STUDY ON THE UNDRAINED STRESS-STRAIN-STRENGTH PROPERTIES OF ANISOTROPICALLY CONSOLIDATED CLAY

異方圧密粘土の非排水応力ーひずみー強度特性に関する研究

by

Toshiyuki Mitachi

三田地　利之

TABLE OF CONTENTS

TABLE OF OFTEN USED SYMBOLS

A = Skempton's pore water pressure coefficient

A_f = Skempton's pore water pressure coefficient at failure

A_{f1}, A_{fn} = Skempton's pore water pressure coefficient at failure in normally and overconsolidated samples

A_o = initial cross sectional area of sample

C_c = compression index

C_f = slope of w versus $\log p_f$ line

C_s, C_{s1} = swelling index in terms of vertical effective swelling pressure

C_{sm} = swelling index in terms of average effective swelling pressure

K_o = coefficient of earth pressure at rest

K_{o1}, K_{on} = coefficient of earth pressure at rest in normal and overconsolidation state

CD = consolidated drained test

CU = consolidated undrained test

UU = unconsolidated undrained test

NCP = K_o normally consolidated undrained plane strain compression test

NEP = K_o normally consolidated undrained plane strain extension test

NIC = isotropically normally consolidated undrained triaxial compression test

NIE = isotropically normally consolidated undrained triaxial extension test

NIEL = isotropically normally consolidated undrained triaxial loading extension test

NK_oC = K_o normally consolidated undrained triaxial compression test with keeping radial strain to be zero during consolidation

$N\overline{K_o}C$ = K_o normally consolidated undrained triaxial compression test with keeping axial strain to be zero during consolidation

NK_oE = K_o normally consolidated undrained triaxial extension test with keeping radial strain to be zero during consolidation

$N\overline{K_o}E$ = K_o normally consolidated undrained triaxial extension test with keeping axial strain to be zero during consolidation

NK_oEL = K_o normally consolidated undrained triaxial loading extension test with keeping radial strain to be zero during consolidation

OCP = K_o overconsolidated undrained plane strain compression test

OEP = K_o overconsolidated undrained plane strain extension test

OIC = isotropically overconsolidated undrained triaxial compression test

OIE = isotropically overconsolidated undrained triaxial extension test

OK_oC = K_o overconsolidated undrained triaxial compression test with keeping radial strain to be zero during consolidation and swelling

$O\overline{K_o}C$ = K_o overconsolidated undrained triaxial compression test with keeping axial strain to be zero during consolidation and swelling

OK_oE = K_o overconsolidated undrained triaxial extension test with keeping radial strain to be zero during consolidation and swelling

$O\overline{K_o}E$ = K_o overconsolidated undrained triaxial extension test with keeping axial strain to be zero during consolidation and swelling

c' = cohesion intercept in terms of effective stress obtained from consolidated undrained test

c_d = cohesion intercept obtained from consolidated drained test

c_e = Hvorslev effective cohesion

e_o = void ratio of clay after consolidation

m = ratio of intermediate principal stress to the sum of the other two principal stresses (Eq.5-3)

m_o = m after K_o consolidation (Eq.5-20)

n = overconsolidation ratio

n_o = overconsolidation ratio at $K_{on} = 1$

p = octahedral effective normal stress (Eqs.3-2 & 5-5)

p_c = vertical effective consolidation pressure

p_e = equivalent consolidation pressure

p_f = effective stress at failure on the 45° plane ($= \frac{\sigma_1' + \sigma_3'}{2}$)

p_1, p_n = preshear vertical effective stress in normal and over-consolidation state

p_o = p after consolidation

p_{oi} = p at the intersection point of consolidation and swelling lines

p_s = vertical effective swelling pressure

p_v = preshear vertical effective stress

q = deviatoric stress (Eq.3-1)

S_u = undrained shear strength

S_{u1}, S_{un} = undrained shear strength in normally and overconsolidated samples

S_{uc}, S_{uE}, S_{up} = S_u in triaxial compression and extension, and plane strain test

Δu = increment of pore pressure

Δu_s = increment of shear induced pore pressure (Eq.5-22)

v = volumetric strain

v^r, v^p = recoverable and irrecoverable component of v

w = water content

x, x_o = stress ratios normalized by M ($x = \eta/M, x_o = \eta_o/M$)

Γ = critical void ratio at $p = 1$

M = octahedral stress ratio τ/p at critical state

$\overline{M}$ = stress ratio q/p at critical state

M_c, M_E = M in compression and extension test

γ = octahedral shear strain $\gamma = \frac{1}{3}\sqrt{(\varepsilon_1-\varepsilon_2)^2+(\varepsilon_2-\varepsilon_3)^2+(\varepsilon_3-\varepsilon_1)^2}$

γ^r, γ^p = recoverable and irrecoverable component of γ

ε = deviatoric strain $\varepsilon = \varepsilon_1 - \frac{1}{3}v$

$\varepsilon_1, \varepsilon_2, \varepsilon_3$ = major, intermediate and minor principal strain

$\varepsilon_x, \varepsilon_y, \varepsilon_z$ = principal strain in x, y and z direction

η = octahedral stress ratio $\eta = \tau/p$

η_o = η after K_o consolidation

$\overline{\eta}$ = stress ratio $\overline{\eta} = q/p$

η_1, η_2 = η at the inflection point in $F(\eta)$ vs. η curve (Fig.3-10) in axi-symmetrical triaxial tests, and η at which interchange of principal stress directions occurs in plane strain extension tests (Fig.5-15)

θ_o = angle representing the magnitude of stress anisotropy (Fig.4-10)

κ = slope of swelling line in e vs. $\ln p$ diagram

$\overline{K}$ = coefficient of cohesion

λ = slope of normal consolidation line in e vs. $\ln p$ diagram

ξ = the ratio C_s/C_c

ξ_m = the ratio C_{sm}/C_c

ρ = the ratio C_s/C_f

μ = dilatancy coefficient

μ_1, μ_2, μ_3 = dilatancy coefficients (Fig.3-10)

ν = coefficient represented by Eq.(3-84)

$\sigma_1', \sigma_2', \sigma_3'$ = major, intermediate and minor effective principal stress

$\sigma_{1c}', \sigma_{mc}'$ = vertical and average effective consolidation pressure

$\sigma_{1s}', \sigma_{ms}'$ = vertical and average effective swelling pressure

σ_a' = effective axial stress in triaxial test

σ_e' = equivalent consolidation pressure

σ_r' = effective radial stress in triaxial test

$\sigma_x', \sigma_y', \sigma_z'$ = effective principal stress in x, y and z direction

$(\sigma_z')_c$ = σ_z' after consolidation

τ = octahedral shear stress $\tau = \frac{1}{3}\sqrt{(\sigma_1-\sigma_2)^2+(\sigma_2-\sigma_3)^2+(\sigma_3-\sigma_1)^2}$

τ_o = τ after K_o consolidation

$\Delta\tau$ = increment of octahedral shear stress

$\Delta\tau_1, \Delta\tau_2, \Delta\tau_3$ = increments of octahedral shear stress (Eqs.5-9 to 5-11)

ψ = plastic strain increment ratio (Eq.3-8)

ϕ' = effective angle of shearing resistance obtained from consolidated undrained test

ϕ_c', ϕ_E' = ϕ' in compression and extension test

ϕ_d = effective angle of shearing resistance obtained from consolidated drained test

ϕ_e = Hvorslev effective angle of internal friction

ω = positive constant in Eq.3-60

$F(\eta)$ = dilatancy function

CHAPTER I INTRODUCTION

1.1 General Description of Stress-Strain-Strength Properties of Cohesive Soils

1.1.1 Introduction

Explication of various phenomena concerning the deformation and failure of cohesive soils is essential to tackle the important practical problems such as bearing capacity, earth pressure and stability of slope. Therefore, a large number of theoretical and experimental investigations on this subject have been done so far. However, since the mechanical properties of soil are the most complicated ones in the engineering material, it is not easy to give the entire picture of the properties.

In this chapter, the major factors which affect the stress-strain-strength properties of cohesive soils and the scope of this thesis will be outlined. Previous investigations concerning these subjects will also be summarized.

1.1.2 Major factors controlling the shear strength of cohesive soil

As it goes without saying that the type of soil gives great influence on the mechanical properties of soil, the density of a given soil has the most important influence on the shear strength of the soil. The fact that the greater the density, the greater the shear strength can intuitively be accepted. Water content of a soil is also important in relation to the drainage condition during shear. Structure of a soil is another important factor comparable to the density.

Defining the effective stress σ' in addition to the type of soil, density, water content and structure, the shear strength of soil τ_f can be represented as follows (Mikasa, 1962 and 1964).

$$\tau_f = F_1(\text{ type of soil, density, water content, soil structure, } \sigma')$$

$$\sigma' = F_2(\text{ type of soil, density, water content, soil structure })$$

These equations are considered to be fundamentals representing shear strength of soils.

1.1.3 Drainage condition and stability analysis

As mentioned previously, the shear strength of soil depends greatly upon the density. When the void of soil is filled with water, very much time is required for the soil to change its volume, especially in cohesive soil. Therefore, the stress-strain-strength properties of soil vary greatly depending on the drainage condition during deformation.

According to the fact mentioned above, laboratory shear tests of soil have been performed under one of three types of standard drainage condition which is regarded approximately close to the drainage condition in situ. These standard test conditions are as follows.

(1) Unconsolidated Undrained (UU) Test; Drainage is not permitted during every stage of test.

(2) Consolidated Undrained (CU) Test; Specimen is first consolidated and then sheared under undrained condition.

(3) Consolidated Drained (CD) Test; Specimen is first consolidated and then sheared under drained condition.

Selection of the drainage condition among these will be connected to what kind of method of stability analysis outlined in the following section is appropriate to the in situ drainage condition.

a) Short term stability analysis

Examples of typical situations in this type of analysis are such as the embankment constructed or strip loading placed rapidly on soft clay deposit. In these cases, practically little drainage takes place during loading, and hence the drainage condition is similar to that in UU test. The shear strength used in stability analysis in such cases is the in situ undrained shear strength that has existed before construction.

b) Long term stability analysis

Examples of this case are such as embankment constructed very slowly in layers over a soft clay deposit or earth dam with steady state seepage. Since there develop no excess pore pressure within the clay layer in such situations, the drainage condition is similar to that in CD test. The shear strength used in those cases is the in situ drained shear strength of the soil.

In situ drained strength is determined from the effective strength parameters (i.e. the cohesion intercept c_d and angle of shear resistance ϕ_d) and the values of effective normal stress acting along the potential failure surface. In order to estimate the effective normal stress, the magnitude of pore pressure is needed. Usually, pore pressure corresponding to the ground water table or steady state seepage is used. Strength parameters c_d and ϕ_d are obtained from CD tests, which are time consuming and

tedious. Fortunately, it has been found experimentally that the values of C_d and ϕ_d from CD tests are almost equal to the values of c' and ϕ' from CU tests (Bjerrum and Simons, 1960). Therefore, CU test is often used in stead of CD test in order to obtain strength parameters for long term analysis.

c) Intermediate term stability analysis

In such a case that additional load is rapidly applied to the clay layer which has already been consolidated, there are two methods of analysis correspond to these situations.

One method is to use the undrained shear strength S_u corresponding to the clay layer that has been consolidated under the existing stress prior to imposition of the additional load.

Another method is to use effective strength parameters c' and ϕ' with the estimation of pore pressure. As in the long term analysis, the value of pore pressure is taken as steady state seepage or that corresponding to the ground water table. In this approach, tacit assumption is made that there does not occur further change in pore pressure, and hence in effective stress with additional loading.

As described above, shear strength parameters, drainage condition and stability analysis are closely connected with one another. From the results of a series of CU test with pore water pressure measurement on saturated clay, rate of change in undrained strength S_u due to consolidation and effective strength parameters c' and ϕ' can be obtained. Since the consolidation condition and stress

system in conventional laboratory CU test are not always the same to those in situ, the validity of the strength parameters obtained from CU test needs to be checked, particularly from the standpoint of the stress history and stress system. Therefore, the investigation of the influence of stress history and stress system during consolidation and shear on the magnitude of strength parameters is one of the most important subjects of this study.

1.1.4 Basic requirements for predicting in situ stress-strain-strength properties of cohesive soils

In order to make successful stability analysis, accurate prediction of stress-strain strength properties of soils is needed. To do so, it is essential to perform the laboratory shear tests that duplicate the in situ conditions, i.e. the following two requirements must be fulfilled.

(1) Obtain samples having the same properties as the in situ soils

Strictly speaking, it is imperative that any soil samples for laboratory shear tests have the same properties as those in situ. Namely, the density, water content, effective stress, soil structure etc. should be the same. Following factors must be examined.

a) Sample disturbance

In order to obtain strength parameters in situ for a soil by laboratory shear test, sample is first removed from some depth of the ground by block sampling or thin wall tube sampling, and then is brought to the laboratory. After storing, it is trimmed and finally mounted in the shear test apparatus. During these processes, the sample is subjected to inevitable disturbance due to the in situ stress release, and mechanical disturbance due to trimming and mounting (Skempton and Sowa, 1963 and Ladd and Lambe, 1963).

b) Stress level and stress system during consolidation

Generally, in situ clay element is consolidated under anisotropic

stress condition, i.e. the vertical stress on the element is not equal to the horizontal one. Since the magnitude of preshear consolidation pressure and the stress system during consolidation give great influence on the stress-strain-strength properties of clay (Henkel,1960 and Henkel and Sowa, 1963), not only the vertical stress but also horizontal stress in triaxial consolidation should be the same as those in situ.

c) Aging effect

It is well known that clay soils undergo secondary consolidation under the constant effective stress after dissipation of the excess pore pressure. Clays which exhibit secondary consolidation generally gain in shear strength with time (Bjerrum, Simons and Torblaa 1958, and Bjerrum and Lo, 1963). The effect of aging on stress-strain and stress path behaviour is even more pronounced (Ladd, 1971).

d) Orientation of the sample

If a clay soil has a difference in soil structure with direction, the stress-strain-strength properties of this clay exhibit anisotropy (Dunkan and Seed, 1966). This type of anisotropy is called "inherent" anisotropy in contrast to the "induced" anisotropy due to the stress system.

(2) Perform the shear test under the same condition as will be imposed in situ

Ideally, the shear tests have to be done under the same conditions

as those in situ. Namely, stress system and rate of strain etc. should be the same. Following factors have to be examined.

a) Stress system

Stress systems typically encountered in the field are illustrated in Fig1-1 for a normally consolidated clay with K_o stress condition, where major principal effective stress σ_1' initially acts in the vertical direction and intermediate and minor principal stresses σ_2' and σ_3', respectively, act in the horizontal direction. Typical examples of stress systems during undrained shear are as follows (Ladd, 1971).

Case (I) Under center line of a circular footing:

The increase in the vertical stress is more than that in the horizontal stress and the directions of the principal stress remain unchanged. The applied stress system is symmetric with respect to the center line. Hence, the stress system is the same as triaxial compression test ($\sigma_2' = \sigma_3'$).

Case (II) Under center line of a circular excavation:

As the decrease in the vertical stress is more than that in the horizontal stress, the horizontal stress can finally exceed the vertical stress. If such circumstances is brought in, the soil will be in a state of triaxial extension ($\sigma_2' = \sigma_1'$). Moreover, an interchange of principal stress directions does occur since the major principal effective stress now acts in the horizontal direction.

Typical Stress Systems in the Field for a Normally Consolidated Clay

(a) Under Centerline of a Circular Footing

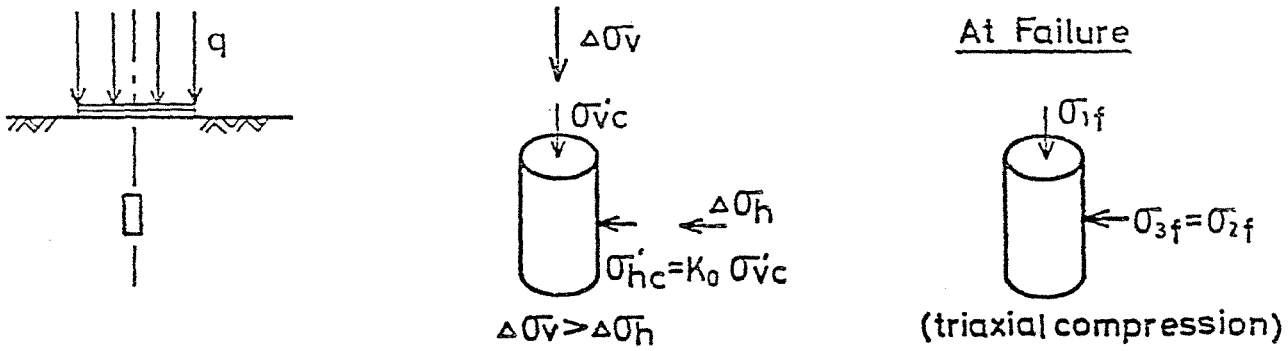

(b) Under Centerline of a Circular Excavation

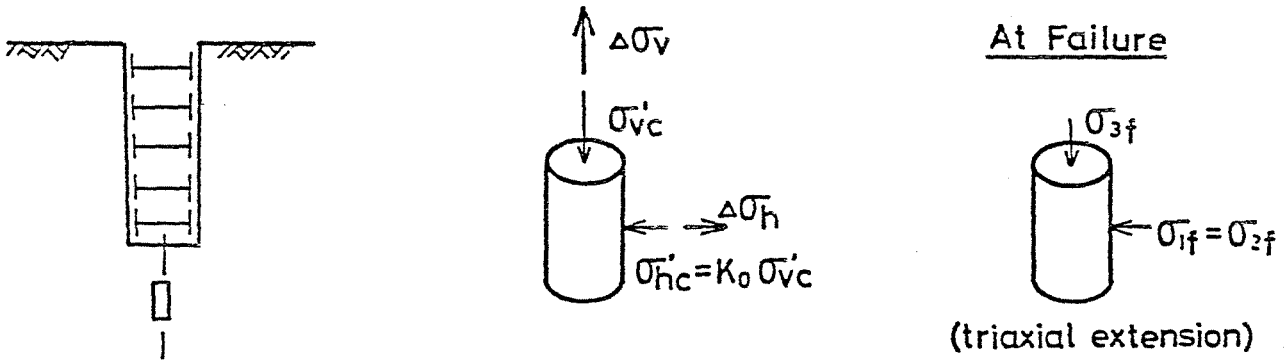

(c) Under Centerline of a Strip Footing

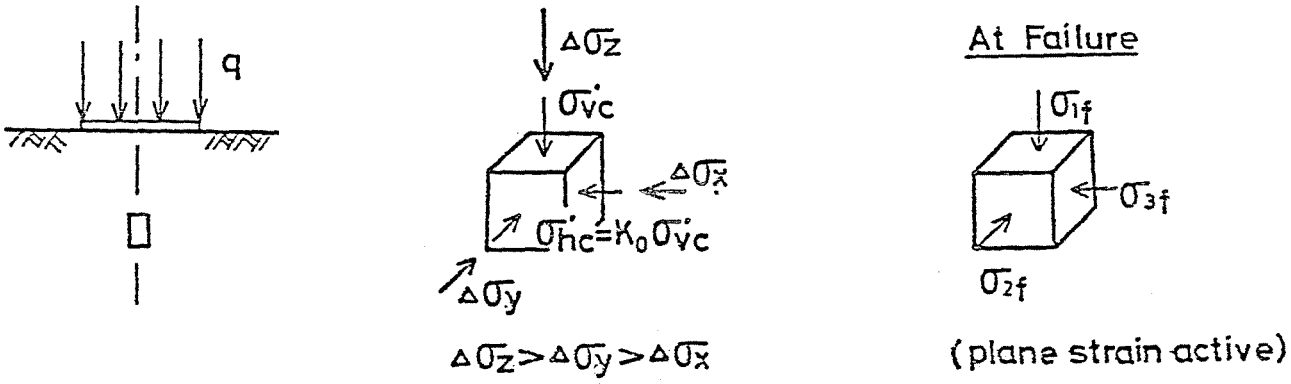

(d) Behind a Retaining Wall with a Passive Pressure

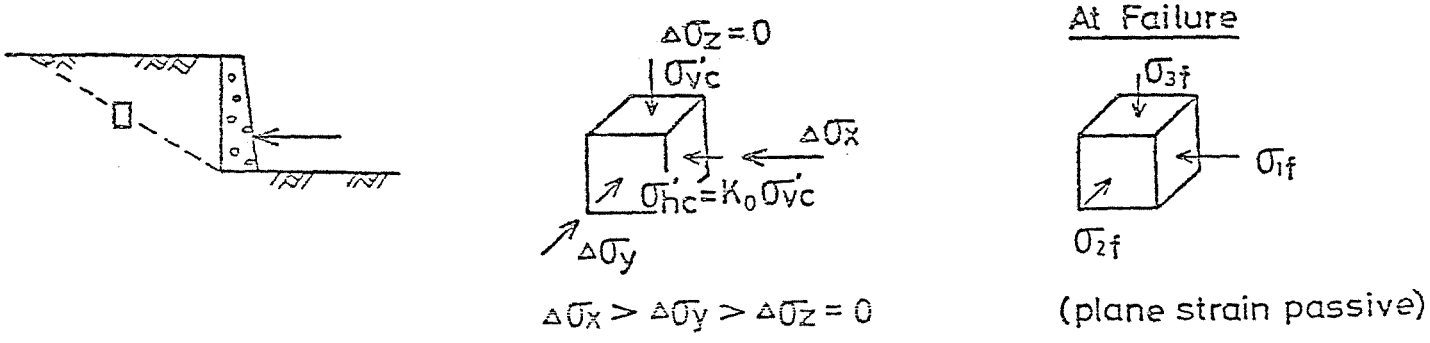

Fig.1-1 Stress systems typically encountered in the field

Case (III) Under centerline of a strip footing:

This case is similar to that of case (I), except that the increase in the longitudinal stress σ_y', which is intermediate principal stress σ_2' in this case, is larger than that in the transverse stress σ_x', which is minor principal stress. As the deformation of the soil in the longitudinal direction is almost equal to zero, the soil is in a plane strain active state with the major principal stress still acting in the vertical direction.

Case (IV) Behind a retaining wall with a passive pressure

This is another case of plane strain, but with an interchange of principal stress directions, since the major principal stress now acts in horizontal direction. It is a plane strain passive case.

b) Interchange of principal stress directions

When the applied stress system causes an interchange of principal stress directions as described above, the soil structure developed during consolidation under anisotropic stress system must change itself in order to resist new direction of the principal stresses. Thus, the stress-strain-strength properties of the soil will be affected by the occurrence of the interchange of principal stress directions.

If a clay had been heavily overconsolidated under the K_o condition, the value of K_o is greater than unity, i.e. the horizontal stress is greater than the vertical stress. Then, the cases (I) and (III) in the preceding article would have

exhibited an interchange of principal stress directions, namely major principal stress σ_1' would have acted in the horizontal direction prior to loading and thereafter in the vertical direction at failure. Conversely, σ_1' would always act in a horizontal direction in the cases (Ⅱ) and (Ⅳ).

c) Rate of strain

There can be no question about the fact that the increase in time to failure in triaxial test causes a decrease in undrained shear strength (e.g. Casagrande and Wilson, 1951). According to the recent experimental data, the rate of strain affects not only the undrained strength but also the dilatancy characteristics of clay, and hence the accurate prediction of stress-strain-strength properties of cohesive soil cannot be accomplished without taking the time effect into consideration, i.e. rate of strain and consolidation duration (Kitago et al., 1980).

In addition to the factors mentioned above, stress-strain-strength properties of cohesive soils is influenced by the following factors such as temperature, pore fluid composition and cyclic loading.

1.2 Brief Review of Previous Investigations

As mentioned previously, the prediction of in situ stress-strain-strength properties of cohesive soils is essential to the solution of the important practical problems. These properties are influenced by many factors, and hence there have been a large number of investigations on these problems. Since it is unable to summarize all the research papers on these subjects, a brief review on the following subjects which are relevant to the present study will be made.

1) Influence of stress history and stress system during consolidation on the stress-strain-strength behaviour
2) Effect of stress system (compression or extension) during shear on the stress-strain-strength behaviour
3) Stress-strain-strength behaviour under plane strain condition
4) Method of predicting stress-strain behaviour of clay

1.2.1 Influence of stress history and stress system during consolidation

The influence of stress anisotropy during consolidation on the strength characteristics of cohesive soil has been investigated in detail for a long time. Theoretical investigation by Hansen and Gibson (1949) is well known and a good example of study on this subject. They suggested that even if the structure of a clay soil is isotropic, the undrained shear strength of this clay is different with direction, because of the anisotropic stress system during consolidation. Henkel and Sowa (1963) studied experimentally, on this subject, by using the lateral strain indicator developed by Bishop and Henkel (1957) so as to control the lateral strain of clay specimen during consolidation in order to establish the K_o condition which is representative of in situ deformation condition during one dimensional consolidation. Akai and Adachi (1965) investigated the one dimensional consolidation and shear strength properties of clay by using the similar indicator as Bishop and Henkel.

Ladd (1965) investigated the difference of strength parameters between isotropically consolidated specimen and anisotropically consolidated one for several cohesive soils. Mikasa et al. (1978) investigated the difference of S_u/p_v, where S_u and p_v are the undrained shear strength and effective vertical consolidation pressure respectively, between the specimen isotropically and

anisotropically consolidated in conjunction with the consolidation duration.

Recently, stress-strain behaviour of anisotropically consolidated clay has become a theme of research in conjunction with the establishment of stress-strain equation of cohesive soil (e.g. Lewin and Burland 1970, Lewin 1975, Prevost 1978 and Mroz et al. 1979).

Effect of overconsolidation on the shear strength characteristics of cohesive soil has also been investigated for a long time (e.g. Hvorslev, 1960). The experimental study using triaxial apparatus by Henkel (1960) is well known, who concluded that the effective angle of shearing resistance ϕ' is almost constant irrespective of stress history and stress system. This experimental fact became a backbone of the effective stress analysis of stability computation.

Nakase et al. (1969) studied the influence of stress anisotropy during consolidation and of preconsolidation on the shear strength parameters of cohesive soil. They suggested that even the effective strength parameter may be affected by the anisotropic overconsolidation, and they proposed a method of estimating the reduction of undrained shear strength due to swelling.

Ladd and Foott (1974) performed elaborate experiments concerning the undrained shear strength of anisotropically overconsolidated clay. They found experimentally an unique relationship between Su/p_v versus logarithm of overconsolidation ratio (OCR).

Experiments in isotropic condition for wide range of OCR values up to 375 were carried out by Yudhbir and Varadarajan (1974).

The effect of sample disturbance on the strength behaviour of clay has also been investigated very actively. Skempton and Sowa (1963) and Noorany and Seed (1965) studied the difference between the in situ undrained shear strength and that obtained from unconsolidated undrained test on "undisturbed" sample by simulating the stress condition in situ and that during sampling process in the triaxial cell. Ladd and Lambe (1963) and Okumura (1969) studied experimentally on the "mechanical" disturbance due to sampling and trimming operation in addition to the disturbance due to stress release. And they proposed methods of modification of undrained strength data obtained from standard triaxial tests.

1.2.2 Effect of stress system (compression or extension) during shear

As mentined previously, Henkel (1960) and Parry (1960) studied systematically the influence of stress history during consolidation and stress system during shear on the shear strength characteristics of remolded clay. In this series of experiment, they performed isotropically consolidated drained and undrained compression and extension tests and suggested that the effective strength parameters are, for practical purposes, independent of the type of test.

Ladd (1965) carried out an undrained extension test on the anisotropically consolidated clay. In accordance with his test result, both effective strength parameter and undrained shear strength in extension test differ extremely from those in compression test.

Parry and Nadarajah (1973) made isotropically and anisotropically consolidated undrained triaxial compression and extension tests in order to study the influence of preconsolidation pressure and anisotropy on the strength and stress-strain characteristics of lightly overconsolidated clay. They found that the failure envelopes for isotropically and anisotropically consolidated specimens differ in both compression and extension, and most markedly in extension.

Based on the critical state concept by Roscoe et al. (1963), Parry (1971) and Karube (1975) suggested equations

estimating the undrained extension strength using the data from compression test.

1.2.3 Plane strain behaviour

The first experiment in the world in which three principal stresses are controlled independently was performed by Kjellman (1936) using dry sand specimen. To the best of the author's knowledge, Wu et al. (1963) carried out the tests controlling the intermediate stress of clay specimen for the first time, using hollow cylindrical specimen. Broms and Ratnam (1963) also performed the tests controlling the intermediate stress with anisotropically consolidated clay.

Shibata and Karube (1965) developed an apparatus, by which plane strain tests can be performed using prismatic specimen whose dimension is similar to that of conventional triaxial test specimen. At that time, Henkel and Wade (1966) carried out a series of plane strain test using the same type of apparatus which was designed by Bishop and Wood and used by Cornforth (1964) for the test with sand specimen. It was suggested by Henkel and Wade that the effective strength parameter $\tan\phi'$ and S_u/p_v are about 8 % greater in plane strain test than those in axi-symmetrical triaxial test.

Campanella and Vaid (1973) further performed plane strain extension and triaxial extension tests in order to investigate the influence of interchange of principal stress directions on the stress-strain behaviour of natural clay.

Sketchley and Bransby (1973) carried out plane strain

compression and extension test on normally and overconsolidated clay by using Hambly and Roscoe (1969) type test apparatus so as to investigate the influence of stress history on the stress-strain-strength behaviour of remolded kaolin.

Recently, Lade (1978) developed an special triaxial apparatus by which the three principal stresses can be controlled independently, and examined the failure criterion of cohesive soil (Lade and Musante, 1978).

1.2.4 Prediction of stress-strain behaviour of cohesive soil

Since the studies by Roscoe et al. (1958), Roscoe and Poorooshasb (1963) and Roscoe et al. (1963), who are considered to be pioneers of this subject, investigations on this subject has been developed rapidly and a large number of researchers have been concerned with this problem.

The theories by Roscoe et al. (1963), which is called original Cam-clay theory, and by Roscoe and Burland (1968) which is called modified Cam-clay theory will be presented in detail later in Chapter III. The theories for predicting stress-strain behaviour of anisotropically consolidated clay, such as Ohta et al. (1975) and Lewin(1975) will also be presented in some detail in Chapter IV.

Wroth and Bassett (1965) proposed a stress-strain equation which has a possibility to apply the overconsolidated clay (Adachi and Tohgi, 1974). Karube (1977) proposed a stress-strain equation for normally consolidated clay which involved the effect of strain rate and consolidation duration.

Recently, the influence of stress history, stress system, consolidation duration and rate of strain on the stress-strain behaviour has become a main theme of research. The studies by Sekiguchi and Ohta (1977), Pender (1978) and Prevost (1978) et al. are the representative of this category.

1.3 Composition of the Present Thesis

As mentioned previously, there are many factors influencing upon the stress-strain-strength characteristics of cohesive soils. Above all, the influences of stress history and stress system during consolidation and shear on the stress-strain behaviour of saturated clay are pronounced. In this study, a method of predicting stress-strain-strength behaviour of normally consolidated saturated clay under the in situ stress condition will be proposed based on the experimental results obtained from variety of tests, in which effects of stress history and stress system are taken into account. A method of predicting in situ undrained strength of overconsolidated clay will also be presented.

The composition of the present study is as follows.

In CHAPTER II, test apparatus, material used and experimental procedure will be presented.

In CHAPTER III, original and modified Cam-clay equations by Roscoe et al. and alternative equations proposed by other research workers for predicting stress-strain behaviour of isotropically consolidated clay will first be outlined. Then, less excellent accuracy of Roscoe's original Cam-clay theory and subsequent theories proposed after him will be shown by predicting the test results of present study, and the problems in their theories will be pointed out, and further will be presented a method proposed by the present author and comparison of predicted and observed stress-strain behaviour.

In CHAPTER IV, the influence of stress condition during consoli-

dation and stress system during shear on the undrained stress-strain-strength properties of saturated clay will be shown, and existing methods for predicting stress-strain behaviour of K_o consolidated clay will be outlined. Furthermore, a new method of prediction by using the parameters obtained from conventional triaxial tests and comparison of predicted stress-strain behaviour by this method with observed one will be presented.

In CHAPTER V, observed stress-strain-strength behaviour of saturated clay in K_o normally consolidated plane strain test will be shown, and the predicted results for this test by both existing methods and proposed one by the present author will be presented for comparison.

In CHAPTER VI, change in undrained strength due to consolidation and swelling obtained from the experimental results will be shown, and the coefficient of earth pressure at rest K_o and the pore pressure coefficient A at failure will be discussed in relation to overconsolidation ratio. Furthermore, a simplified method of predicting in situ undrained strength of overconsolidated clay by using the data from a series of conventional laboratory test will be presented.

In CHAPTER VII, conclusions drawn from this study will be presented.

CHAPTER II TEST APPARATUS, MATERIAL USED AND EXPERIMENTAL PROCEDURE

2.1 Test Apparatus

Test apparatuses used in this study can be divided roughly into two types. One is conventional triaxial compression apparatus and the other is plane strain apparatus.

Since the triaxial compression apparatus used for the present study is nothing but conventional, its detailed explanation will be abbreviated, but the circumstances of the specimen mounted in the triaxial apparatus are illustrated in Fig.2-1. As the observation and recording of data for triaxial test much time and efforts are needed, digital strain meter and pressure and displacement transducer were used in this study. In conventional triaxial compression test, measured variables were major and minor principal stress, pore water pressure and axial displacement. In this study, minor principal stress (cell pressure) and pore water pressure were measured by pressure transducer, and axial displacement was measured by displacement transducer. Axial load was measured through the water pressure within the bellofram cylinder by pressure transducer (see Fig.2-2). Electrical signals from the pressure and displacement transducers were recorded automatically by the digital strain meter according to time intervals set prior to the start of test.

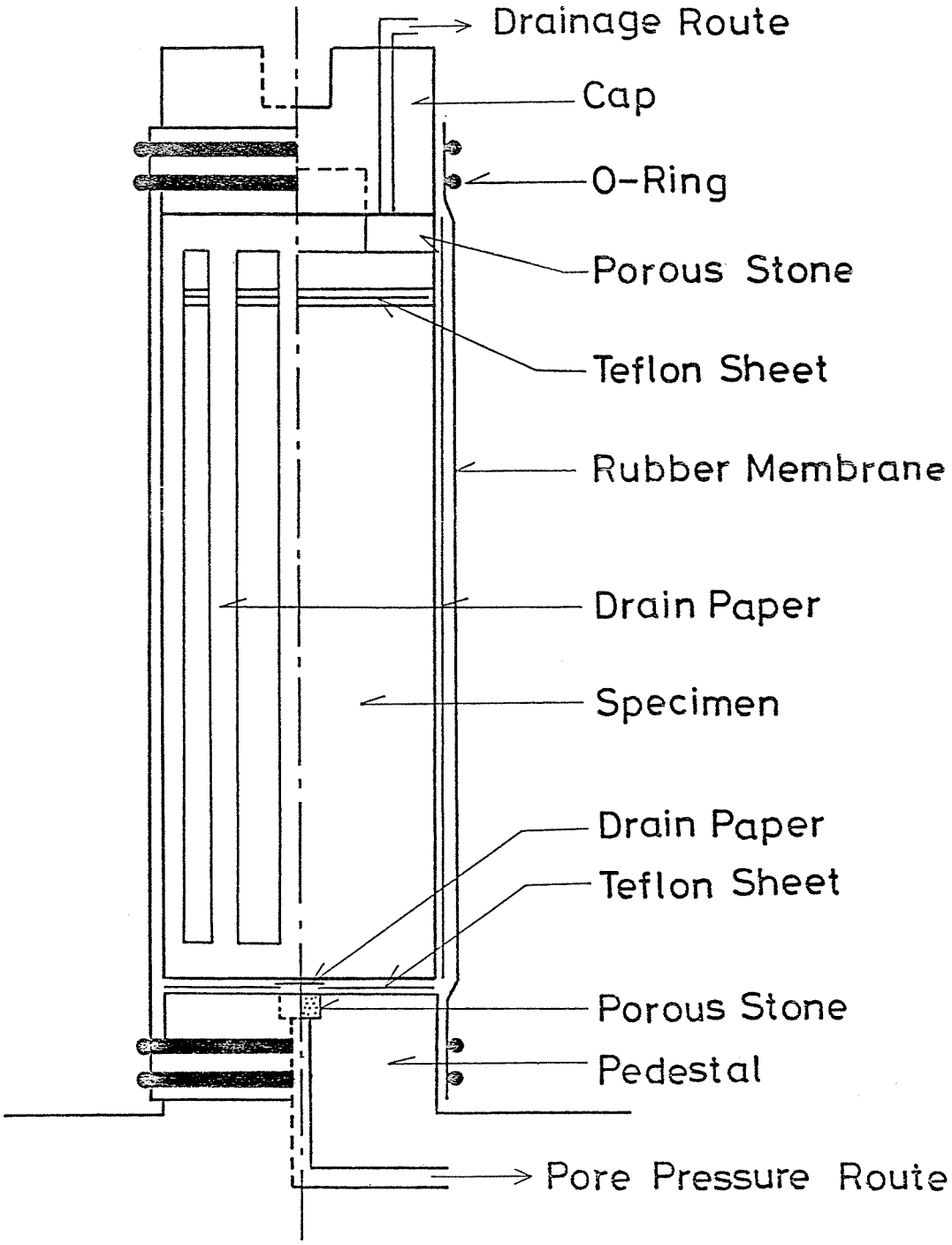

Fig. 2-1 Triaxial test specimen

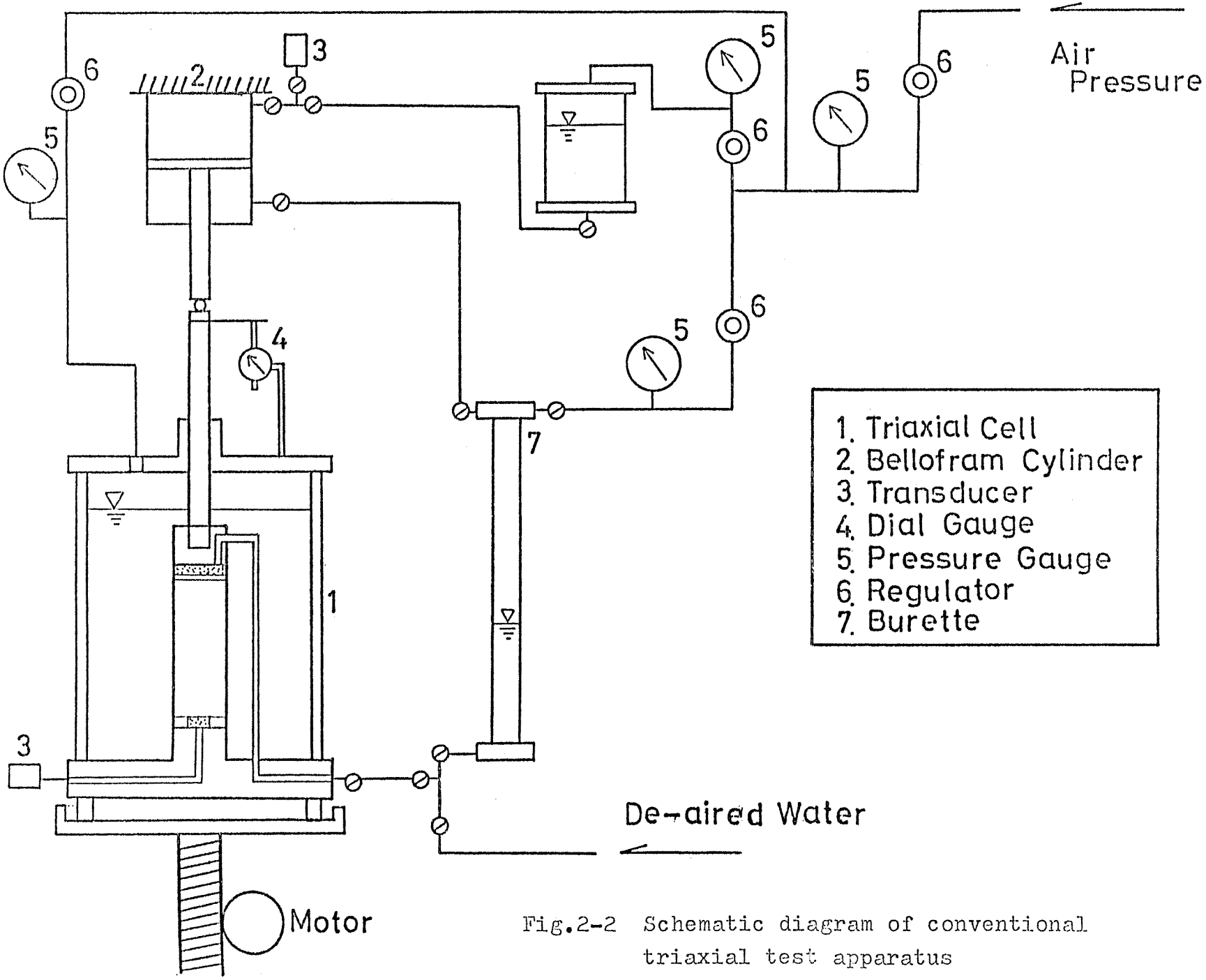

Fig.2-2 Schematic diagram of conventional triaxial test apparatus

Brief explanations of the plane strain apparatus and other equipments attached to the standard triaxial apparatuses are as follows.

1) K_0 control system

There are two kinds of method of K_0 consolidation by using triaxial apparatus. The first method is to control the axial or lateral stress so as to keep the diameter of specimen unchanged by detecting directly the lateral deformation during consolidation. The second method is to control the stresses so as to establish the K_0 condition in such a manner that the change in volume ΔV of specimen is made equal to the axial displacement ΔH multiplied by the original cross sectional area A_0 of the sample, i.e.

$$\Delta V = A_0 \cdot \Delta H \qquad (2\text{-}1)$$

Various types of lateral strain indicator have been developed (Bishop and Henkel 1957, Brown and Snaith 1974, El-Ruwayih 1976 and Boyce and Brown 1976) for the purpose of the first method.

Several automatic K_0 control systems have been proposed (Lewin 1971, Mitachi et al. 1973, and Menzies et al. 1977) which are attached to the conventional apparatus, and specially designed triaxial apparatus (Campanella and Vaid, 1972) so as to establish the condition represented by Eq.(2-1).

Fig.2-3 schematically illustrates an equipment designed by the present author (Mitachi and Kitago, 1976) for controlling automatically the K_0 condition during consolidation, on referring to Lewin's

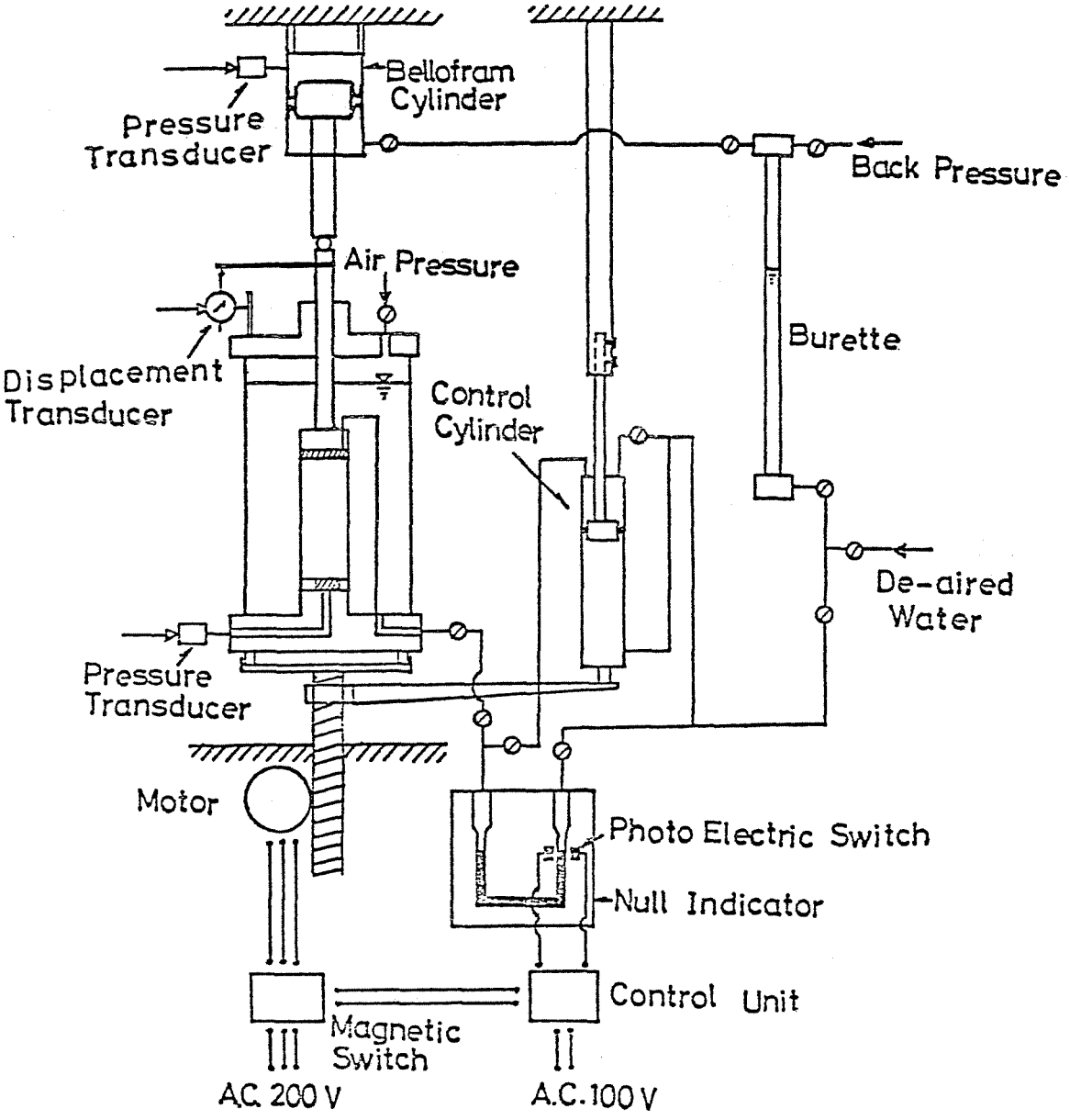

Fig.2-3 Schematic diagram of automatic K_o control system

method. Drainage water from specimen is led to burette via null indicator and control cylinder. This route is filled with de-aired water. Sectional area of the upper room of control cylinder(sectional area of piston rod is subtracted) is made to be equal to the sectional area A_0 of the specimen. This equipment establishes the K_0 condition in accordance with the principle represented by Eq.(2-1).

Mechanism of this equipment is as follows. The specimen is mounted in a conventional triaxial cell in an usual manner and the K_0 control system is connected to the specimen just prior to consolidation. The test procedure involves increasing the cell pressure in steps. Subsequent volume change due to consolidation under all-round pressure makes an movement to the mercury in the null indicator. Photo-electric switch mounted on the null indicator detects this movement and switches on, through delay relay and magnetic switch, the motor which drives the loading shaft to initiate the vertical compression of the specimen. At the same time, the movement of the shaft carries up with it the control cylinder. This displacement of the control cylinder sucks back the mercury and so switches off the motor. In the consolidation stage, the control unit of photo-electric switch is set to "dark on" and the change-over switch of the motor to "forward" so that the interception of the light of the photo-electric switch by the mercury switches on and rotates the motor in the direction compressing the specimen. K_0 swelling

test can be performed in similar manner as the K_0 consolidation by setting the controlling unit to "light on" and the motor to "reverse". In this case, if the overconsolidation ratio exceeds about 3, the value of K_0 becomes greater than unity, and it is needed to connect tightly the piston rod and top cap of specimen.

The present author formerly developed a lateral strain indicator for K_0 consolidation (Mitachi and Ueda, 1969) as shown in Fig.2-4, which was mounted in the triaxial cell. Observing lateral strain by this indicator, control of stress was manually performed so as to fulfill the condition of zero lateral strain. This indicator was mounted tentatively in the triaxial cell in order to check the magnitude of lateral strain during K_0 consolidation which was performed by using the automatic K_0 control system. The test result is shown in Table 2-1. It is clear that the condition of zero lateral strain is well established by the use of automatic K_0 control system, in which the lateral strain is not measured directly, but the average diameter of the specimen is kept constant.

2) Loading extension apparatus

In extension tests, in which axial stress is decreased while lateral stress is maintained constant, the conventional triaxial apparatus was used after slight modification of loading ram tightly connected with top cap.

On the other hand, in such a type of extension test as axial

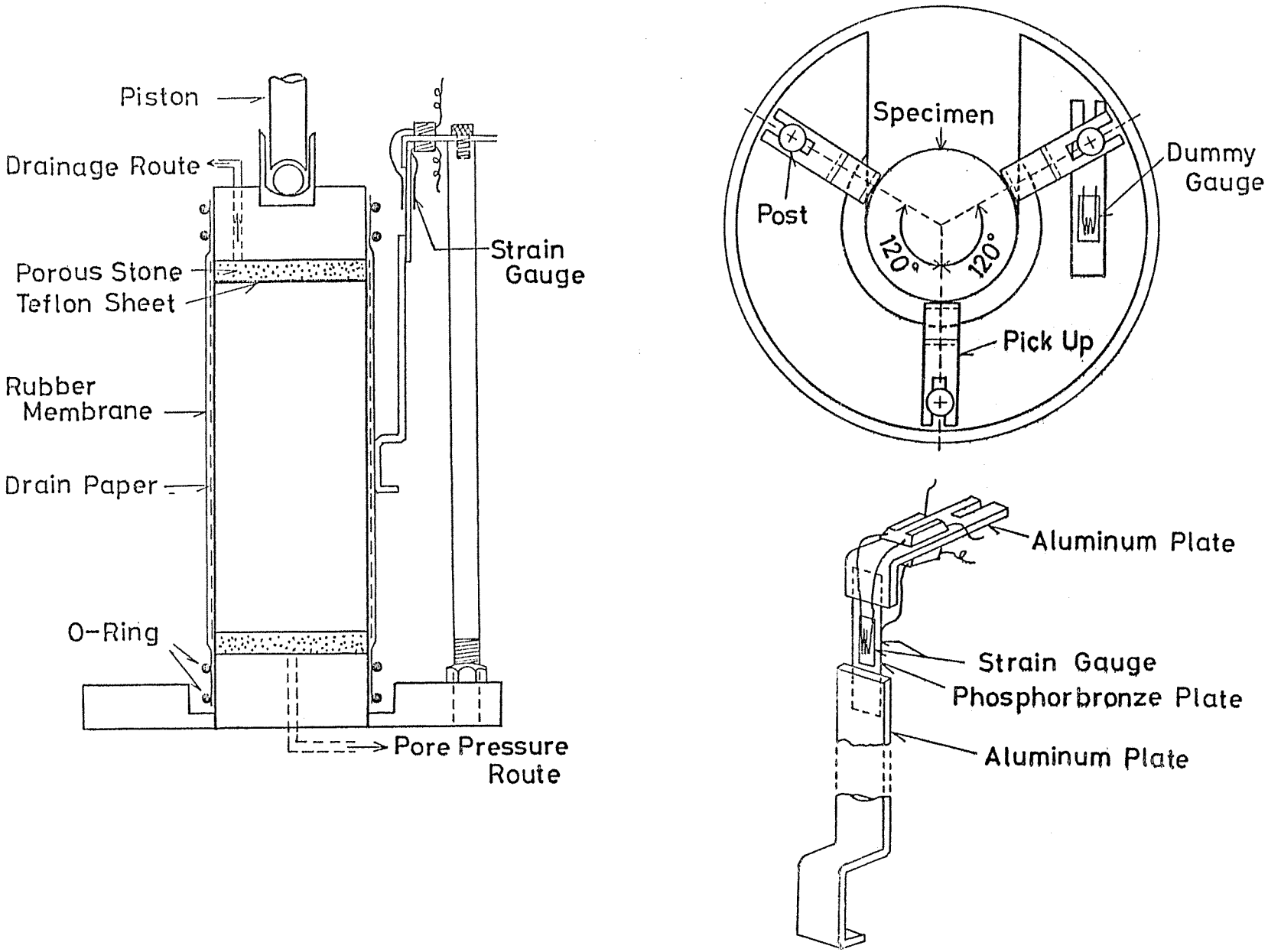

Fig.2-4 Lateral strain indicator

σ_r (kPa)	$\Delta\sigma_r$ (kPa)	Elapsed Time (min.)	Radial Deformation ($\times$ 1/100mm)
5	5	60	-2.0
10	5	60	+2.0
15	5	70	0.0
22	7	850	-0.7
32	10	100	+1.6
45	13	70	+1.3
58	13	70	0.0
78	20	90	+1.3
105	27	90	+1.6
135	30	60	+1.6
170	40	60	+1.6
210	40	80	+1.6
250	40	840	-2.3
310	60	60	0.0
400	90	80	0.0
500	100	1440	+2.6
Total	500	4080	+10.2

Total radial strain as a percentage (diameter of specimen = 50mm);

$$\frac{10.2 \times 10^{-2}}{50} \times 100 = 0.2\%$$

Table 2-1 Check data of the magnitude of lateral strain during K_o consolidation

stress constant and lateral stress increased, the apparatus shown schematically in Fig.2-5 was used in order to perform strain controlled test by increasing lateral stress. The loading ram of the triaxial cell is sealed to the top of the cell by means of bellofram. The control cylinder connected to the cell is filled with water which is pushed at a constant rate into the cell to increase all-round pressure.

3) Plane strain test apparatus

Plane strain compressin and extension tests were carried out with the apparatus shown schematically in Fig.2-6 which was designed taking the following consideration into account;

i) Friction between specimen and confining plates must be made as small as possible. ii) Control system of plane strain condition (i.e. intermediate principal strain $\varepsilon_2 = 0$) must be accurate enough. iii) For the purpose of correlations of the plane strain test data with those of axi-symmetrical tri-axial test, dimension of specimen should be close to each other. iv) For the purpose of simulation of the initial stress condition of soils in situ, specimens must initially be consolidated under K_0 condition. Special feature of main parts of this apparatus are as follows;

a) Triaxial cell and specimen; Dimension of specimen is 50x50mm in side and 120mm in height, which is very close to that of cylindrical specimen, 50mm in diameter and 120mm high.

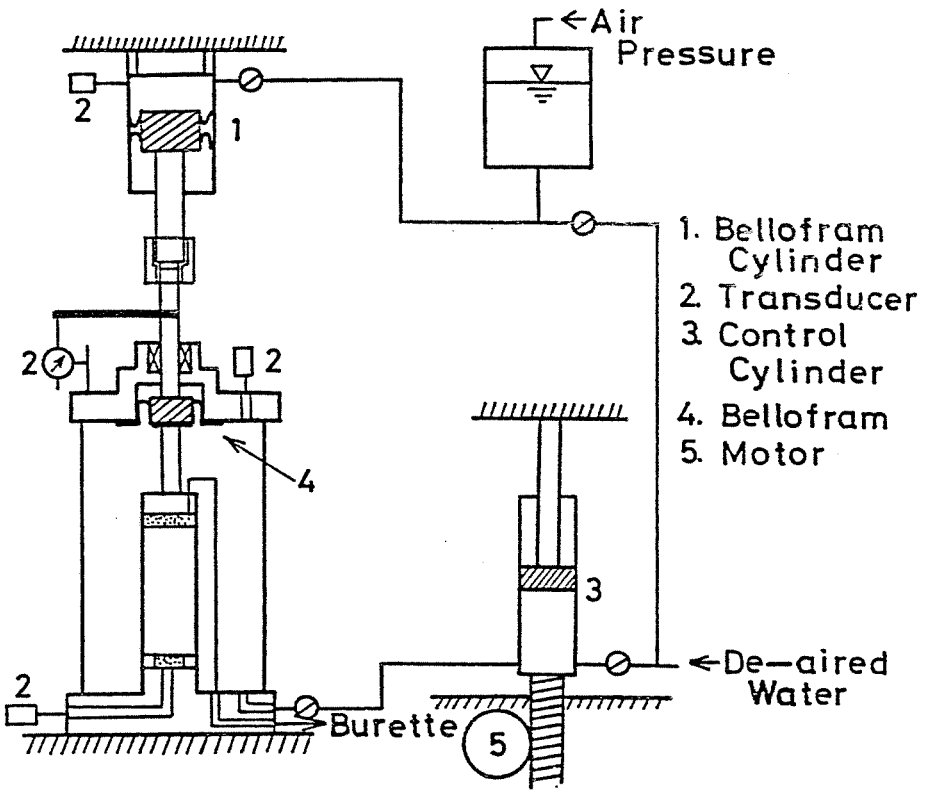

Fig.2-5 Schematic diagram of loading extension test apparatus

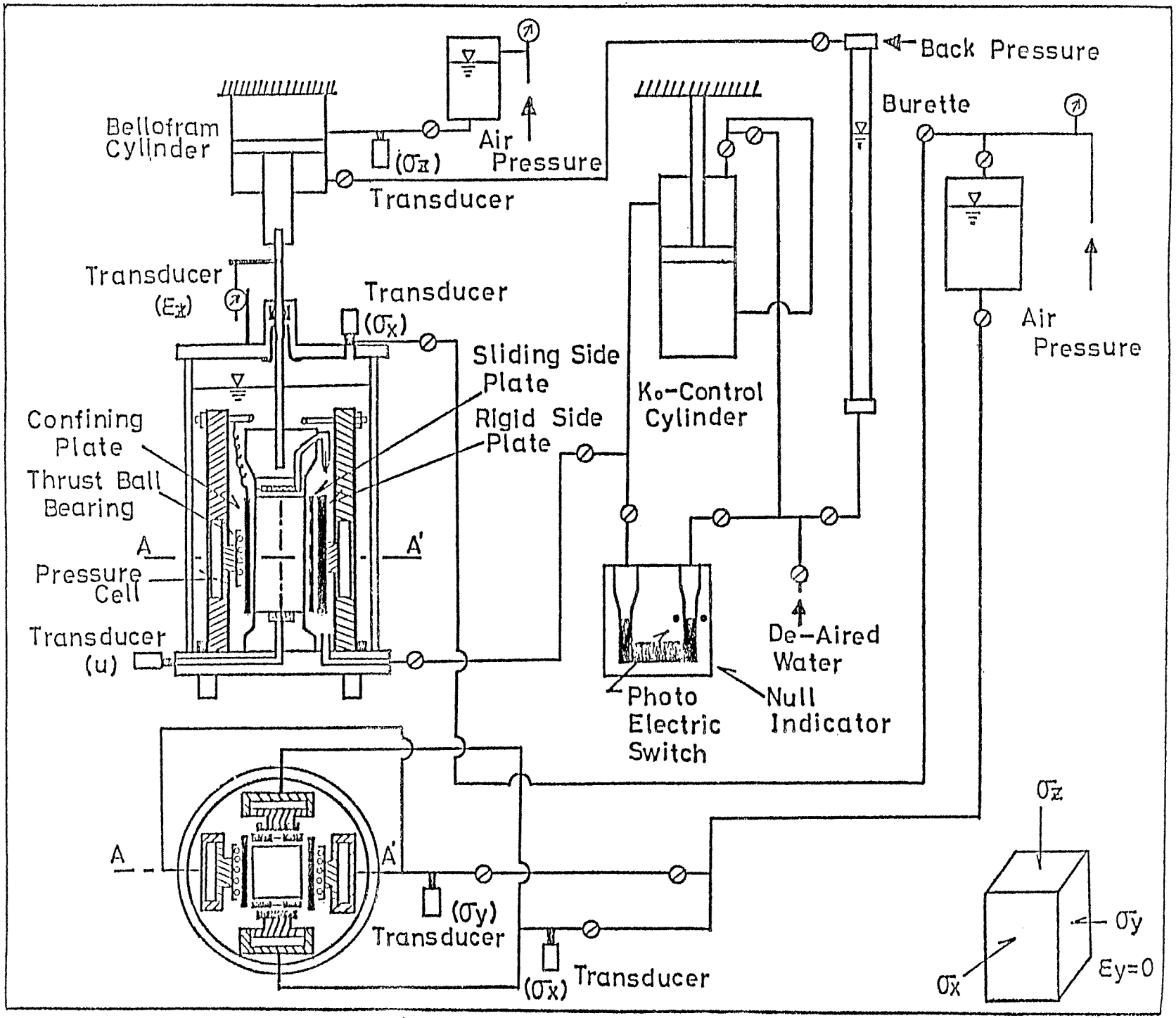

Fig.2-6 Schematic diagram of plane strain test apparatus

Construction of base and top of the triaxial cell was almost the same as that of conventional one. Lubrication by teflon sheet with silicone grease was applied to top and bottom of the specimen.

b) Automatic K_o control system; Automatic K_o control system was connected to the triaxial cell in order to simulate the consolidation condition in situ.

c) $\varepsilon_2 = 0$ control system; Two sets of pressure cells can be fixed with triaxial cell base. In plane strain compression test, only one set of pressure cells in y direction was used. Specially designed bellofram cylinder installed in the pressure cell was filled with de-aired water and at the end of bellofram piston, thrust ball bearing was fitted. In K_o consolidation stage, confining plate which was suspended by spring was pushed against specimen by the bellofram piston with a small water pressure (about 5 kPa) to insure contact between specimen and confining plate before starting shear test. During shear, water supplying route to pressure cell was closed and internal pressure developed during shear was measured by pressure transducer. In plane strain extension test, one more set of pressure cells was attached in x direction, construction of which was almost the same as that of y direction except that rigid side plate was attached at the end of bellofram piston. Sliding side plate as shown in Fig.2-7 which was designed so as to move itself freely in vertical direction as the specimen extended, was inserted between specimen and rigid side plate. Teflon sheets

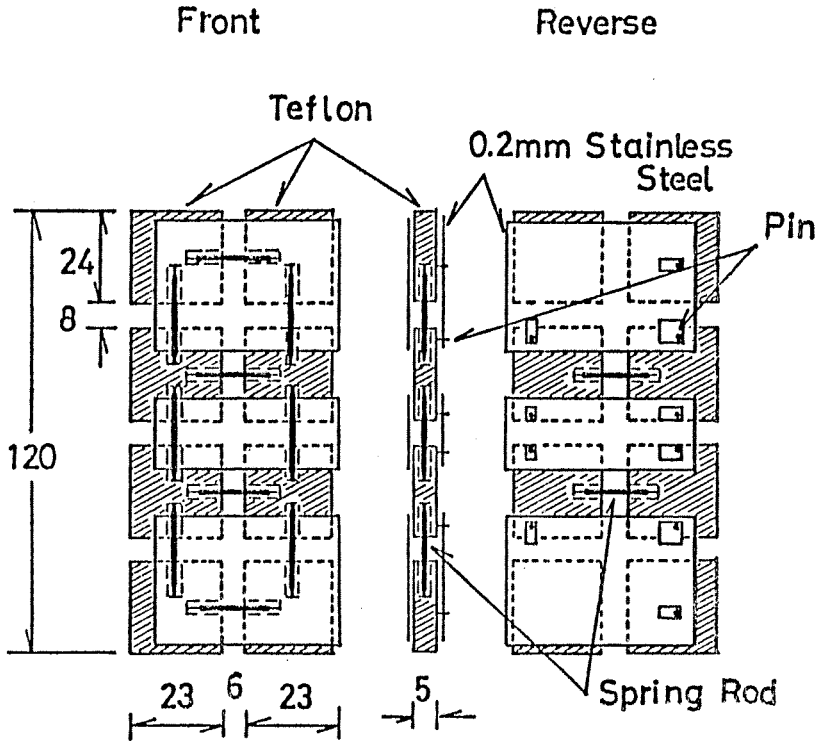

Fig.2-7 Construction of sliding side plate

with silicone grease were inserted between specimen and confining plate, and if needed, specimen and sliding side plate to minimize the friction between them.

2.2 Preparation of Sample

Index properties of clay samples used in this study are listed in Table 2-2. These soils were sampled at the sites of river improvement near Sapporo, and were thoroughly mixed with distilled water, sieved by a 420μm size sieve and stored in the state of slurry. Before making test specimen, the slurry were stirred again in a soil mixer for about an hour and then transfered under a vacuum to a preconsolidation cell shown in Fig. 2-8, the diameter and the height of which are 165mm and 350mm, respectively. Then the slurry was initially consolidated one-dimensionally under an axial stress of 78kPa for more than 4 days. Specimens, 50x50mm sided and 120mm high for triaxial test were trimmed from this preconsolidated sample. Trimming of the prismatic specimens was performed as in the following manner. After completion of preconsolidation, block sample within the preconsolidation cell is extruded carefully through the trimming wires attached to the end of preconsolidation cell. Prismatic specimen of 50x120mm sided and about 70mm high is thus made. Then, the final dimension 50x50x120mm is formed by using miter box. The situation of trimming of prismatic specimen is shown in Fig. 2-9.

The specimens for triaxial compression and extension tests were then further consolidated isotropically or anisotropically in the triaxial cell and then sheared under undrained condition, while specimens for plane strain tests were further consolidated

Sample number	Liquid limit	Plasticity index (%)	Specific gravity	Clay fraction ($< 2\mu m$) %
1	52	21	2.70	21
2	51	21	2.72	19
3	72	32	2.69	26
4	86	49	2.66	70

Table 2-2 Index properties of samples

(a) preconsolidation cell

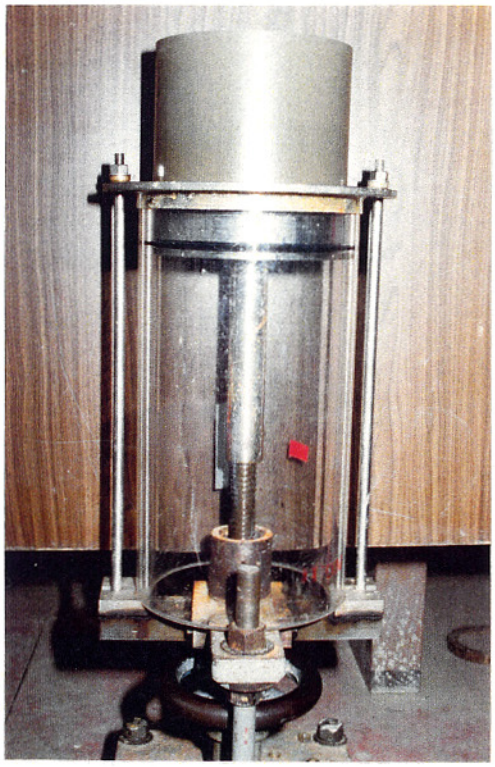

(b) extruded sample for making triaxial test specimen

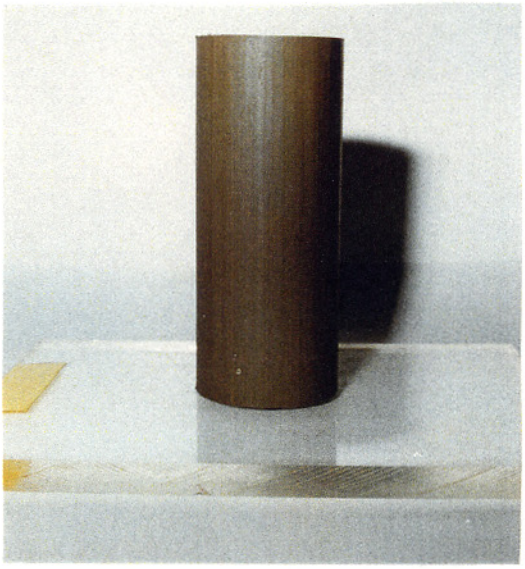

(c) triaxial test specimen

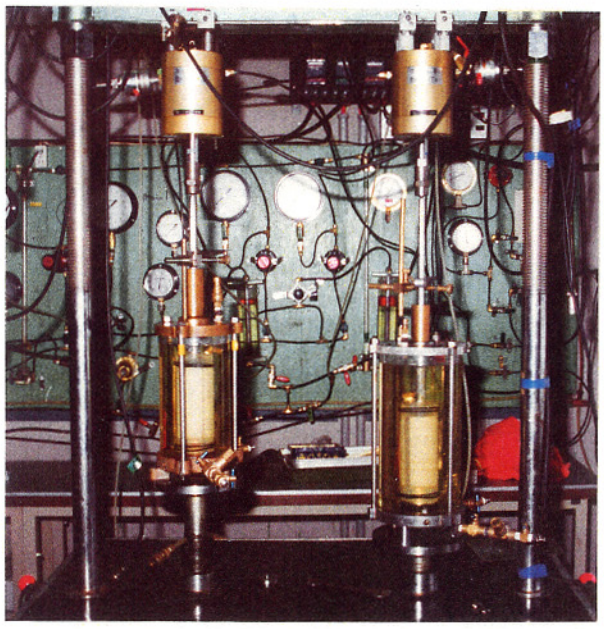

(d) conventional triaxial test apparatus

Fig.2-8 Preconsolidation cell and specimen and apparatus for axi-symmetrical triaxial test

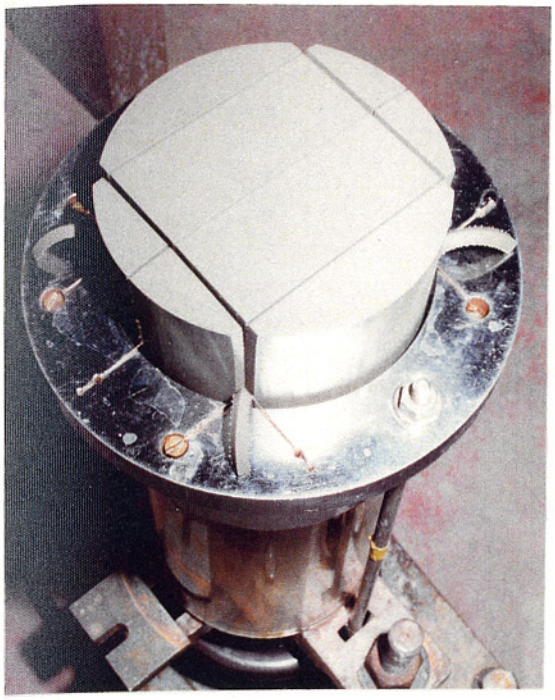

(a) extruded specimens for plane strain test

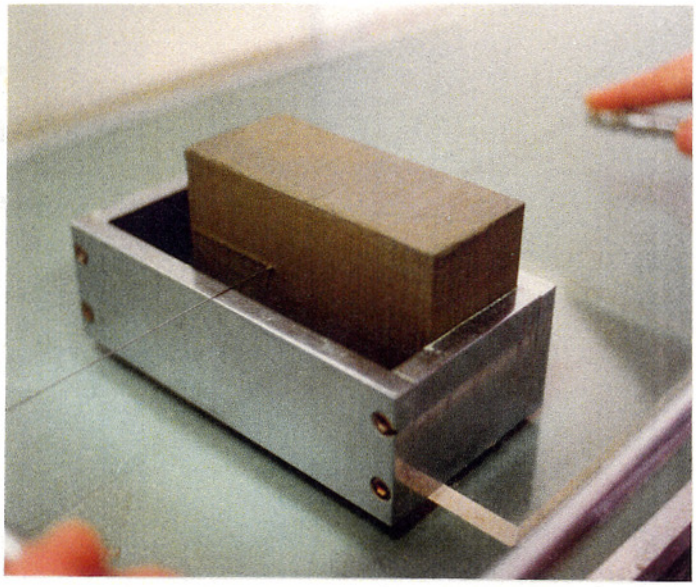

(b) trimming of prismatic specimen for plane strain test

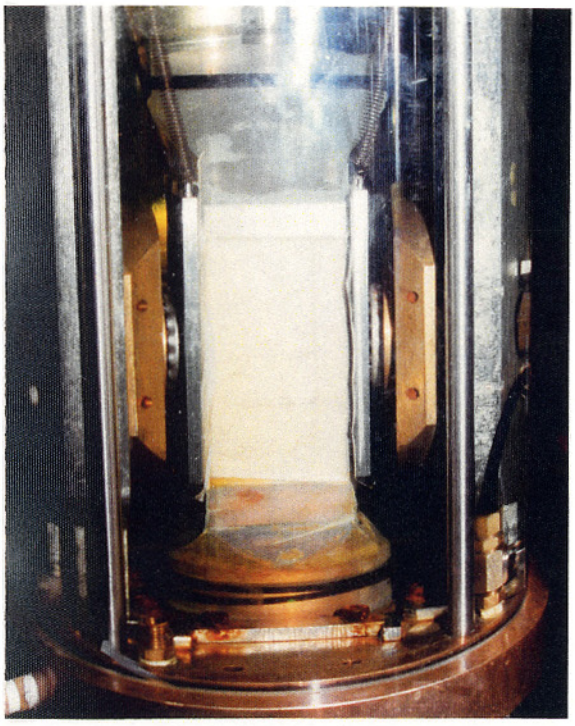

(c) specimen mounted on plane strain test apparatus

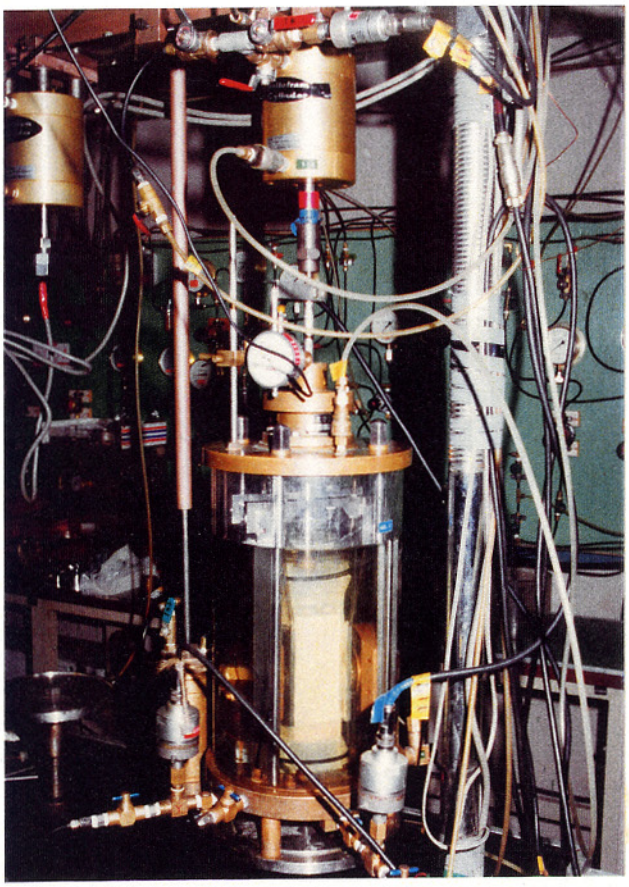

(d) plane strain test apparatus

Fig.2-9 Situation of making prismatic specimen and specimen mounted on plane strain test apparatus

under K_o condition in the plane strain apparatus and then sheared under undrained plane strain condition.

Samples No.1,2 and 3 were mainly used for the study on the prediction of undrained shear strength of overconsolidated clay in axi-symmetrical triaxial compression condition (Chapter Ⅵ).

Sample No.4 was mainly used for the study on the prediction of stress-strain behaviour of isotropically and K_o consolidated clay and on the stress-strain behaviour of clay under plane strain condition (Chapter Ⅲ, Ⅳ and Ⅴ).

2.3 Testing Method and Test Case

Four series of consolidated undrained triaxial and plane strain test with pore water pressure measurement were performed under following conditions:

(I) Isotropically consolidated undrained compression and extension test series (Fig.2-10);

a) NIC Test; Specimens are consolidated isotropically and then sheared under undrained compression by increasing axial stress while lateral stress is maintained constant.

b) NIE Test; After isotropic consolidation, specimens are sheared under undrained extension by decreasing axial stress while lateral stress is maintained constant.

c) NIEL Test; Same as NIE test but with axial stress constant and lateral stress increased.

d) OIC Test; Specimens are first consolidated under all-round pressure, allowed to swell under reduced isotropic pressure and finally subjected to undrained compression by increasing axial stress while lateral stress is maintained constant.

e) OIE Test; After isotropic consolidation and swelling, specimens are sheared under undrained extension by decreasing axial stress while lateral stress is maintained constant.

(II) Anisotropically consolidated undrained compression and extension test series (i) (Fig.2-11);

a) NK_oC Test; Before undrained compression by increasing axial stress and keeping lateral stress constant, specimens are

(I) Isotropically Consolidated and Rebounded Undrained Triaxial Compression and Extension Test Series

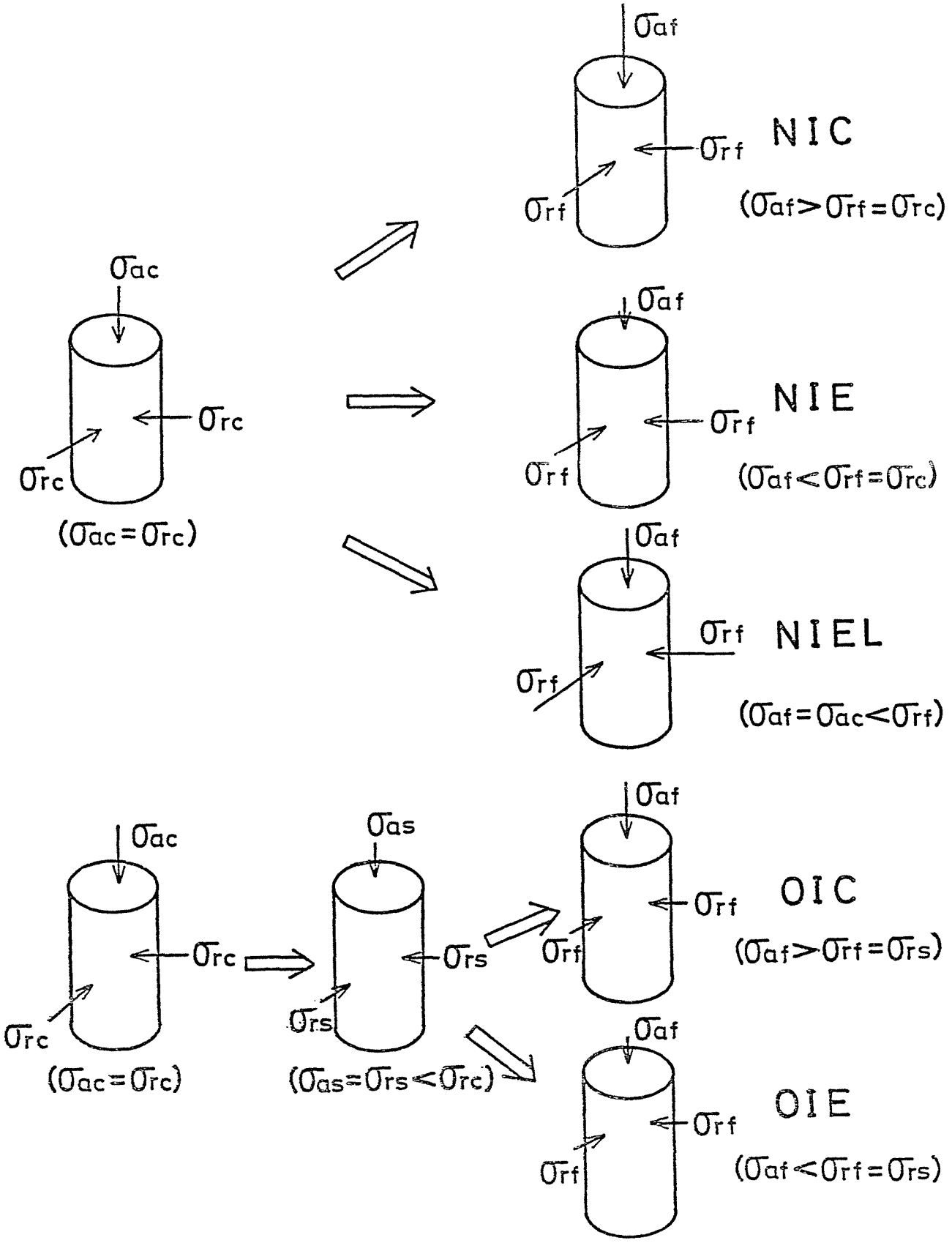

Fig.2-10 Isotropically consolidated undrained tests

(II) Anisotoropically Consolidated and Rebounded Undrained Triaxial Compression and Extension Test Series(i)

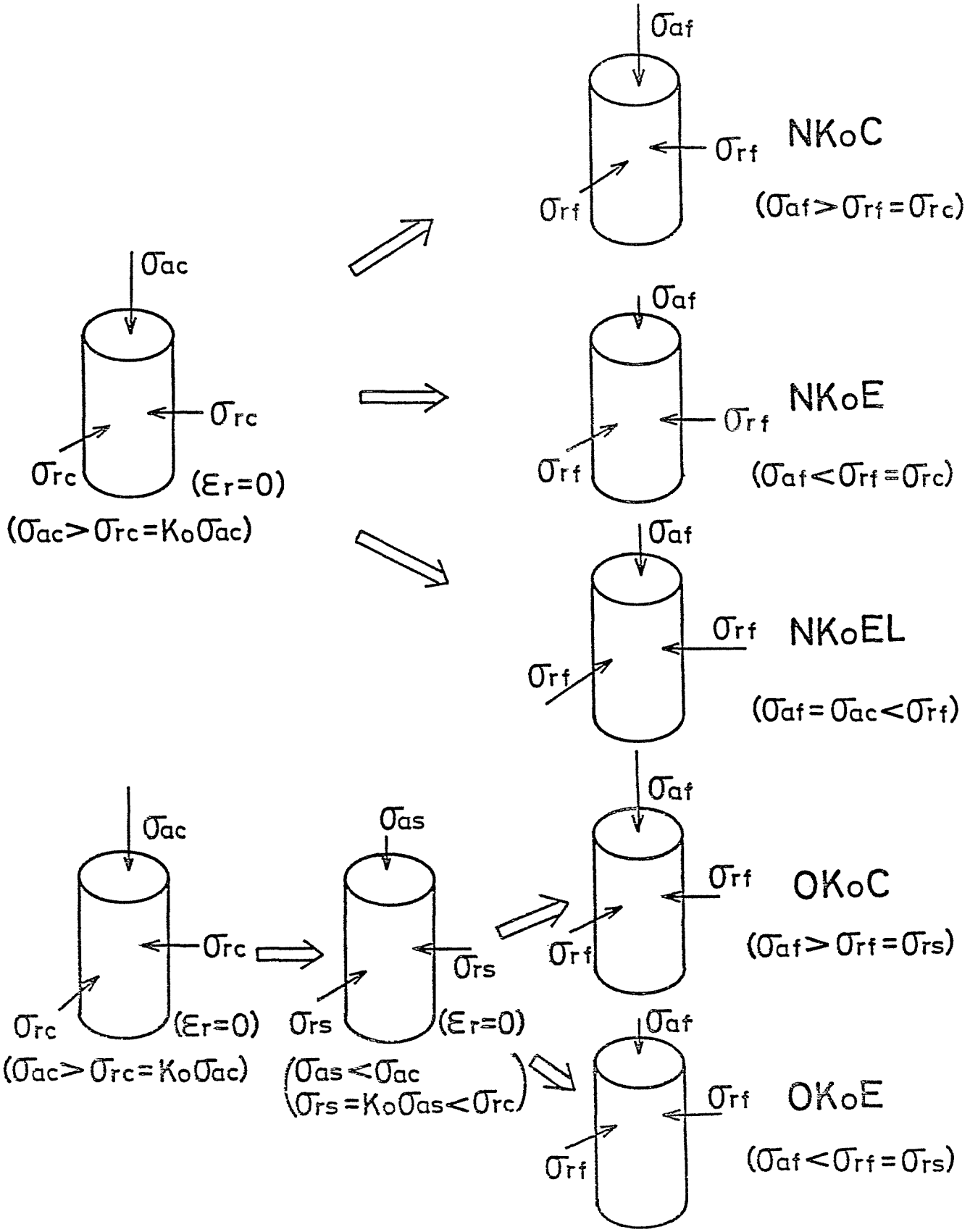

Fig.2-11 Anisotropically consolidated undrained tests (i)

consolidated under K_o condition, keeping the radial strain to be zero.

b) NK_oE Test; After K_o consolidation, specimens are sheared by decreasing axial stress while lateral stress is maintained constant.

c) NK_oEL Test; Same as NK_oE test but with axial stress constant and lateral stress increased.

d) OK_oC Test; Before undrained compression by increasing axial stress and keeping lateral stress constant, the consolidation and following swelling are carried out under K_o condition.

e) OK_oE Test; After K_o consolidation and swelling, specimens are sheared under undrained extension by decreasing axial stress while lateral stress is maintained constant.

(Ⅲ) Anisotropically consolidated undrained compression and extension test series (ⅱ) (Fig.2-12);

a) $N\overline{K_o}C$ Test; Before undrained compression, specimens are consolidated under K_o condition, keeping the axial strain to be zero. Symbol $\overline{K_o}$ denotes the condition of zero axial strain.

b) $N\overline{K_o}E$ Test; After $\overline{K_o}$ consolidation, specimens are sheared by decreasing axial stress while lateral stress is maintained constant.

c) $O\overline{K_o}C$ Test; Before undrained compression by increasing axial stress and keeping lateral stress constant, the consolidation and following swelling are carried out under $\overline{K_o}$ condition.

d) $O\overline{K_o}E$ Test; After $\overline{K_o}$ consolidation and swelling, specimens

(III) Anisotropically Consolidated and Rebounded Undrained Triaxial Compression and Extension Test Series (ii)

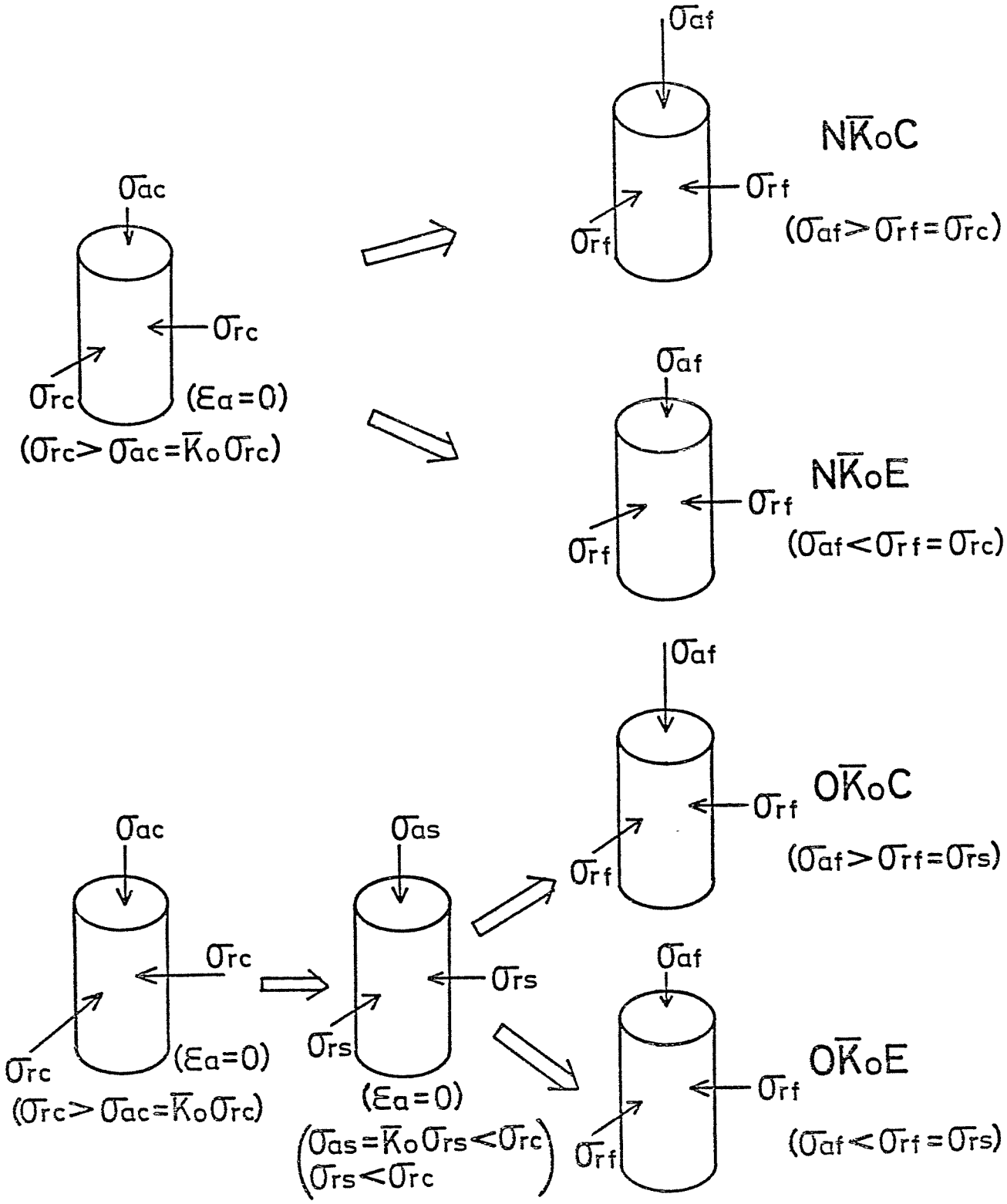

Fig. 2-12 Anisotropically consolidated undrained tests (ii)

are sheared under undrained extension by decreasing axial stress while lateral stress is maintained constant.

(Ⅳ) Plane strain compression and extension test series (Fig. 2-13);

a) NCP Test; Specimens are consolidated under K_o condition and then sheared under plane strain condition by increasing axial stress σ_z while one of the two lateral stresses σ_x is maintained constant.

b) NEP Test; After K_o consolidation, specimens are sheared under plane strain condition by decreasing σ_z while σ_x is maintained constant.

c) OCP Test; Before undrained plane strain compression by increasing σ_z and keeping σ_x constant, the consolidation and following swelling are carried out under K_o condition.

d) OEP Test; After K_o consolidation and swelling, specimens are sheared under plane strain condition by decreasing σ_z while σ_x is maintained constant.

Test series with isotropic and $\overline{K_o}$ consolidation and swelling were carried out with conventional triaxial apparatus. In test series with K_o consolidation and swelling, the automatic K_o control system mentioned previously was connected to the conventional triaxial apparatus just prior to K_o consolidation.

For the shear stage of NIEL and NK_oEL test, the apparatus shown schematically in Fig. 2-5 was used to perform strain controlled test by increasing lateral stress. Since variation of both cell

(Ⅳ)Anisotropically Consolidated and Rebounded Undrained Prane Strain Compression and Extension Test Series

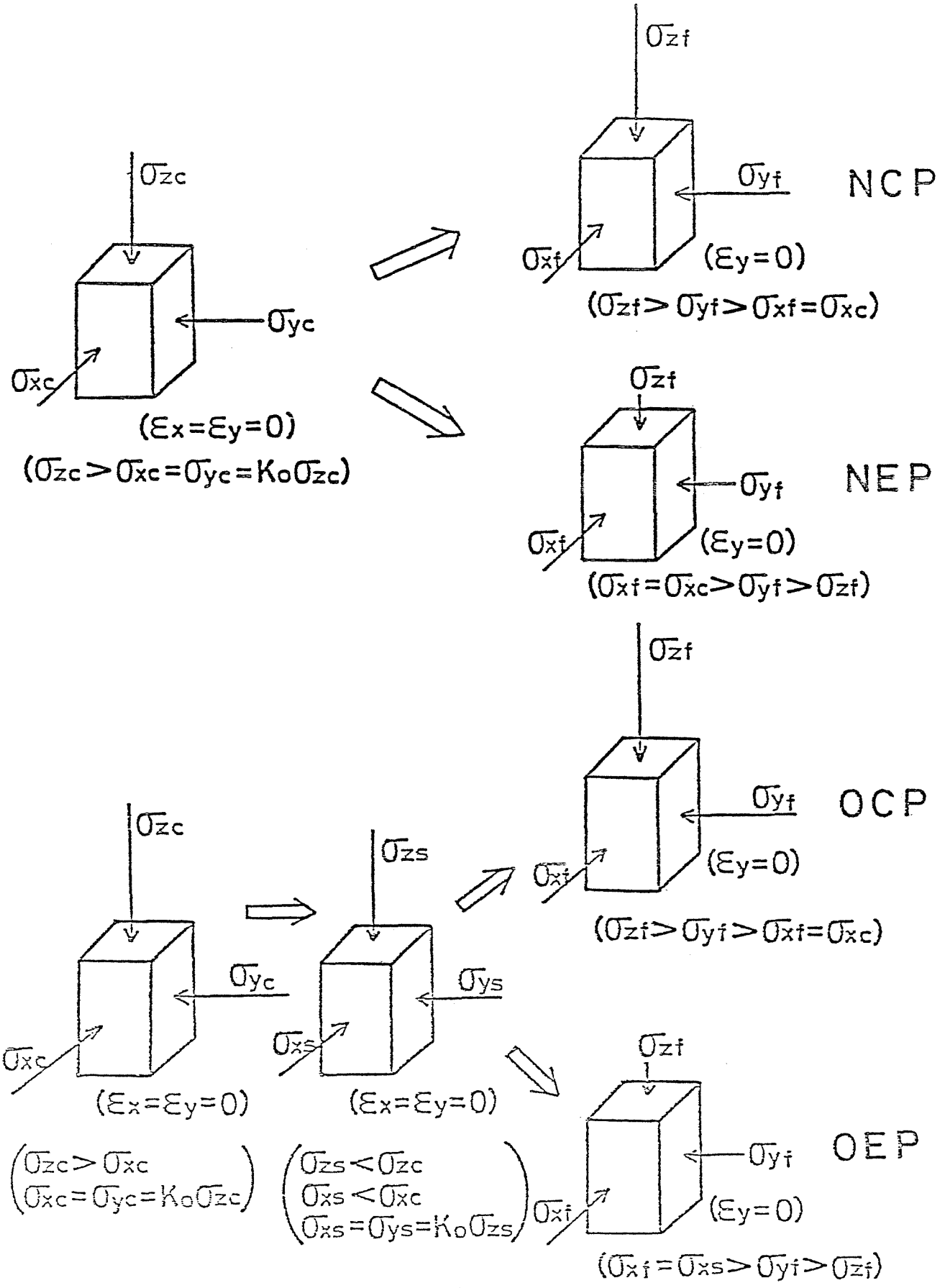

Fig.2-13 Undrained plane strain tests

pressure and sectional area of the specimen in NIEL and NK_oEl tests changes the value of axial stress, air pressure in the upper room of the bellofram cylinder was manually controlled to cancel the axial stress change in order to maintain the axial stress constant.

Plane strain compression and extension tests were carried out with the apparatus shown previously in Fig. 2-6.

In all type of test, specimen is mounted on the cell base under water in order to avoid air entraining, and cell pressure of 49 kPa is applied for about an hour to squeeze out the excessive water between specimen and membrane,entrained possibly during mounting.

During consolidation stage of all the tests involved, all-round pressure was increased in several steps, and so the consolidation took 3 to 6 days in isotropic condition and 6 to 9 days in K_o condition depending on the magnitude of the final pressure. Consolidation duration after reaching the final cell pressure was specified to be 24 hours in both K_o and isotropic conditions.

Cell pressure in isotropic swelling was decreased to final pressure in one step, while, in K_o swelling, it was decreased in 3 to 4 steps. However, the time allowed for swelling was 24 hr. irrespective of steps in cell pressure decrease. Initial back pressure of 98 kPa was applied to all specimens.

In all the tests other than NEP test, specimens were sheared

in undrained condition just after completion of consolidation or swelling. In NEP test, at the start of final stage of consolidation, the all-round pressure was reduced to 40% of its existing value, keeping σ_z, σ_x and σ_y values as they were, by increasing the pressure in the bellofram cylinder in z direction and those in the pressure cells in x and y directions, respectively, in order that σ_x and σ_y may vary independently during shear. Then, specimens were sheared by decreasing σ_z and keeping σ_x constant.

The rate of axial strain in undrained shear was 0.05%/min. for all tests, and pore water pressure was measured at the bottom of the specimen.

As there occurs the interchange of principal stress directions in these test series, following notations were used.

In all the test series other than plane strain test, axial and lateral stresses are represented by σ_a and σ_r, respectively. Therefore, axial stress σ_a at failure is major principal stress in compression tests, while it is equal to minor principal stress in extension tests.

In the plane strain test series, fixed coordinates x, y and z were used and z and y direction are coincident with the vertical and $\varepsilon_y = 0$ direction, respectively. Stresses σ_x, σ_y and σ_z in NCP test imply minor, intermediate and major principal stresses, respectively, whereas in NEP test, immediately after interchange of principal stress directions, they are coincident with major, intermediate and minor principal stresses, respectively.

CHAPTER III STRESS-STRAIN-STRENGTH BEHAVIOUR OF ISOTROPICALLY CONSOLIDATED CLAY

3.1 Introduction

Recently, finite element method has been frequently used for the analysis of the stress-strain-strength behaviour of natural stratum or earth structure (e.g. Wroth,1977). In this case, as the stress-strain characteristics of a particular soil is an input of computer analysis, the input data should be as universal as possible to follow up the various states and processes of stress-strain change of the soil in situ.

It should be noted that the output data of stress-strain behaviour of soil stratum or earth structure obtained by putting an equation representing limited experimental condition into computer analysis should not be gobbled up indiscriminately. It is essential to develop a constitutive equation which is able to fully describe the stress-strain-time behaviour of soil, because soil is a material which depends strongly on the stress and time history. In order to extend the applicability of a constitutive equation, it is convenient to represent the complicated properties by some parameters, as less as possible in number, and at the same time, it is necessary to rely only on relatively simple and reliable testing method to obtain these parameters.

As mentioned previously, stress condition during consolidation of earth structure as well as natural soil stratum are anisotropic, and moreover, soil element is, for the most part, consolidated under the condition of no lateral strain, i.e. K_0 condition. As the stress-strain-strength properties of soil is greatly influenced by the stress history during consolidation, it is necessary to examine the stress-strain behaviour of the specimen consolidated under the condition which represent the in situ consolidation condition in order to make accurate prediction of the in situ stress-strain behaviour.

As it is possible to conduct K_0 consolidation by attaching a simple control system developed by the present author, K_0 consolidation will become a routine work in the near future. But, the actual situation of the testing of strength properties of cohesive soil conducted by consulting engineer in Japan is as follows. In many cases of stability analysis, unconfined compression strength is used and consolidated undrained type triaxial compression test is performed for only a special case, and moreover, is seldom performed the triaxial test with measurement of pore water pressure. Taking the circumstances mentioned above into account, it will be advisable to await to come into wide use of conventional triaxial test. In this paper, the method of predicting in situ undrained stress-strain behaviour of cohesive soil by using the parameters obtained from isotropically consolidated undrained triaxial tests.

In order to estimate the stress-strain behaviour of clay imposed by external loads by using the parameters obtained from laboratory tests, it is essential to establish a constitutive equation. There are two methods of approach to do this.

1) The first approach is to search for the establishment of the universal constitutive equation by analyzing and sythesizing macroscopically stress-strain behaviour under the various conditions, and not to come into microscopic internal mechanism of soil. This approach is so to speak phenomenological method, and already systematized theory, such as elastoplasticity, visco-elasticity etc. is widely used, and moreover, well established experimental facts, e.g. linearity of virgin compression line, can be included into constitutive equation. Typical example of research work belonging to this category is original Cam-clay theory by Roscoe et al.(1963).

2) The second method is to intend the derivation of a macroscopic constitutive equation based on the microscopical analysis of soil behaviour. Although, there has not yet been the definite method of analysis, Rowe's stress-dilatancy theory (Rowe, 1962) of sand is famous as an early work of constitutive equation of this type of approach.

Recently, a large number of research works have been done, intending to establish an universal constitutive equation of soil, most of which are influenced more or less by the studies mentioned above.

The present author assigns the goal to predict the stress-strain behaviour of soil which is consolidated under K_o condition and imposed by various in situ stress and strain conditions, by using a simple calculation procedure based on the parameters obtainable by simple and reliable method of testing.

In this chapter, less excellent accuracy of Roscoe's original theory and subsequent theories proposed after him will be shown by predicting the test results of present study, and the problems in their theories will be pointed out, and further will be presented the modification of existing theory and comparison of observed and predicted stress-strain behaviour.

3.2 Original Cam-clay Theory by Roscoe et al.

3.2.1 Introduction

The present author intend to modify the original Cam-clay theory by Roscoe et al. and establish a modified method of predicting stress-strain behaviour of clay under in situ stress condition by using experimental parameters obtained from conventional isotropically consolidated undrained triaxial test. As almost all assumptions used in the modified method are similar to those used by Roscoe et al., original theory by Roscoe et al. will, first of all, be introduced in this chapter.

Roscoe et al. considered that the basic parameters used in stress-strain prediction are those obtained from standard triaxial compression test, and they selected stress parameters p and q which are represented as follows by the observed values of two effective principal stresses σ_1' and σ_3'.

$$q = \sigma_1' - \sigma_3' \tag{3-1}$$

$$p = \frac{1}{3}(\sigma_1' + 2\sigma_3') \tag{3-2}$$

From the experimental results, it was found that the state path during triaxial test for saturated normally consolidated clay constitutes an unique curved surface, which was called "state boundary surface" in p, q and e space, where e is void ratio.

In Fig.3-1, ACEF is a part of state boundary surface and AC is isotropic normal consolidation line. Wherein, the linearity of e versus $\ln p$ curve is assumed as shown by the following equation,

$$e = e_a - \lambda \ln p \ , \tag{3-3}$$

where e_a is void ratio at $p = 1$. Roscoe et al. also assumed that the soil element subjected to shear deformation finally reaches ultimate condition, "critical state", where the element of soil continues to deform without further change of p , q and e . This critical state is represented by EF in Fig.3-1. Projection of this curve on the p , q plane is represented by the following equation

$$q = \overline{M} \cdot p \tag{3-4a}$$

and projection onto $e - \ln p$ plane is

$$e = \Gamma - \lambda \ln p \ , \tag{3-4b}$$

where Γ is critical void ratio at $p = 1$ and λ is a material constant, the same as used in Eq.(3-3).

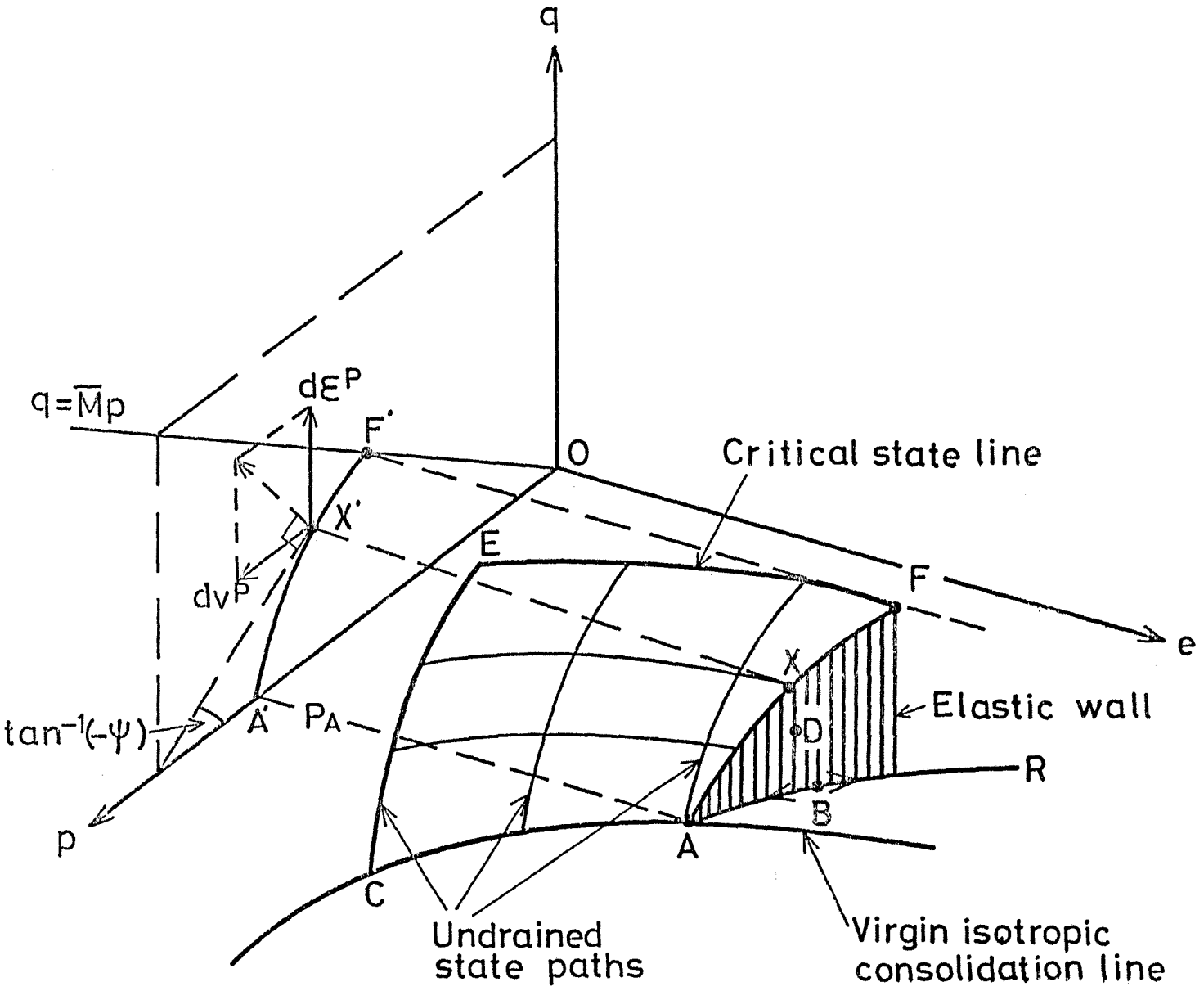

Fig.3-1 State boundary surface (after Roscoe and Burland,1968)

3.2.2 Definition of strain and concept of yield loci

Roscoe et al. defined the volumetric and deviatoric strain as follows

$$\delta v = \frac{\delta V}{V} = -\frac{\delta e}{1+e} = \delta\varepsilon_1 + \delta\varepsilon_2 + \delta\varepsilon_3 = \delta\varepsilon_1 + 2\delta\varepsilon_3 \qquad (3\text{-}5)$$

$$\delta\varepsilon = \delta\varepsilon_1 - \frac{1}{3}\delta v = \frac{2}{3}(\delta\varepsilon_1 - \delta\varepsilon_3) \qquad (3\text{-}6)$$

where ε_1 , ε_2 and ε_3 are principal natural strains.

The reason for the choice of p , q , δv and $\delta\varepsilon$ as done in Eqs. (3-1), (3-2), (3-5) and (3-6) is that the sum of the product of the parameters should be equal to the sum of the product of the principal strains and stresses (Schofield and Wroth, 1968), i.e.,

$$p\,\delta v = \left(\frac{\sigma_1' + 2\sigma_3'}{3}\right)\cdot(\delta\varepsilon_1 + 2\delta\varepsilon_3) = \frac{1}{3}(\sigma_1'\delta\varepsilon_1 + 4\sigma_3'\delta\varepsilon_3 + 2\sigma_3'\delta\varepsilon_1 + 2\sigma_1'\delta\varepsilon_3)$$

$$q\,\delta\varepsilon = \frac{2}{3}(\sigma_1' - \sigma_3')(\delta\varepsilon_1 - \delta\varepsilon_3) = \frac{1}{3}(2\sigma_1'\delta\varepsilon_1 + 2\sigma_3'\delta\varepsilon_3 - 2\sigma_3'\delta\varepsilon_1 - 2\sigma_1'\delta\varepsilon_3)$$

$$\therefore \quad p\,\delta v + q\,\delta\varepsilon = \sigma_1'\delta\varepsilon_1 + 2\sigma_3'\delta\varepsilon_3$$

Roscoe et al. defined yield loci in (e,p,q) space as follows. Now, a normally consolidated clay which reached equilibrium state (point A in Fig. 3-1) under isotropic stress p_A is considered. If the isotropic stress p is first decreased and then the stress p larger than p_A is reloaded, the stress path will become A → B → A → C and point A is to be yield point. If the curve which include A, B in elastic region is assumed to be a straight line in e-ln p plane, then the following equation is obtained, assuming κ as a material constant.

$$\delta v^r = \frac{\kappa}{1+e} \frac{\delta p}{p} \tag{3-7}$$

As it was assumed that plastic deformation occurs only when the stress state is on the state boundary surface, shear strains exerted by the change of q which is not large enough to reach the state boundary surface are entirely recoverable, i.e. the state of the soil will be confined to an 'elastic' surface in (e,p,q) space which cuts the $q = 0$ plane along the swelling curve ABR. Roscoe et al. assumed that the elastic limit curve AF lies directly above the swelling curve ABR. They also assumed that there is never any recoverable energy associated with shear deformation, i.e. $\delta\varepsilon^r = 0$ and at all times $\delta\varepsilon = \delta\varepsilon^p$. The projection of AF on the p , q plane is yield locus.

3.2.3 Normality condition

When stress increment (δp , δq) is applied on a soil element whose stress state is represented by a point X' (p,q) which is on the current yield locus A'F' and the vector of stress increment orientates to the outside of OA'F', the deformation includes plastic components. If the soil element is at "stable state" by Drucker's definition (1959), strain increment vector, the components of which are represented by $\delta\varepsilon^p$, δv^p , must be normal to A'F' at point X'. Therefore,

$$\frac{\delta\varepsilon^p}{\delta v^p} = -\left(\frac{dp}{dq}\right)_{A'F'} = \frac{1}{\psi} \qquad (3\text{-}8)$$

where $(dq/dp)_{A'F'} = -\psi$ is the slope of the current yield locus A'F' at the point X'.

The condition represented by Eq. (3-8) is called normality condition. Most research workers concerning with the study for predicting stress-strain behaviour of soils have conveniently been using this condition in order to obtain shear strain increment. Based on the stress probe tests on normally consolidated clay, Lewin and Burland (1970) suggested that the normality condition of plasticity theory provides a reasonable basis for the prediction of shear strain. On the other hand, Lade (1976) performed a series of consolidated undrained test with three different principal stresses and found that the normality condition is satisfied or

very nearly satisfied in the octahedral plane, but not in the triaxial plane. Therefore, he concluded that the normality condition is not fulfilled in general for normally consolidated clay.

According to the facts mentioned above, there is yet a room for studying the validity of the application of normality condition to soils.

Those mentioned in preceding sections 3.2.1 through 3.2.3 are the basic assumptions in Cam-clay theory. Stress-strain relationship will be expressed using these assumptions in the remainder part of this chapter.

3.2.4 Expression of yield locus by ψ

In Fig. 3-2 slope $\acute{A}_1\acute{F}_1$ of yield locus at point X' is represented by Eq. (3-8). And, $dq = \bar{\eta}\,dp + p\,d\bar{\eta}$ as $q = \bar{\eta}p$. Combining above equation and Eq. (3-8), following equation is obtained.

$$\frac{dp}{p} - \frac{d\bar{\eta}}{\psi + \bar{\eta}} = 0 \qquad (3\text{-}9)$$

Integration of Eq. (3-9), gives the following equation.

$$\ln p - \int_0^{\bar{\eta}} \frac{d\bar{\eta}}{\psi + \bar{\eta}} = \ln p_0 \qquad (3\text{-}10)$$

where p is the effective principal mean stress at the intersection point of normal consolidation line with current elastic limit line. Eq. (3-10) represents a yield locus.

If the stress increment is applied upon the clay element whose state is represented by the point X on the state boundary surface, clay element yields in such a way that the total strain increments δv and $\delta\varepsilon$ contain plastic components δv^p and $\delta\varepsilon^p$, and then the clay element will come to equilibrium at some other point Y on the state boundary surface (Fig. 3-2).

The elastic limit curve through Y will now correspond to a new yield locus $\acute{A}_2\acute{F}_2$ still obeying Eq. (3-10) but with p_0 now having a value $p_0 + \delta p_0$. In other words, Eq. (3-10) can be

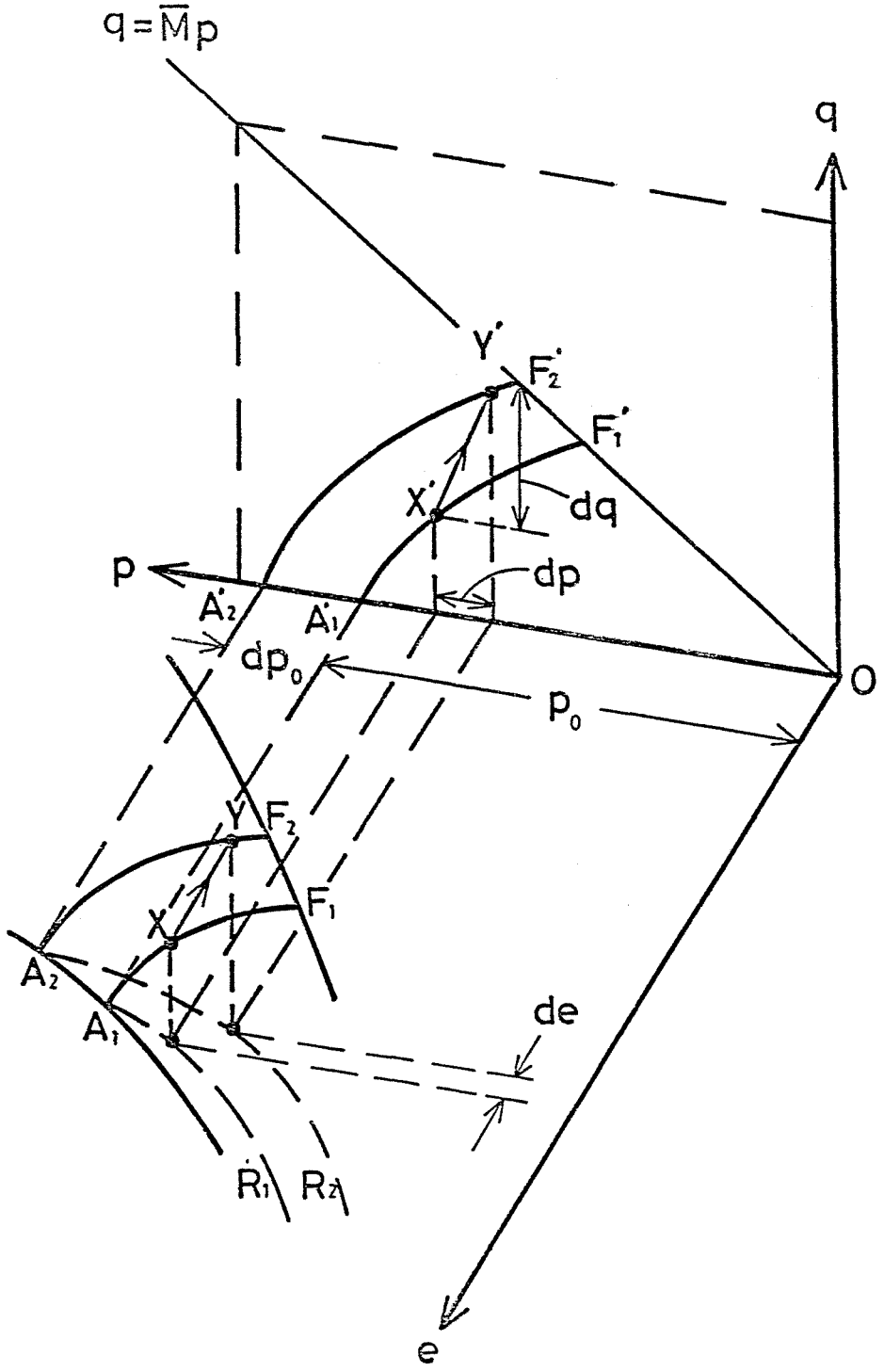

Fig.3-2 Successive yield loci (after Roscoe and Burland,1968)

equation for all yield loci corresponding to all elastic limit curves on the state boundary surface, provided that p_o is treated as a variable which has a fixed value for individual yield locus. Expressed in differential form, all yield loci are therefore represented by

$$\frac{dp_o}{p_o} - \frac{dp}{p} - \frac{d\bar{\eta}}{\varphi+\bar{\eta}} = 0 \qquad (3\text{-}11)$$

where dp_o is a measure of the distance between the elastic wall $A_1F_1R_1$ associated with point X and $A_2F_2R_2$ associated with point Y.

Considering the isotropic consolidation, the over all void ratio change from point A_1 to A_2 is

$$\delta e = -\lambda (dp_o/p_o)$$

The elastic component of this change has already been shown to be

$$\delta e^r = -\kappa (dp_o/p_o)$$

Consequently, the plastic component of the void ratio change will be

$$\delta e^p = \delta e - \delta e^r = -(\lambda-\kappa)\delta p_o/p_o \qquad (3\text{-}12)$$

Combining Eq.(3-11)and(3-12), following equation is obtained.

$$\delta e^p = -(\lambda-\kappa)\left(\frac{\delta p}{p} + \frac{\delta \bar{\eta}}{\psi+\bar{\eta}}\right) \tag{3-13}$$

Therefore,

$$\delta v^p = -\frac{\delta e^p}{1+e} = \frac{\lambda-\kappa}{1+e}\left(\frac{\delta p}{p} + \frac{\delta \bar{\eta}}{\psi+\bar{\eta}}\right) \tag{3-14}$$

As the elastic component of the volumetric strain for the state of sample to change from X to Y is

$$\delta v^r = \frac{\kappa}{1+e}\frac{\delta p}{p}$$

the total volumetric strain will be

$$\delta v = \delta v^p + \delta v^r = \frac{\lambda}{1+e}\left[\frac{\delta p}{p} + (1-\kappa/\lambda)\frac{d\bar{\eta}}{\psi+\bar{\eta}}\right] \tag{3-15}$$

Considering the definition of ψ and the assumption mentioned in section 3.2.2 that $\delta \varepsilon^r = 0$, Eq.(3-14) gives

$$\delta \varepsilon = \frac{1}{\psi}\frac{\lambda-\kappa}{1+e}\left(\frac{\delta p}{p} + \frac{\delta \bar{\eta}}{\psi+\bar{\eta}}\right) \tag{3-16}$$

Since $\delta v = -\delta e/(1+e)$, Eq.(3-15) becomes

$$-\frac{\delta e}{\lambda} = \frac{\delta p}{p} + (1-\kappa/\lambda)\frac{\delta \bar{\eta}}{\psi+\bar{\eta}} \tag{3-17}$$

Eq.(3-17) represents a short range of the state path between X and Y in Fig.(3-2), and since void ratio e is related to the equivalent pressure p_e, it may be written in the form

$$\frac{\delta p_e}{p_e} = \frac{\delta(e_a - e)}{\lambda} = \frac{\delta p}{p} + (1 - \kappa/\lambda)\frac{d\bar{\eta}}{\psi + \bar{\eta}} \qquad (3\text{-}18)$$

where the parameter p_e, which was proposed by Hvorslev(1936), represents the pressure corresponding to that void ratio on the virgin isotropic consolidation line.

Integrating Eq.(3-18), following equation representing state boundary surface is obtained.

$$\ln(p_e/p) = (1 - \kappa/\lambda)\int_0^{\bar{\eta}} \frac{d\bar{\eta}}{\psi + \bar{\eta}} - (1 - \kappa/\lambda) F(\bar{\eta}) \qquad (3\text{-}19)$$

3.2.5. Determination of ψ as a function of $\bar{\eta}$

Roscoe et al. derived a relationship between ψ and $\bar{\eta}$ from considerations of internal work. When an element of soil, initially in equilibrium under principal effective stress (σ_1', σ_2', σ_3'), is subjected to a stress increment ($\delta\sigma_1'$, $\delta\sigma_2'$, $\delta\sigma_3'$), it undergoes principal strain increments of ($\delta\varepsilon_1$, $\delta\varepsilon_2$, $\delta\varepsilon_3$). The total energy per unit volume transmitted to the soil skeleton across its boundaries is

$$\delta E' = \sigma_1'\delta\varepsilon_1 + \sigma_2'\delta\varepsilon_2 + \sigma_3'\delta\varepsilon_3 \qquad (3\text{-}20)$$

As total energy $\delta E'$ is the sum of recoverable energy δU and dissipated energy δW,

$$\left.\begin{aligned} \delta E' &= \delta U + \delta W \\ \delta U &= \sigma_1'\delta\varepsilon_1^r + \sigma_2'\delta\varepsilon_2^r + \sigma_3'\delta\varepsilon_3^r \\ \delta W &= \sigma_1'\delta\varepsilon_1^p + \sigma_2'\delta\varepsilon_2^p + \sigma_3'\delta\varepsilon_3^p \end{aligned}\right\} \qquad (3\text{-}21)$$

These equations are applicable to any homogeneous deformable continuum in which the principal axes of stress and strain-increment coincide.

Expressed in terms of the Cambridge stress and strain parameters for triaxial compression conditions, these equations become

$$\left.\begin{aligned} \delta E' &= p\delta v + q\delta\varepsilon \\ \delta U &= p\delta v^r + q\delta\varepsilon^r \\ \delta W &= p\delta v^p + q\delta\varepsilon^p \end{aligned}\right\} \qquad (3\text{-}22)$$

From the assumption by Roscoe et al. $\delta\varepsilon^r = 0$. Consequently since

$$\delta v^r = \frac{\kappa}{1+e} \cdot \frac{\delta p}{p}$$

it follows from Eq.(3-22) that

$$\delta v = \frac{\kappa}{1+e} \delta p \tag{3-23}$$

They also assumed that the dissipated energy δW per unit volume of the material, when undergoing deformation (δv, $\delta\varepsilon$) at any state (e,p,q) corresponding to a point on the state boundary surface, is $\bar{M} p \delta\varepsilon$.
Substituting $\delta W = \bar{M} p \delta\varepsilon$ and $\delta\varepsilon = \delta\varepsilon^p$ in Eq.(3-22), following equation is obtained.

$$p \delta v^p + q \delta\varepsilon = \bar{M} p \delta\varepsilon$$

Therefore, plastic strain increment ratio $\delta\varepsilon / \delta v^p$ is as follows.

$$\frac{1}{\psi} = \delta\varepsilon / \delta v^p = \frac{1}{\bar{M} - \bar{\eta}} \tag{3-24}$$

Substituting Eq.(3-24) into Eqs.(3-11), (3-17) and (3-19), following equations for δv, $\delta\varepsilon$, yield locus and state boundary surface as a function of p and $\bar{\eta}$ are obtained.

$$\delta v = \frac{1}{1+e}\left(\frac{\lambda-\kappa}{\bar{M}}d\bar{\eta}+\lambda\frac{\delta p}{p}\right) \tag{3-25}$$

$$\delta\varepsilon = \frac{\lambda-\kappa}{1+e}\left[\frac{p\delta\bar{\eta}+\bar{M}\delta p}{\bar{M}p(\bar{M}-\bar{\eta})}\right] \tag{3-26}$$

$$\bar{\eta} = \bar{M}\ln p_0/p \tag{3-27}$$

$$\bar{\eta} = \frac{\bar{M}}{1-(\kappa/\lambda)}\ln p_e/p \tag{3-28}$$

Since $dv = 0$ in undrained test, Eq.(3-25) gives

$$\delta\bar{\eta} = \frac{\bar{M}\lambda}{(\kappa-\lambda)}\cdot\frac{\delta p}{p}$$

Inserting above equation into Eq.(3-26), following equation is obtained

$$\delta\varepsilon = \frac{\kappa(\lambda-\kappa)}{\bar{M}\lambda(1+e)}\cdot\frac{d\bar{\eta}}{\bar{M}-\bar{\eta}}$$

Integration of above equation under the initial condition $\varepsilon = 0$ for $\bar{\eta} = 0$, gives

$$\varepsilon = \frac{\kappa(\lambda-\kappa)}{\bar{M}\lambda(1+e)}\ln\left|\frac{\bar{\eta}}{\bar{M}-\bar{\eta}}\right| \tag{3-29}$$

And it follows from Eq.(3-28) that

$$p = p_e \cdot \exp\left\{ \frac{\kappa - \lambda}{\lambda \bar{M}} \bar{\eta} \right\} \tag{3-30}$$

Thus, the stress path and stress ratio-strain relationship of isotropically consolidated clay during undrained test can be calculated by using Eqs.(3-29) and (3-30).

3.3 Modified Theory by Roscoe and Burland

As shown previously, the increment of work dissipated per unit bulk volume of an isotropic continuum during deformation δW can be written by using the Cambridge parameters p, q, δv and $\delta \varepsilon$ as follows.

$$\delta W = p \cdot \delta v^p + q \cdot \delta \varepsilon^p \tag{3-31}$$

Assuming that there exist dissipated energy under isotropic stress condition (q = 0), Eq.(3-31) gives

$$(\delta W)_{q=0} = p \cdot \delta v^p \tag{3-32}$$

At the critical state condition ($\eta = \bar{M}$ and $\delta v^p = 0$), Eq.(3-31) becomes

$$(\delta W)_{q=\bar{M}p} = p \cdot \bar{M} \cdot \delta \varepsilon^p \tag{3-33}$$

A generalization of these two particular conditions would be

$$\delta W = p \sqrt{(\delta v^p)^2 + (\bar{M} \delta \varepsilon^p)^2} \tag{3-34}$$

Burland(1965) adopted this equation for the value of dissipated energy instead of $\delta W = \bar{M} p \delta \varepsilon^p$ in original Cam-clay equation. Retaining the concept $\delta \varepsilon^r = 0$, the plastic strain increment

ratio is given as follows by combining Eq.(3-34) with Eq.(3-31).

$$1/4 = \delta\varepsilon^p/\delta v^p = \frac{2\bar{\eta}}{\bar{M}^2-\bar{\eta}^2} \qquad (3\text{-}35)$$

Burland noted that "It is important to note that Eq.(3-34) represents one of many possible generalizations of Eqs.(3-32) and (3-33). The ultimate choice between original Cam-clay and modified Cam-clay model, or other similar models, may well depend on mathematical expediency and must, in any case, await the results of further tests,particularly of the stress controlled type." By the way,Table 3-1 shows the examples of the expression of plastic strain increment ratio used by recent research workers including Roscoe et al. From this table, it can be seen that the models by Wong and Mitchell (1975), Pender(1978)and Cheney(1979) are the modification of original Cam-clay theory and that by Eekelen et al. (1978) is that of modified Cam-clay theory.

Substituting Eq. (3-35) into the Eqs. (3-11), (3-17) and (3-19), the following expressions may be obtained.

$$\delta v^p = \frac{\lambda-\kappa}{1+e}\left(\frac{2\bar{\eta}\,d\bar{\eta}}{\bar{M}^2+\bar{\eta}^2}+\frac{dp}{p}\right) \qquad (3\text{-}36)$$

$$\delta v = \frac{1}{1+e}\left[(\lambda-\kappa)\frac{2\bar{\eta}\,d\bar{\eta}}{\bar{M}^2+\bar{\eta}^2}+\lambda\frac{dp}{p}\right] \qquad (3\text{-}37)$$

Authors	$\delta\varepsilon^p/\delta v^p$
Roscoe et al. (1963)	$1/(\bar{M}-\bar{\eta})$
Roscoe & Burland (1968)	$2\eta/(\bar{M}^2-\bar{\eta}^2)$
Wong & Mitchell (1975)	$(1-C)/(b\bar{M}-\bar{\eta})$
Pender (1978)	$1/(P_0/P_{cs}-1)\{\bar{M}-(P/P_{cs})\bar{\eta}\}$
Eekelen & Potts (1978)	$2(\frac{\Lambda}{2\Lambda-1})\bar{\eta}/(\bar{M}^2-\bar{\eta}^2)$
Cheney (1979)	$(1-\alpha)/(\bar{M}-\bar{\eta})$

$\Lambda = 1 - \kappa/\lambda$

P_{cs} ; the value of P at the point on the critical state line

α, b, c : numerical constants

Table 3-1 Examples of the expression of plastic strain increment ratio

$$\delta\varepsilon = \delta\varepsilon^p = \frac{\lambda-\kappa}{1+e}\left(\frac{2\bar{\eta}}{\bar{M}^2-\bar{\eta}^2}\right)\left(\frac{2\bar{\eta}\,d\bar{\eta}}{\bar{M}^2+\bar{\eta}^2} + \frac{\delta p}{p}\right) \qquad (3\text{-}38)$$

And yield locus becomes from Eq.(3-12)

$$p/p_0 = \frac{\bar{M}^2}{\bar{M}^2+\bar{\eta}^2} \qquad (3\text{-}39)$$

while the state boundary surface is represented as follows.

$$p/p_e = \left(\frac{\bar{M}^2}{\bar{M}^2+\bar{\eta}^2}\right)^{1-\kappa/\lambda} \qquad (3\text{-}40)$$

Since $dv = 0$ in undrained test, Eq.(3-37) gives

$$-\delta p/p = (1-\kappa/\lambda)\left(\frac{2\bar{\eta}}{\bar{M}^2+\bar{\eta}^2}d\bar{\eta}\right)$$

Inserting above equation and integrating resulting equation under the condition $\varepsilon = 0$ at $\bar{\eta} = 0$, then, following equation is obtained.

$$\varepsilon = \frac{\kappa(\lambda-\kappa)}{\bar{M}\lambda(1+e)}\left[\ln\left|\frac{\bar{M}+\bar{\eta}}{\bar{M}-\bar{\eta}}\right| - 2\tan^{-1}\bar{\eta}/\bar{M}\right] \qquad (3\text{-}41)$$

3.4 Comparison of Observed and Predicted Stress-Strain Behaviour by Existing Theories

3.4.1 Introduction

The present author has long intended to find out a method to predict the stress-strain relationship of K_0 consolidated clay, using the parameters obtained from the conventional consolidated undrained (CU) triaxial test results. To do this, establishment of an appropriate stress-strain theory for predicting the isotropically consolidated undrained case has first been made, and then, in order to apply this theory to the K_0 consolidated clay, some modifications to the theory so as to fill up the discrepancy which comes from the stress and the structural anisotropy resulting from K_0 consolidation have been carried out.

Now, the validity of the existing theories is examined, using the present CU triaxial test results. The test data used for this purpose are from NIC-No.4 and the computed parameters are as follows.

$$M = 0.578 \qquad \lambda = 0.221 \qquad \kappa = 0.113 \qquad e_0 = 1.339 \ ,$$

where M is equal to η at critical state, λ and κ correspond to compression and swelling indices, respectively, and e_0 is void ratio after consolidation. The parameter η represents the ratio of octahedral shear stress τ to octahedral effective normal stress p, where τ and p are defined as follows.

$$\tau = \frac{1}{3}\sqrt{(\sigma_1-\sigma_2)^2+(\sigma_2-\sigma_3)^2+(\sigma_3-\sigma_1)^2} \qquad (3\text{-}42)$$

$$p = \sigma_m' = \frac{1}{3}(\sigma_1'+\sigma_2'+\sigma_3') \qquad (3\text{-}43)$$

By considering axi-symmetrical stress condition, it follows from Eqs.(3-1), (3-2),(3-4a), (3-42) and (3-43) that

$$\left.\begin{aligned} \tau &= \frac{\sqrt{2}}{3}\,q \\ \eta &= \frac{\sqrt{2}}{3}\,\bar{\eta} \\ M &= \frac{\sqrt{2}}{3}\,\bar{M} \end{aligned}\right\} \qquad (3\text{-}44)$$

Numerical values of M and λ given in the preceding page are average values obtained from the series of NIC tests. Determination of the value of κ is not easy in general because of the non-linearity of swelling line. Following the suggestion by Karube(1975), its value was obtained by drawing a line passing observed two points which locate far away from the virgin consolidation line.

3.4.2 Prediction by original and modified Cam-clay equation

In the original Cam-clay theory, the equations for undrained stress path and stress ratio-strain curve are as follows in terms of the notation of the present study

$$p/p_0 = \exp\left[(\kappa/\lambda - 1)\,\eta/M\right] \tag{3-45}$$

$$\gamma = \frac{\kappa(\lambda-\kappa)}{3\lambda M(1+e_0)} \ln\left|1-\eta/M\right| \tag{3-46}$$

where γ is octahedral shear strain defined as follows.

$$\gamma = \frac{1}{3}\sqrt{(\varepsilon_1-\varepsilon_2)^2+(\varepsilon_2-\varepsilon_3)^2+(\varepsilon_3-\varepsilon_1)^2} \tag{3-47}$$

Fig. 3-3 shows the comparison of observed stress paths and stress ratio-strain relationships with calculated ones by original Cam-clay equation. In this figure, calculated stress paths and stress ratio-strain relationships for additional two cases assuming κ/λ = 0.3 and κ/λ = 0.1 with the fixed value of λ = 0.221 are also illustrated. Calculated stress ratio versus strain curve for κ/λ = 0.5 follows approximately the observed values. On the other hand, effective mean stress p in the predicted stress paths monotonously decreases as shear stress increases toward the critical state point, whereas in

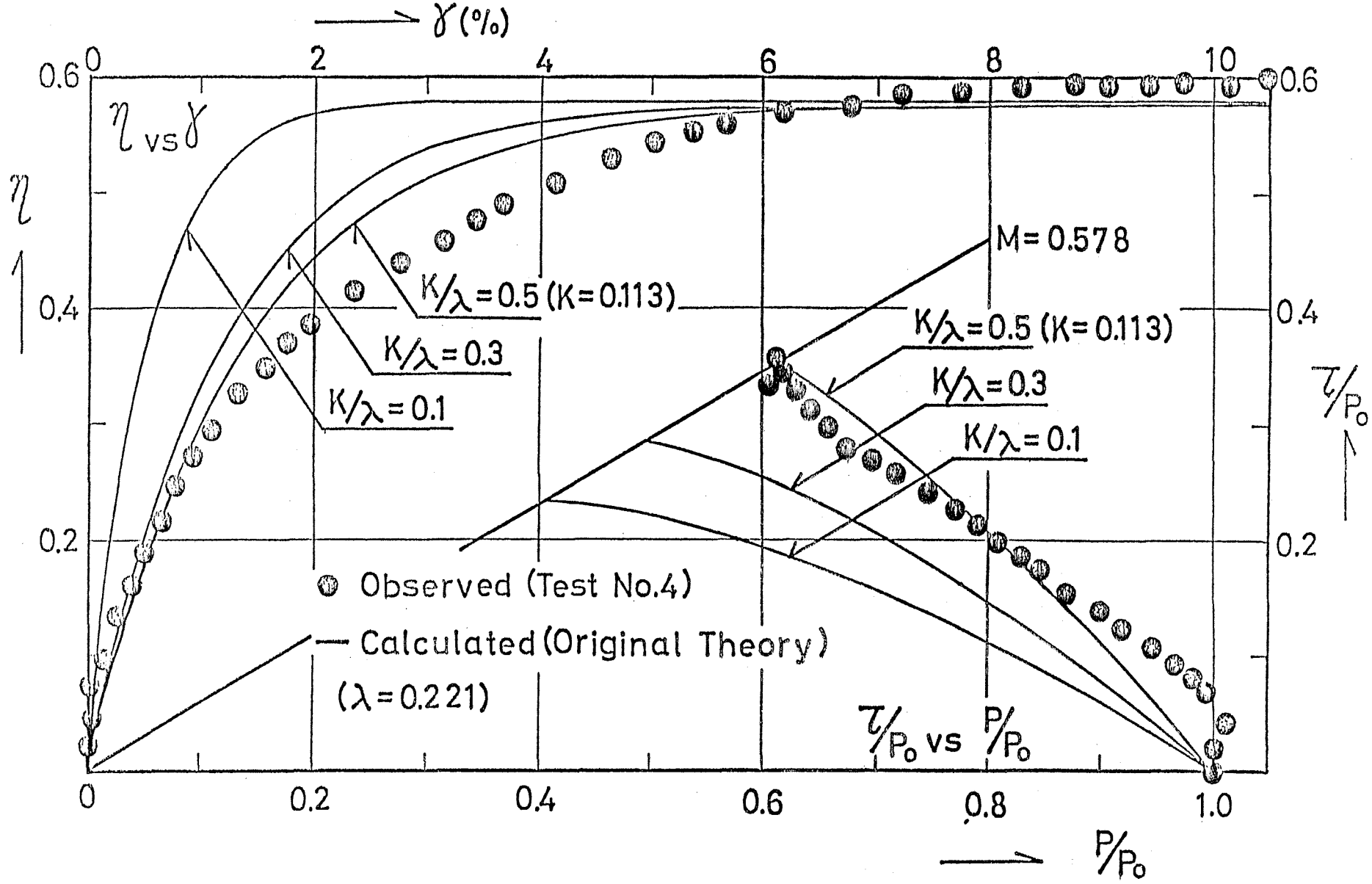

Fig.3-3 Observed and predicted stress-strain relationship by original Cam-clay equation

the measured stress path, p increases slightly in the earlier part of shear. Thus, the stress paths predicted by the original theory show an appreciable difference from the observed ones, and this can be demonstrated by the data from other tests of the present study.

It should be noted that the pattern of predicted stress path and stress ratio-strain curve are greatly influenced by the value of K as shown in Fig. 3-3 , i.e. the smaller value of K gives the smaller prediction of γ and the greater rate of decrease of p for a given stress ratio η .

As mentioned previously, Roscoe and Burland(1968) introduced a new energy equation to their original concept to make some modifications to their previous theory. The equations thus obtained to calculate the undrained stress path and stress ratio-strain curve are as follows in terms of the notation of the present study

$$p/p_0 = \left(\frac{M^2}{M^2+\eta^2}\right)^{1-K/\lambda} \tag{3-48}$$

$$\gamma = \frac{1}{3}\frac{K(\lambda-K)}{M\lambda(1+e)}\left[\ln\left|\frac{M+\eta}{M\,\eta}\right| - 2\tan^{-1}\eta/M\right] \tag{3-49}$$

Fig. 3-4 illustrates the comparison of observed stress paths and stress ratio-strain curves with calculated ones by the above two equations. As it was in Fig. 3-3 , the influence of

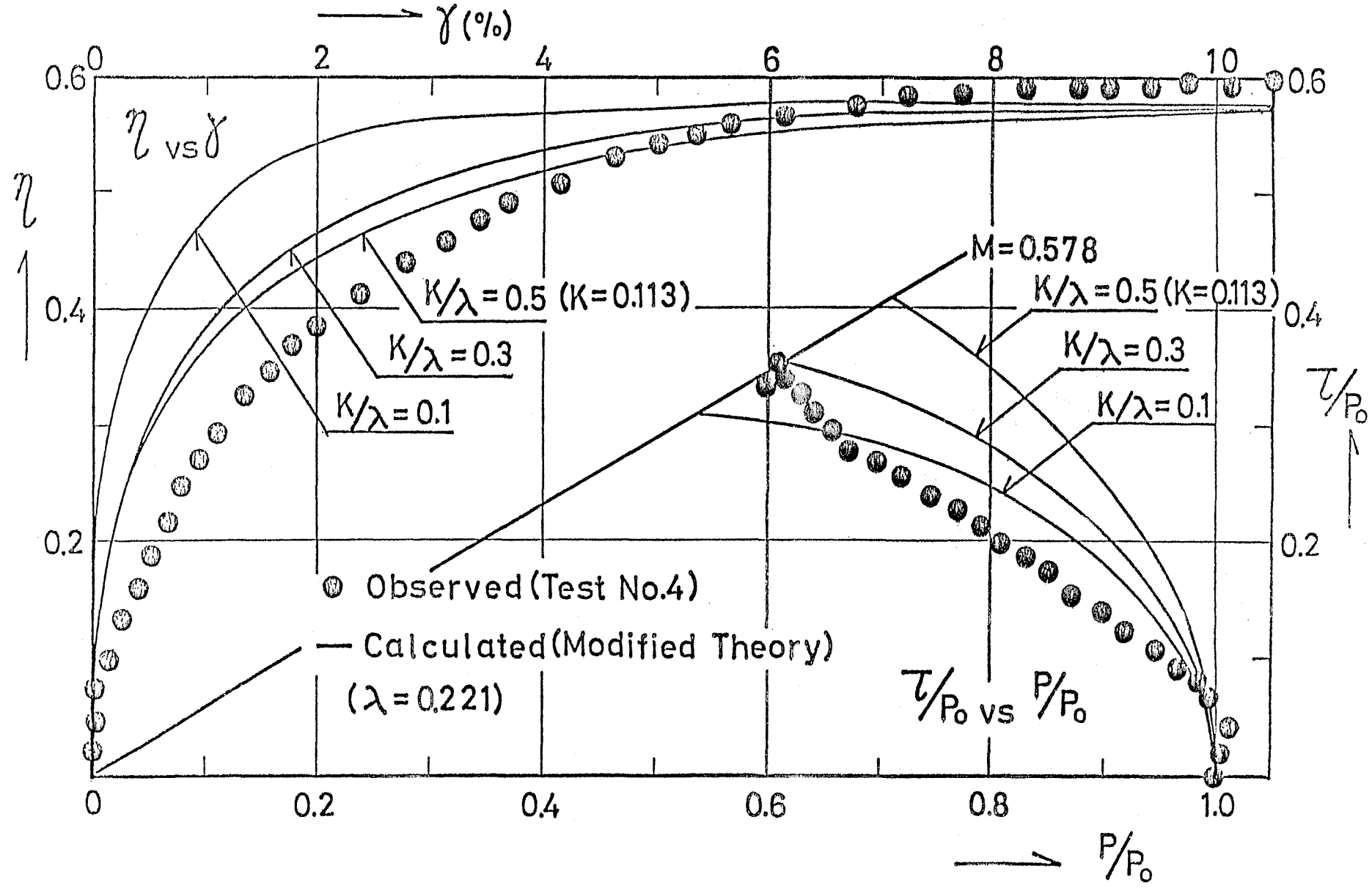

Fig.3-4 Observed and predicted stress-strain relationship by modified Cam-clay equation

the magnitude of K value on the prediction of the stress-strain relationships is obviously dominant.

3.4.3 Suggested methods of predicting stress-strain behaviour of clay by other research workers

Wroth & Bassett(1965) and Wroth(1965) proposed a new predicting method of stress-strain relationship of soils based on the energy theory and exponential function. The equations for predicting undrained stress path and stress ratio-strain curve are as follows

$$\eta = \frac{a_0 K}{1+e_0} \ln p/p_0 \tag{3-50}$$

$$\eta = M\left[1-\exp(-\sqrt{2}\, a_0 \gamma)\right] \tag{3-51}$$

Wroth represents the parameter a_0 for normally consolidated undrained test by the following equation

$$a_0 = \frac{3}{\sqrt{2}} \cdot \frac{M(1+e_0)\lambda}{(\lambda-K)K} \tag{3-52}$$

Putting Eq.(3-52) into Eqs.(3-50)and(3-51), the equations quite the same as Eqs.(3-45)and(3-46) can be obtained.

Parameters a and b in the theory of Wroth and Bassett, which was primarily concerned on sandy soil, have to be determined so as to the predicted values best fitted to the experimental data. In application of this theory to normally consolidated

clay, Wroth assumed the parameter b to be zero, which necessitated the parameter a to be a function of M, λ, κ and e_0. Therefore, determination of the parameter κ in Wroth's stress-strain equation still remains as a problem because the parameter a, which was originally an experimental constant, became to be dependent on the parameter κ.

Ohta et al.(1975) developed a stress-strain theory for anisotropically consolidated clay, extending their previous theory (e.g. Hata et al.1969) for isotropically consolidated clay. Their equations for undrained stress path and stress ratio-strain curve after isotropic consolidation are as follows

$$\eta = -\frac{\lambda}{(1+e_0)\mu} \ln p/p_0 \tag{3-53}$$

$$\gamma = -\frac{\kappa\mu}{3\lambda} \ln\left|1-\frac{(1+e_0)\mu}{\lambda-\kappa}\eta\right| \tag{3-54}$$

In this theory, they derived following equation using the condition of critical state.

$$\mu = \frac{\lambda-\kappa}{(1+e_0)M} \tag{3-55}$$

The parameter μ was originally defined (shown later in section 3.5) as dilatancy index, but now it has a different definition, being dependent on M, λ and κ. In any case, putting Eq.(3-55)

into Eqs.(3-53) and(3-54), equations quite the same as Eqs.(3-45) and (3-46) can be obtained. Predicted values by the theories of Wroth and Ohta et al. will be exactly the same as in Fig. 3-3 , provided that the same value of M , λ and K are used.

Karube (1977 and 1978) recently proposed a method to obtain incremental stress-strain relationship, based on an experimental relationship between strain increment ratio versus stress ratio. His equations which predict the undrained stress path and stress ratio-strain curve are as follows in terms of the notation of the present study

$$\gamma = \frac{\sqrt{2}}{3}\alpha \int_{x_0}^{x} \frac{\exp(Hx)}{1-x}\,dx \tag{3-56}$$

$$p/p_0 = \exp\left[\frac{3.6M^2(1+e_0)x}{\lambda}\left\{\exp(Hx_0) - \exp(Hx)\right\}\right] \tag{3-57}$$

where

$$x = \eta/M \tag{3-58}$$

$$H = \left\{\frac{3.6}{\sqrt{2}}M\left(1+\frac{3}{2\sqrt{2}}M\right)^{K}/\lambda\right\}^{-1} \tag{3-59}$$

and α is an experimental parameter which is determined so as to make the best fit to observed stress ratio-strain curve.

Fig. 3-5 shows the comparison between observed and predicted

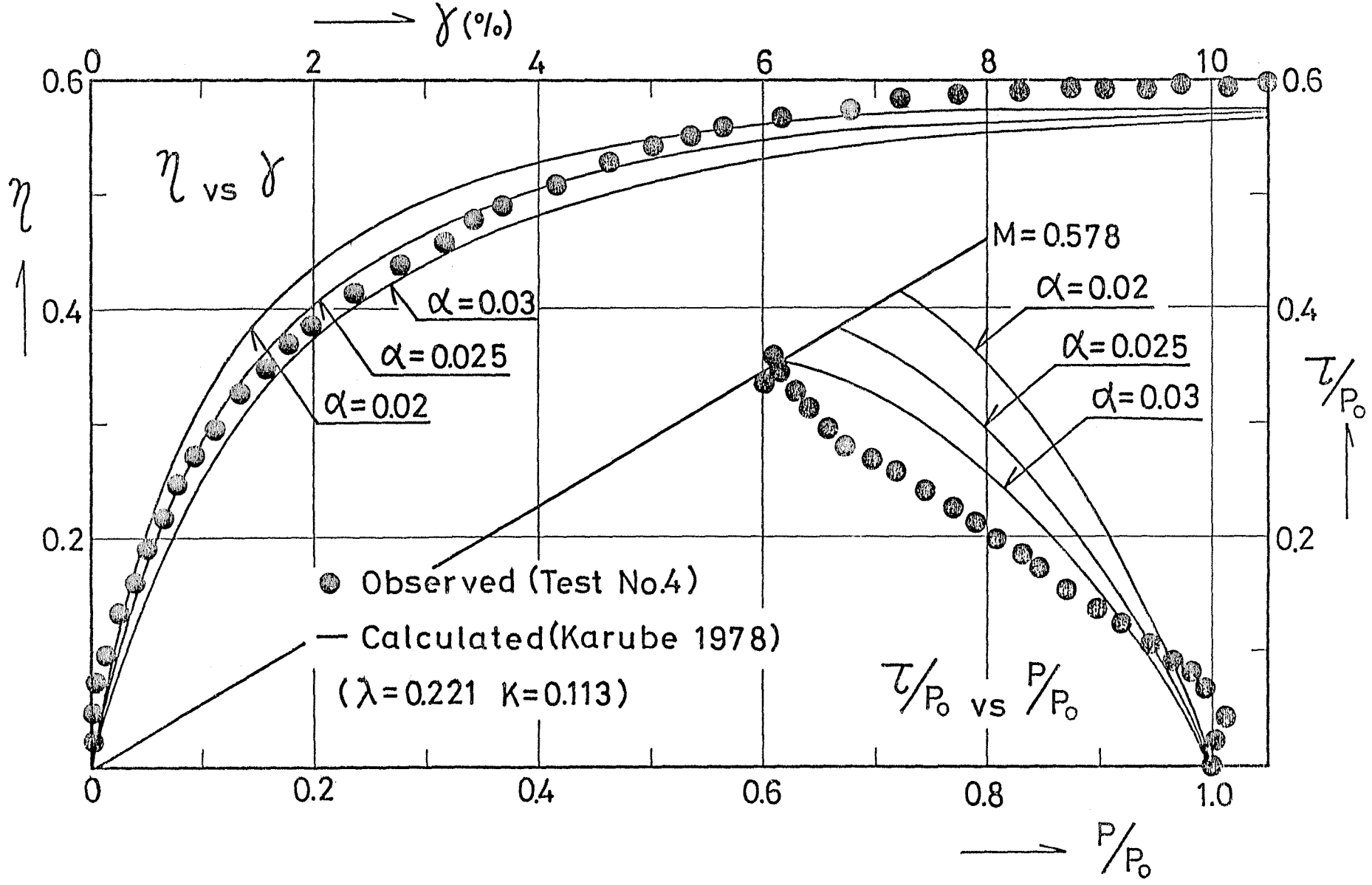

Fig.3-5 Observed and predicted stress-strain relationship by equations of Karube

stress path and stress ratio versus strain curve. Stress ratio-strain curve for α = 0.025 gives the best fit, but the failure point in the predicted stress path is appreciably different from the observed one. Calculated stress paths for α = 0.02 and 0.03 are also illustrated in the same figure, and they indicate that a satisfying stress path prediction can not be obtained by merely modifying the value of α .

3.5 Modified Equation by the Present Author

Roscoe et al. assumed that the dissipated energy is to be $\delta W = M p \delta \varepsilon^p$. But, calculation based on this assumption overpredict the magnitude of shear strain at given stress ratio. Consequently, Roscoe and Burland newly assumed δW as follows

$$\delta W = p\sqrt{(\delta v^p)^2 + (M \delta \varepsilon^p)^2} \qquad (3\text{-}34 \text{ bis})$$

Eq.(3-34)was brought out from the concept that the dissipated energy be equal to $p\delta v^p$after isotropic consolidation and be equal to$pM\delta\varepsilon^p$ at critical state condition. Since there are many possible generalization of above two conditions, the present author suggested a new equation which satisfies the two conditions mentioned above (Mitachi et al. 1979).

$$\delta W = p\delta v^p + q\delta\varepsilon^p = \frac{p}{\sqrt{\omega}}\sqrt{(\sqrt{\omega}\delta v^p - M\delta\varepsilon^p)^2 + (\omega-1)(M\delta\varepsilon^p)^2} \qquad (3\text{-}60)$$

where ω is a positive constant.

Rearrangement of Eq.(3-60) after dividing it by $p\delta v^p$ gives strain increment ratio as follows.

$$1/4 = \delta\varepsilon^p / \delta v^p = \frac{2(\eta + M/\sqrt{\omega})}{M^2 - \eta^2} \qquad (3\text{-}61)$$

Substituting Eq.(3-61) into basic equations(3-16) and (3-19) which give shear strain increment and undrained stress path, following equations are obtained

$$\delta\varepsilon = \frac{4K(\lambda-K)}{\lambda(1+e_0)} \cdot \frac{(\eta+M/\sqrt{\omega})^2}{(M^2+\frac{2}{\sqrt{\omega}}M\eta+\eta^2)(M^2-\eta^2)}\delta\eta \qquad (3\text{-}62)$$

$$\frac{dp}{p} = 2(K/\lambda-1) \cdot \frac{\eta+M/\sqrt{\omega}}{(M^2+\frac{2}{\sqrt{\omega}}M\eta+\eta^2)}d\eta \qquad (3\text{-}63)$$

Fig.3-6 illustrates an example of effective stress paths during undrained triaxial compression test for various values of ω. From this figure it is seen that the stress path for small value of ω is approximate to that of original Cam-clay theory, and the stress path is the same as that of modified Cam-clay theory when the value ω approaches to infinity.

Fig. 3-7 shows the stress paths and stress ratio-strain curves obtained from Eqs. (3-62) and (3-63) by changing the value of ω as 5,20 and 100. Stress ratio-strain curve for ω = 5 gives the best fit. But the following fundamental defects are still inevitable.

1) The appropriate value of K is difficult to determine objectively, since it varies with overconsolidation ratio.

2) As this equation is based on the energy concept, dilatancy characteristics of particular soil can not be introduced directly into the predicting equation.

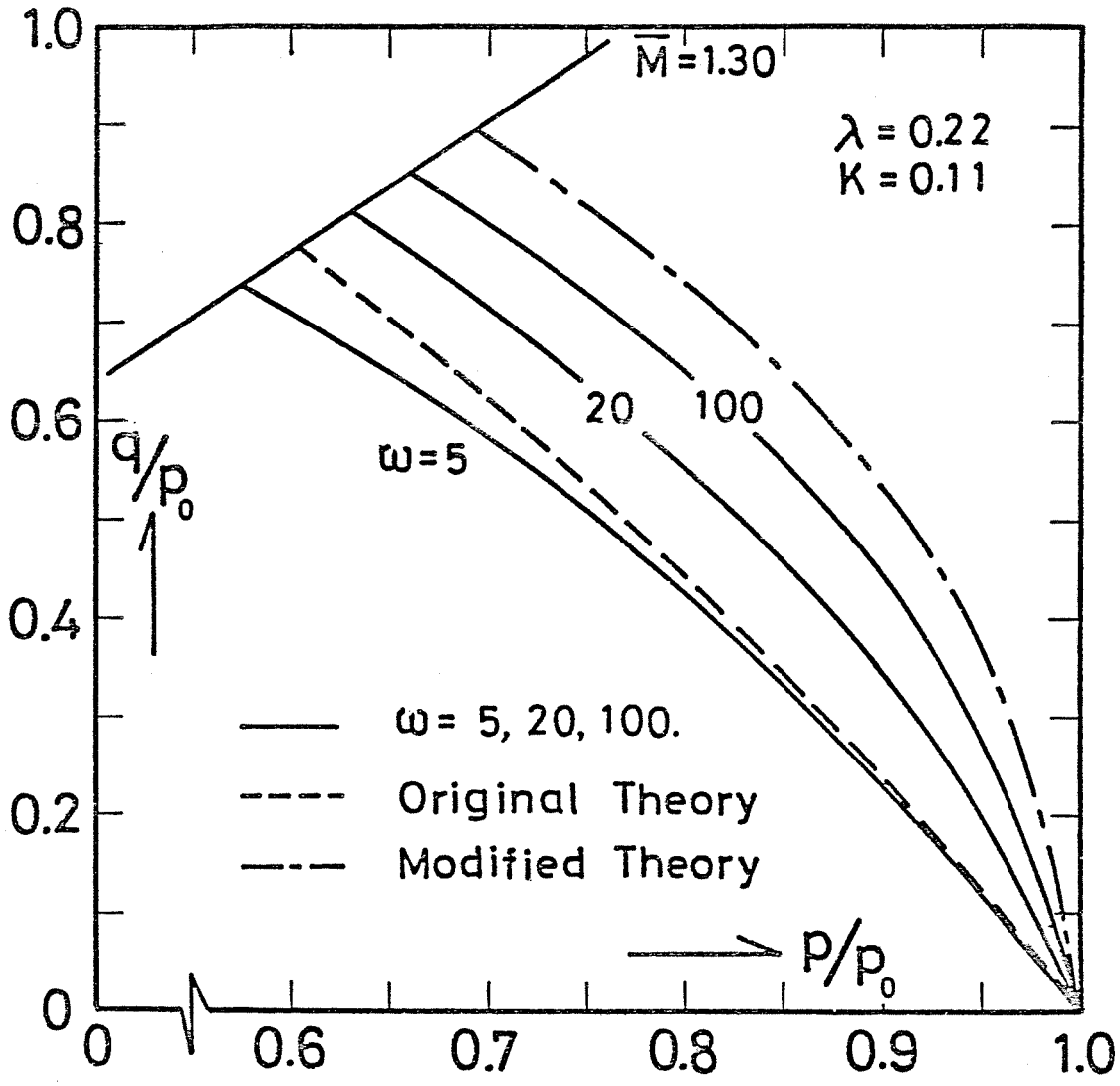

Fig.3-6 Undrained effective stress paths for various values of ω

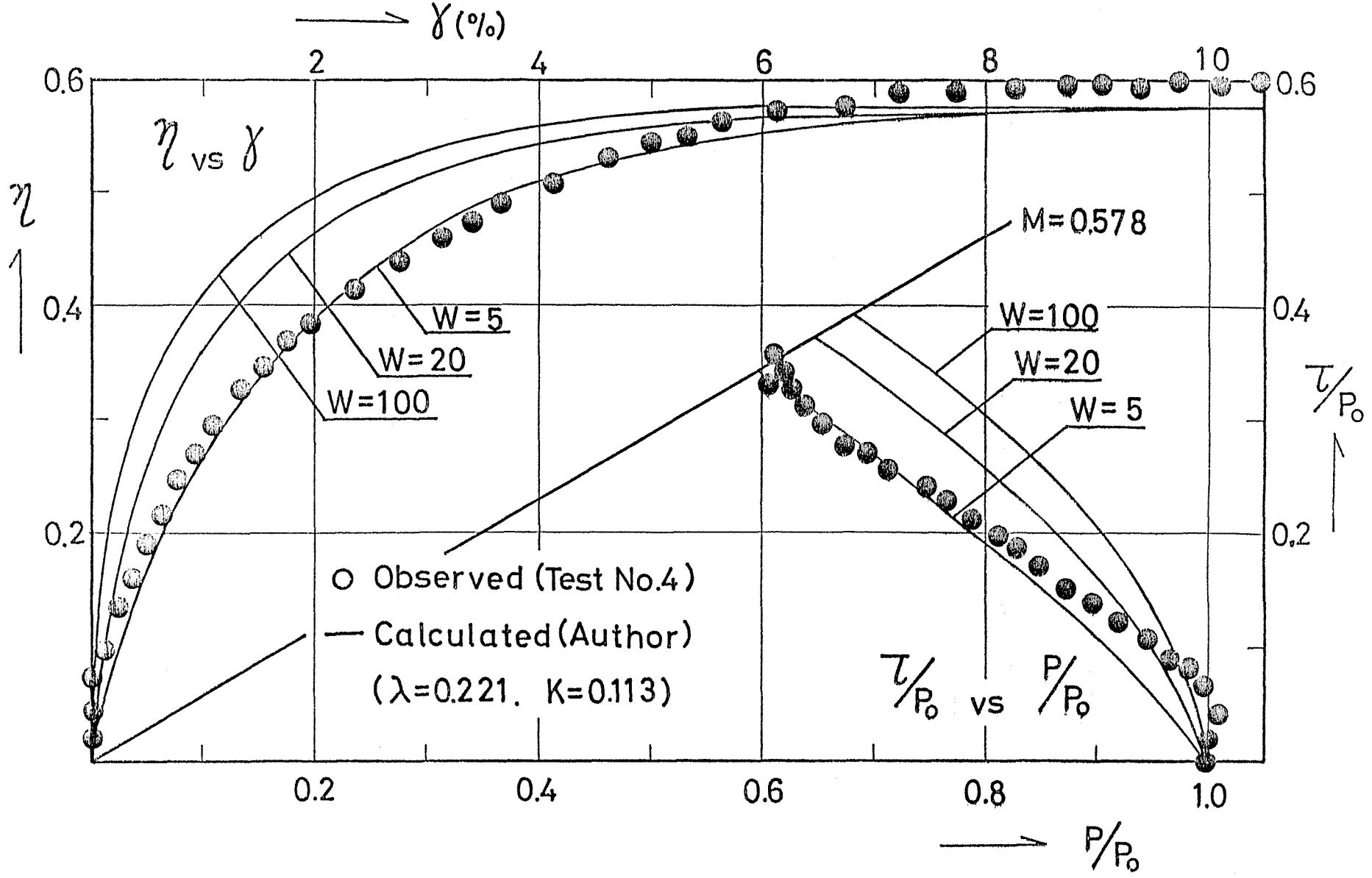

Fig.3-7 Observed and predicted stress-strain relationship by Eqs.(3-62) & (3-63)

In spite of those defects mentioned above, since the change of the value of ω is, in a sense, equivalent to the change of the value of χ, it would be possible to obtain a equation that can predict more accurately the stress-strain behaviour of clay, by changing the value of ω corresponding to the change of η.

3.6 Stress-Strain Prediction with Dilatancy Function

3.6.1 Introduction

In the preceding section, the validity of the existing theories by comparing the observed with predicted stress-strain relationship was examined. In Cam-clay equation (and also Wroth's and Ohta's theory), three basic parameters M, λ and K are needed to fix. Among these parameters, the appropriate value of K is difficult to determine objectively, since it varies with overconsolidation ratio. Modified theory by Roscoe and Burland, and Karube's theory also have the same problem concerning the value of K.

The present author derived a new stress-strain equation under the assumptions as shown in the following section. Special features of the equation are as follows

1) the equation involves the dilatancy function $F(\eta)$ which represent appropriately the dilatancy characteristics of soils, and

2) K is not considered to be a material constant, but a parameter which is determined from the critical state condition. Since the value of K thus determined is not a material constant, a new symbol ν in place of K will be used in this paper to make clear the difference of their outcoming. Although the two parameters K and ν are determined by different

ways, their functions are exactly the same in the sense of Cam-clay equations.

3.6.2 Basic assumptions

Referring to the existing theories and taking $F(\eta)$ and ν into consideration, the present author has made following assumptions to derive a new stress-strain equations.

1) Total change of void ratio during shear is represented by summation of void ratio change due to isotropic stress component $(de)_c$ and that due to deviatoric one, $(de)_d$,i.e.

$$de = (de)_c + (de)_d \tag{3-64}$$

2) The change of void ratio due to isotropic stress is represented as follows

$$(de)_c = -\lambda \frac{dp}{p} \tag{3-65}$$

3) Dilatancy characteristics of clays are represented by a function of stress ratio η , i.e.

$$\frac{V_0 - V}{V_0} = F(\eta)$$

, which gives the following equation for void ratio change due to deviatoric stress

$$(de)_d = -(1+e_0) F'(\eta) d\eta \tag{3-66}$$

4) Recoverable component of the change of void ratio is given as follows

$$(de)^r = -\nu \frac{dp}{p} \tag{3-67}$$

5) There is no recoverable component of shear strain during shear, and so

$$(d\gamma)^r = 0 \tag{3-68}$$

6) Normality rule can be applied to the soil if it is stable in the sense by Drucker(1959).

$$\frac{\frac{1}{3} d v^p}{d\gamma^p} = -\frac{d\tau}{dp} \tag{3-69}$$

3.6.3 Incremental stress-strain equations

Total change of void ratio during shear is represented by using Eqs.(3-64),(3-65)and(3-66) as follows

$$de = (de)_c + (de)_d = -\lambda \frac{dp}{p} - (1+e_o)F'(\eta)d\eta \qquad (3\text{-}70)$$

In order to derive an equation which represents the state boundary surface, integration of Eq.(3-70) is made with the initial condition $e = e_o$ when $p = p_o$ and $\eta = \eta_o$, where η_o is the octahedral stress ratio after completion of anisotropic consolidation. The result of integration is as follows

$$e - e_o + \lambda \ln p/p_o + (1+e_o)[F(\eta) - F(\eta_o)] = 0 \qquad (3\text{-}71)$$

For undrained shear test, putting the conditions $e = e_o$ and $F(\eta_o) = 0$ into Eq.(3-71), the following equation is obtained.

$$F(\eta) = -\frac{\lambda}{1+e_o} \ln \frac{p}{p_o} \qquad (3\text{-}72)$$

Based on the concept of Scott(1963) on the volume change in the soil structure, Tsushima and Miyakawa(1977) derived a similar equation to Eq.(3-72) (combining their Eq.(3) and (7), the same form of Eq.(3-72) of this study is obtained), and they called the function $F(\eta)$ as equivalent dilatancy. In this paper,

it will preferably be called dilatancy function. Ohta et al. (1975) developed a theory for stress-strain relationship for anisotropically consolidated clay, assuming that

$$F(\eta) = \mu (\eta - \eta_0)$$

where μ is a coefficient expressing the dilatancy intensity. Ohta's assumption is based on the experimental studies by Shibata (1963) et al.

Fig.3-8 and Fig.3-9 illustrate the relationship between stress ratio η and dilatancy function $F(\eta)$ for 6 series of the present shear test. In compression test, the observed values for $F(\eta) - \eta$ curves could be approximated by a straight line, excluding their initial parts of positive dilatancy. Hata et al. (1969) inferred that the positive dilatancy would disappear if the strain rate is set to be very small. Most research workers interesred in the stress-strain behaviour of clays seem to support this inferrence, but there are some published data which are against it (e.g. Roscoe and Thurairajah 1964, Lambe and Whitman 1969, and Sawada et al. 1977). Moreover, Shibata et al. (1976) mentioned that even though the strain rate is set to be extremely small, the deviation of the observed $F(\eta) - \eta$ relationship from Ohta's assumption will be large with the increase of silt and sand fraction of a given soil.

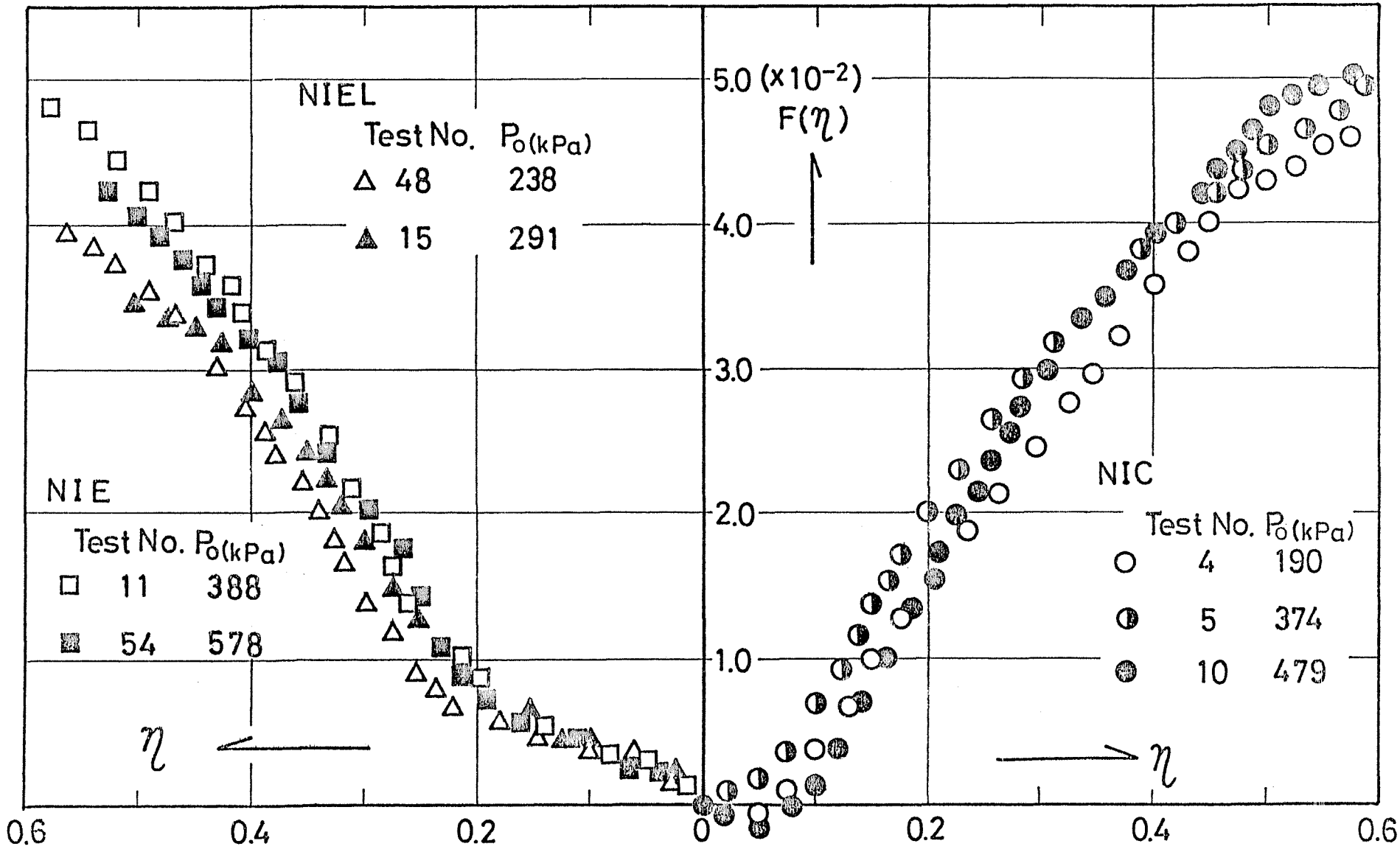

Fig.3-8 Octahedral stress ratio vs. dilatancy of isotropically consolidated clay

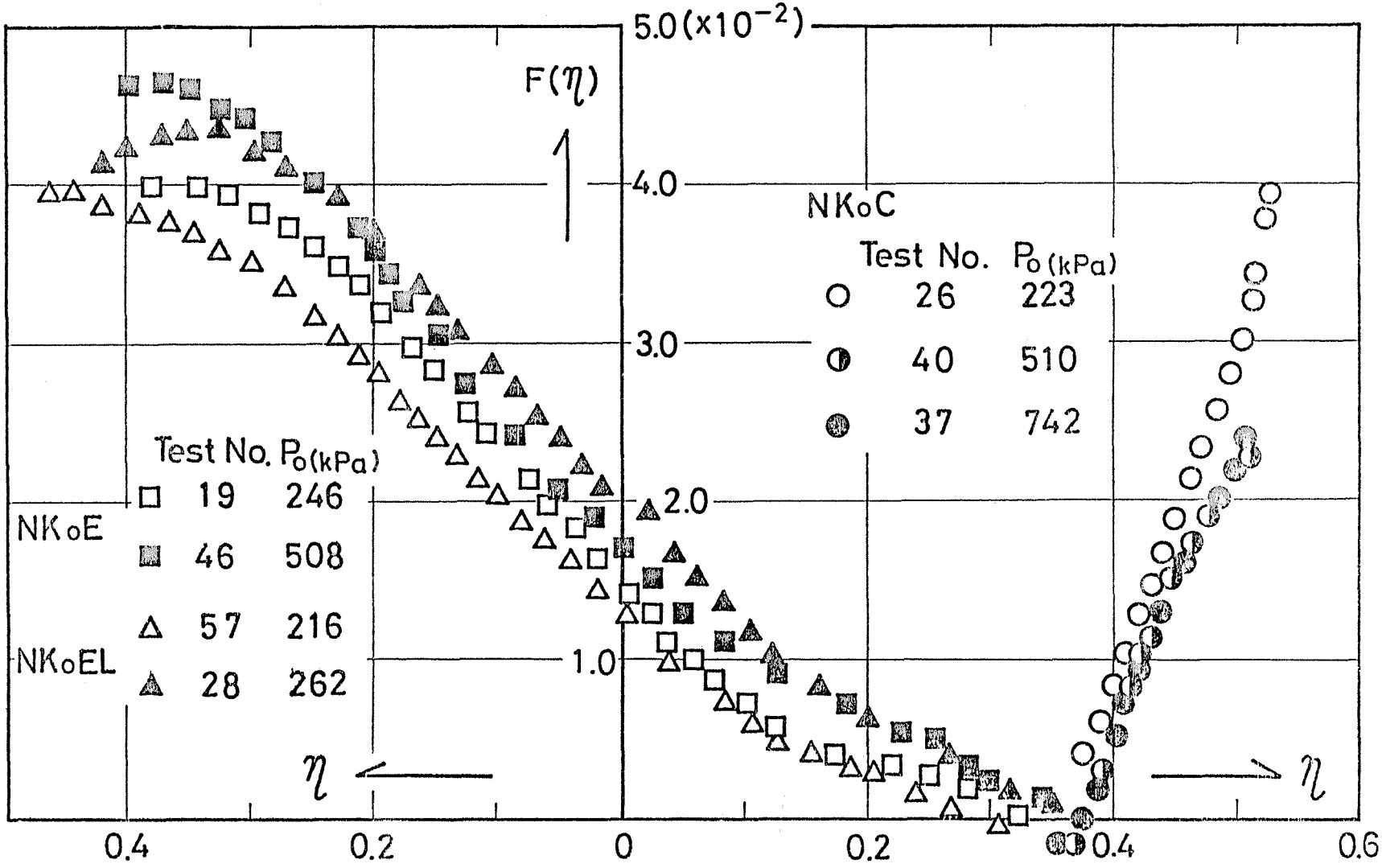

Fig.3-9 Octahedral stress ratio vs. dilatancy

Recently, the present author and his co-workers (Kitago et al. 1979) reported that the development of positive dilatancy in the initial part of shear increases with the increase in consolidation duration, and that the influence of consolidation duration is more significant than that of strain rate during shear. Therefore, the present author presumes that positive dilatancy does develop in the initial part of shear within the conventional strain rate range used in the undrained test carried out in the present study.

Combining Eqs.(3-5) and (3-67), plastic volumetric strain increment $d\upsilon^p$ is given as follows

$$d\upsilon^p = d\upsilon - d\upsilon^r = -\frac{1}{1+e}\left(de + \nu\frac{dp}{p}\right) \tag{3-73}$$

From Eq.(3-70) and (3-73),

$$d\upsilon^p = -\frac{1}{1+e}\left[-\lambda\frac{dp}{p} - (1+e_0)F'(\eta)d\eta + \nu\frac{dp}{p}\right]$$

$$= \frac{1+e_0}{1+e}\left[\frac{\lambda-\nu}{1+e_0}\cdot\frac{dp}{p} + F'(\eta)d\eta\right] \tag{3-74}$$

Integrating Eq.(3-67) with the condition $e = e_0$ and $p = p_0$, and combining the resulting equation with Eq.(3-71), following equation is obtained to represent the current yield locus.

$$\frac{\lambda-\nu}{1+e_0}\ln\frac{p}{p_0}+F(\eta)-F(\eta_0)=0 \tag{3-75}$$

Accordingly, successive yield loci is given by the equation

$$\frac{\lambda-\nu}{1+e_0}\ln\frac{p}{p_{0i}}+F(\eta)-F(\eta_0)=0 \tag{3-76}$$

where p_{0i} is effective mean stress at the intersection point of consolidation and swelling lines.

Differentiation of Eq.(3-76) leads to

$$\frac{d\tau}{dp}=\frac{-\frac{\lambda-\nu}{1+e_0}}{F'(\eta)}+\eta \tag{3-77}$$

Substituting Eq.(3-77) into Eq.(3-69), relationship between plastic strain increment ratio versus stress ratio is obtained as follows

$$\frac{d\gamma^p}{d\nu^p}=-\frac{1}{3}\frac{dp}{d\tau}=-\frac{1}{3}\left[\frac{F'(\eta)}{\eta F'(\eta)-\frac{\lambda-\nu}{1+e_0}}\right] \tag{3-78}$$

and substitution of Eq.(3-74) into the above equation gives

$$d\gamma^p=-\frac{1}{3}\cdot\frac{1+e_0}{1+e}\left[\frac{\lambda-\nu}{1+e_0}\frac{dp}{p}+F'(\eta)d\eta\right]\frac{F'(\eta)}{\eta F'(\eta)-\frac{\lambda-\nu}{1+e_0}} \tag{3-79}$$

Furthermore, from Eq.(3-70)

$$d\nu = \frac{-de}{1+e_0} = \frac{\lambda}{1+e_0}\cdot\frac{dp}{p} + F'(\eta)d\eta \qquad (3\text{-}80)$$

Since $d\nu = 0$ in the undrained test,

$$\frac{\lambda}{1+e_0}\cdot\frac{dp}{p} + F'(\eta)d\eta = 0 \qquad (3\text{-}81)$$

Combining Eq.(3-81) with (3-79) and assuming $e = e_0$, following incremental stress ratio-strain equation for undrained test is obtained.

$$d\gamma = d\gamma^p = -\frac{\nu}{3\lambda}\cdot\frac{[F'(\eta)]^2}{\eta F(\eta) - \frac{\lambda-\nu}{1+e_0}}d\eta \qquad (3\text{-}82)$$

Roscoe et al. defined the critical state to be the state that shear strain continues to increase without further change of void ratio or of the effective stresses. Considering the critical state to be that shear strain continues to increase without the change of stress ratio, following condition is satisfied at the critical state.

$$\left(\frac{d\eta}{d\gamma}\right) = 0 \qquad \text{at } \eta = M \qquad (3\text{-}83)$$

From Eqs.(3-82) and (3-83), the parameter ν is determined as follows

$$\nu = \lambda - (1+e_0) M F'(M) \qquad (3\text{-}84)$$

Thus the parameter ν can be obtained by the known parameters λ, e_0, M and $F'(M)$.

3.6.4 Determination of $F(\eta)$

The stress-strain equation mentioned in previous section includes the dilatancy function $F(\eta)$. Therefore, to describe accurately the stress-strain behaviour of a soil, it is necessary to find out the appropriate function of $F(\eta)$ to represent the stress-dilatancy characteristics of the soil.

As can be seen in Figs.3-8 and 3-9, it appears almost impossible to approximate the stress ratio-dilatancy plot by a single straight line. Instead, it would be better to assume an appropriate curve or to approximate by a set of two straight lines. As a first approximation, the latter is assumed. According to this assumption, observed stress ratio-dilatancy relationships obtained from NIC and NIE tests are represented as follows (see Fig.3-10). In NIC test,

$$F_1(\eta) = \mu_1 \eta \qquad \text{for} \qquad 0 \leqq \eta \leqq \eta_1 \tag{3-85a}$$

and

$$F_2(\eta) = \mu_1 \eta_1 + \mu_2(\eta - \eta_1) \quad \text{for} \quad \eta_1 \leqq \eta \leqq \mu_c \tag{3-85b}$$

and in NIE test,

$$F_1(\eta) = \mu_1 \eta \qquad \text{for} \qquad 0 \leqq \eta \leqq \eta_2 \tag{3-86a}$$

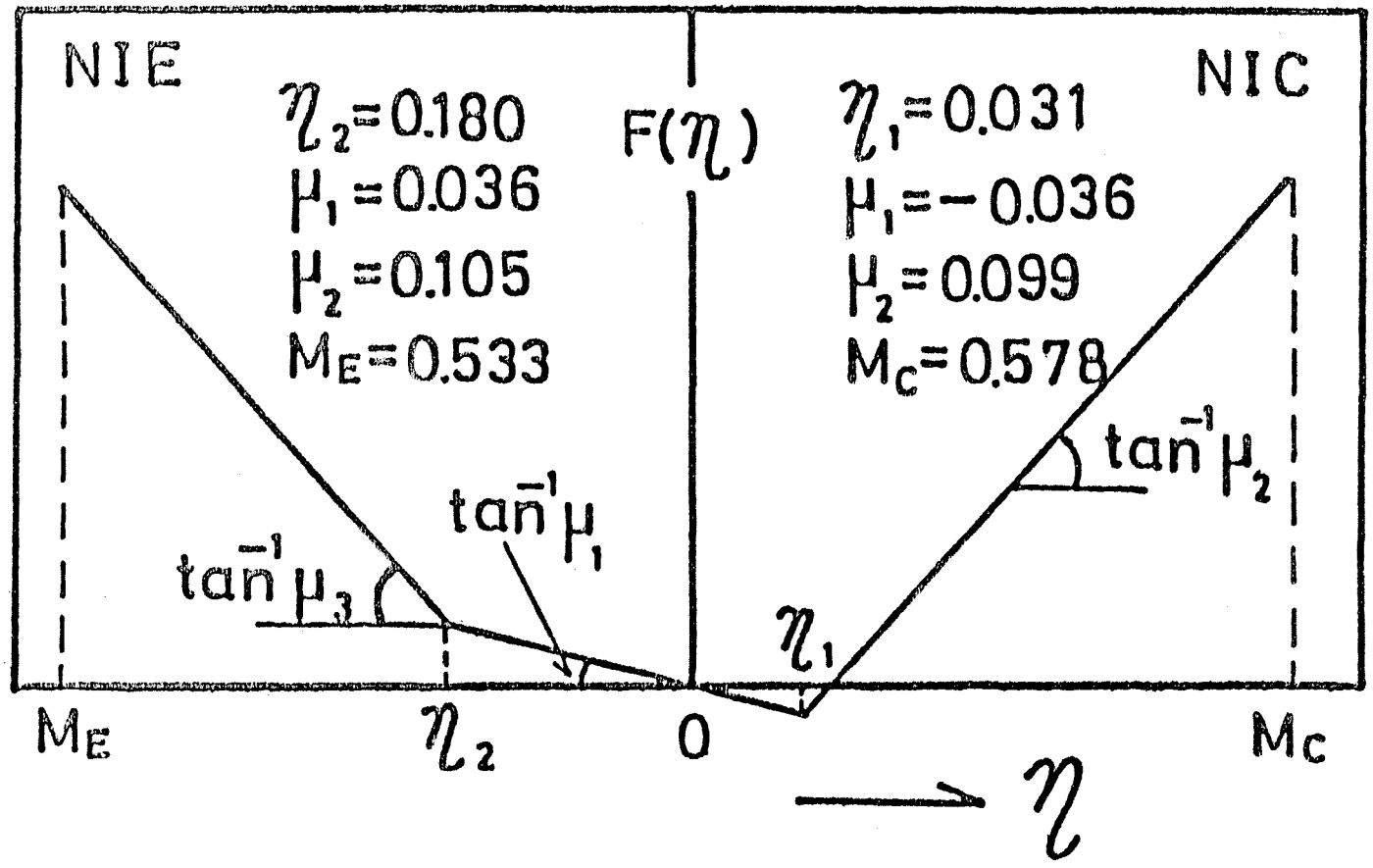

Fig.3-10 Schematic diagram of stress ratio vs. dilatancy

and

$$F_2(\eta) = \mu_1 \eta_2 + \mu_3 (\eta - \eta_2) \quad \text{for} \quad \eta_2 \leqq \eta \leqq M_E \tag{3-86b}$$

where η_1 and η_2 are the stress ratios at which dilatancy coefficient changes its value in compression and extension test respectively, and μ_1, μ_2 and μ_3 are the dilatancy coefficients as shown in Fig.3-10, and M_c and M_E are equal to η at the critical state in compression and extension tests, respectively.

Stress path for NIC test is obtained by inserting Eqs.(3-85a) and (3-85b) into Eq.(3-72) as follows

$$p/p_0 = \exp\left[- \frac{(1+e_0)\mu_1}{\lambda} \eta \right] \quad \text{for} \quad 0 \leqq \eta \leqq \eta_1 \tag{3-87a}$$

$$p/p_0 = \exp\left[- \frac{1+e_0}{\lambda} \{ \mu_1 \eta_1 + \mu_2 (\eta - \eta_1) \} \right] \quad \text{for} \quad \eta_1 < \eta \leqq M_c \tag{3-87b}$$

Combining Eqs.(3-85a) and (3-85b) with Eq.(3-82) and integrating the resulting equations with initial condition $\gamma = 0$ at $\eta = 0$, equations for stress ratio-strain prediction can be derived as follows

$$\gamma = \frac{\nu \mu_1}{3\lambda} \left[\ln \left| \frac{\frac{\lambda - \nu}{1+e_0}}{\mu_1 \eta - \frac{\lambda - \nu}{1+e_0}} \right| \right] \quad \text{for} \quad 0 \leqq \eta \leqq \eta_1 \tag{3-88a}$$

and

$$\gamma = \frac{\nu}{3\lambda}\left[\mu_1 \ln\left|\frac{\frac{\lambda-\nu}{1+e_o}}{\mu_1\eta_1 - \frac{\lambda-\nu}{1+e_o}}\right| + \mu_2 \ln\left|\frac{\mu_2\eta_1 - \frac{\lambda-\nu}{1+e_o}}{\mu_2\eta - \frac{\lambda-\nu}{1+e_o}}\right| \right. \quad \text{for } \eta_1 < \eta \leq M_c \qquad (3\text{-}88b)$$

For NIE test, similar equations as shown above can be obtained.

3.6.5 $F(\eta)$ in existing theories

Dilatancy function $F(\eta)$ involved in the stress-strain equations mentioned above is a function which relates the equivalent volumetric strain in undrained test due to octahedral shear stress with octahedral stress ratio. The present author intended to simplify the observed $F(\eta)$ versus η curve to be represented by the two straight lines. Herein, the functions equivalent to $F(\eta)$ in the existing theories are examined.

As described before, Ohta et al. assumed that $F(\eta)$ versus η relationship can be expressed by a single straight line. Now, how about in original and modified Cam-clay theories.

1) Original Cam-clay theory

Eq.(3-45) can be rewritten as follows

$$\lambda \ln p/p_0 + \frac{\lambda-\kappa}{M}\eta = 0$$

Comparison of Eq.(3-72) with the above equation leads to

$$F(\eta) = \frac{\lambda-\kappa}{M(1+e_0)}\eta \qquad (3\text{-}89)$$

Since M, λ, κ and e_0 are regarded as soil constants, $F(\eta)$ versus η relationship in original theory implies a single straight line.

2) Modified Cam-clay theory

Undrained stress path in modified theory is given by Eq. (3-48), which is written as follows

$$\lambda \ln p/p_0 + (\lambda - \kappa) \ln \left(\frac{M^2+\eta^2}{M^2} \right) = 0$$

Combination of Eq.(3-72) with above equation gives

$$F(\eta) = \frac{\lambda - \kappa}{1+e_0} \ln \left\{ 1 + (\eta/M)^2 \right\} \qquad (3\text{-}90)$$

Relationships between $F(\eta)$ versus η by Eq.(3-89) and (3-90) are illustrated in Fig. 3-11 . It should be noted that the latter part of $F(\eta) - \eta$ curve by modified theory is almost parallel to the straight line by original one.

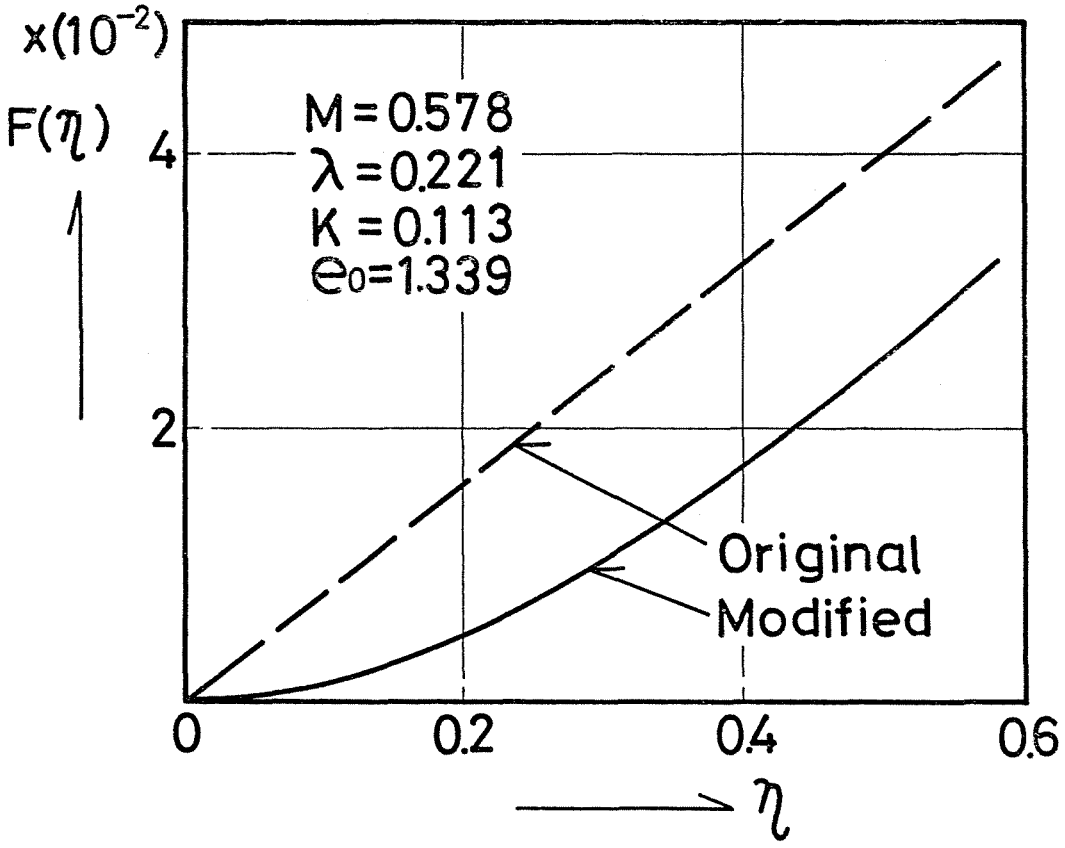

Fig.3-11 Octahedral stress ratio-dilatancy relationship by original and modified Cam-clay equations

3.6.6 Comparisons of predicted with observed stress-strain relationship

In this section, the validity of the present method for estimating the undrained stress-strain behaviour of isotropically consolidated clay is examined. The data used for this purpose are those from NIC-No.4, which was also used in preceding section. Parameters prepared for prediction are as follows

$M = 0.578$ $\lambda = 0.221$ $e_o = 1.339$

$M_1 = -0.036$ $M_2 = 0.099$ $\eta_i = 0.031$

where the parameters except for e_o are average values obtained from the series of NIC test.

Fig.3-12 shows the comparison of the calculated stress paths and stress ratio-strain relationship with the observed ones. Figs.3-13 and 3-14 illustrate another example of comparisons including that of NIE test. As seen from these figures, both calculated stress paths and stress ratio-strain curves agree fairly well with the observed ones. It is a natural result that the calculated stress path agrees with the observed one, because the predicted stress path was based on the measured $F(\eta)$ versus η relationship. However, the fact that the calculated stress ratio-strain curve agrees well with the observed one suggests that the normality rule may be conveniently used as

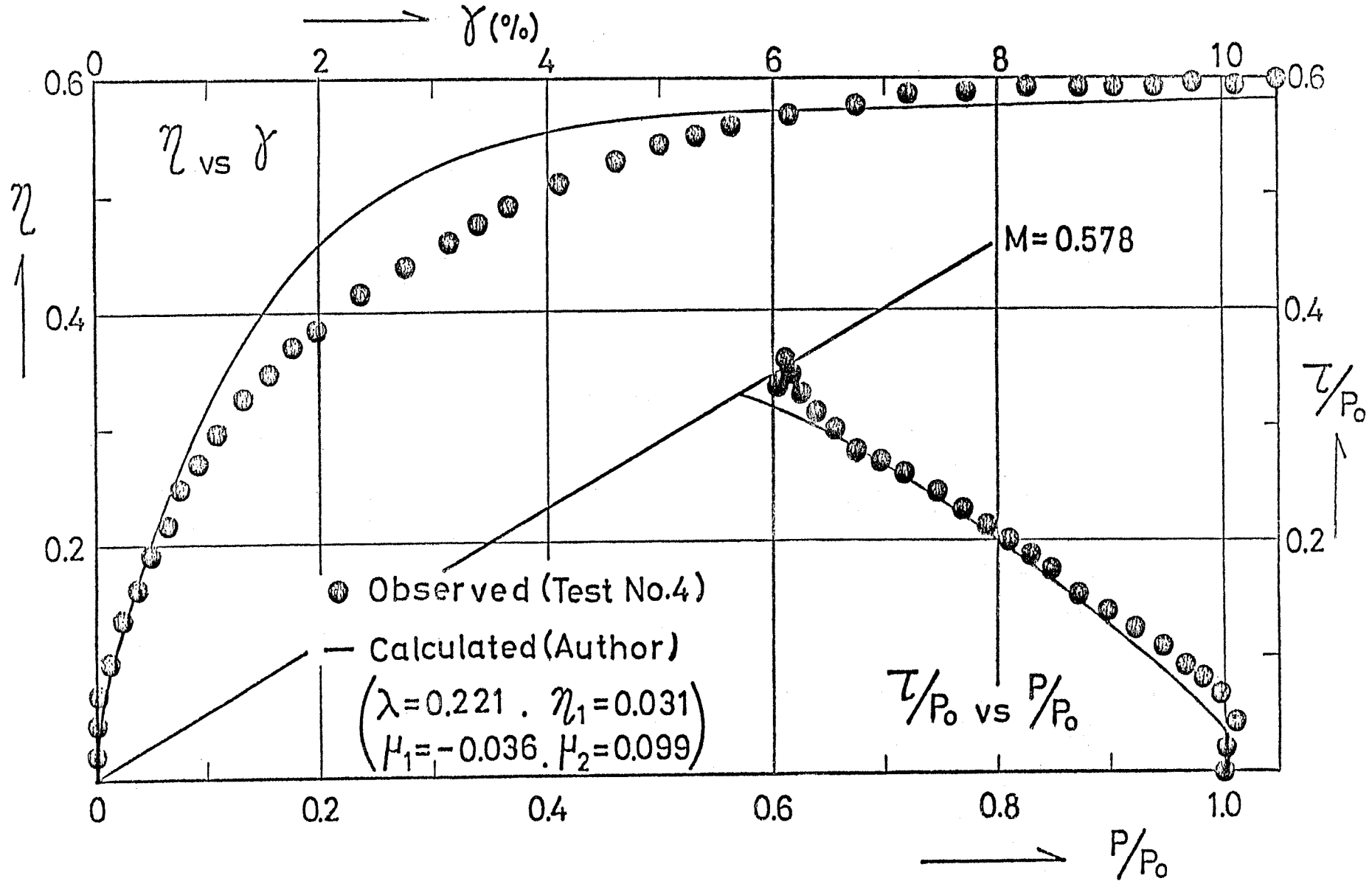

Fig.3-12 Observed and predicted stress-strain relationship by the present author

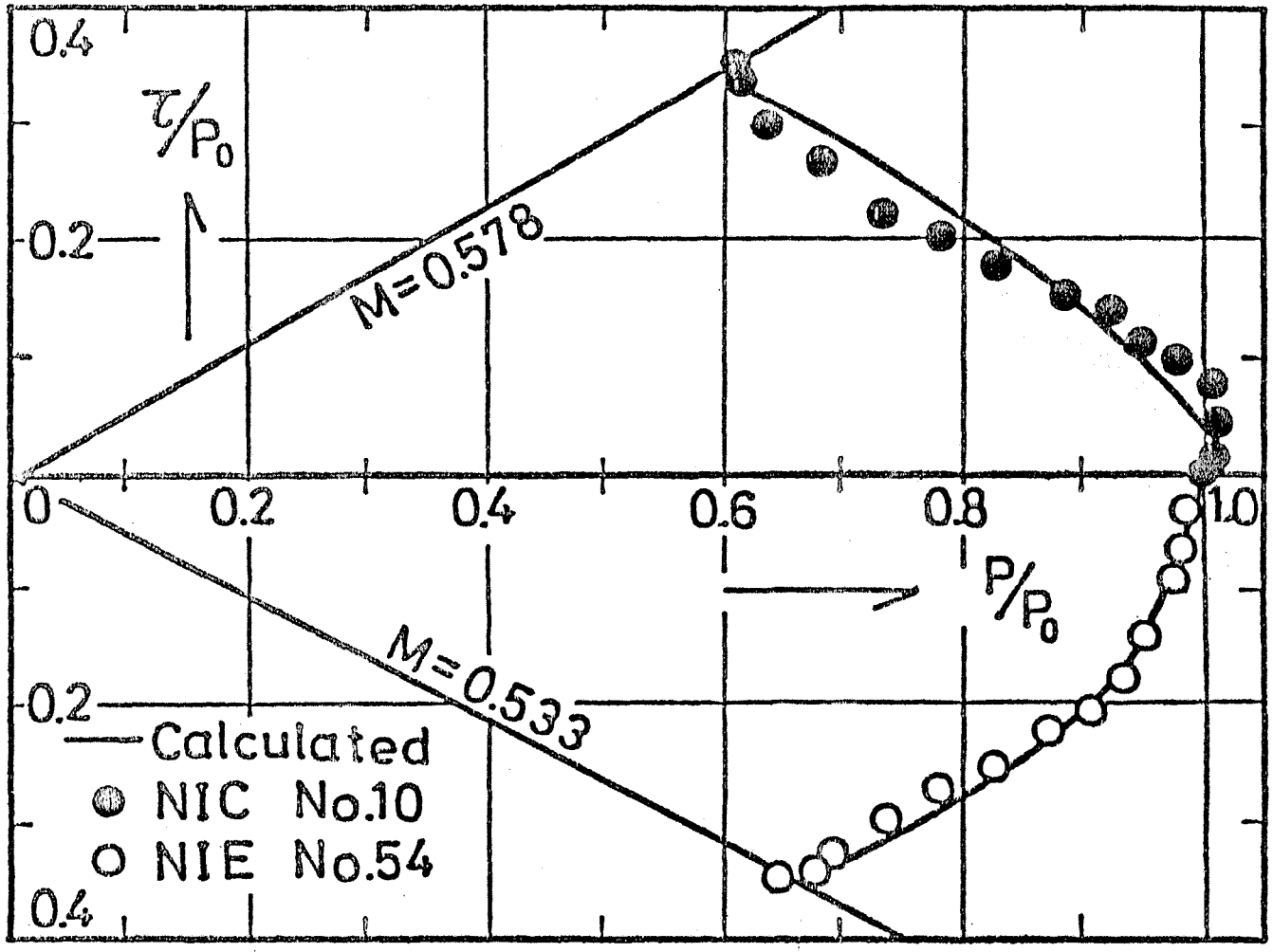

Fig.3-13 Observed and predicted stress paths for both compression and extension tests by the present author

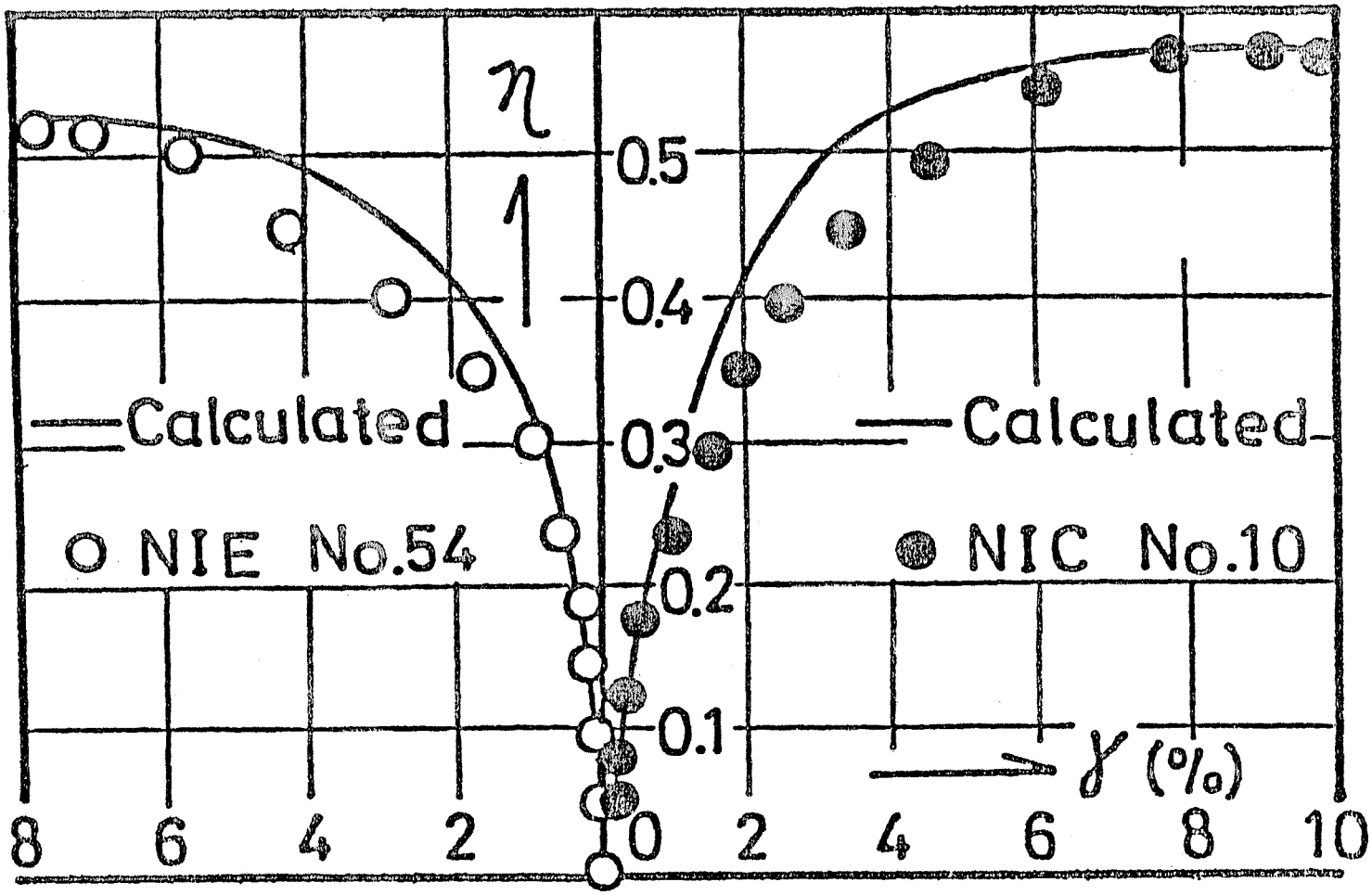

Fig.3-14 Observed and predicted stress ratio-strain relationship by the present author

far as the stress ratio-dilatancy characteristics could be closely approximated by appropriate function, in spite of some criticism on the validity of normality rule in soils.

CHAPTER IV PREDICTION OF STRESS-STRAIN BEHAVIOUR OF K_o CONSOLIDATED CLAY

4.1 Introduction

Geotechnical problems in practice such as slope stability or bearing capacity of foundation are usually solved by using the strength parameters obtained from triaxial compression test conducted under initial isotropic stress condition. However, the stress and strain conditions of soil elements differ from each other by the position they exist in situ. In general, the stress-strain-strength properties of soils are greatly influenced by the stress or strain to which they have been or will be subjected before or during shear. Although it is desirable to test soils under exactly the same conditions as those in situ, laboratory strength tests are usually performed under the condition of isotropically consolidated triaxial compression. Therefore, from the practical point of view, real stress-strain-strength properties of soils which might be obtained only by the special tests simulating the stress and strain conditions in situ would be conveniently related to those obtained from conventional tests for design purpose.

In this chapter, the influence of stress condition during consolidation and stress system during shear on the undrained

stress-strain-strength properties of saturated clay will be shown, and existing methods for predicting stress-strain behaviour of K_o consolidated clay will be outlined. Furthermore, a new method of prediction by using the parameters obtained from conventional triaxial tests and comparison of predicted stress-strain behaviour by this method with observed one will be presented.

4.2 Stress-Strain Behaviour of Clay in K_0 Consolidated Undrained Test

4.2.1 Stress ratio-strain relationship and effective stress path

Figs.4-1 and 4-2 illustrate the octahedral stress ratio-strain relationship for 6 series of test. In these figures, η represents the ratio of octahedral shear stress τ to octahedral effective normal stress p, and γ and p_o are octahedral shear strain and octahedral effective normal stress after consolidation, respectively. As can be seen from these figures, the stress ratio-strain curves in each test series are almost the same irrespective of the magnitude of consolidation pressure, and the curves of NIEL test almost coincide with those of NIE test. This may also be true for the relationship between NK_0EL and NK_0E test, although the scattering of the data is relatively large.

In NIE and NIEL test, axial stress is equal to the minor principal stress σ_3', and the other two principal stresses σ_1', σ_2' are equal to each other in magnitude and major one, whereas in NIC test σ_2' is equal to σ_3'. In NK_0E and NK_0EL test, however, axial stress remains initially as major principal stress until the interchange of principal stress directions takes place at about 0.5% of octahedral shear strain, and there-

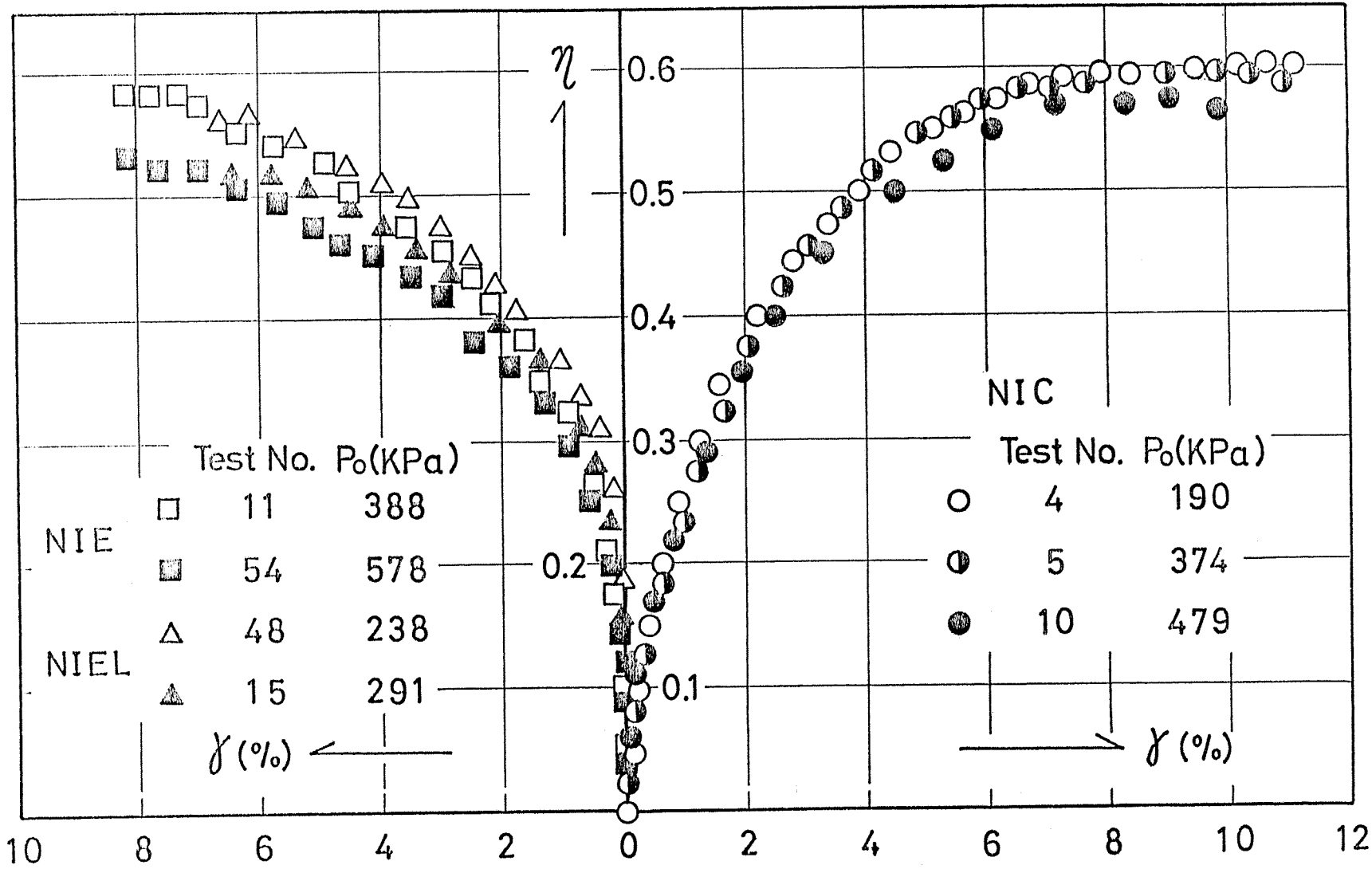

Fig.4-1 Octahedral stress ratio vs. strain relationship

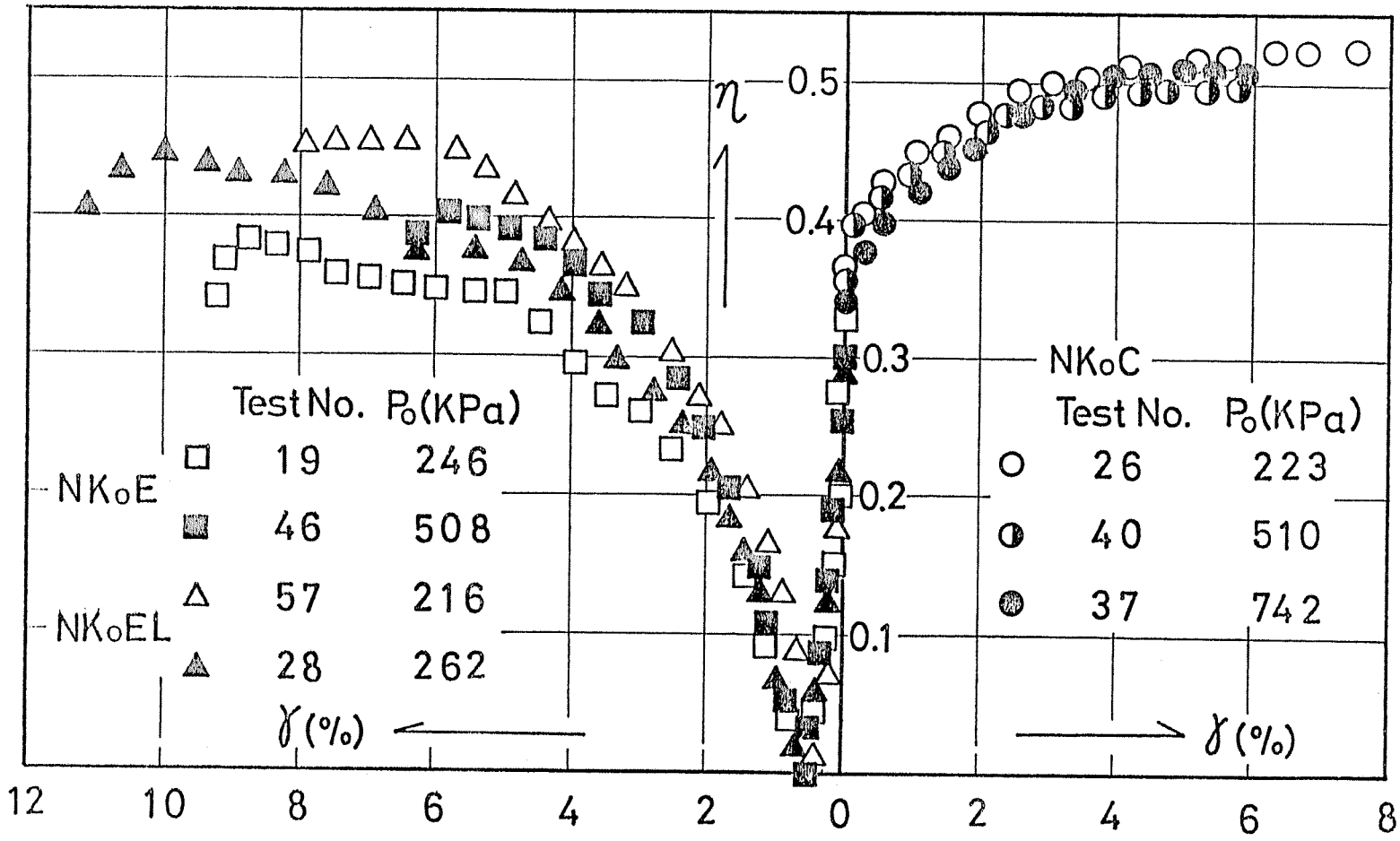

Fig.4-2 Octahedral stress ratio vs. strain relationship

after it is transfered to minor one. On the other hand, in NK_oC test, axial stress is always the major principal stress, because the interchange of principal stress directions does not occur in this test, and the cell pressure is always the minor principal stress, which is equal to the intermediate one in magnitude. Therefore, it can be concluded that the difference of stress system (or the difference of relative magnitude of intermediate stress) during shear affects the stress ratio-strain relationship, but the type of stress change, i.e. increasing or decreasing, in extension tests gives little influence upon the stress ratio-strain properties of clay, irrespective of the stress system during consolidation.

Figs.4-3 and 4-4 show the effective stress paths in the octahedral stress space for 6 series of test. Fig.4-5 illustrates typical stress paths among the 6 series of test, normalized by the octahedral effective normal stress after consolidation. Parry and Nadarajah(1973) reported that there is a distinct measure of symmetry about the $\tau = 0$ line for compression and extension test stress paths for isotropically consolidated specimens. As can be seen in Fig.4-3 to 4-5 inclusive, however, the test results of the present author do not show the symmetry of stress paths.

The stress paths for both NIE and NIEL test in Fig.4-5 seem to almost coincide with each other. This coincidence is also seen between the stress paths of NK_oE and NK_oEL test.

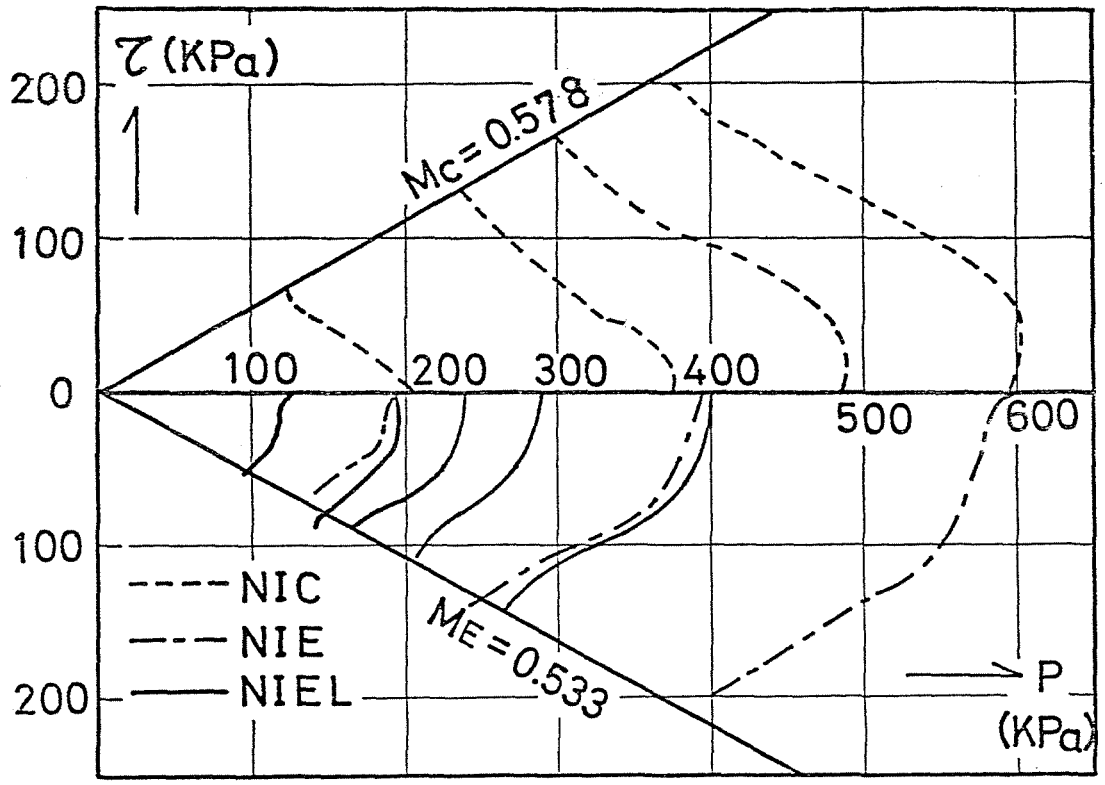

Fig.4-3 Effective stress paths in octahedral stress space

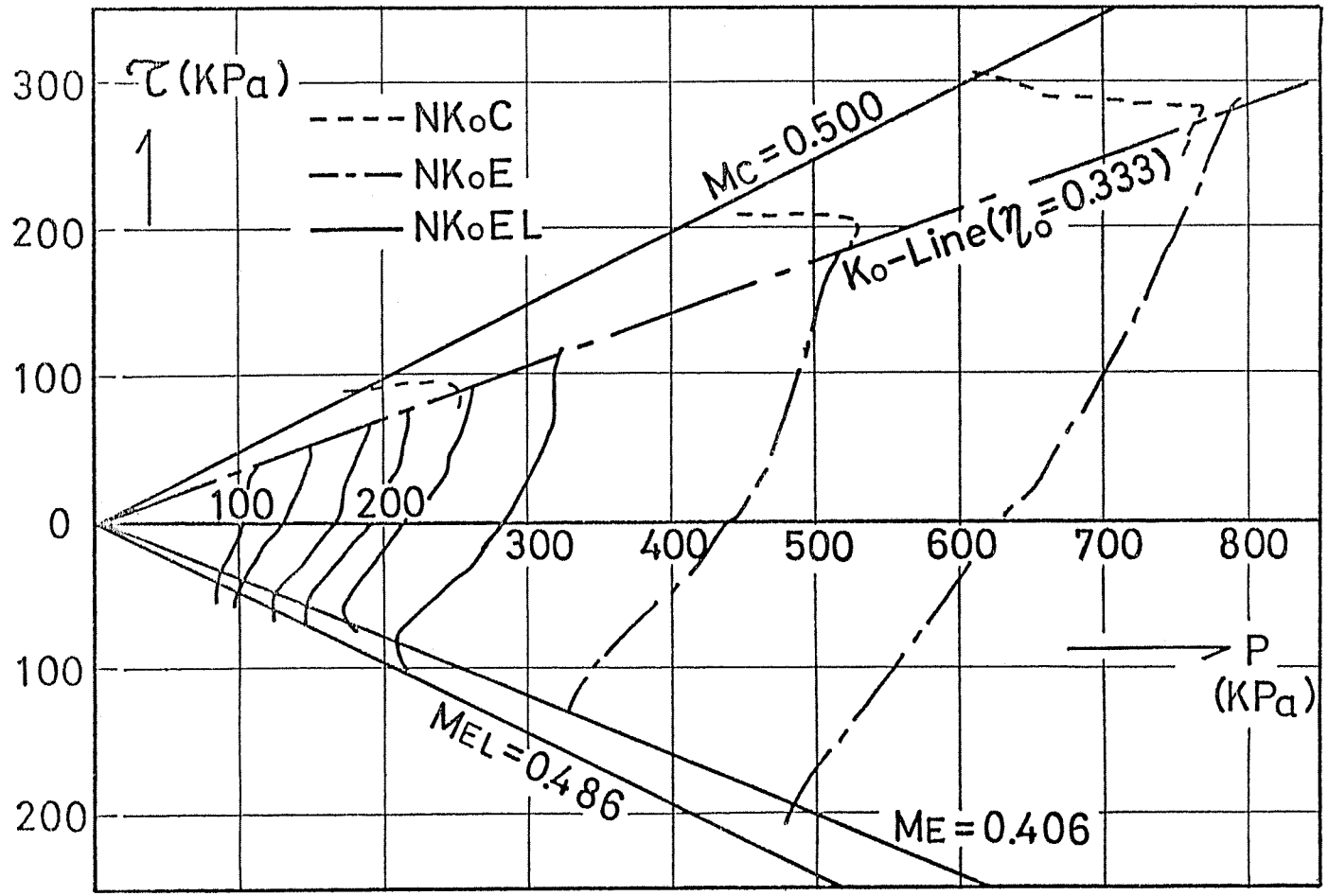

Fig.4-4 Effective stress paths in octahedral stress space

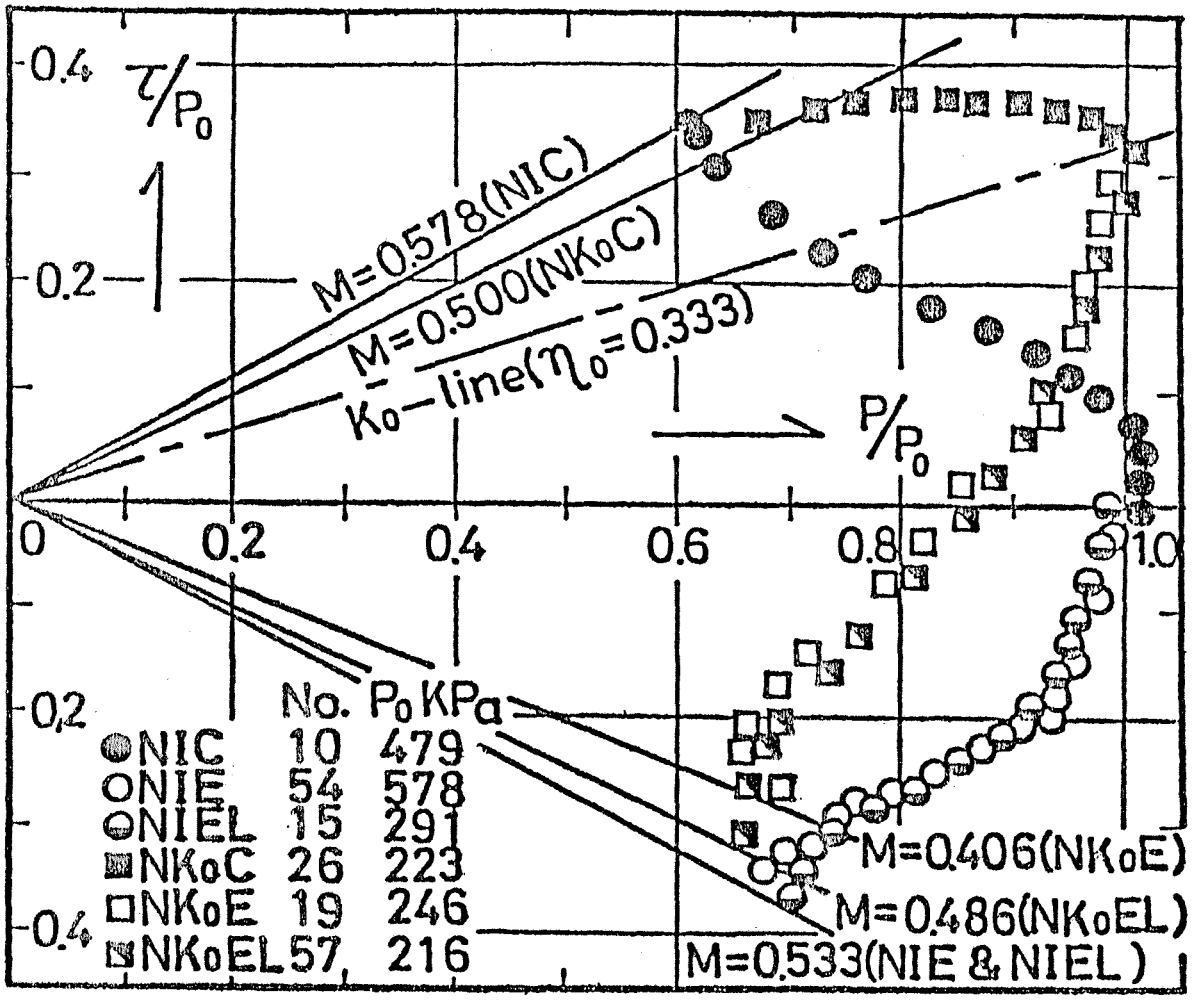

Fig.4-5 Comparison of normalized stress paths obtained from six series of test

From the η versus γ and τ versus p relationships mentioned above, it may be concluded that the type of stress application, i.e. increasing or decreasing stress, during shear does not affect the effective stress-strain behaviour of clay irrespective of the stress system during consolidation, as far as the magnitude of σ_2' during shear is equal to σ_1' or it is equal to σ_3'.

4.2.2 Fffective strength parameter ϕ', and undrained shear strength

Effective angle of shearing resistance ϕ' determined from the deviator stress maximum criterion, and the ratio of undrained shear strength S_u to effective vertical consolidation pressure p_v for 6 series of test are listed in Table 4-1. Paying attention to the ϕ' values of extension tests, those of NIE and NIEL are almost coincident, but those of NK_oE and NK_oEL differ as much as 8 degrees. This difference can be attributed to significant develoment of pore pressure in NK_oEL test, reducing effective mean stress at failure as small as 200kPa, whereas the cell pressure at failure rose as high as 800 kPa. Thus the data points at failure concentrated around the range of 0 to 200kPa of effective mean principal stress as shown in Fig.4-4, and this seemed to make the calculated value of ϕ' larger than the actual one.

Table 4-2 shows the comparison of the published data on ϕ' value, where suffix C and E denote compression and extension test, respectively. Although it has been reported that the stress anisotropy during consolidation does not make any difference on the ϕ' value in compression test for normally consolidated clay (Henkel and Sowa 1963, Akai and Adachi 1965, et al.), taking especially into account of the test results by Parry and Nadarajah (1973) and those by the present author, it should rather be concluded that the ϕ' values both in com-

Consol. Condition	ϕ_c' (°)	ϕ_E' (°)	ϕ_{EL}' (°)	$\sin\phi_c'/\sin\phi_E'$	$(Su/p_v)_c$	$(Su/p_v)_E$	$(Su/p_v)_{EL}$	Suc/SuE	I_p (%)
Iso.	30.6	44.2	44.4	0.73	0.383	0.382	0.405	0.95	49
K_o	26.8	30.2	38.5	0.90	0.301	0.192	0.235	1.57	49
Iso.('76)	34.5	46.1	——	0.79	0.40	0.38	——	1.05	20
K_o ('76)	32.0	42.4	——	0.79	0.32	0.21	——	1.52	20

Table 4-1 Strength parameters obtained from 6 series of test on Sample No.4 including those from earlier ones (Kitago et al., 1976)

Authors	Henkel	Parry	Parry et al.		Ladd	Vaid et al.	Leon et al.	Lade	Shibata et al.	Wu et al.	Broms et al.
	('60)	('60)	('73)		('65)	('74)	('77)	('76)	('65)	('63)	('65)
Consol. Condition	Iso.	Iso.	Iso.	K_0	K_0	K_0	Iso.	Iso.	Iso.	Iso.	Iso.
ϕ_c' (°)	21.7	22.6	22.6	20.8	26.5	29.8	44	29.3	33.7	33.2	29.2
ϕ_E' (°)	21.1	21.3	20.5	28.0	38.8	33.8	78	32.5	33.7	33.1	36.0
$\sin\phi_c'/\sin\phi_E'$	1.03	1.06	1.10	0.75	0.71	0.89	0.71	0.91	1.00	1.00	0.83
$(Su/p_v)_c$	0.28	0.29	0.215	0.205	0.33	0.268	0.51	0.49	0.42	0.50	0.43
$(Su/p_v)_E$	0.23	0.24	0.205	0.175	0.165	0.168	0.51	0.45	0.37	0.33	0.34
Suc/Su_E	1.22	1.21	1.05	1.17	2.00	1.59	1.00	1.09	1.14	1.52	1.26
I_p (%)	25	25	32	32	15	18	290	30	49	24	25

Table 4-2 Comparison of published data on strength parameters obtained from undrained compression and extension tests

pression and extension are affected to a certain degree by the stress anisotropy during consolidation.

Fig.4-6 illustrates the comparison of ϕ' values between compression and extension tests. The values with cross mark in this figure were obtained from the experiments using clay-glass beads mixtures (Kitago et al. 1978) which indicate that the ratio of the ϕ_C' to ϕ_E' decreases with the increase in plasticity index. The test results by other reseach workers on clay, however, do not exihibit a distinct trend. In any case, the difference between ϕ_C' and ϕ_E' is greater in K_O consolidated clay than in isotropically consolidated one.

Comparison of published data of undrained shear strength in compression with those in extension is shown in Table 4-2. Fig.4-7 also illustrates the published data on this subject including those of the present author. From this figure and Table 4-2, it can be seen that the value of S_u/p_v is greatly influenced by the difference of stress system, especially in K_O consolidated clay. Ladd(1973) performed 3 series of consolidated undrained test and presented the undrained strength ratio of triaxial compression to direct shear, and the ratio of triaxial extension to direct shear. He concluded that each ratio approaches asymptotically to unity as the plasticity index of clay increases. Solid line in Fig.4-7 is obtained by using average values of Ladd's data. Cross marks in this figure are the data on clay-glass beads mixtures mentioned above. Although the data points of present author including those by other

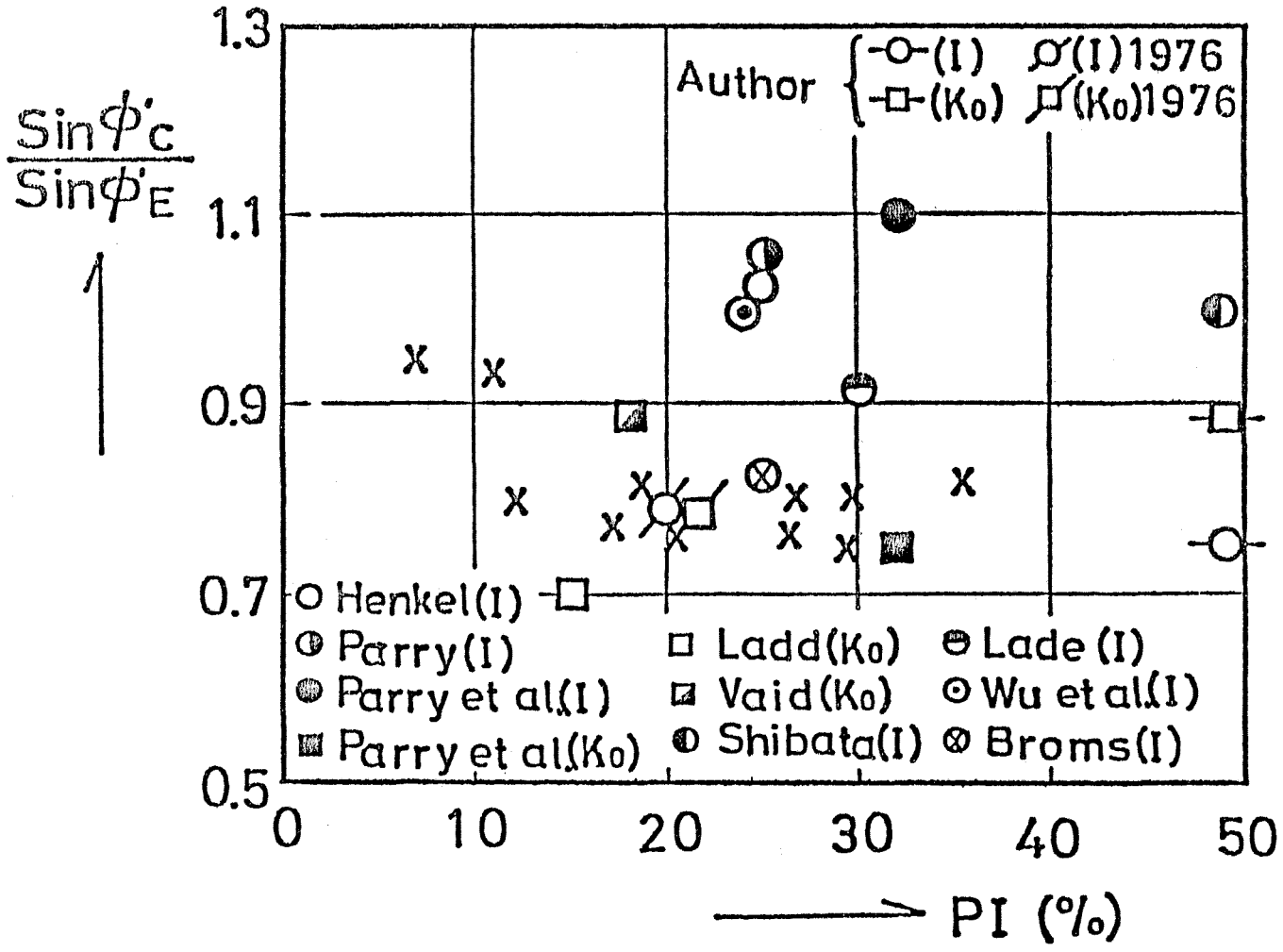

Fig.4-6 Ratio of ϕ' value by compression to that by extension tests

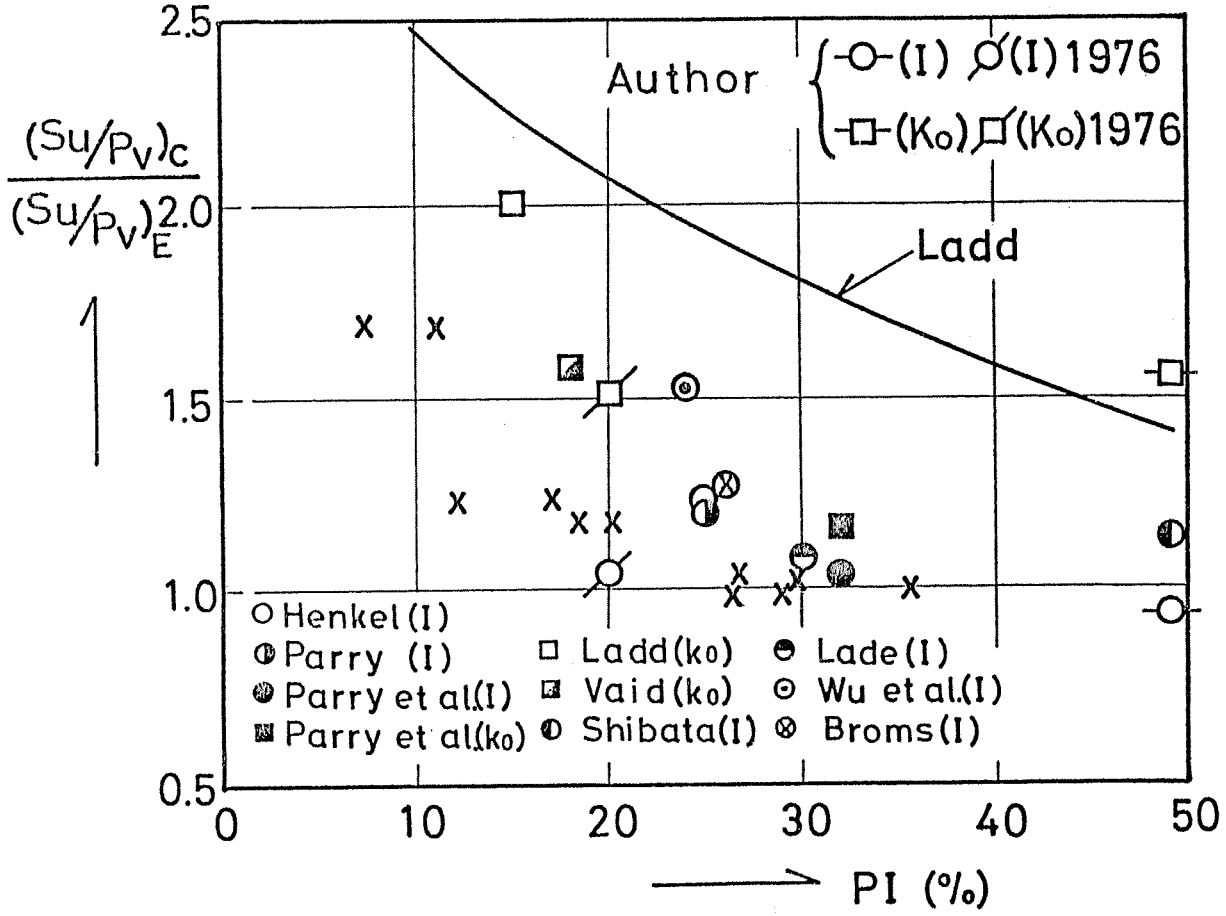

Fig.4-7 Undrained strength ratio vs. plasticity index

research workers have considerable deviation from Ladd's experimental line, they have a general trend that the ratio approaches to unity with the increase of plasticity index.

Parry (1971) deduced an equation to represent the ratio of S_u/p_v in compression to that in extension, assuming that the value of ϕ' is independent of stress paths. However, as mentioned previously, the value of ϕ' is affected by stress system during shear, and so his equation can not always be applied to estimate the undrained strength ratio as already pointed out by Shibata (1975) and Mitachi et al.(1976).

Recently, Mikasa et al. (1978) reported that the S_u/p_v ratio for K_o consolidated specimen is almost equal to that for isotropically consolidated one, especially for clays with higher plasticity (PI = 75%). This fact and the trend shown in Fig.4-7 may probably be subjected to common rule, i.e. the higher the plasticity of clay, the smaller the influences of stress anisotropy during consolidation and stress system during shear on the undrained strength.

4.3 Existing Methods for Estimating Stress-Strain Behaviour of K_o Consolidated Clay

In the Cam-clay model, normally consolidated clay is idealized as an elastoplastic material exhibiting isotropic strain hardening.

Sekiguchi and Ohta (1977) explained the inadequacy of the assumption that the yield loci expand isotropically with the increase of plastic strain, as follows.

A clay specimen consolidated under K_o condition along the line O-a in Fig.4-8 is now considered. According to the Cam-clay model, the specimen undergoes successive yielding in the process of consolidation, and the yield loci expand exactly in the same manner on both compressional and extensional sides, while the straining is carried out on the compressional side only. Thus the yield loci OBA, OCA are symmetric about the axis of $\sigma_a' = \sigma_r'$, where σ_a' and σ_r' are the effective axial and radial stresses, respectively.

Undrained stress path in undrained extension test starting at point a is predicted as follows. As mentioned above, the yield loci have already expand, on the extensional side, to the curve OCA. Therefore, yielding would not occur until the effective stress path touches the yield locus OCA. This means that the undrained effective stress path on the extensional side should follow line a-b, on which the mean effective stress p

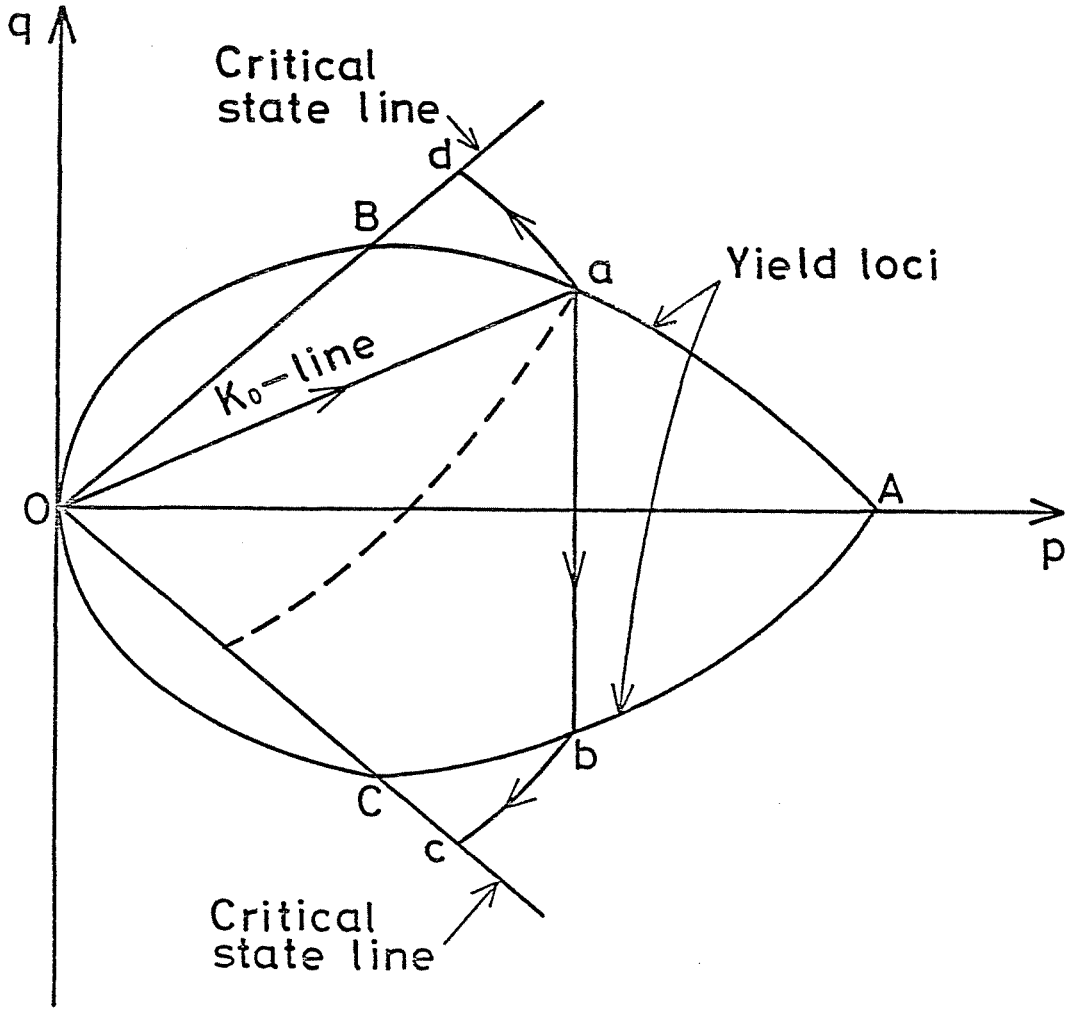

Fig.4-8 Yield loci for compression and extension test (after Sekiguchi and Ohta, 1977)

remains unchanged, because non-occurrence of yielding under undrained conditions leads neither to plastic nor to elastic changes in volumetric strain. And after reaching the yield locus OCA, the undrained effective stress path will now follow curve b-c, and finally reach a critical state at point c.

In K_0 consolidated undrained compression test, on the other hand, an effective stress path predicted by the Cam-clay model is curve a-d in Fig.4-8. It should be noted that the curves a-d and b-c are symmetric about the axis of $\sigma_a' = \sigma_r'$.

There are a number of experimental evidence indicating that in normally K_0 consolidated clays, effective stress path during undrained extension test is something like the dotted curve in Fig.4-8, being far from the curve a-b-c aforementioned. As implied in Fig.4-8, the Cam-clay model predicts that undrained strength of a K_0 consolidated clay in extension test is the same as that in compression test. However, the experimental results mentioned previously in section 4.2 shows the distinct anisotropy in undrained strength of K_0 consolidated clay.

Sekiguchi and Ohta suggested that such inadequacy of assuming isotropic strain hardening for K_0 consolidated clays mentioned above are primarily due to ignoring the influence of the interchange of principal stress directions on their dilatancy characteristics.

They assumed as

$$\delta v = \mu \cdot \delta \eta$$

under 'active loading', where η increases from its initial value, and

$$\delta v = -\mu \cdot \delta \eta$$

under 'passive loading', where η decreases initially from its initial value. They also assumed that the soil constants λ, κ and μ remain essentially unchanged.

Pender(1978) proposed a model for the behaviour of anisotropically overconsolidated soil. Proposed model is based on four assumptions, three of which are the same as in original and modified Cam-clay theories. In addition to these assumptions, three hypotheses were built up. Second and third hypotheses are as follows.

The second hypothesis is that the generalized form of the undrained stress path is

$$\left(\frac{\bar{\eta}-\bar{\eta}_0}{A\bar{M}-\bar{\eta}_0}\right)^2 = \frac{p_{cs}}{p}\left\{\frac{1-p_0/p}{1-p_0/p_{cs}}\right\}$$

where p_{cs} is the value of effective mean principal stresses at the point on the critical state line corresponding to the current void ratio and A is +1 for loading towards the critical

state in compression and -1 for extension.

The third hypothesis is that the ratio of plastic distorsion increment to the volumetric strain increment is given by

$$\frac{d\varepsilon^p}{d\upsilon^p} = \frac{(A\bar{M}-\bar{\eta}_0)^2}{(A\bar{M})^2(p_0/p_{cs}-1)\{(A\bar{M}-\bar{\eta}_0)-(\bar{\eta}-\bar{\eta}_0)p/p_{cs}\}}$$

Above equation is the generalization of the equation in Table 3-1.

In order to predict the stress-strain behaviour of anisotropically consolidated clay by using this model, four soil constants are required. These are $\bar{M}$, λ, κ and Γ, which are the same parameters needed for the Cam-clay models.

The predicting methods by Sekiguchi and Ohta, and by Pender both have the same problem concerning the determination of the value of κ as in the predicting method of the stress-strain behaviour of isotropically consolidated clay.

Lewin (1975) suggested a method to obtain the undrained stress path for anisotropically consolidated clay using that of isotropically consolidated clay. Proposed method, which is based on the extensive experiments (Lewin and Burland 1970, and Lewin 1973), is as follows. Rendulic stress path for isotropically consolidated undrained test is regarded as being symmetrical about the space diagonal. For a specimen consolidated anisotropically along the anisotropic consolidation line at an angle α to space diagonal, the new axis of symmetry is drawn at an

angle θ from the 'hinge point' taken to be halfway along the space diagonal (see Fig.4-9). Then stress path for anisotropically consolidated specimen is produced by rotating the stress path for isotropically consolidated specimen by the angle θ about the hinge point, where the relationship between α and θ for a soil must in advance be determined experimentally.

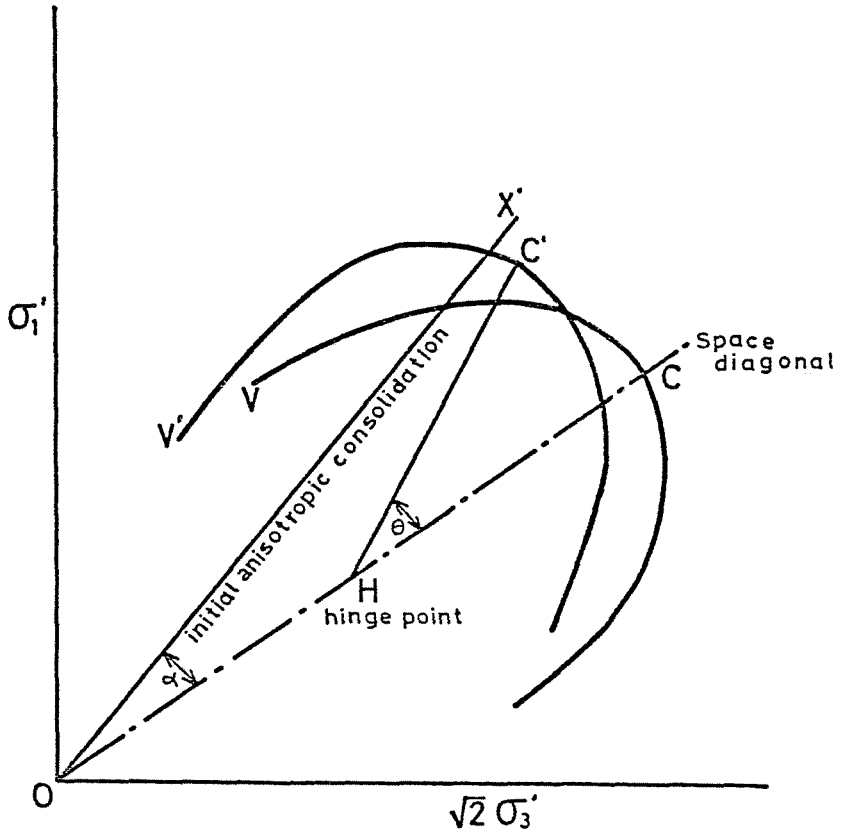

Fig.4-9 Undrained stress paths for anisotropically consolidated clay (after Lewin, 1975)

4.4 Proposed Method for Predicting the Stress-Strain Behaviour of K_o Consolidated Clay

4.4.1 Assumptions

Referring to the methods mentioned above, the present author made following hypotheses in order to establish the predicting method of stress-strain relationship for K_o consolidated clay.

1) Stress path for K_o consolidated compression test

Stress path for NK_oC test in $p/p_o - \tau/p_o$ co-ordinate is similar to that obtained by rotating the NIC stress path by an angle θ_o after shifting the NIC stress path from the point (1,0) to $(1, \tau_o/p_o)$, where

$$\theta_o = \tan^{-1} \tau_o/p_o$$

and p_o and τ_o are the octahedral normal and shear stresses after K_o consolidation.

2) Stress path for K_o consolidated extension test

Stress path is similar to that obtained by rotating the NIE stress path by an angle $\theta_o/2$, after shifting the NIE stress path from the point (1,0) to $(1, \tau_o/p_o)$. In addition, the effective mean stress at failure is equal to that of isotropically consolidated specimen.

Two hypotheses mentioned above are based on the following consideration that the stress-strain-strength properties of initially K_0 consolidated clay are clearly different from isotropically consolidated clay due not only to induced anisotropic stress system but also to structural anisotropy developed during consolidation. The present author assumed that the stress anisotropy is covered by shifting the starting point of shear from $\tau = 0$ plane to $\tau = \tau_0$ plane. Although quantitative evaluation of structural anisotropy is a difficult problem to solve, it may roughly be done as follows. Structural difference between test specimens after K_0 and isotropic consolidation appears markedly in compression test, because the direction of major principal stress during shear is the same as that in consolidation. Therefore, the structural difference for this case is assumed as being expressed by the magnitude of rotating angle θ_0. On the other hand, structural difference between NIE and NK_0E almost disappears during initial part of shear, during which interchange of principal stress directions occurs, and the stress-strain behaviour during latter part of shear is almost the same in two tests, especially at critical state. These considerations lead to the assumption that the difference may roughly be expressed by the angle $\theta_0/2$ and the effective mean stress at failure in NK_0E test is almost equal to that in NIE test.

4.4.2 Predicted stress-strain behaviour

Based on the preceding hypotheses, prediction of NK_oC and NK_oE stress-strain relationship using NIC and NIE test data will be made.

1) Prediction of stress-strain behaviour from NIC test data

As shown in preceding section, stress ratio-dilatancy characteristics in NIC test is expressed approximately by Eq.(3-85). Shifting these relations from $F(\eta) = 0$ at $\eta = 0$ to $F(\eta) = 0$ at $\eta = \eta_o$, following equations are obtained.

$$F_1(\eta) = \mu_1(\eta - \eta_o) \quad \text{for} \quad 0 < \eta - \eta_o \leqq \eta_1 \tag{4-1a}$$

$$F_2(\eta) = \mu_1\eta_1 + \mu_2(\eta - \eta_o - \eta_1) \quad \text{for} \quad \eta - \eta_o > \eta_1 \tag{4-1b}$$

Octahedral effective normal and shear stresses normalized by the initial octahedral normal stress p_o at any value of η ($\eta > \eta_o$) after shifting the NIC stress path are represented, referring to Eq. (3-72), as follows

$$p/p_o = \exp\left[-\frac{1+e_o}{\lambda} F(\eta)\right] \tag{4-2a}$$

$$\tau/p_o = \eta \cdot p/p_o \tag{4-2b}$$

Next step is to rotate the stress path by an angle θ_o around

the point $(1, \tau_0/p_0)$. Then, the co-ordinates of stress point after rotation are represented, referring to Fig. 4-10, as follows

$$\tau'/p_0 = \eta_0 + \sqrt{(\tau/p_0 - \eta_0)^2 + (1 - p/p_0)^2}\ \cos(\beta + \theta_0) \qquad (4\text{-}3a)$$

$$p'/p_0 = 1 - \sqrt{(\tau/p_0 - \eta_0)^2 + (1 - p/p_0)^2}\ \sin(\beta + \theta_0) \qquad (4\text{-}3b)$$

where

$$\beta = \tan^{-1} \frac{p_0 - p}{\tau - \tau_0}$$

Combination of Eqs. (3-72) with (3-93b) gives a new $F(\eta)$ versus η relationship, and new dilatancy equations equivalent to Eq. (3-85) can also be obtained as follows

$$F_1(\eta) = \mu_1'(\eta - \eta_0) \quad \text{for} \quad 0 < \eta - \eta_0 \leqq \eta_1' \qquad (4\text{-}4a)$$

$$F_2(\eta) = \mu_1'(\eta_1' - \eta_0) + \mu_2'(\eta - \eta_1') \quad \text{for} \quad \eta_1' < \eta \qquad (4\text{-}4b)$$

Parameters η_1', μ_1' and μ_2' are equivalent to η_1, μ_1 and μ_2 in Eqs. (4-1a) & (4-1b), respectively. A new strength parameter M' is obtained by putting $\eta = M$ into Eqs. (4-2) and (4-3). Furthermore, replacing the value M and $F(M)$ in Eq. (3-84) by M' and $F(M')$, following equation is obtained.

$$\nu' = \lambda - (1 + e_0) M' F(M') \qquad (4\text{-}5)$$

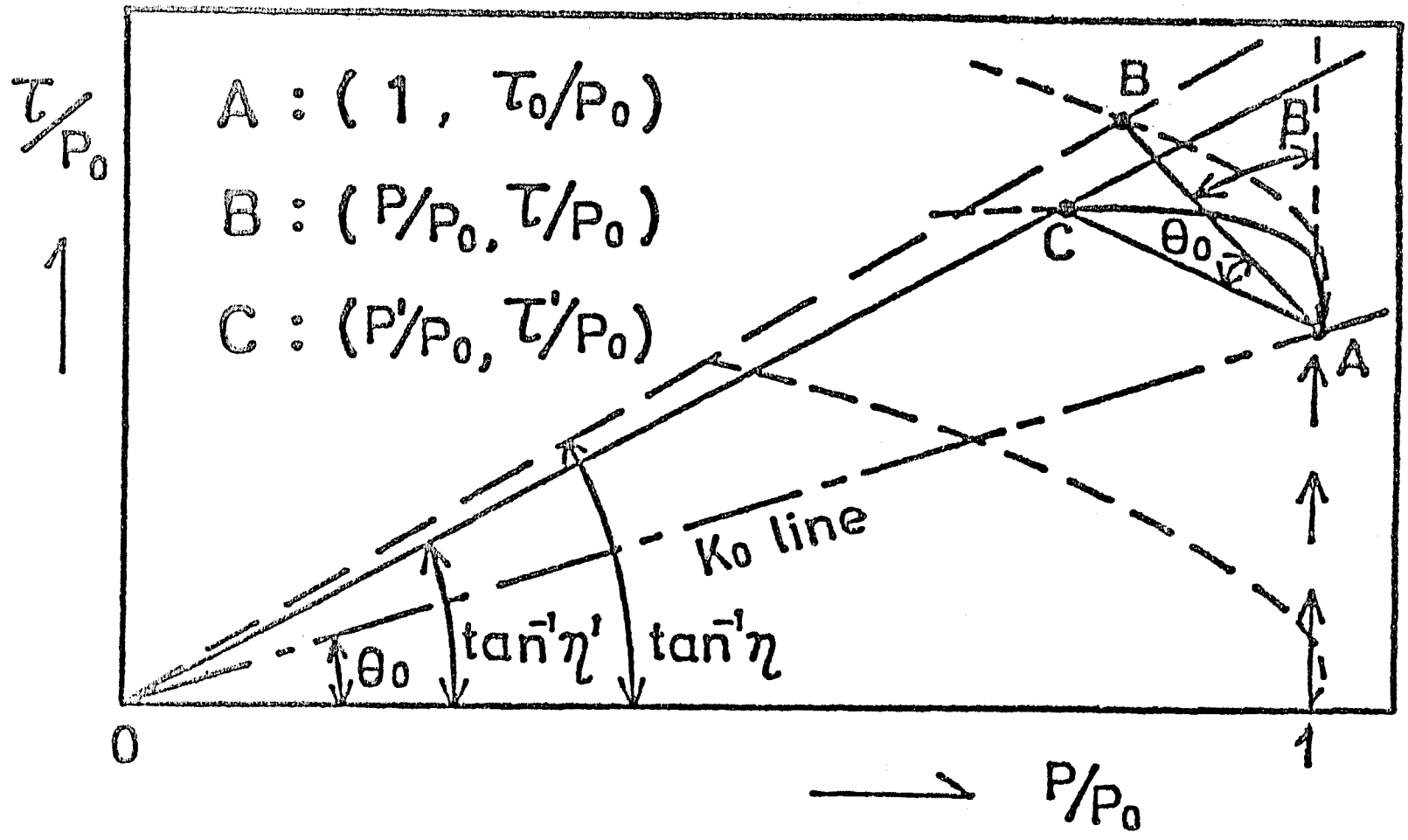

Fig.4-10 Stress path prediction for NK_oC test

Combination of Eqs. (4-4) & (4-5) with Eq. (3-82) and integration of the resulting equations with initial condition $\gamma = 0$ at $\eta = \eta_0$, following stress ratio-strain equations for K_0 consolidated clay can be obtained.

$$\gamma = \frac{\nu' \mu_1'}{3\lambda} \ln \left| \frac{\mu_1' \eta_0 - \frac{\lambda - \nu'}{1 + e_0}}{\mu_1' \eta - \frac{\lambda - \nu'}{1 + e_0}} \right| \qquad \text{for} \quad 0 < \eta - \eta_0 \leqq \eta_1' \qquad (4\text{-}6a)$$

$$\gamma = \frac{\nu'}{3\lambda} \left[\mu_1' \ln \left| \frac{\mu_1' \eta_0 - \frac{\lambda - \nu'}{1+e_0}}{\mu_1' \eta_1' - \frac{\lambda - \nu'}{1+e_0}} \right| + \mu_2' \ln \left| \frac{\mu_2' \eta_1' - \frac{\lambda - \nu'}{1+e_0}}{\mu_2' \eta - \frac{\lambda - \nu'}{1+e_0}} \right| \right] \text{for} \quad \eta_1' < \eta \qquad (4\text{-}6b)$$

2) Prediction of NK_0E stress-strain behaviour from NIE test data

Stress-strain prediction of NK_0E test using NIE test data can be performed by almost the same procedure as in compression test, except that the angle of rotation is $\theta_0/2$ and the effective mean stress at failure is set to be equal in NIE and NK_0E test.

The comparison of the stress paths and stress ratio-strain curves for NK_0C & NK_0E tests predicted by the present method with those observed indicates fairly good agreement as shown in Figs.4-11 & 4-12. By the way, the values of strength parameter M' for NK_0C and NK_0E in Fig. 4-11 are the predicted ones, while the corresponding observed average values are given previously in Fig. 4-4. Comparison of these values with each other indicates a good agreement.

Therefore, estimation is now possible on the undrained compression and extension stress-strain-strength behaviour

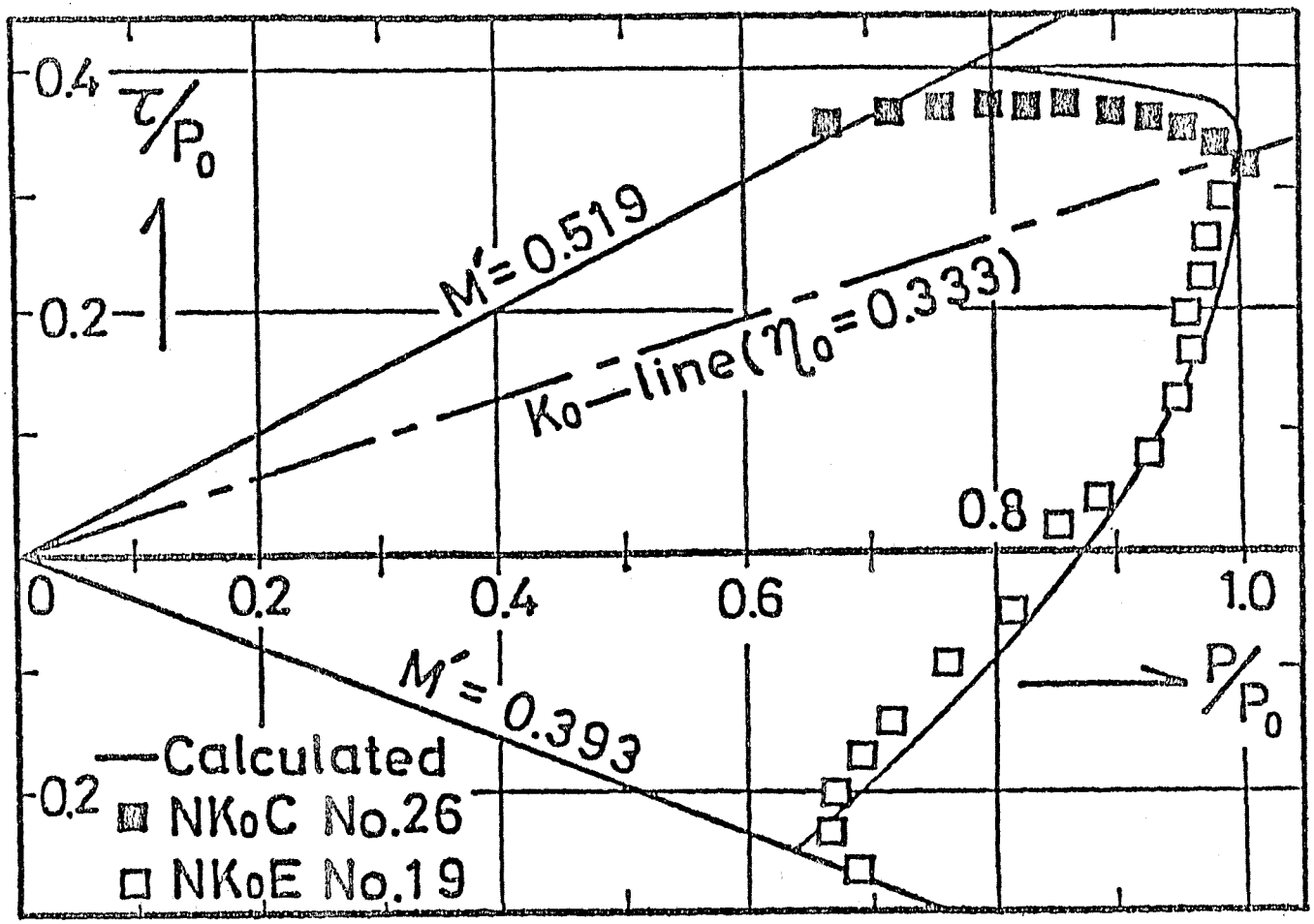

Fig.4-11 Observed and predicted stress paths for K_o consolidated clay

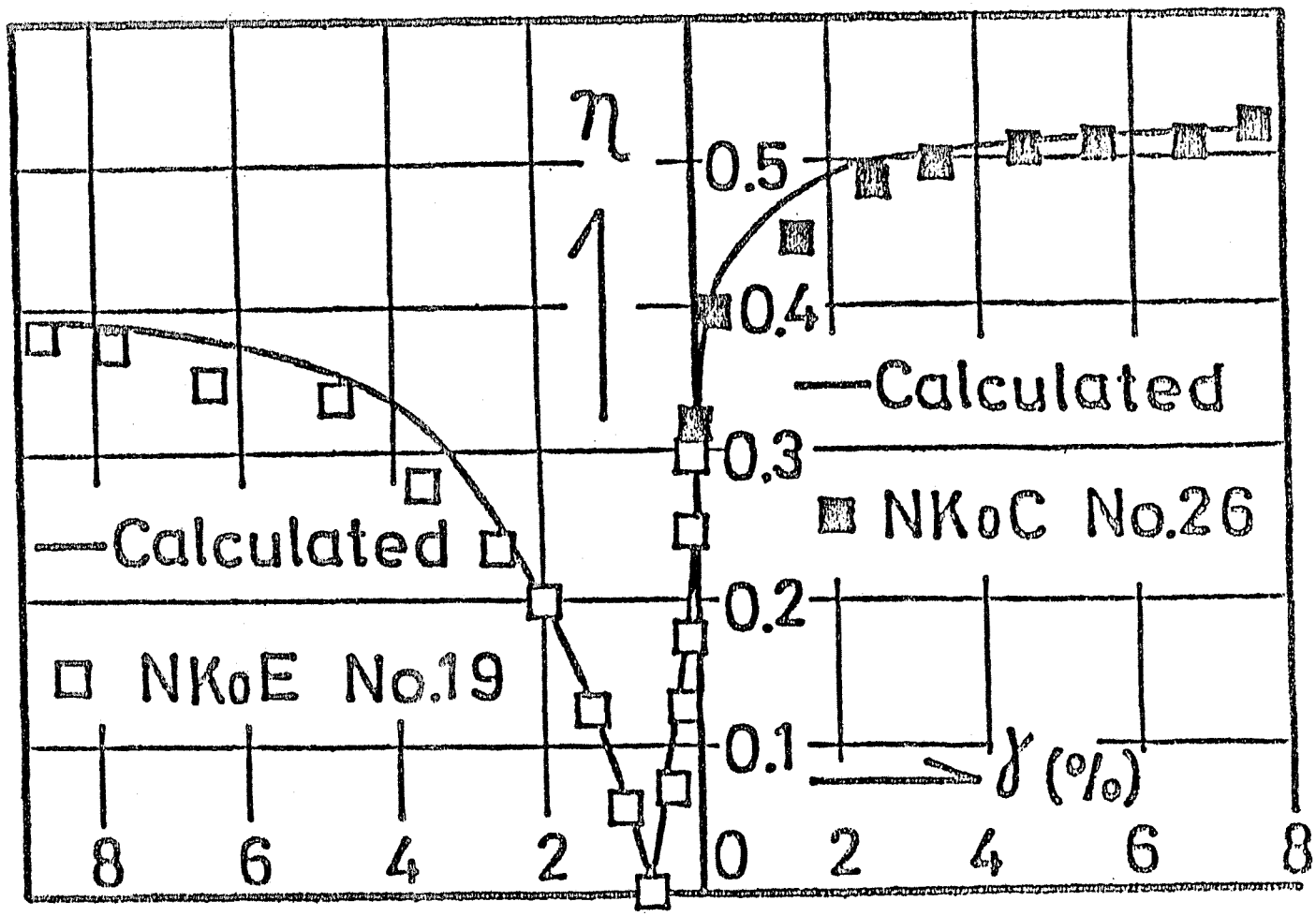

Fig.4-12 Observed and predicted stress ratio-strain relationship for K_0 cosolidated clay

of K_o consolidated clay using the data obtained from isotropically consolidated undrained compression and extension tests. Parameters needed for estimation are the coefficient of earth pressure at rest K_o, strength parameter M, compression index λ and dilatancy function $F(\eta)$.

CHAPTER V STRESS-STRAIN-STRENGTH BEHAVIOUR OF CLAY UNDER PLANE STRAIN CONDITION

5.1 Introduction

In order to estimate the in situ behaviour of soils from laboratory test results, it is essential to test them under exactly the same conditions as exist in situ. Although the deformation conditions of soil in the majority of field problems closely approximate to those of plane strain, test data concerning the shear strength characteristics of cohesive soil under plane strain condition are limited in number. Above all, the data obtained under K_o consolidated plane strain extension condition are extremely limited.

Four series of consolidated undrained test under the condition of plane strain with pore water pressure measurement were performed on a saturated remolded clay to investigate the correlation of triaxial and plane strain test results. Based on the experimental results, a tentative method for predicting stress-strain behaviour of K_o normally consolidated plane strain condition by using the parameters obtained from conventional triaxial test is presented.

5.2 Observed Stress-Strain-Strength Behaviour of Clay in Plane Strain Test

5.2.1 Effective strength parameter ϕ' and undrained shear strength

Table 5-1 shows strength parameters obtained from K_o consolidated plane strain tests including those from isotropically and K_o consolidated axi-symmetrical triaxial tests. The ratio of undrained shear strength S_u to effective vertical consolidation pressure p_v in isotropically consolidated clay is almost the same in compression and extension. But in K_o consolidated clay, S_u/p_v in compression is greater than that in extension by about 35% for plane strain and 60% for axi-symmetrical triaxial tests. It has been reported that the clay particles orientate perpendicular to the direction of major principal stress during anisotropic consolidation. This fact may have resulted in great strength anisotropy of K_o consolidated clay. Effective angle of shearing resistance ϕ' in extension is larger than that in compression by more than 10 degrees for both K_o consolidated plane strain and isotropically consolidated triaxial tests. These results coincide with those from Broms and Casbarian (1965) in isotropically consolidated clay and Ladd(1973), Parry and Nadarajah(1973), and Vaid and Campanella(1974) in K_o consolidated clay.

Karube(1975) suggested following equation representing the

Test Condition	NIC	NIE	NK_oC	NK_oE	NCP	NEP
S_u/P_v	0.383	o.382	0.309	0.192	0.350	0.261
$\phi'(°)$	30.6	44.2	28.1	30.2	33.4	51.0
A_f	0.84	1.12	1.24	0.93	1.06	0.89
M	0.578	0.533	o.526	0.406	0.523	0.576

Table 5-1 Strength parameters obtained from 6 series of test on Sample No.4

strength ratio of undrained compression and extension based on the Cam-clay equation and several assumptions, including one in which ϕ' is assumed as a material constant, irrespective of stress paths.

$$S_{UE}/S_{UC} = \frac{3}{3+\bar{M}} \exp\left\{\frac{\bar{M}}{1.75}\left(\frac{\bar{M}}{3+\bar{M}} - \frac{3}{6-\bar{M}}\right)\right\} \qquad (5\text{-}1)$$

where

$$\bar{M} = \frac{6\sin\phi'}{3-\sin\phi'}$$

Parry(1971) deduced following equations to represent undrained strength ratio of axi-symmetrical compression and extension, and that of axi-symmetrical compression and plane strain, assuming that ϕ' and effective mean stress at failure are independent of stress paths.

$$S_{UE}/S_{UC} = \frac{3-\sin\phi'}{3+\sin\phi'} \quad , \quad S_{UP}/S_{UC} = \frac{3-\sin\phi'}{2(1+m)} \qquad (5\text{-}2)$$

where

$$m = \sigma_y'/(\sigma_x' + \sigma_z') \qquad (5\text{-}3)$$

Fig.5-1 is the plot of undrained strength ratio to effective angle of shearing resistance obtained from Eqs.(5-1) and (5-2), and the author's test results. Some discrepancies seen in the

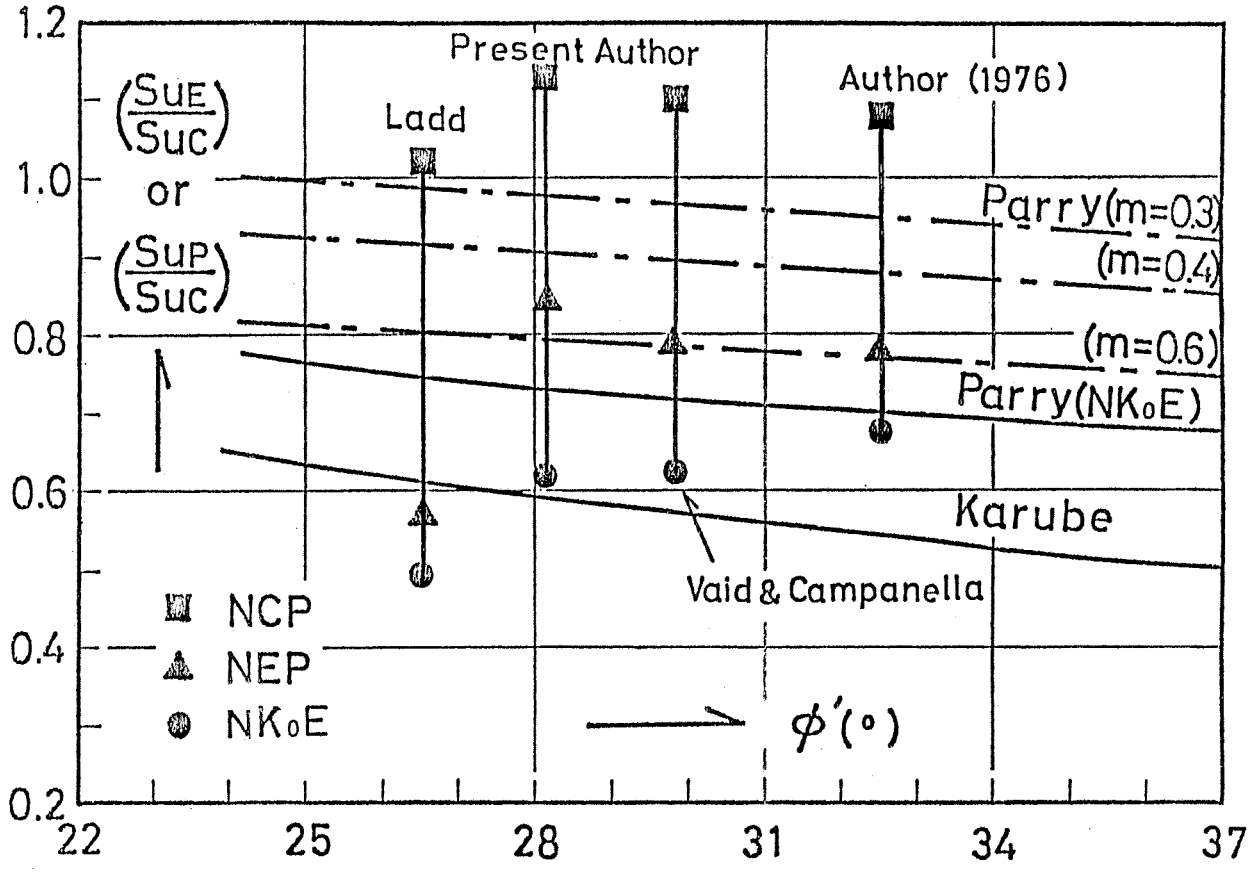

Fig.5-1 Undrained strength ratio vs. effective angle ofshearing resistance

figure between predicted values and experimental data might have come from the fact that the two assumptions on ϕ' and effective mean principal stress are not satisfied simultaneously.

Recently, Prevost(1979) derived following equations representing undrained shear strength of plane strain compression and extension test as a function of undrained shear strength in axi-symmetrical triaxial compression and extension test.

$$(S_{up})_c = \frac{\sqrt{3}}{3}(S_{uc} + S_{uE}) + \frac{1}{2}(S_{uc} - S_{uE})$$

$$(S_{up})_E = \frac{\sqrt{3}}{3}(S_{uc} + S_{uE}) - \frac{1}{2}(S_{uc} - S_{uE})$$

Calculation of the values of S_u/p_v in NCP and NEP test by using the above equations with observed data of NK_oC and NK_oE test in Table 5-1 gives 0.348 and 0.231, respectively. Comparison of these values with observed ones in Table 5-1 indicates a good agreement, especially in NCP test.

5.2.2 Normalized stress-strain behaviour

Stress-strain data of the present test were obtained for more than three steps of consolidation pressure, and for each consolidation pressure two tests were carried out. Typical stress-strain behaviour normalized by preshear effective stress are discussed in this section.

Fig.5-2 illustrates the relationship between stress difference $|\sigma_z - \sigma_x|$ normalized by preshear vertical effective stress $(\sigma_z')_c$ and axial strain ε_z. The curves with cross mark were obtained from axi-symmetrical triaxial tests. This figure indicates that $|\sigma_z - \sigma_x|/(\sigma_z')_c$ versus ε_z relationship is independent of consolidation pressure, and the magnitude of strain at failure in compression test is smaller in plane strain (4 to 5%) than that in axi-symmetrical test (>6%). Henkel and Wade(1966) reported similar results. Decrease in stress difference after its peak has been reached is more distinct in NCP than in NK_oC test. In extension test, the interchange of principal stress directions occurs at about 0.4% axial strain in NEP and 0.8% in NK_oE test. And peak stress difference takes place at 6 to 8% of axial strain in NEP and at 8 to 10% in NK_oE test. Comparing $|\sigma_z - \sigma_x|$ versus ε_z relationship of compression with extension test, it is seen that $|\sigma_z - \sigma_x|$ in compression test is greater than that in extension test at any vertical strain. Vaid and Campanella(1974) reported similar results, using undisturbed clay specimen.

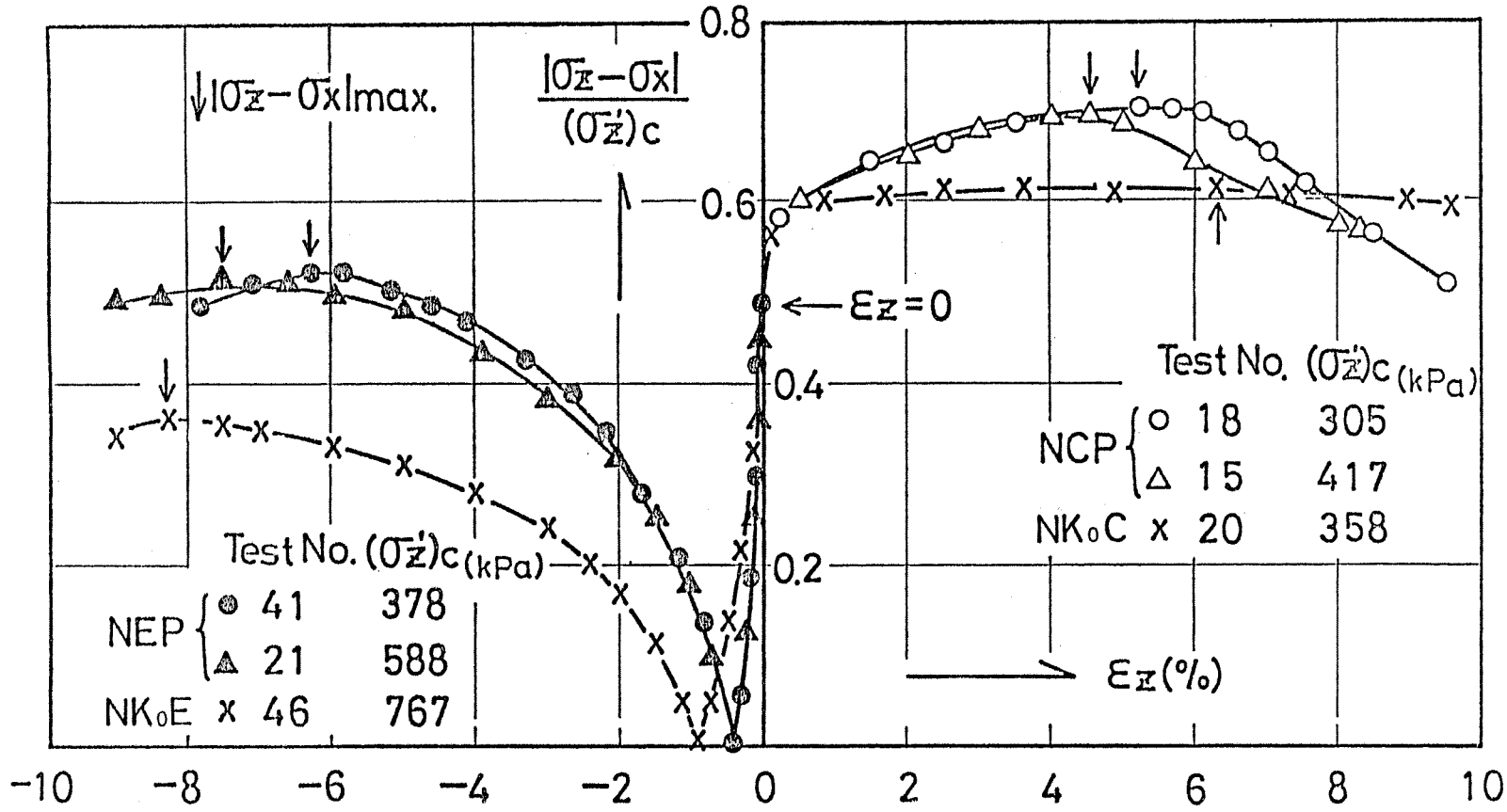

Fig.5-2 Normalized deviator stress vs. axial strain

Stress ratio η versus shear strain γ relationship for normally consolidated plane strain tests mentioned above in octahedral stress plane is shown in Fig.5-3, where octahedral shear stress τ, effective normal stress p and shear strain γ are defined as follows.

$$\tau = \frac{1}{3}\sqrt{(\sigma_x - \sigma_y)^2 + (\sigma_y - \sigma_z)^2 + (\sigma_z - \sigma_x)^2} \tag{5-4}$$

$$p = \frac{1}{3}(\sigma_x' + \sigma_y' + \sigma_z') \tag{5-5}$$

$$\gamma = \frac{1}{3}\sqrt{(\varepsilon_x - \varepsilon_y)^2 + (\varepsilon_y - \varepsilon_z)^2 + (\varepsilon_z - \varepsilon_x)^2} \tag{5-6}$$

Relationships between octahedral shear strain and axial strain in axi-symmetrical and plane strain tests under undrained condition are expressed as follows.

$$\gamma = \frac{1}{\sqrt{2}}\varepsilon_z \qquad \text{for axi-symmetrical test} \tag{5-7}$$

$$\gamma = \frac{\sqrt{6}}{3}\varepsilon_z \qquad \text{for plane strain test} \tag{5-8}$$

In compression test, η versus γ curve in plane strain test is almost identical with that in axi-symmetrical test, whereas in extension test such a coincidence cannot be observed. Rather,

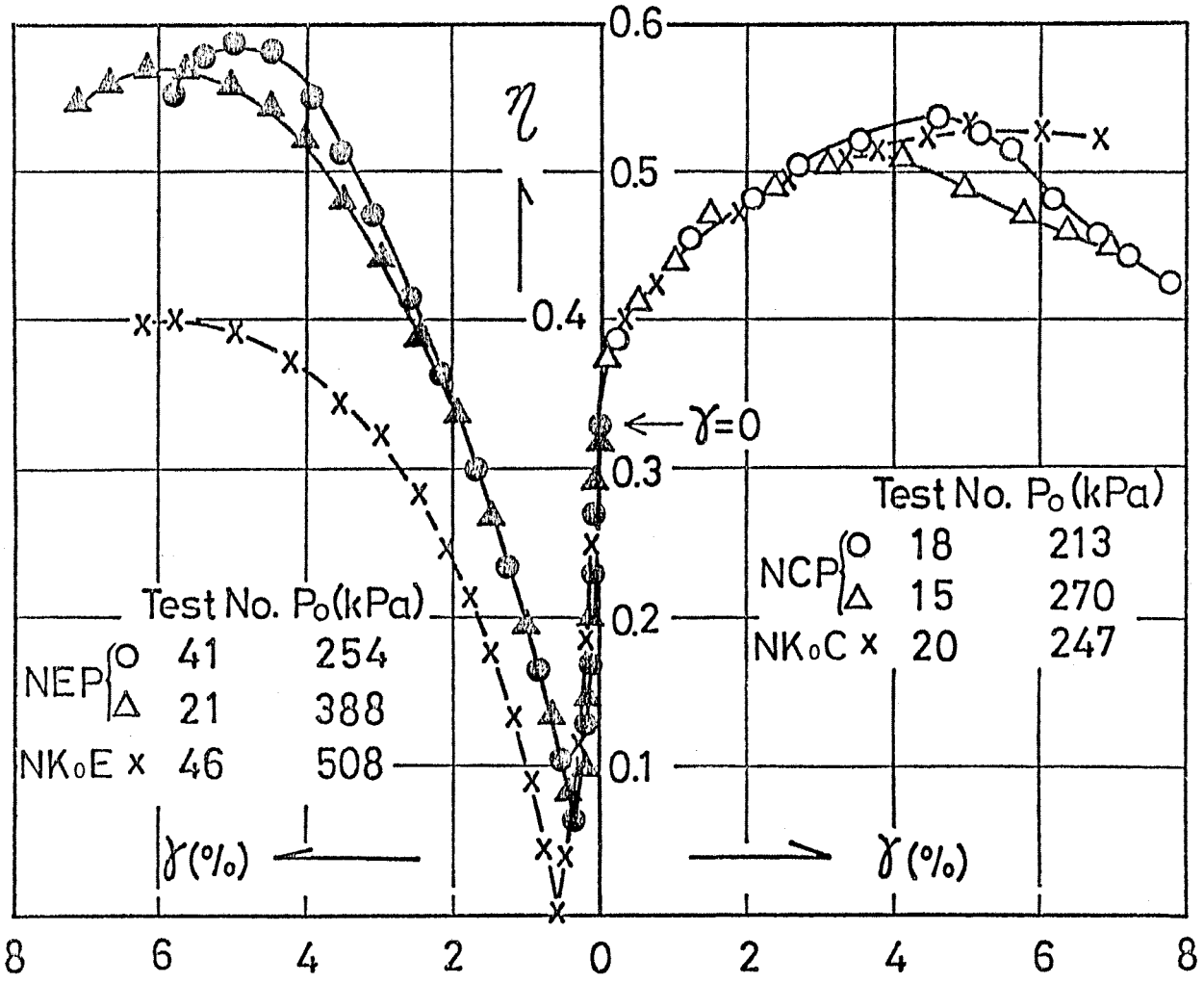

Fig.5-3 Octahedral stress ratio-strain relationship in normally consolidated plane strain tests

there exists a great difference in η versus γ relationship between NEP and NK_oE tests, i.e. τ does not reduce to zero in NEP, whereas it does reduce to zero in NK_oE test when σ_z becomes equal to σ_x during unloading. M, the maximum value of η for the present tests, are computed as shown in Table 5-1.

Fig.5-4 illustrates η versus γ relationship for overconsolidated plane strain compression and extension tests, where n denotes overconsolidation ratio. Although it cannot be concluded whether the η versus γ curves in plane strain test coincide with those in axi-symmetrical test not shown in this figure, because of the lack of test data of plane strain test at the same value of n in axi-symmetrical test, there was a case that the η versus γ curve in plane strain test at $n = 4.9$ almost coincide with that in axi-symmetrical test at $n = 4.2$. It is natural that the stress ratio versus strain relationships at small strain in two types of test for different value of n are different from one another, since the preshear stress ratio differs from one another. It is seen in Fig.5-4 that stress ratio versus strain curves for $n \leqq 6$ converge to a single curve at $\gamma > 10\%$ in two types of test. Although there appears a clear peak in η versus γ curves in compression test, it cannot be found in extension test. It is noticeable that even the curve of $n = 9.9$ in compression test becomes close to that of normally consolidated clay at large strain.

In Fig.5-5, the increment of octahedral shear stress normalized by octahedral normal stress after consolidation is plotted against shear strain. In connection to the expression of octahedral shear stress increment, the following three equations have been suggested.

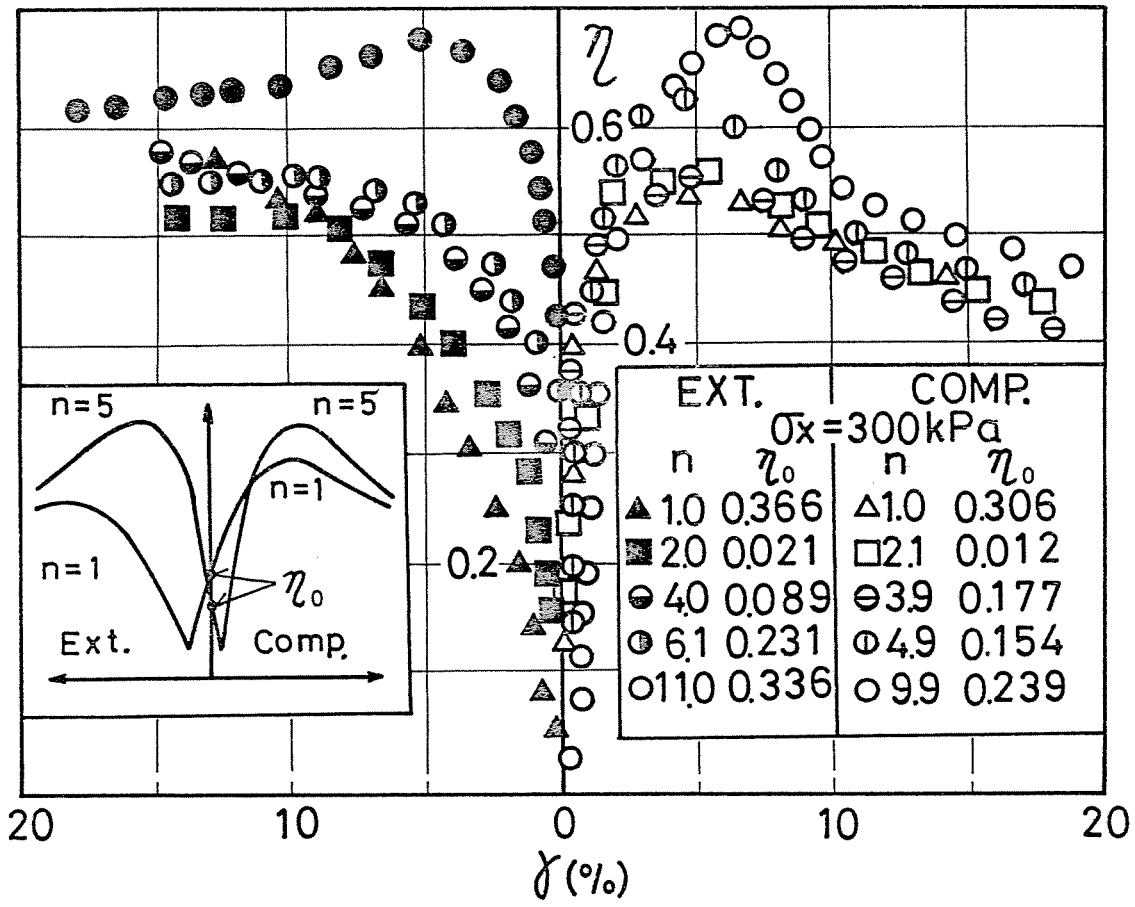

Fig.5-4 Octahedral stress ratio-strain relationship in overconsolidated plane strain tests

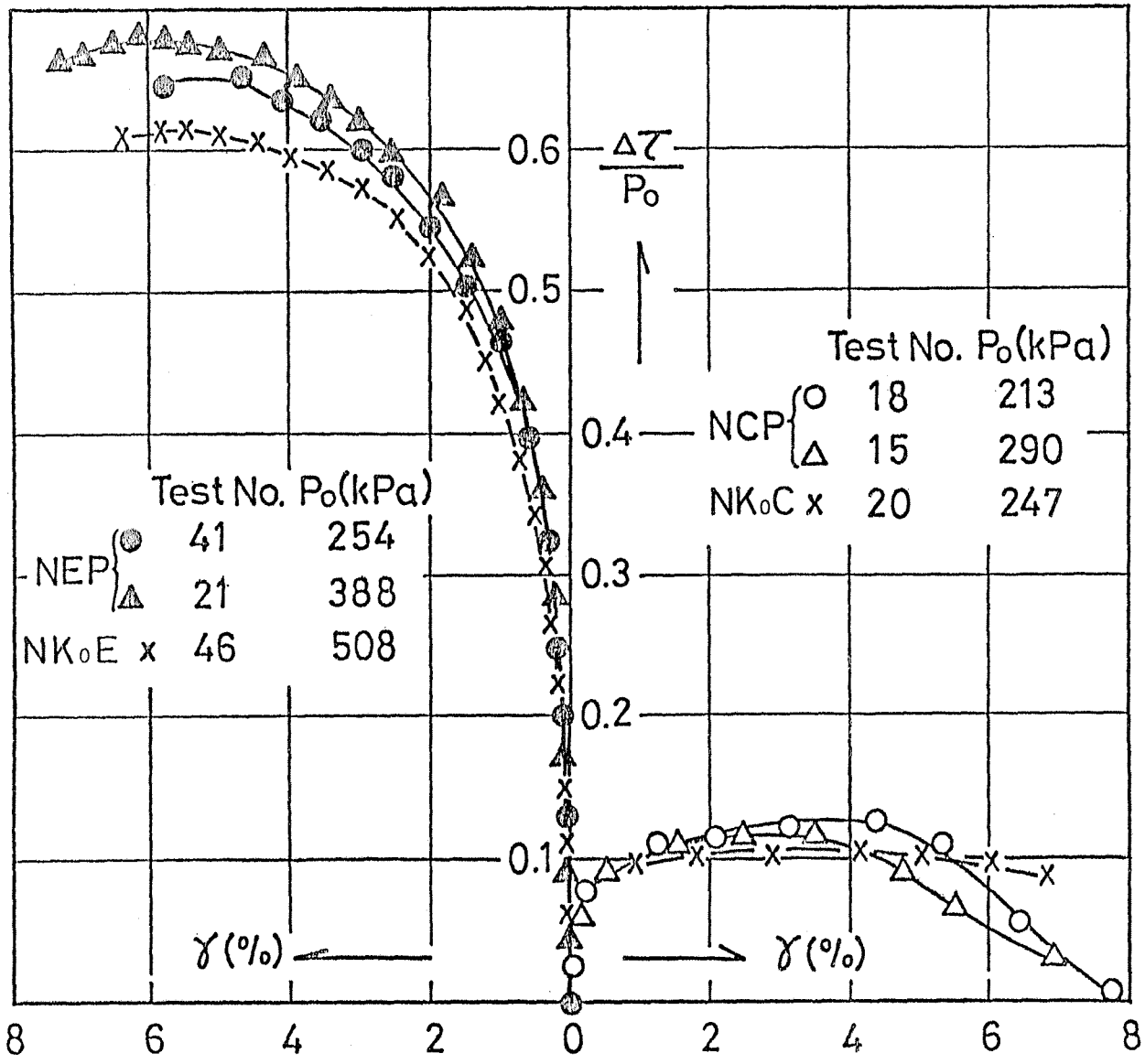

Fig.5-5 Octahedral shear stress increment vs. shear strain

$$\Delta\tau_1 = \frac{1}{3}\sqrt{(\Delta\sigma_1-\Delta\sigma_2)^2+(\Delta\sigma_2-\Delta\sigma_3)^2+(\Delta\sigma_3-\Delta\sigma_1)^2} \quad (5\text{-}9)$$

$$\Delta\tau_2 = \frac{1}{3}\Delta\sqrt{(\sigma_1-\sigma_2)^2+(\sigma_2-\sigma_3)^2+(\sigma_3-\sigma_1)^2} \quad (5\text{-}10)$$

$$\Delta\tau_3 = \frac{1}{3}\sqrt{(\Delta\sigma_x-\Delta\sigma_y)^2+(\Delta\sigma_y-\Delta\sigma_z)^2+(\Delta\sigma_z-\Delta\sigma_x)^2} \quad (5\text{-}11)$$

Comparing Eqs.(5-9) with (5-11), $\Delta\tau_1 = \Delta\tau_3$ in compression test. In extension test, $\Delta\tau_3$ continues to increase even after interchange of principal stress directions, whereas $\Delta\tau_1$ and $\Delta\tau_2$ turn to decrease. Therefore, Eq.(5-11) has been adopted in this paper to represent the increment of octahedral shear stress. Fig.5-5 shows that the octahedral shear stress increment in plane strain test is almost identical with that in axi-symmetrical test for both compression and extension condition.

The values of m ($= \sigma_y'/\sigma_x'+\sigma_z'$) for normally consolidated plane strain test are plotted against axial strain in Fig.5-6, where m is a measure of the relative magnitude of effective intermediate principal stress during shear. It should be noted that σ_y' was not always the intermediate principal stress during extension test as shown later in Fig.5-17. In compression test, the value of m decreases slightly in the initial part of shear and then increases gradually with axial strain. This tendency is

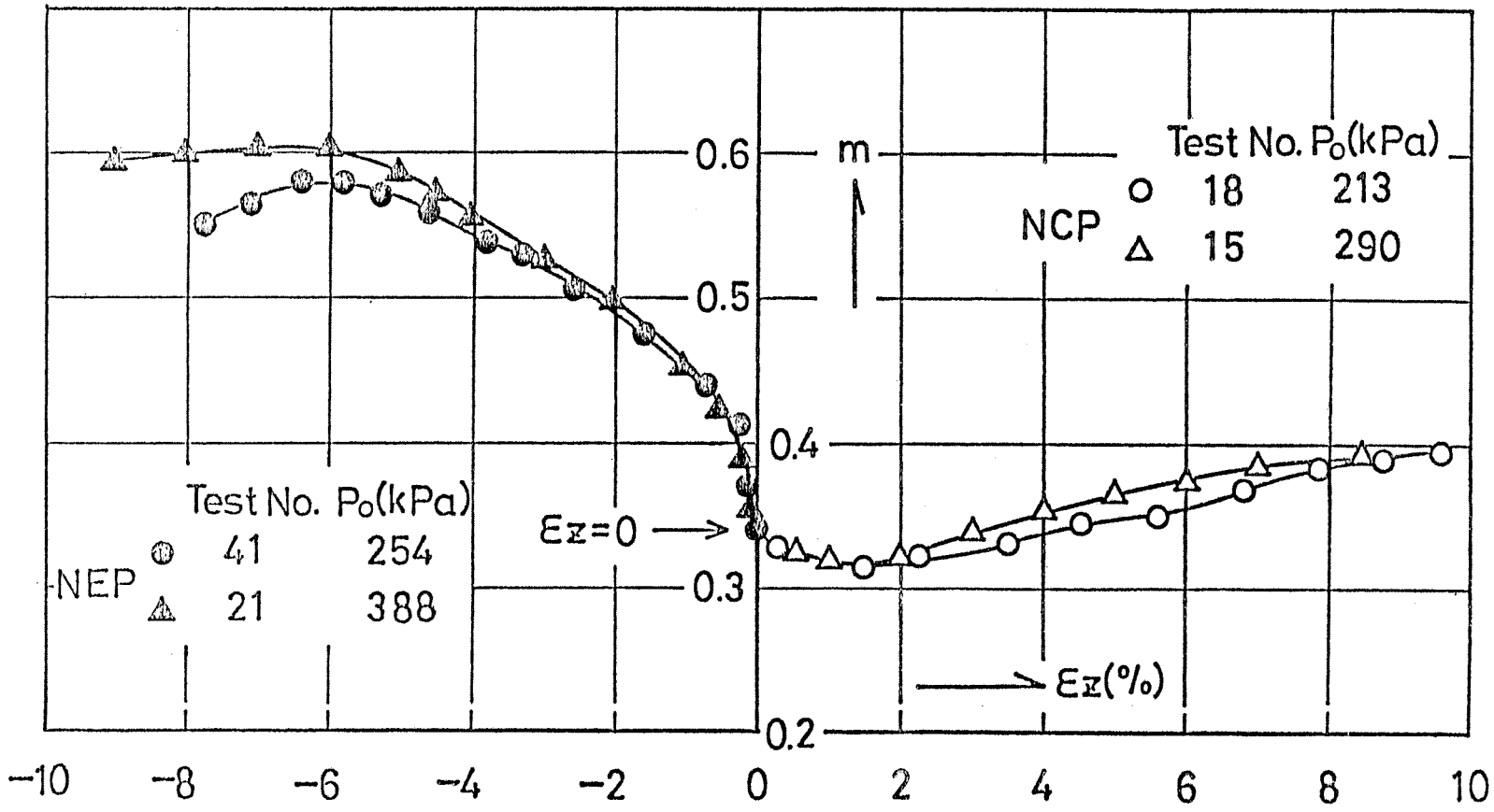

Fig.5-6 Variation of the stress ratio m in normally consolidated plane strain tests

also evident in the report by Henkel and Wade (1966). Campanella and Vaid (1973) reported that the value of m remained constant throughout the test irrespective of stress system (compression or extension). In the present test, it increased up to 0.6 at 5 % axial strain in extension test. As the stress condition of the specimen consolidated under K_o condition is $\sigma_x' = \sigma_y' = K_o \sigma_z'$, the value of m immediately after consolidation is equal to $m = \sigma_y'/\sigma_x' + \sigma_z' = K_o/1+K_o$. Based on the elastic theory, Cornforth (1964) derived a relationship between intermediate principal stress and the other two as follows.

$$\sigma_2' = \frac{K_o}{1+K_o}(\sigma_1' + \sigma_3') \qquad (5\text{-}12)$$

Table 5-2 shows the comparison of the values ever reported on m, K_o and $K_o/1+K_o$, respectively.

Fig.5-7 illustrates the value of m versus ε_z relationship for overconsolidated plane strain compression and extension tests. In compression test, the value of m at $\varepsilon_z = 0$ is equal to $K_o/1+K_o$ and decreases to $m \fallingdotseq 0.3$ at small strain. But m value at $\varepsilon_z > 10$ % is equal to 0.35 to 0.37 and is almost constant irrespective of overconsolidation ratio. Calculation of the value of $K_o/1+K_o$ by using the mean value of $K_o = 0.53$ in normally consolidated clay gives the value of 0.35 . This value is nearly equal to the m value at $\varepsilon_z > 10$ % .

Authors	K_o	$K_o/1+K_o$	m_c	m_E
Present Author	0.52	0.34	0.32	0.61
Henkel & Wade ('66)	0.58	0.37	0.40	——
Campanella & Vaid ('73)	0.55	0.35	0.36	0.39
Sketchley & Bransby ('73)	0.64	0.39	0.40	0.40

Table 5-2 Comparison of the values of m , K_o and $K_o/1+K_o$, repectively

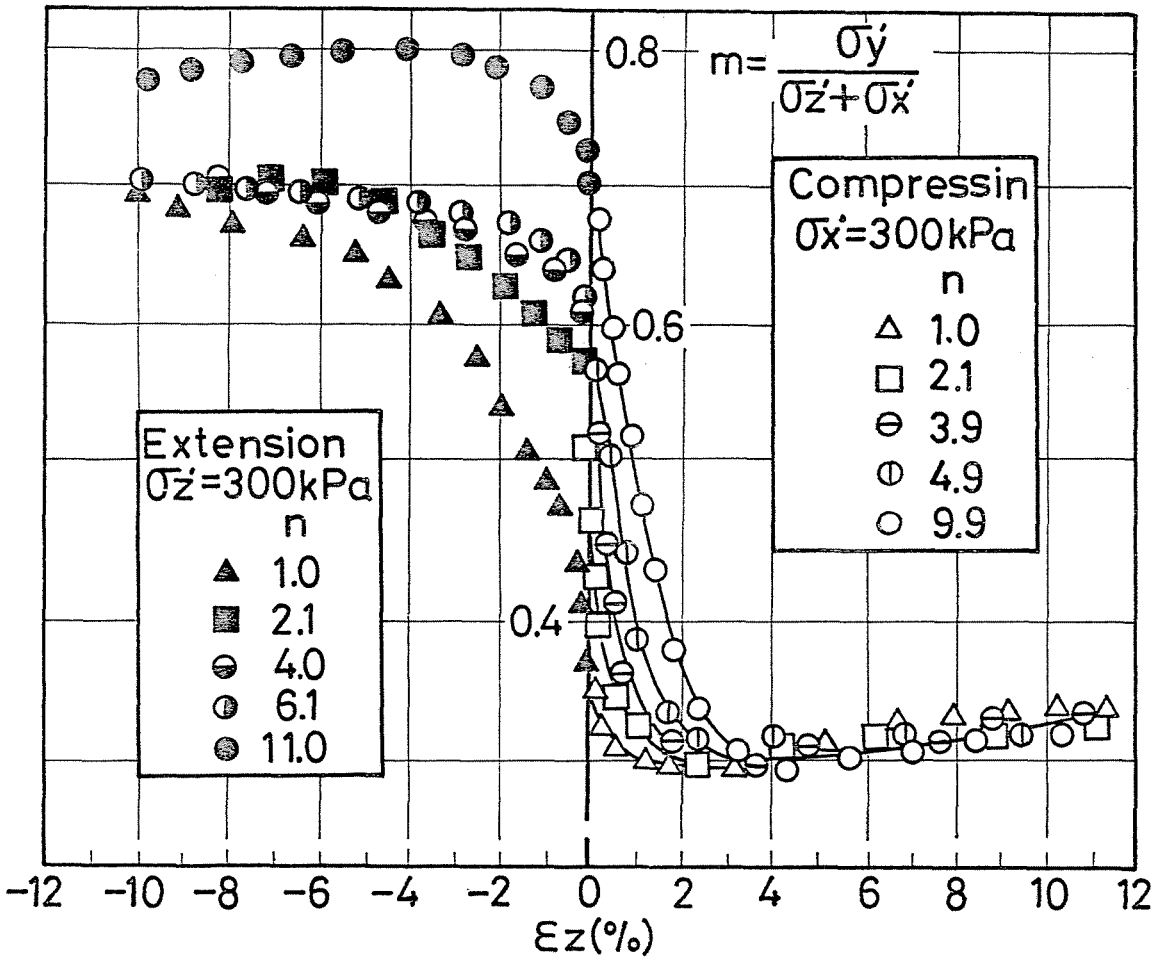

Fig.5-7 Variation of the stress ratio m in overconsolidated plane strain tests

According to their experimental data on lightly overconsolidated ($n < 4$) clay, Sketchley and Bransby (1973) suggested that the value of m at failure converges to a constant value ($m \fallingdotseq 0.4$) irrespective of compression or extension test. On the other hand, the value of m in extension test obtained from the author's experimental results greatly differs from that of compression test. Namely, the initial slope of m versus ε_z curve increases with the value of n , and m converges about 0.7 at the strain greater than 8 %.

Ohta et al. (1975) derived an equation which gives information about the relative magnitude of intermediate principal stress during plane strain test, based on the following assumption. Although the intermediate principal strain increment $d\varepsilon_2 = 0$ in plane strain test, it was assumed that the plastic component of $d\varepsilon_2$ is approximately equal to zero, which implies that both recoverable and plastic component of $d\varepsilon_2$ are simultaneously equal to zero. Then the stress state under plane strain condition should satisfy the following equation, assuming f as plastic potential.

$$\frac{\partial f}{\partial \sigma_2'} = 0 \qquad (5\text{-}13)$$

Referring to Roscoe et al. (1963), and Ohta et al. (1975), the present author derived following equation representing successive yield loci for normally consolidated clay as stated in chapter III.

$$\frac{\lambda-\nu}{1+e_0}\ln\frac{p}{p_{oi}} + F(\eta) - F(\eta_0) = 0 \qquad \text{(3-76 bis)}$$

Parameter ν whose functions are exactly the same as κ in the sense of Cam-clay equations, is determined by the following equation.

$$\nu = \lambda - (1+e_0) M F'(M) \qquad \text{(3-84 bis)}$$

Thus the plastic potential of normally consolidated clay including both compression and extension side is represented as follows.

$$f = \frac{\lambda-\nu}{(1+e_0)}\ln\frac{p}{p_{oi}} \pm \{F(\eta) - F(\eta_0)\} \qquad \text{(5-14)}$$

Applying the condition expressed by Eq.(5-13) to Eq.(5-14), following equation is obtained.

$$\frac{\sigma_2'}{p} = \frac{3m}{1+m} = 1 \mp \eta\left\{\frac{\lambda-\nu}{(1+e_0)F'(\eta)} \mp \eta\right\} \qquad \text{(5-15)}$$

Eq.(5-15) is essentially the same as Eq.(38) by Ohta et al. (1975). Combination of Eq.(3-84) with above equation gives

$$m = \frac{1 \mp \eta\left\{M\frac{F'(M)}{F'(\eta)} \mp \eta\right\}}{2 \pm \eta\left\{M\frac{F'(M)}{F'(\eta)} \mp \eta\right\}} \qquad \text{(5-16)}$$

Ohta et al. assumed that $F(\eta)$ versus η relationship can be expressed by a single straight line as

$$F(\eta) = \mu\eta \tag{5-17}$$

where μ is a coefficient expressing the dilatancy intensity.

In original Cam-clay theory, $F(\eta)$ can be written as follows.

$$F(\eta) = \frac{\lambda - \kappa}{M(1+e_0)}\eta \tag{3-89 bis}$$

Since M, λ and κ are regarded as soil constants, $F(\eta)$ versus η relationship shown above implies a single straight line as mentioned in section 3.6.5. By the way, $F(\eta)$ versus η relationship in modified Cam-clay theory is given as follows.

$$F(\eta) = \frac{\lambda - \kappa}{1+e_0} \ln\left\{1 + (\eta/M)^2\right\} \tag{3-90 bis}$$

$F(\eta)$ versus η relationship obtained from normally consolidated plane strain test results is conveniently approximated by a set of straight lines as shown in next section, and so $F(\eta)$ in Eq.(3-76) can be replaced by a straight line equation. This leads to a conclusion in Eq.(5-16) that $F'(M) = F'(\eta)$ = a constant, which gives a simplified expression for m as follows.

$$m = \frac{1 \mp \eta\ (M \mp \eta)}{2 \pm \eta\ (M \mp \eta)} \tag{5-18}$$

In order to obtain the value of m during plane strain test for K_0 consolidated clay, η and M must be replaced by $(\eta - \eta_0)$ and $(M - \eta_0)$ respectively, since the dilatancy function $F(\eta)$ in Eq.(3-76) is concerned with the shear test starting from $\eta = \eta_0$. Therefore, Eq.(5-18) is rewritten as follows.

$$m = \frac{1 \mp (\eta-\eta_0)\{(M-\eta_0) \mp (\eta-\eta_0)\}}{2 \pm (\eta-\eta_0)\{(M-\eta_0) \mp (\eta-\eta_0)\}} \qquad (5\text{-}19)$$

m_0, the value of m at completion of K_0 consolidation is represented by octahedral stress ratio after consolidation as follows.

$$m_0 = \frac{K_0}{1+K_0} = \frac{\sqrt{2} - \eta_0}{\eta_0 + 2\sqrt{2}} \qquad (5\text{-}20)$$

On the other hand, m value obtained from Eq.(5-19) by inserting $\eta = \eta_0$ is computed as 1/2. As the initial value of m after K_0 consolidation can never be equal to 1/2 except for the case of $K_0 = 1$, Eq.(5-19) must be modified by the magnitude of $(m_0 - 1/2)$. Therefore, a tentative expression of m for Ko consolidated plane strain test will be as follows.

$$m = \frac{1 \mp (\eta-\eta_0)\{(M-\eta_0) \mp (\eta-\eta_0)\}}{2 \pm (\eta-\eta_0)\{(M-\eta_0) \mp (\eta-\eta_0)\}} - \frac{3\eta_0}{2(\eta_0+2\sqrt{2})} \qquad (5\text{-}21)$$

Comparison of calculated values of m by Eq.(5-21) with observed ones will be shown in latter part of this chapter.

Fig.5-8 illustrates the relationship between pore water

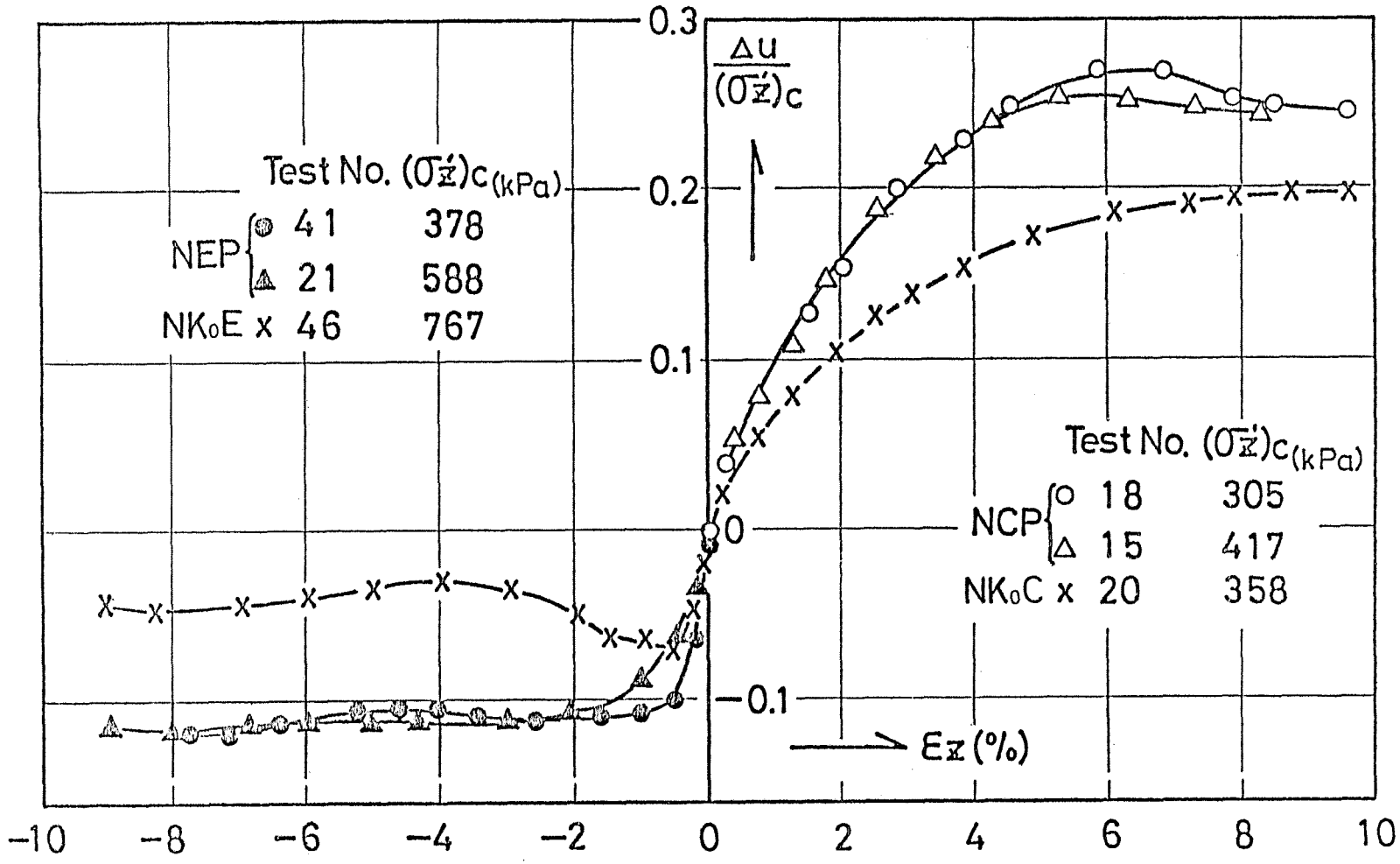

Fig.5-8 Pore pressure change in normally consolidated plane strain tests

pressure change Δu normalized by the preshear effective vertical stress $(\sigma_z')_c$ and axial strain ε_z. In compression test, Δu increases with axial strain and it reaches maximum at about 6% strain in NCP and 8% in NK_oC test. The difference of the magnitude of strain at maximum pore pressure in NCP and NK_oC may be attributed to the difference of the strain at which maximum stress difference occurs. The difference of pore pressure development in NCP and NK_oC test at any equal strain may be due to the relative magnitude of intermediate principal stress. In NEP test, Δu decreases rapidly till about -1.0% axial strain and then increases slightly and becomes almost constant at larger strain. In NK_oE test, the pattern of pore pressure change is almost the same as in NEP test, but the magnitude of change is almost one half of the NEP test. From these test results it can be concluded that the influence of deformation condition (axi-symmetrical or plane strain condition) upon the development of pore pressure is greater in extension than in compression.

Undrained stress paths in octahedral stress plane obtained from four types of test are shown in Fig.5-9. In compression test, the stress paths almost coincide with each other, as reported by Shibata and Karube (1965), Henkel and Wade (1966), and Vaid and Campanella (1974). In extension test, as stated previously, τ does not become equal to zero, and stress paths in NK_oE and NEP test after interchange of principal stress directions are appreciably different as reported by Vaid and Campanella (1974).

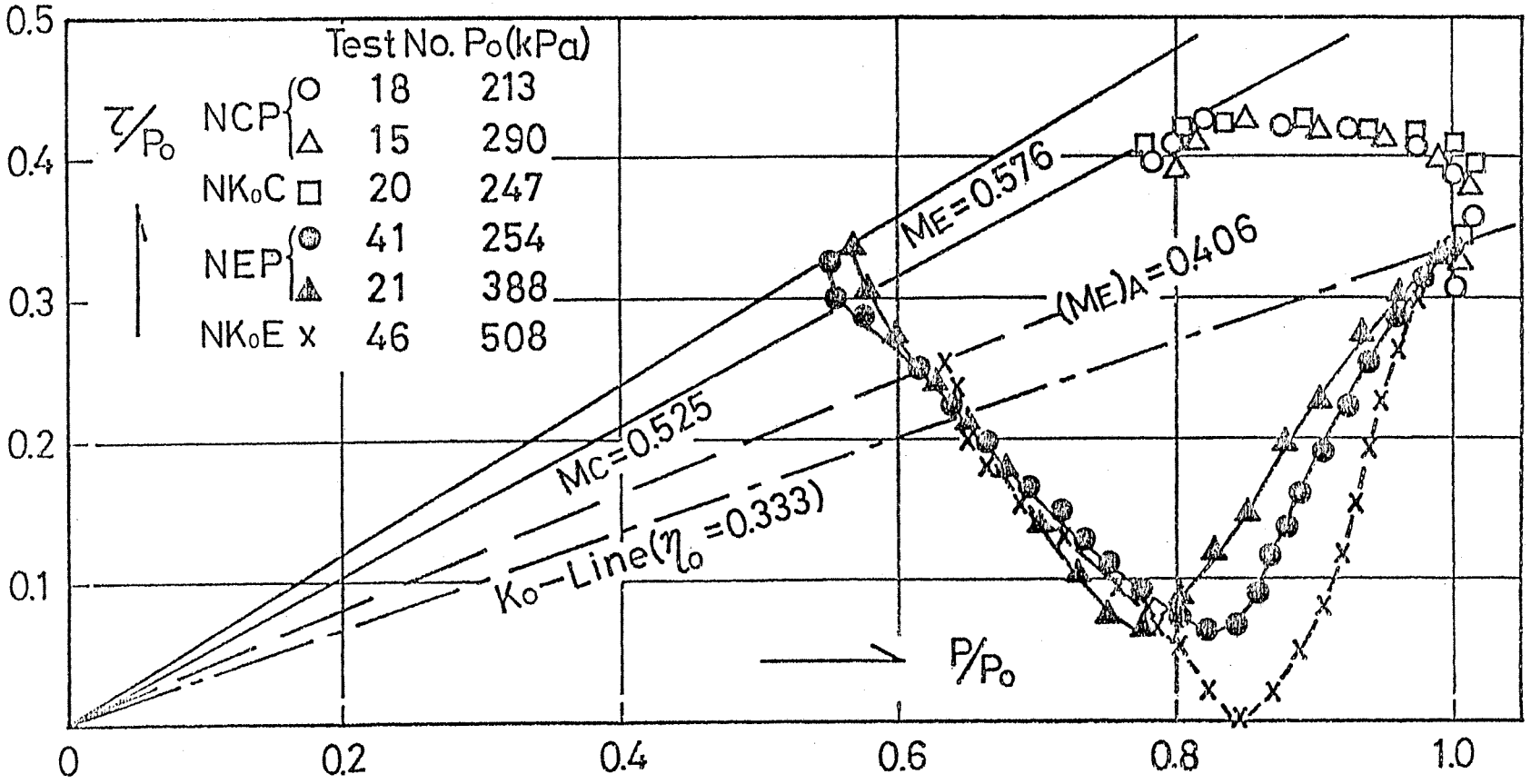

Fig.5-9 Effective stress paths in octahedral stress plane

5.2.3 Dilatancy characteristics

Henkel and Wade (1966) suggested that pore water pressure of saturated clay which develops during shear can be divided into two components, one of which is due to the increment of mean principal stress and the other is due to shear stress increment as shown by Eq.(5-22).

$$\Delta u = \Delta p + a \cdot \Delta \tau \quad \text{or} \quad \Delta u_s = \Delta u - \Delta p = a \cdot \Delta \tau \qquad (5\text{-}22)$$

where a is a constant representing the dilatancy characteristics of a soil. Fig.5-10 shows the development of Δu_s in the present tests due to $\Delta \tau$ normalized by the preshear effective mean stress p_o. In this figure, $\Delta \tau$ was computed in accordance with the definition represented by Eq.(5-11). It is seen from this figure that Δu_s versus $\Delta \tau$ relationships in plane strain compression and extension tests were substantially identical with those in axi-symmetrical compression and extension tests, respectively.

Fig.5-11 is the plot of $\Delta u_s / p_o$ against octahedral shear strain γ. This figure shows that for compression tests, Δu_s is almost identical for axi-symmetrical and plane strain condition. In extension tests, however, Δu_s in plane strain condition is larger than that in axi- symmetrical condition. Lo (1969) suggested that the value of Δu_s (according to Lo's notation, this value is represented by Δu_{sp}, i.e. $\Delta u - \Delta p = \Delta u_{sp}$) depends

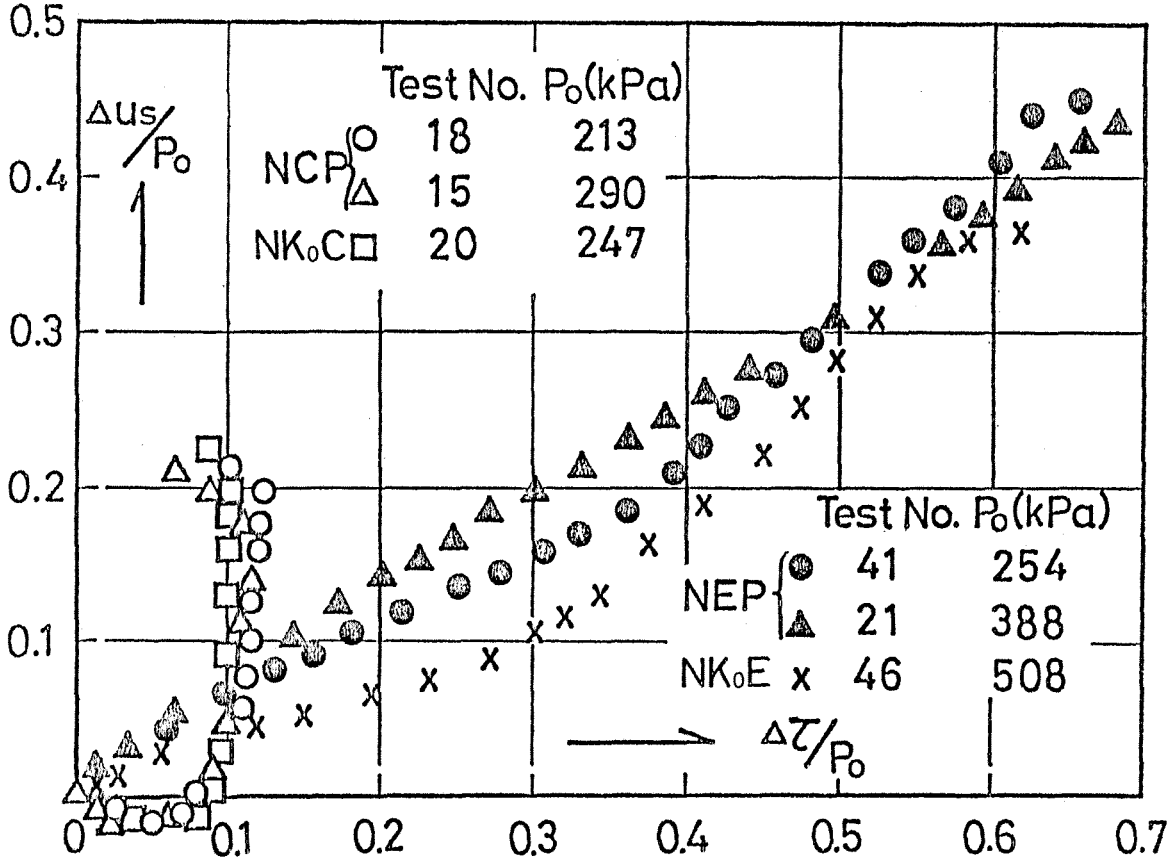

Fig.5-10 Relationship between shear induced pore pressure and octahedral shear stress increment

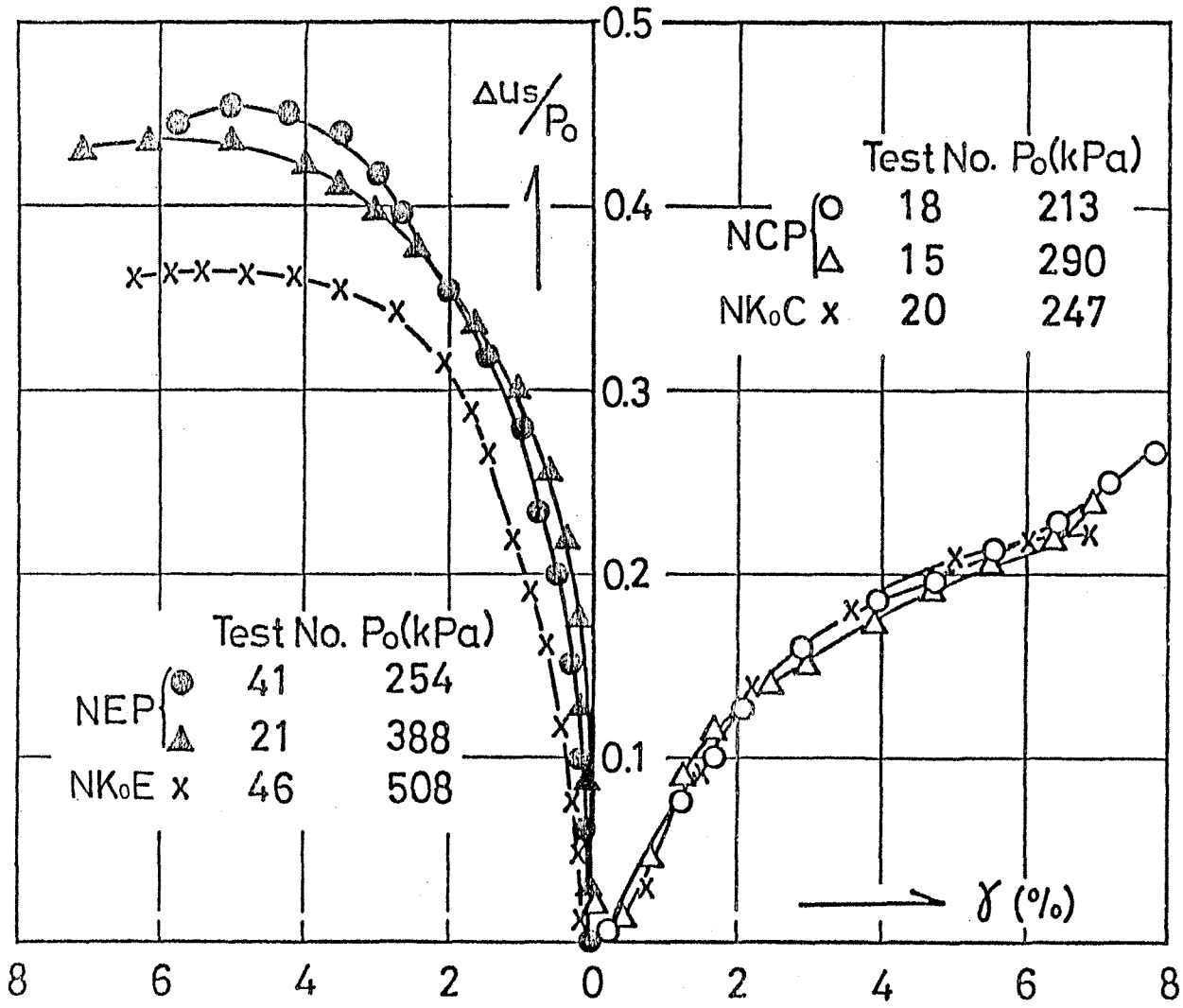

Fig.5-11 Shear induced pore pressure vs. octahedral shear strain

only on the axial strain ε_z and independent of deformation condition (axi-symmetrical or plane strain) during undrained shear. According to the test results shown in Figs.5-10 and 5-11, and Eqs.(5-7) and (5-8), it is rather concluded that the value of Δu_s depends not on axial strain, but on both the octahedral shear strain and shear stress increment.

As shown previously in chapter III and IV effective mean stress during undrained shear under axi-symmetrical stress condition is represented by a function of octahedral stress ratio η . This function has been called as dilatancy function by the present author. Now the influence of strain condition during shear on the $F(\eta)$ versus η relationship is illustrated in Fig.5-12. Observed $F(\eta)$ versus η curves for the NCP test, likely for the NK_oC test, could be approximated by a straight line, excluding their initial parts of positive dilatancy. Those for the NEP test could also be approximated by a set of two straight lines. Slope of straight portion of $F(\eta)$ versus η curves in compression is greater than that in extension. Comparing plane strain with axi-symmetrical test data, it can be concluded that the $F(\eta)$ versus η relationships in plane strain and axi-symmetrical test are similar in qualitative sense for both compression and extension test. In compression test, the slope of the straight portion of $F(\eta)$ versus η curves for NCP is almost equal to that for NK_oC. In extension test, the slope of NEP curve before interchange of principal stress directions is greater than that of NK_oE curve,

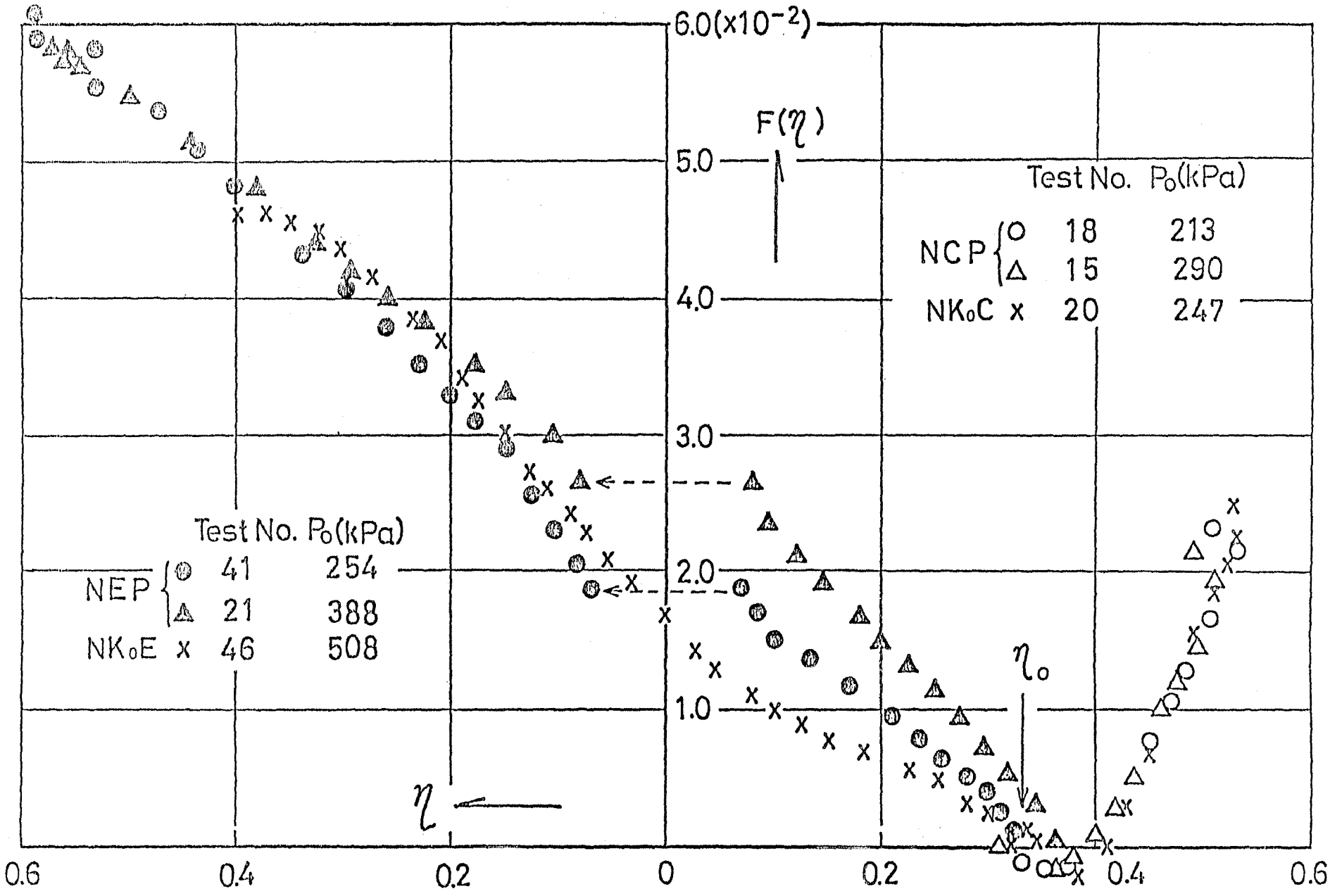

Fig. 5-12 Octahedral stress ratio vs. dilatancy

but its slope after interchange of principal stress directions is almost equal to that of NK_oE curve. In any case, as the $F(\eta)$ versus η relationship in extension test appreciably differs from that in compression test even in axi-symmetrical test as well as in plane strain test, it is concluded that dilatancy characteristics of K_o consolidated clay is greatly influenced by the interchange of principal stress directions.

5.3 Existing Theory for Predicting Stress-Strain Behaviour of Clay under Plane Strain Condition

5.3.1 Stress-strain equation by Roscoe and Burland

Roscoe and Burland (1968) derived general three dimensional incremental stress-strain relationships by extending their Cam-clay equation for axi-symmetrical stress condition.

The volumetric yield locus and state boundary surface are represented as follows.

$$p/p_0 = \frac{M^{*2}}{M^{*2}+\eta^{*2}} \tag{5-23}$$

$$p/p_e = \left(\frac{M^{*2}}{M^{*2}+\eta^{*2}}\right)^{(1-\kappa/\lambda)} \tag{5-24}$$

where

$$\eta^* = \sqrt{3}\,\eta \quad , \quad M^* = \sqrt{3}M$$

And shear and volumetric strain increment are as follows.

$$\delta v^* = \frac{1}{1+e}\left[(\lambda-\kappa)\frac{2\eta^* d\eta^*}{M^{*2}+\eta^{*2}} + \frac{\lambda dp}{p}\right] \tag{5-25}$$

$$\delta\varepsilon^* = \frac{\lambda-\kappa}{(1+e)}\left(\frac{2\eta^*}{M^{*2}-\eta^{*2}}\right)\left(\frac{2\eta^* d\eta^*}{M^{*2}+\eta^{*2}} + \frac{dp}{p}\right) \qquad (5\text{-}26)$$

Combining above two equations under the condition of $\delta v^* = 0$, following equation representing incremental shear strain for undrained condition is obtained.

$$\delta\varepsilon^* = \frac{\kappa(\lambda-\kappa)}{\lambda(1+e)}\left(\frac{4\eta^{*2}}{M^{*4}-\eta^{*4}}\right)d\eta^* \qquad (5\text{-}27)$$

where

$$\delta\varepsilon^* = \frac{1}{\sqrt{3}}\sqrt{(\delta\varepsilon_1-\delta\varepsilon_2)^2+(\delta\varepsilon_2-\delta\varepsilon_3)^2+(\delta\varepsilon_3-\delta\varepsilon_1)^2}$$

$$\delta v^* = \delta\varepsilon_1 + \delta\varepsilon_2 + \delta\varepsilon_3$$

The general equations shown above can be made to satisfy plane strain condition by setting $\delta\varepsilon_2 = 0$. However, it is difficult to find out the relationship between effective principal stresses σ_1', σ_2', σ_3' and principal strains ε_1, ε_2, ε_3, individually.

Roscoe and Burland simplified the problem by assuming that the recoverable components of all strains are negligible compared to that of plastic components. This is equivalent to assuming that κ is negligible compared to λ.

Introducing this assumption into the general equation mentioned above, equations for stress path and axial strain during shear under undrained plane strain condition are obtained as follows.

$$\eta' = t/s = \frac{\bar{M}}{\sqrt{3}}\sqrt{\left(\frac{S_o}{S} - 1\right)} \tag{5-28}$$

$$\varepsilon_1 = \frac{\sqrt{3}\,\lambda}{\bar{M}(1+e)}\left[\ln\left|\frac{\bar{M}/\sqrt{3}+\eta'}{\bar{M}/\sqrt{3}-\eta'}\cdot\frac{\bar{M}/\sqrt{3}-\eta'_{K_o}}{\bar{M}/\sqrt{3}+\eta'_{K_o}}\right| + 2\tan^{-1}\left\{\frac{\sqrt{3}\bar{M}(\eta'_{K_o}-\eta')}{\bar{M}^2+3\eta'_{K_o}\cdot\eta'}\right\}\right] \tag{5-29}$$

where

$$t = \frac{\sigma_1' - \sigma_3'}{2} \qquad S = \frac{\sigma_1' + \sigma_3'}{2}$$

$$\eta'_{K_o} = \frac{1-K_o}{1+K_o}$$

and, S_o is the value of S at the completion of K_o consolidation. Moreover, intermediate effective principal stress σ_2' is given by the following equation.

$$\sigma_2' = \frac{3\bar{M}^2 S_o + 2(9-2\bar{M}^2)S}{2(\bar{M}^2+9)} \tag{5-30}$$

5.3.2 Stress-strain equation by Ohta et al.

As shown previously, Ohta et al (1975) developed a stress-strain equation for anisotropically consolidated clay. Their equations for undrained stress path in octahedral stress space and stress ratio-strain curve after anisotropic consolidation are as follows.

$$\lambda \ln \frac{p}{p_0} + (1+e_0)\mu(\eta-\eta_0) = 0 \tag{5-31}$$

$$\gamma_{oct} = -\frac{\mu K}{3\lambda} \ln \left| \frac{\frac{\lambda-K}{(1+e_0)\mu} - \eta}{\frac{\lambda-K}{(1+e_0)\mu} - \eta_0} \right| \tag{5-32}$$

where μ denotes the coefficient of dilatancy and η_0 is the stress ratio η at the completion of anisotropic consolidation. As mentioned previously in section 5.2.2, they derived an equation which gives information about the relative magnitude of intermediate principal stress during plane strain test based on the following assumption. Although the intermediate principal strain increment $d\varepsilon_2 = 0$ in plane strain test, it was assumed that the plastic component of $d\varepsilon_2$ is approximately equal to zero, which implies that both recoverable and plastic component of $d\varepsilon_2$ are simultaneously equal to zero. Based on this assumption, intermediate principal stress σ_2' is given by the following equation.

$$\sigma_2' = p \mp \tau \left\{ \frac{\lambda-K}{(1+e_0)\mu} \mp \frac{\tau}{p} \right\} \tag{5-33}$$

5.3.3 Comparison of predicted stress-strain relationships by Roscoe and Burland, and by Ohta et al. with observed ones

Fig.5-13 illustrates the comparison of predicted stress-paths in σ_1' , σ_3' and σ_2' , σ_3' space by the equation of Roscoe and Burland with observed ones.

As shown previously in chapter III, undrained stress path and stress ratio-strain curve are greatly influenced by the magnitude of κ . Hence, the assumption of $\kappa = 0$ may be one of the causes of discrepancy between prediction and observation. Fig.5-14 shows the comparison of prediction of stress path and stress-strain curve by the equation of Ohta et al. with observed values. The discrepancy between predicted and observed stress path may be due to the difference between assumed stress ratio-dilatancy relationship with observed one, i.e. the development of positive dilatancy at low stress level was neglected in this equation. Moreover, Ohta et al. assumed that the dilatancy coefficient μ is not affected by the stress and strain conditions during consolidation and shear. According to the present author's test results, however, the value of μ appears to be influenced by these conditions. This cannot nevertheless be stated positively due to the following reason. Although the value of μ have to be obtained from drained test under the condition of constant mean effective stress, the value of μ in this test was obtained from σ_3 constant undrained test.

The stress ratio at critical state is represented as follows.

$$M = \frac{\lambda - \kappa}{(1+e_0)\mu} \qquad (5\text{-}34)$$

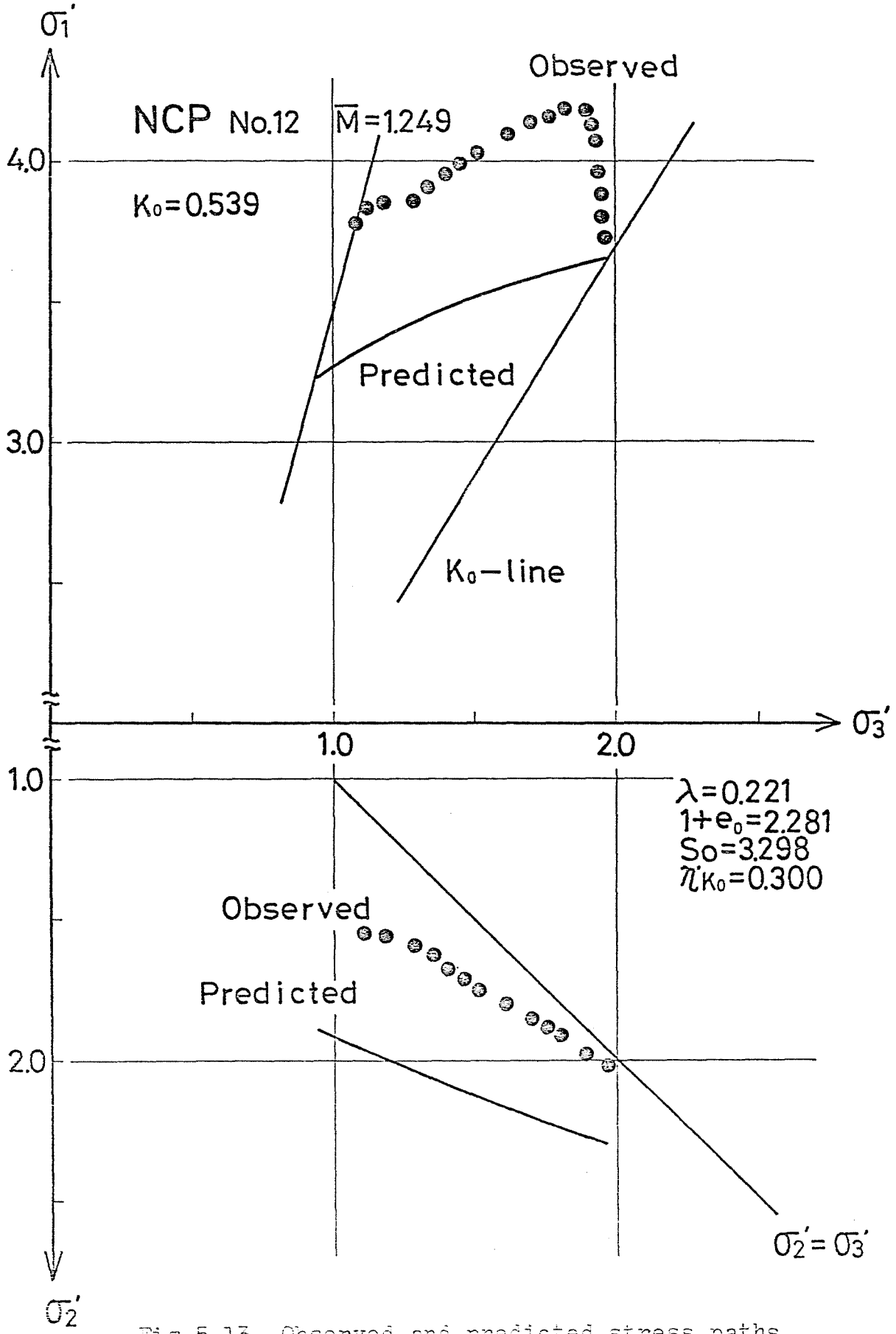

Fig.5-13 Observed and predicted stress paths by modified Cam-clay equations

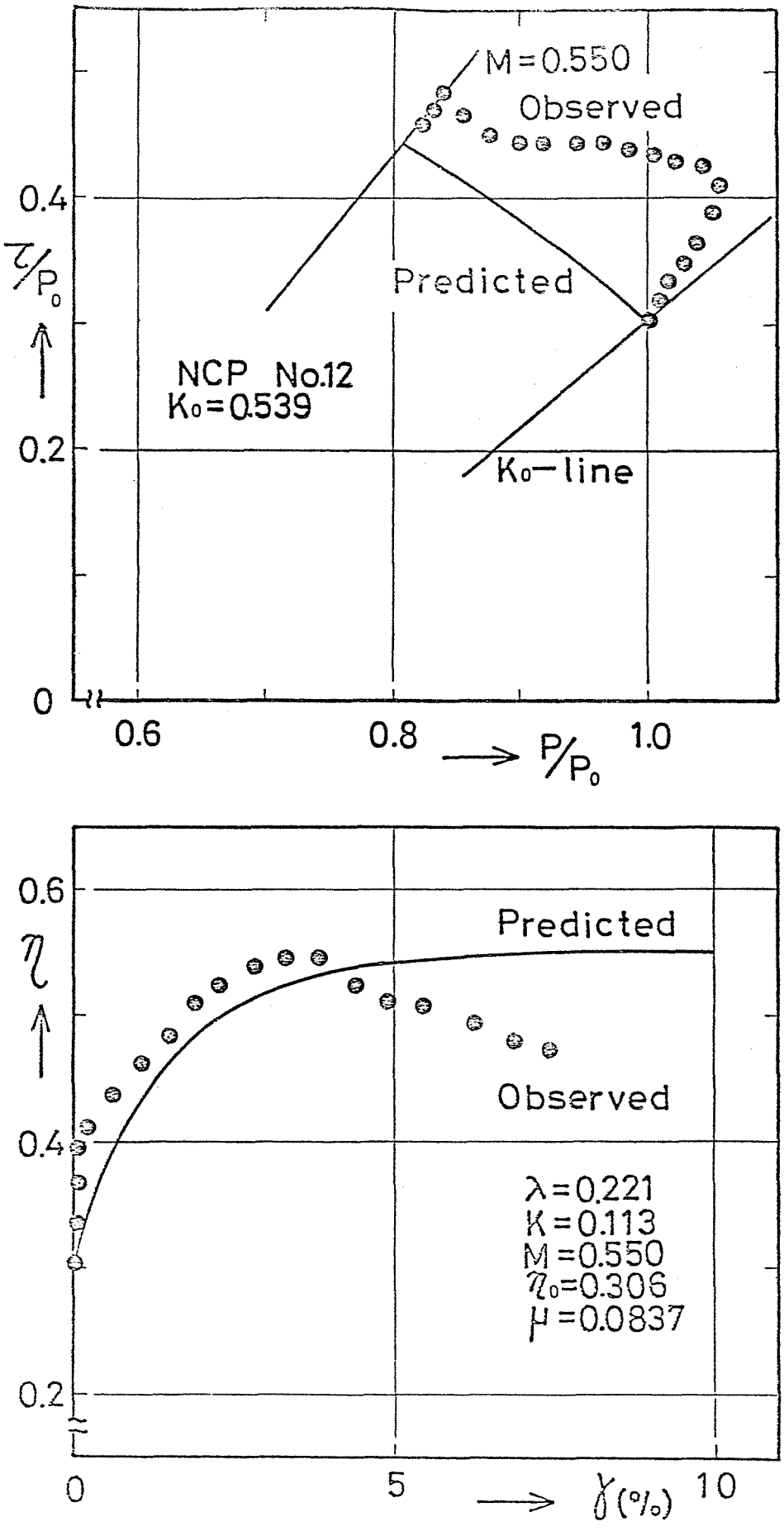

Fig.5-14 Observed and predicted stress-strain relationship by equations of Ohta et al.

Hata et al. (1969) described that the value of M calculated by the above equation using the observed values of λ , κ , μ and e_0 does not coincide with observed one. Accordingly, they adopted such a method as to vary the value of λ so as to let the calculated value of M coincide with observed one. This method leads to the result that the calculated undrained stress path can be coincident with the observed one , because there does not appear the value of κ in the stress-path equation. In accordance with the experiment by the present author shown in the preceding section, there is no evidence that the value of μ is constant irrespective of the stress and strain conditions during consolidation and shear. Therefore, it would be adequate to deal with the value of μ to be a variable depending on the conditions during consolidation and shear. The value of μ used in the prediction in Fig.5-14 was determined so as to let the calculated value of M coincide with the observed one.

As mentioned above, there is some ambiguity about the method of determination of soil constants in the predicting equation of stress-strain behaviour by Ohta et al.

5.4 Proposed Method for Predicting Stress-Strain Behaviour of K_o Consolidated Clay under Undrained Plane Strain Condition

The present author suggested previously, in chapter Ⅳ, a method of predicting stress-strain behaviour of K_o consolidated clay under axi-symmetrical stress condition by using the parameters obtained from isotropically consolidated undrained test. In this section, a tentative method of predicting undrained plane strain stress-strain behaviour will be discussed.

As mentioned in section 5.3.1, Roscoe and Burland (1968) developed a method of predicting plane strain stress-strain behaviour, assuming that $\kappa = 0$, i.e. recoverable components of all strains are to be zero. In this section, the information about the relative magnitude of intermediate principal stress, which can be obtained by a method mentioned in previous section, is utilized for the present purpose, retaining κ not to be zero.

The procedure for predicting undrained plane strain stress-strain behaviour of K_o consolidated clay will be as follows. By conducting a series of isotropically consolidated undrained compression and extension tests, compression index λ, octahedral stress ratio at critical state M_c for compression and M_E for extension, and the relationship between dilatancy function $F(\eta)$ and octahedral stress ratio η are obtained. Then, undrained stress path and incremental stress ratio versus strain relationship for isotropically consolidated clay are represented

as follows.

$$p/p_o = \exp\left[-\frac{1+e_o}{\lambda} F(\eta)\right] \qquad (3\text{-}72 \text{ bis})$$

$$d\gamma = -\frac{\nu}{3\lambda} \cdot \frac{[F(\eta)]^2}{\eta F(\eta) - \frac{\lambda-\nu}{1+e_o}} d\eta \qquad (3\text{-}82 \text{ bis})$$

For example, if the $F(\eta)$ versus η relationship is represented simply by a straight line equation such as $F(\eta) = \mu\eta$, then Eq.(3-82) can easily be integrated by giving initial condition of $\gamma = 0$ at $\eta = 0$, and following equation will be obtained.

$$\gamma = -\frac{\nu\mu}{3\lambda} \ln\left|1 - \frac{(1+e_o)\mu}{\lambda-\nu}\eta\right| \qquad (5\text{-}35)$$

It has been assumed in section 4.4 that the stress path for K_o consolidated compression test (NK_oC) in $\tau/p_o - p/p_o$ co-ordinate is similar to that obtained by rotating the stress path for isotropically consolidated clay (NIC) by an angle θ_o after shifting the NIC stress path from the point (1,0) to (1, τ_o/p_o), where

$$\theta_o = \tan^{-1} \tau_o/p_o$$

and, p_o and τ_o are the octahedral normal and shear stresses after K_o consolidation. In the light of the experimental results illustrated previously, the stress path for plane strain compre-

ssion (NCP) in octahedral stress plane is thus obtained by assuming it to be identical with that for axi-symmetrical stress condition (NK_oC).

It has also been assumed that stress path for K_o consolidated axi-symmetrical extension test (NK_oE) is similar to that obtained by rotating the stress path for isotropically consolidated clay (NIE) by an angle $\theta_o/2$, after shifting the NIE stress path from the point (1,0) to (1, τ_o/p_o), and that effective mean stress at failure in NK_oE is equal to that of NIE test. As shown in previous section, the stress paths for plane strain extension and axi-symmetrical extension are appreciably different from each other, especially for the path after interchange of principal stress directions. Therefore, following assumptions are made to determine approximately the stress path for plane strain extension test, as far as the present tests are concerned. As already stated and can be seen in Fig.5-9, the stress path for NEP test in octahedral stress plane does not have a point of $\eta = 0$, and stress ratio η_1, at which interchange of principal stress directions takes place, is roughly equal to 20% of the value of M_E obtained from NK_oE tests. If it is assumed that the length of stress path for NEP test is nearly equal to that for NK_oE test, the stress ratio M_E in NEP test is to be greater by about 40% than that in NK_oE test. Thus, the unknown quantity of M_E and η_1 in NEP test can be obtained by using NK_oE test data. Fig.5-15 illustrates schematically the $F(\eta)$ versus η relationship shown in Fig. 5-12.

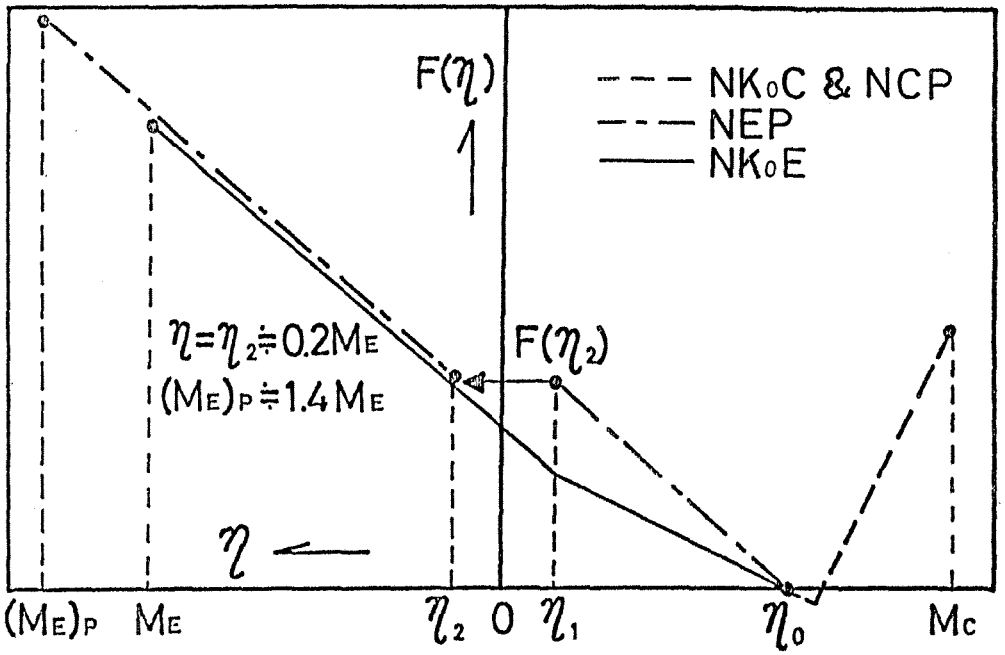

Fig.5-15 Schematic diagram of stress ratio vs. dilatancy

The slope of $F(\eta)$ versus η curve of NEP test after interchange of principal stress directions is almost equal to that of NK_0E, and the slope of NEP test curve before the interchange is greater than that of NK_0E test. Therefore, the following method can be proposed to estimate $F(\eta)$ vs. η relationship of NEP test. From the $F(\eta)$ vs. η curve of NK_0E, the value of $F(\eta_2)$ is obtained by setting $\eta_2 = 0.2M_E$. Then $F(\eta)$ vs. η curve of NEP test before interchange of principal stress directions is obtained by connecting the points ($\eta_1 = 0.2M_E$, $F(\eta_2)$) and (η_0, 0) by a straight line. $F(\eta)$ vs. η curve of NEP test after interchange of principal stress directions can simply be obtained by extending the $F(\eta)$ vs. η curve of NK_0E test up to the point $\eta = 1.4M_E$. Thus the octahedral stress ratio vs. strain relationship and stress path in octahedral stress plane can be obtained by using Eqs.(3-72) and (5-35).

Any information other than those on octahedral stress ratio versus strain and stress path are not needed to obtain undrained stress-strain behaviour under axi-symmetrical stress condition. In order to describe undrained stress-strain behaviour of clay under plane strain condition, however, it is essential to know further the relative magnitude of intermediate principal stress. In this paper, Eq.(5-21) is used to estimate the intermediate principal stress at any value of octahedral stress ratio η.

Effective principal stresses normalized by the preshear effective mean stress p_0 during undrained plane strain tests can be obtained by the known parameter η, m and p as follows. According to the definition of η,

$$\eta = \frac{\tau}{p} = \frac{\frac{1}{3}\sqrt{(\sigma_x' - \sigma_y')^2 + (\sigma_y' - \sigma_z')^2 + (\sigma_z' - \sigma_x')^2}}{\frac{1}{3}(\sigma_x' + \sigma_y' + \sigma_z')}$$

Inserting Eq. (5-3) into above equation, following equation is obtained.

$$\eta = \frac{1}{1+m}\sqrt{2m(m-1) + \frac{1}{2}\left\{1 + 3\left(\frac{\sigma_z' - \sigma_x'}{\sigma_z' + \sigma_x'}\right)^2\right\}} \qquad (5\text{-}36)$$

Combination of Eq. (5-3) with (5-5) gives

$$p = \frac{1}{3}(\sigma_x' + \sigma_z')(1+m) \qquad (5\text{-}37)$$

Effective principal stresses normalized by the preshear effective mean stress are obtained by combining Eq. (5-36) with (5-37) as follows.

$$\sigma_x'/p_o = \frac{\sqrt{3}\, p/p_o}{2(1+m)}\left\{\sqrt{3} \mp \sqrt{2(1+m)^2\eta^2 - (2m-1)^2}\right\} \qquad (5\text{-}38)$$

$$\sigma_y'/p_o = \frac{3m}{1+m}\, p/p_o \qquad (5\text{-}39)$$

$$\sigma_z'/p_o = \frac{\sqrt{3}\, p/p_o}{2(1+m)}\left\{\sqrt{3} \pm \sqrt{2(1+m)^2\eta^2 - (2m-1)^2}\right\} \qquad (5\text{-}40)$$

The comparison of the effective stress vs. axial strain curves of undrained plane strain compression predicted by the present method with those observed is shown in Fig. 5-16. Solid lines are obtained by using the observed η vs. γ and τ/p_o vs. p/p_o data of Nk_oC test and Eqs. (5-21), (5-38), (5-39), and (5-40), whereas dotted lines are obtained by using the observed parameters from NIC test and Eqs. (5-21) to (5-40). Predicted curves by using NK_oC test agree well with the observed ones, especially for σ_z'/p_o and σ_x'/p_o curves. Therefore, undrained plane strain stress-strain behaviour in compression can successfully be predicted by using the axi-symmetrical test data. Prediction by using the parameters obtained from conventional isotropically consolidated undrained compression test may even be possible, although some errors might be accompanied. Fig. 5-17 illustrates the comparison of effective stress-strain curves of observed NEP test data with predicted ones by using the observed η vs. γ and τ/p_o vs. p/p_o data of NK_oE test and the Eqs. (5-21), (5-38), (5-39), and (5-40). Although the predicted values of σ_z'/p_o agree fairly well with the observed ones, degree of coincidence between predicted values and observed ones for σ_y'/p_o is not so good. The discrepancies between predicted and observed stress-strain curves can be attributed to the predicted m vs. η relationship shown in Fig. 5-18 .

In any case, prediction of undrained plane strain stress-strain behaviour of clay is now possible by using the data obtainable from

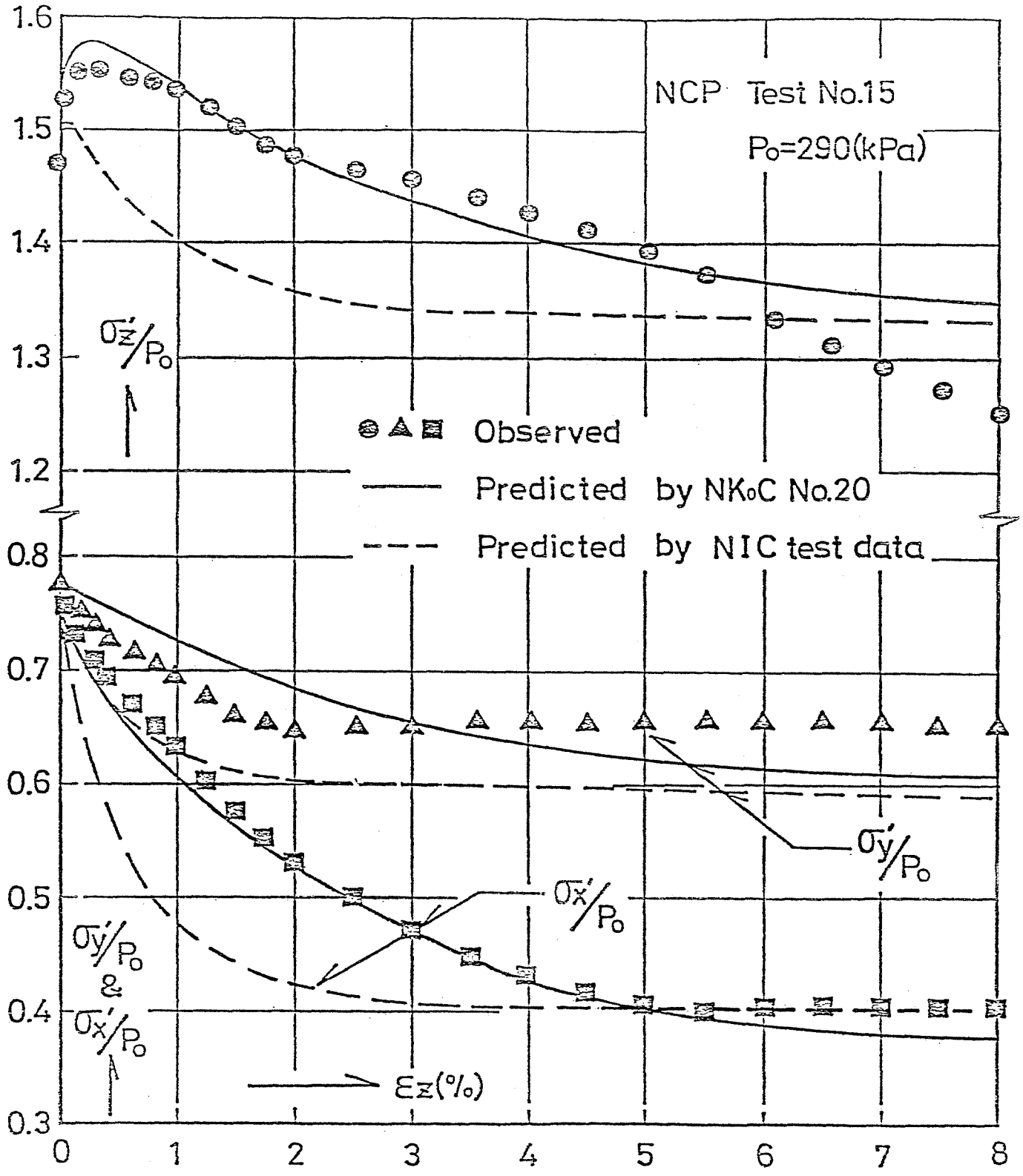

Fig.5-16 Observed and predicted stress-strain relationship for plane strain compression test

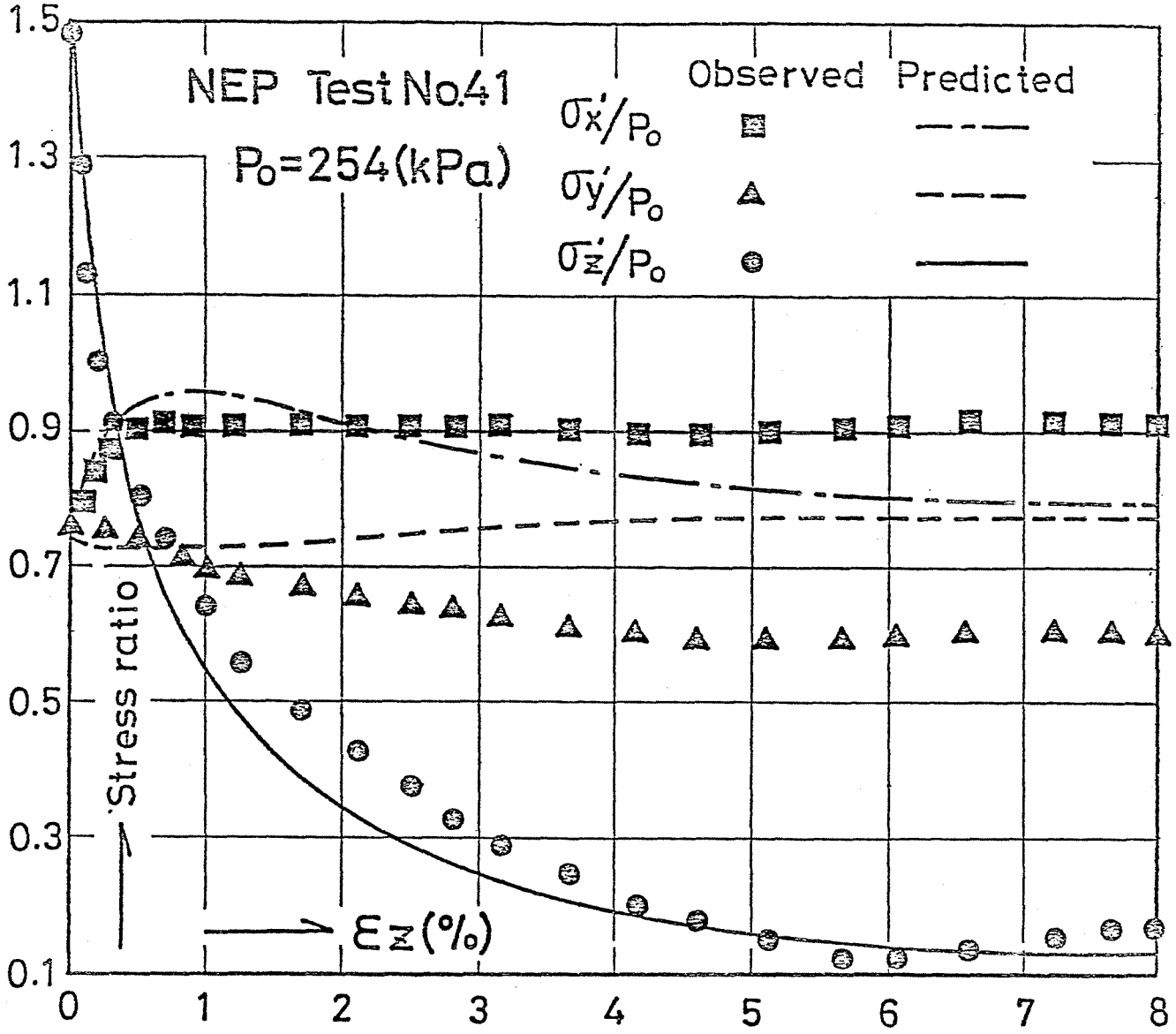

Fig.5-17 Observed and predicted stress-strain relationship for plane strain extension test

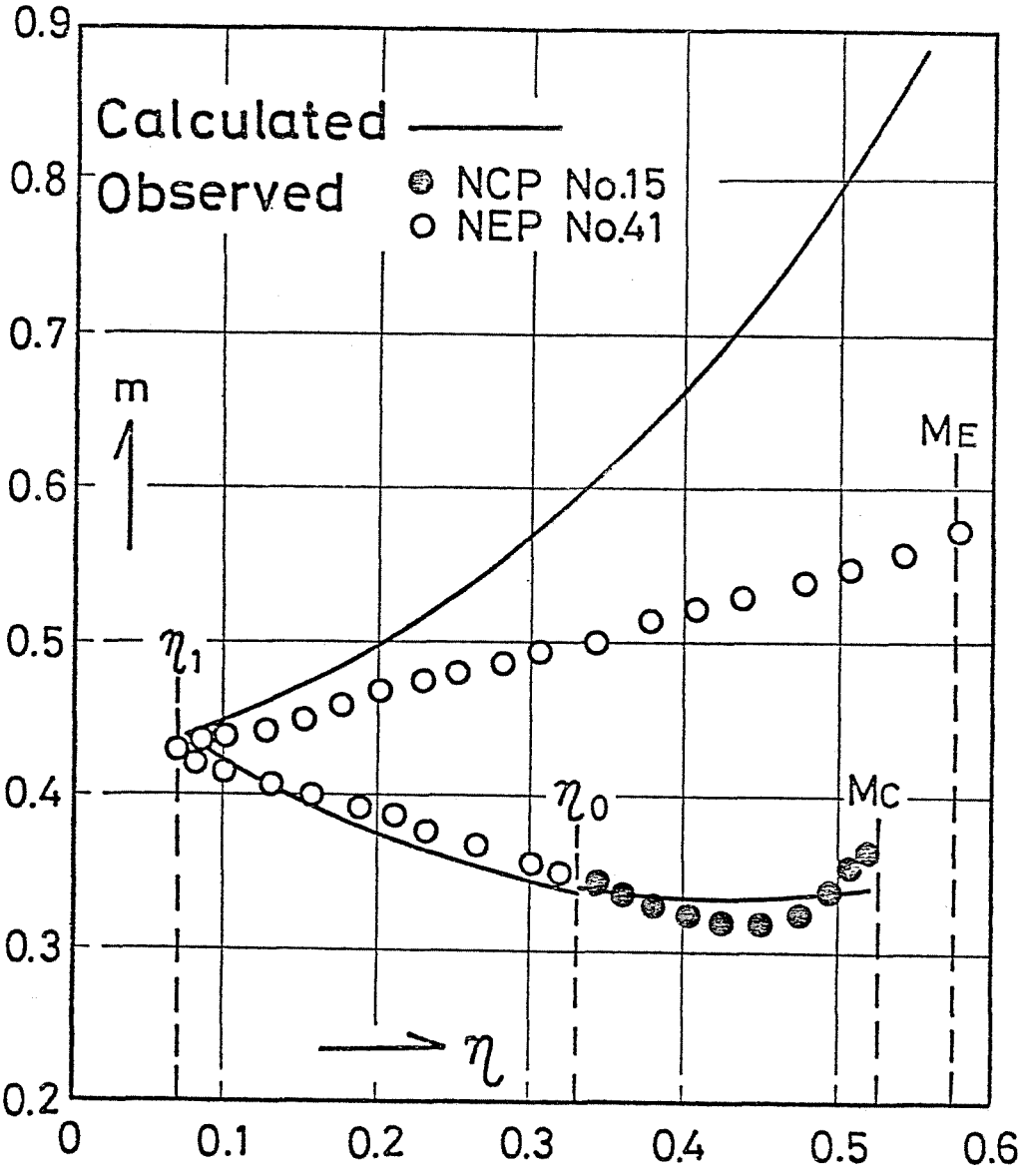

Fig.5-18 Comparison of observed and predicted relationships between m and η

axi-symmetrical compression and extension tests under the condition of securing some informations on the intermediate principal stress and effective stress path as mentioned above.

CHAPTER VI PREDICTION OF UNDRAINED SHEAR STRENGTH OF OVERCONSOLIDATED CLAY

6-1 Introduction

Excavations in saturated clay deposits lead to gradual decrease in shearing resistance of the clay due to swelling. So-called "long term " type problems correspond to such cases and effective strength parameters c' and ϕ' have been proposed to apply to this type of problems (Bishop and Bjerrum, 1960). In such cases, the failure of the clay layer is assumed to occur at a sufficiently slow rate so that little or no excess pore pressures are developed, and the pore pressures used to calculate the effective normal stresses acting on the potential failure surface are those corresponding to the ground water table or steady state seepage.

However, there is no evidence that the failure of the clay layer occurs at a sufficiently slow rate as in a drained test. Moreover, it is very difficult, in general, to measure accurately small values of cohesion intercept c' (Ladd, 1971). Therefore, taking the position that the stability problems should always be treated conservatively, it might be more practical to apply the $\phi_u = 0$ analysis to the long term type problem, based on the estimation of the rate of decrease in undrained shear strength S_u in relation to overconsolidation ratio n .

In this chapter, change in undrained strength due to consolidation and swelling obtained from the experimental results will be

shown, and the coefficient of earth pressure at rest K_o and the pore pressure coefficient A at failure will be discussed in relation to overconsolidation ratio. Furthermore, a simple method of predicting in situ undrained strength of overconsolidated clay by using the data from a series of conventional laboratory test will be presented.

6.2 Su/p_v in overconsolidated clay

In order to find the relationship between the ratio Su/p_v in overconsolidated clay and that in normally consolidated clay, assumptions are made as follows (refer to Fig.6-1), where p_v is preshear effective stress.

(1) In normal consolidation state, the relation between water content w after consolidation and effective vertical consolidation pressure p_c is represented by a straight line in semi-logarithmic plot. And the slope of this line, i.e. compression index C_c, is a constant for a given clay, irrespective of the stress systems during consolidation.

(2) In overconsolidation state, the relation between water content w after swelling and effective vertical swelling pressure p_s is also represented approximately by a straight line in semi-logarithmic plot. And the inclination of this line, i.e. swelling index C_s, is a constant for a given clay, irrespective of the stress systems in swelling process.

(3) In normally consolidated clay, w versus $\log p_f$ line is parallel to the w versus $\log p_c$ line mentioned above, where p_f is $(\sigma_1' + \sigma_3')/2$, and σ_1' and σ_3' are the major and minor principal effective stresses at failure, respectively.

(4) In overconsolidated clay, w versus $\log p_f$ relationship is approximated by a straight line within the range of $n \leqq 10$. In this study, a symbol C_f is applied to the slope of this line.

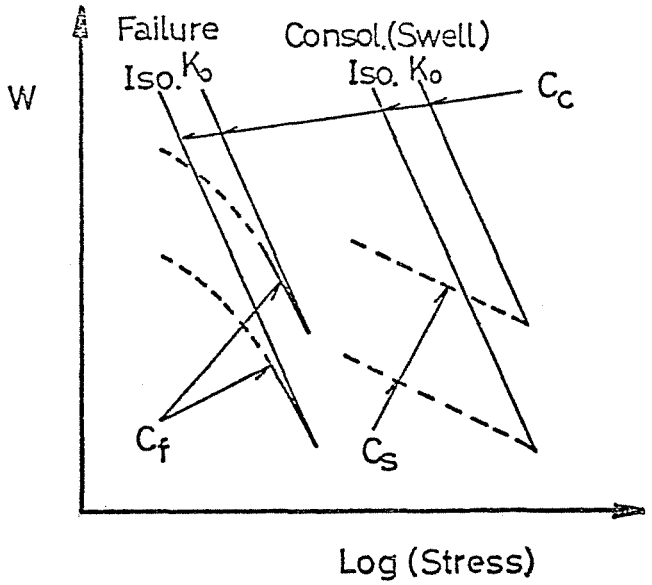

Fig.6-1 Assumptions on water content vs. effective stresses

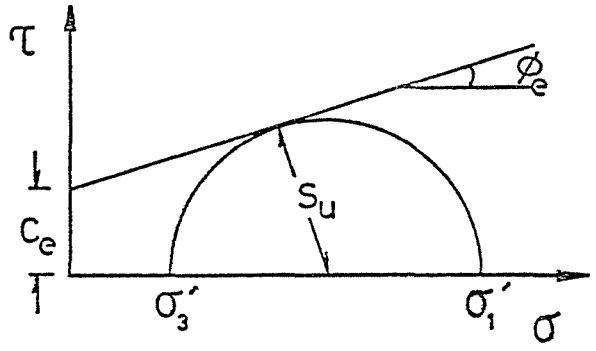

Fig.6-2 Hvorslev failure criterion

Based on these assumptions, relationship between S_{ui}/p_i versus S_{un}/p_n can be derived as follows, where subscripts i and n represent the state of normal and overconsolidation, respectively.

According to Hvorslev failure criterion, following equation is obtained referring to Mohr's stress circle in Fig.6-2.

$$S_u = \frac{\sigma_1 - \sigma_3}{2} = c_e \cos\phi_e + \frac{\sigma_1' + \sigma_3'}{2} \sin\phi_e$$

or

$$S_u = \bar{\kappa} \cdot \sigma_e' \cos\phi_e + p_f \sin\phi_e \qquad (6\text{-}1)$$

where c_e and ϕ_e are effective cohesion and effective angle of internal friction, respectively. $\bar{\kappa}$ is the coefficient of cohesion, and σ_e' is the equivalent consolidation pressure. In this paper, effective vertical stress is adopted as equivalent consolidation pressure. Idealized relationships for w versus $\log p$, and w versus $\log p_f$ are illustrated in Fig. 6-3. From this figure, following equations are obtained.

$$w_a - w_b = C_c \log p_b/p_a = C_s \log p_b/p_c = C_f \log p_{fb}/p_{fc} \qquad (6\text{-}2)$$

Combination of $\xi = C_s/C_c$ and $n = p_b/p_c$ with Eq. (6-2), gives

$$p_b/p_a = n^{\xi} \qquad (6\text{-}3)$$

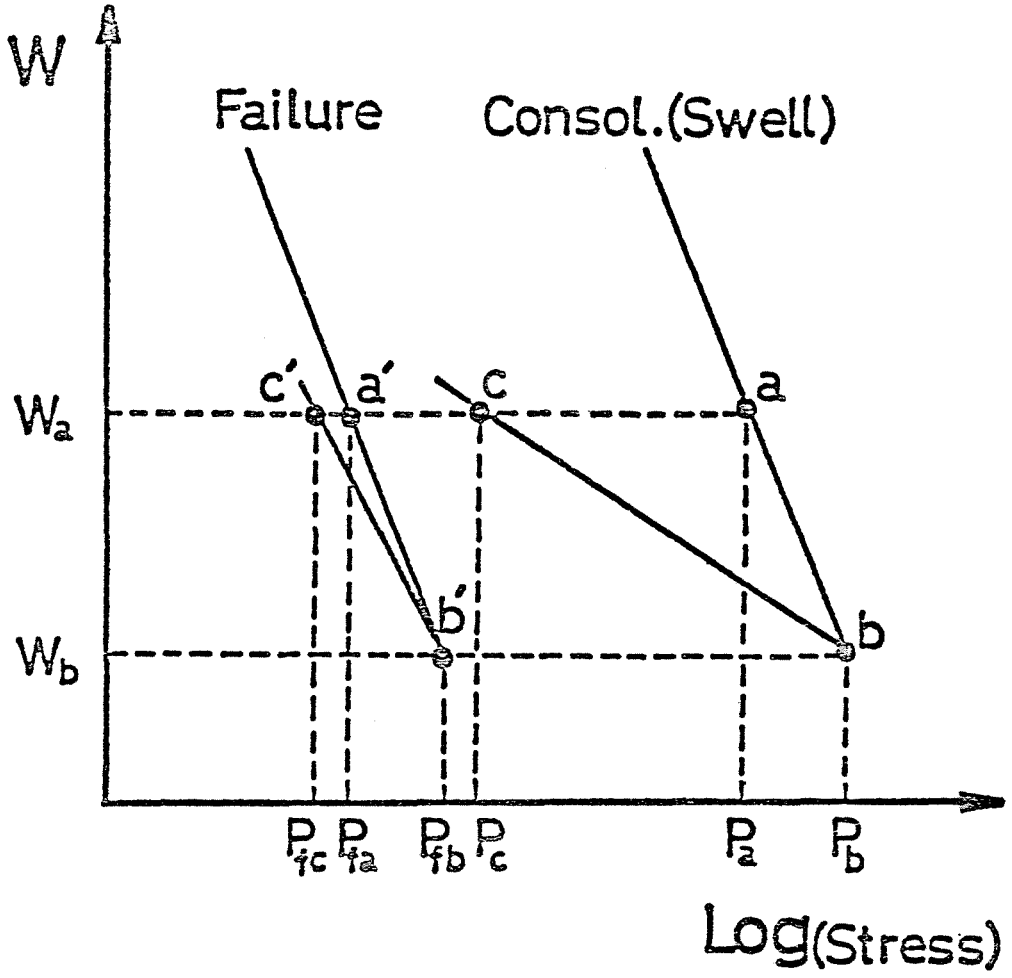

Fig.6-3 Idealized relationships between water content and effective stresses

And putting $\rho = C_s/C_f$ into Eq. (6-2), following equation is obtained

$$p_{fb}/p_{fc} = n^{\rho} \tag{6-4}$$

The ratio of undrained shear strength S_{uc} to effective swelling pressure p_c at point C in Fig. 6-3 is expressed as follows. Since the equivalent consolidation pressure at point C is p_a, following equation is obtained on referring to Eq. (6-1).

$$S_{uc}/p_c = \bar{K} \cdot p_a/p_c \cos\phi_e + p_{fc}/p_c \sin\phi_e \tag{6-5}$$

Meanwhile, combination of Eqs. (6-3), (6-4) and $n = p_b/p_c$ gives

$$p_a/p_c = n^{1-\xi} \quad , \quad p_{fc}/p_c = p_{fb}/p_b \; n^{1-\rho} \tag{6-6}$$

Substituting these into Eq. (6-5), following equation is derived.

$$S_{uc}/p_c = \bar{K} n^{1-\xi} \cos\phi_e + p_{fb}/p_b \; n^{1-\rho} \sin\phi_e \tag{6-7}$$

On the other hand, S_u/p_v at point b, which is in the state of normal consolidation, is represented as follows.

$$S_{ub}/p_b = \bar{K} \cos\phi_e + p_{fb}/p_b \sin\phi_e \tag{6-8}$$

Introducing the assumption that $\xi \fallingdotseq \rho$ within the range of $n \leqq 10$ into Eq. (6-7), following equation is obtained.

$$S_{uc}/p_c \fallingdotseq (K \cos\phi_e + p_{fb}/p_b \sin\phi_e) n^{1-\xi} \qquad (6\text{-}9)$$

Therefore, from Eqs. (6-8) and (6-9) following approximate equation is derived.

$$S_{uc}/p_c \fallingdotseq S_{ub}/p_b \, n^{1-\xi}$$

In general,

$$S_{un}/p_n \fallingdotseq S_{u1}/p_1 \, n^{1-\xi} \qquad (6\text{-}10)$$

This equation is valid for any clay provided that the clay satisfies the assumptions (1) through (4) and the condition $\xi \fallingdotseq \rho$.

6.3 Pore Water Pressure and Effective Stresses in Overconsolidated Undrained Test under Axi-symmetrical Triaxial Condition

6.3.1 Relationship between water content and preshear effective stress

It was reported that the relationship between the water content w and the average consolidation pressure $\bar{\sigma}_{mc}$ in K_o consolidation was almost identical with that in isotropic consolidation (Henkel and Sowa, 1963).

Fig. 6-4 illustrates the w versus $\log p$ relationship for 4 tests (Results of oedometer test are also plotted in this figure). For K_o test, w is plotted against both vertical and average effective stresses. In the consolidation range, w versus $\log p_c$ lines are almost parallel and K_o consolidation gives lower water content when compared to that of isotropic consolidation at the same average effective stress. By the way, Akai and Adachi (1965) demonstrated that the volumetric strain in the K_o test was larger than that in isotropic consolidation test at the same average effective stress. Khera and Krizek (1967) found that the water content decreases with the increase in stress ratio at the same average effective stress. These test results indicate that the water content depends not only on the average effective stress but also on the stress ratio.

Results such as shown in Fig. 6-4 are also obtained by others

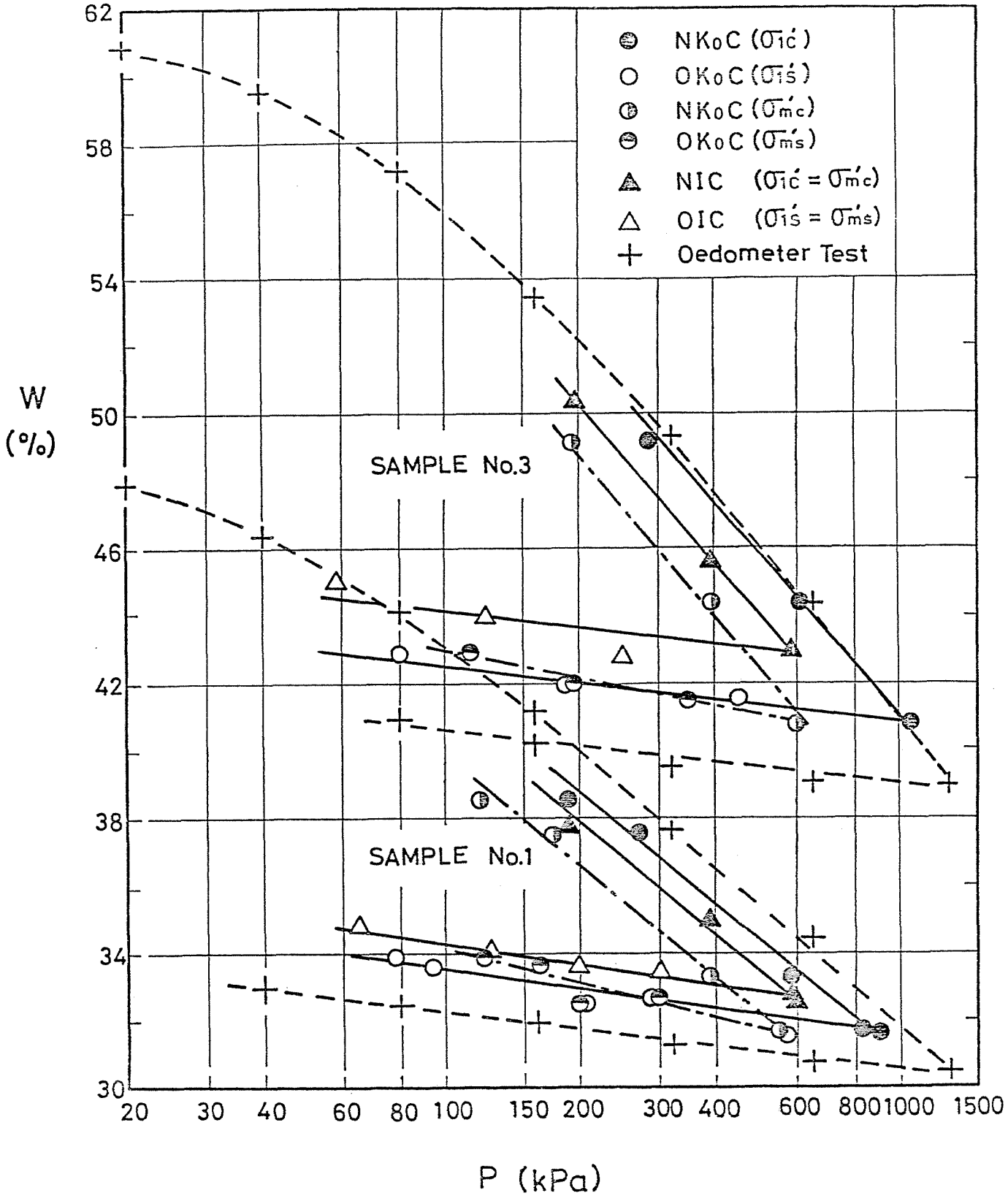

Fig.6-4 Effective consolidation (swelling) pressure vs. water content

(e.g. Lewin and Burland 1970, Campanella and Vaid 1972). Moreover, Henkel and Sowa (1963) described their own experimental results as "the fact that the water content and p' lines for both types of consolidation almost coincide must be regarded as fortuitus".

In the light of these experimental results, it will be reasonable to consider as follows. Since in the K_o consolidation there exists a volume change due to dilatancy exerted by the increase in deviator stress in addition to isotropic stress, the water content after K_o consolidation should be lower than that in isotropic consolidation at the same average effective stress.

Apart from above discussion, the fact that w versus $\log p_c$ lines are almost parallel in normal consolidation range, indicates that compression index C_c is almost constant for both K_o and isotropic stress conditions. And this verifies the adequacy of the preceding assumption (1) in section 6.2.

Turning attention to w versus $\log p_s$ relationship in swelling range, their curves can be approximated to straight lines within the range of $n \leqq 10$. And the lines representing w versus $\log p_s$ in terms of effective vertical swelling pressure σ'_{is} in K_o and isotropic swelling tests are almost parallel. This means that the swelling index is constant and satisfies the assumption (2) in section 6.2. Moreover, ξ, which is the ratio of compression index C_c to swelling index C_s in terms of vertical effective stress, is almost identical for both K_o and isotropic stress conditions. The values ξ are computed as 0.20, 0.16 and 0.11 for Sample No. 1,2 and 3, respectively.

6.3.2 Coefficient of earth pressure at rest

The coefficient of earth pressure at rest K_0 is defined as the ratio of the minor principal effective stress to the major one after consolidation or swelling under the condition of no lateral strain. Table 6-1 shows the average K_0 value in normal consolidation and the effective angle of shearing resistance ϕ' obtained from NIC test. Brooker and Ireland (1965) reported that the value K_0 in normally consolidated clay could be approximated by the empirical relationship

$$K_0 = 0.95 - \sin \phi' \qquad (6\text{-}11)$$

whereas the original relationship proposed by Jaky

$$K_0 = 1 - \sin \phi' \qquad (6\text{-}12)$$

were more valid for cohesionless soils.

However, Akai and Adachi (1965) and Yamaguchi (1972) described that both equations were open to question because K_0 value after consolidation were combined to the angle of shearing resistance at failure. Yamaguchi (1972) derived the equation expressing the relation between K_0 value and interparticle friction angle ϕ_μ, and combining ϕ_μ and ϕ' by Caquot's equation, he finally obtained the following equation.

Sample number	K_o			ϕ'	
	Observ.	Eq.(6-12)	Eq.(6-13)	NIC	NK_oC
1	0.45	0.40	0.39	37.2	35.1
2	0.45	0.43	0.42	35.1	34.9
3	0.47	0.41	0.41	36.1	34.0
4	0.52	0.49	0.48	30.6	26.8

Table 6-1 Coefficient of earth pressure at rest and effective angle of shearing resistance in normally consolidated samples

$$K_o = \frac{1-0.404\ \tan\phi'}{1+\tan\phi'} \qquad (6\text{-}13)$$

In Table 6-1, there listed the values of K_o calculated by Eqs. (6-12) and (6-13) using ϕ' obtained from NIC test. K_o values calculated by Eq. (6-12) are closer to the observed ones.

Brooker and Ireland (1965) found that the K_o values in overconsolidation state could be expressed by the function of overconsolidation ratio n and plasticity index I_p. In this section, the relationship between the earth pressure at rest in overconsolidation state K_{on} and overconsolidation ratio n is investigated.

Fig. 6-5 schematically illustrates the general trend existing in between observed water content and consolidation pressure, which can be seen in Fig. 6-4. From this figure, following equation is obtained.

$$w_a - w_b = C_{sl} \log p_b/p_d = C_{sm} \log p_b'/p_d' \qquad (6\text{-}14)$$

where, C_{sl} is the slope of the swelling line $\overline{bd}$ which is represented in terms of vertical effective stress and C_{sm} is that of the swelling line $\overline{b'd'}$ in terms of average effective stress. While, there exists the following relationship.

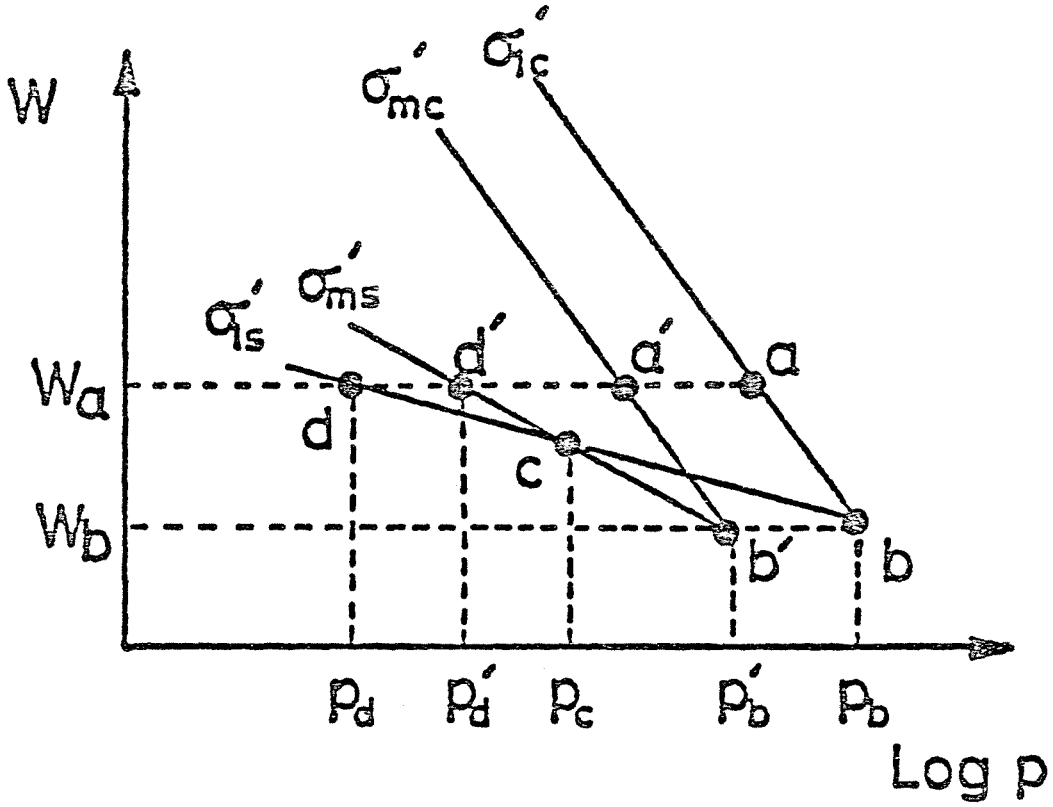

Fig.6-5 Schematic representation of preshear effective stress vs. water content relationship

$$p_b' = \frac{p_b(1+2K_{o1})}{3}, \quad p_d' = \frac{p_d(1+2K_{on})}{3}, \quad p_b/p_d = n \tag{6-15}$$

Combination of Eq.(6-15) with Eq.(6-14) gives

$$1 + 2K_{on} = (1+2K_{o1})\, n^{(1 - C_{s1}/C_{sm})} \tag{6-16}$$

As $\overline{bd}$ and $\overline{bd'}$ lines intersect each other at point c , it follows

$$C_{s1} \log p_b/p_c = C_{sm} \log p_b'/p_c \tag{6-17}$$

where $p_b/p_c = n_o$ is overconsolidation ratio at point c . Combination of Eqs. (6-15), (6-17) and $p_b/p_c = n_o$ gives

$$C_{s1}/C_{sm} = 1 + \frac{\log \frac{1+2K_{o1}}{3}}{\log n_o} \tag{6-18}$$

Putting above equation into Eq. (6-16), following equation is obtained.

$$1 + 2K_{on} = (1+2K_{o1})\, n^{\alpha} \tag{6-19}$$

where

$$\alpha = - \frac{\log \frac{1+2K_{o1}}{3}}{\log n_o} \tag{6-20}$$

Comparison of K_{on} values calculated by Eq. (6-20) with those observed in the tests are shown in Fig. 6-6, where the values of K_{oI} and n_o required to calculate the value of K_{on} were read from Table 6-1 and Fig. 6-4, respectively. Based on the theoretical consideration, Yamanouchi and Yasuhara (1974) described that K_{on} is defined as $K_{on} = f(n, I_p)$. Further, they reviewed the data reported up to that time and found that the slope of $\log(1 + 2K_{on})$ vs. $\log n$ line, i.e. ξ_m varies with I_p, where, $\xi_m = C_{sm}/C_c$.

As it is apparent from the above mentioned investigation and from the data shown in Fig. 6-6 by the present author, K_{on} can be expressed as a function of n. But, finding out the dominant factor, which governs the value ξ_m of Yamanouchi and Yasuhara or n_o in the present author's Eq.(6-20), is the subject for a future study.

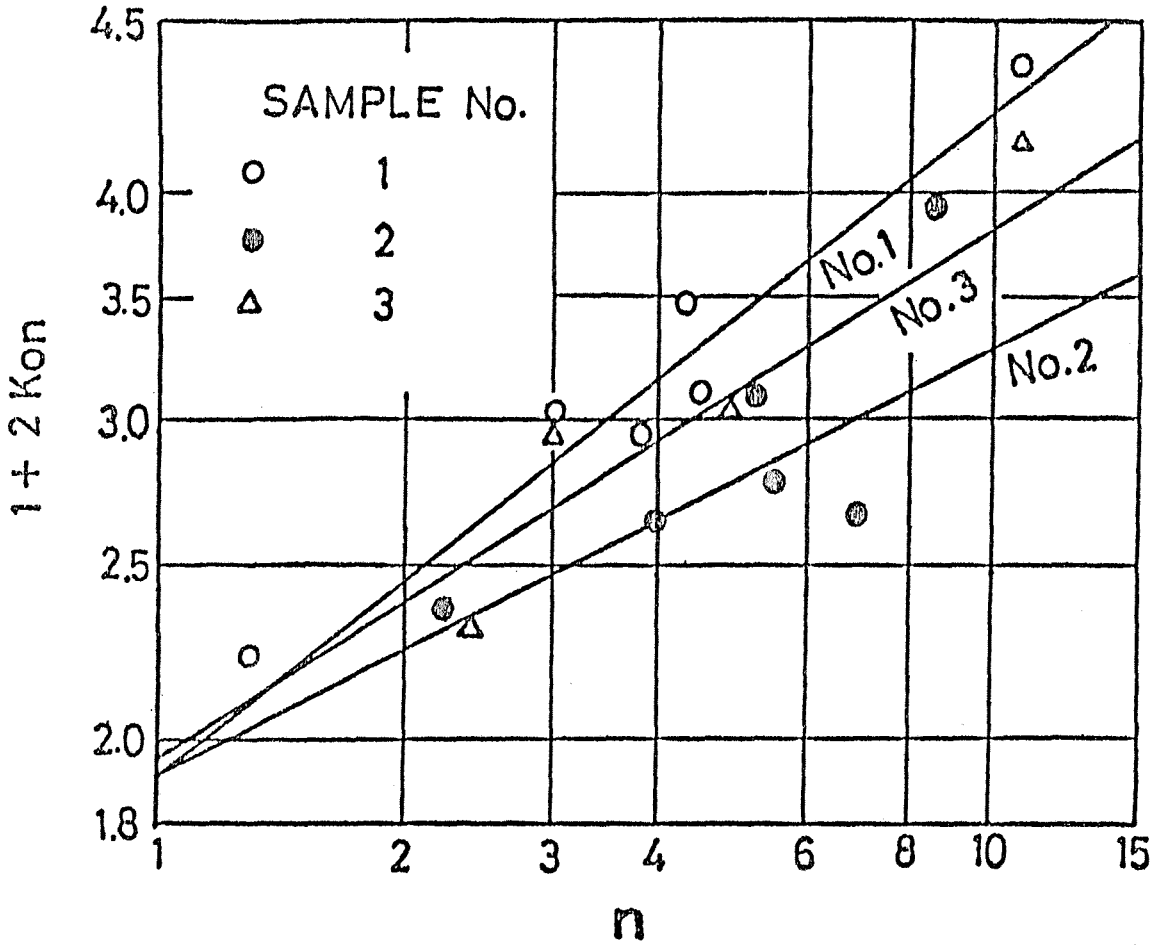

Fig.6-6 Coefficient of earth pressure at rest in overconsolidation state vs. overconsolidation ratio

6.3.3 Pore water pressure coefficient at failure

Fig. 6-7 shows the variation of the pore water pressure coefficient at failure A_f with the overconsolidation ratio n, where the value A_f at $n = 1$, i.e. in normal consolidation state, is the average of values obtained from the tests in different consolidation pressures.

Curves in Fig. 6-7 were obtained by the following manner. As stated before, if the assumption $\xi \fallingdotseq \rho$ is permitted, C_f is nearly equal to C_c, and hence p_{fa} is equal to p_{fc} in Fig. 6-2. For NK_oC and OK_oC test, p_{fa} and p_{fc} can be expressed in terms of undrained shear strength S_u, preshear effective stress p, coefficient of earth pressure at rest K_o and the pore water pressure coefficient at failure A_f as follows.

$$\left.\begin{aligned} p_{fa} &= p_a \{K_{oa} + A_{fa}(1-K_{oa})\} + S_{ua}(1-2A_{fa}) \\ p_{fc} &= p_c \{K_{oc} + A_{fc}(1-K_{oc})\} + S_{uc}(1-2A_{fc}) \end{aligned}\right\} \quad (6\text{-}21)$$

According to Hvorslev failure criterion, undrained strength S_{ua} of normal consolidation will be equal to the undrained strength S_{uc} of overconsolidation, provided that the water content at point a is equal to that at c and $p_{fa} = p_{fc}$. Putting above condition and the relationship $S_{uc}/p_c = S_{ua}/p_a \, n^{1-\xi}$ into Eq. (6-21) following equation is obtained.

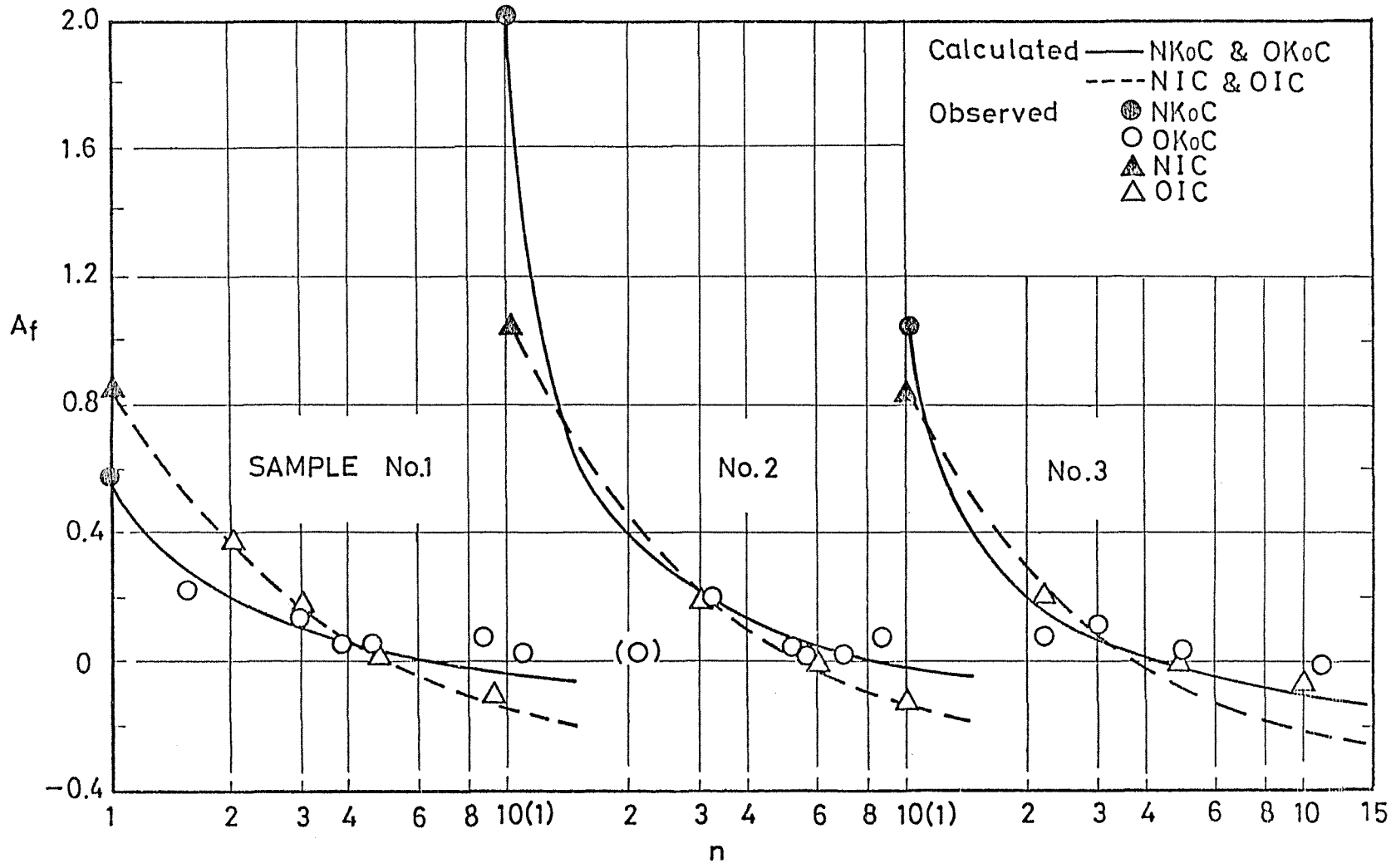

Fig.6-7 Pore water pressure coefficient at failure vs. overconsolidation ratio

$$A_{fc} = \frac{A_{fa}\left\{1 - p_a/2S_{ua}(1-K_{oa})\right\} - p_a/2S_{ua}(K_{oa} - K_{oc}n^{\xi-1})}{1 - p_a/2S_{ua}\ (1-K_{oc})n^{\xi-1}}$$

In general

$$A_{fn} = \frac{A_{f1}\left\{1 - p_1/2S_{u1}(1-K_{o1})\right\} - p_1/2S_{u1}(K_{o1} - K_{on}n^{\xi-1})}{1 - p_1/2S_{u1}\ (1-K_{on})n^{\xi-1}} \qquad (6\text{-}22)$$

where subscripts 1 and n represent the state of normal and overconsolidation, respectively.

For OIC test, the condition $K_{o1} = K_{on} = 1$ is combined with Eq. (6-22), giving

$$A_{fn} = A_{f1} - p_1/2S_{u1}\ (1-n^{\xi-1}) \qquad (6\text{-}23)$$

Eq. (6-23) is substantially the same as equation (22) of Roscoe et al. (1958), although the form of the equation is different to each other. Putting the values of A_{f1} (average value of A_f at $n=1$), S_{u1}/p_1 (shown later in Table 6-2), $1-\xi$ (also shown later in Table 6-3), K_{o1} (read from Table 6-1) and K_{on} (calculated by Eq. 6-19) into Eqs. (6-22) and (6-23), the curves in Fig. 6-7 are obtained. As seen in the figure, the calculated values of A_{fn} agree well with the observed ones, especially in the number 1 and 2 samples.

6.3.4 Effective stress at failure

Fig. 6-8 represents the relation between the water content w after consolidation or swelling and effective stress p_f, where p_f is equal to the average value of major and minor effective principal stresses at failure. From this figure, it is obvious that w versus $\log p_f$ lines in normally consolidated clay are straight and the slopes of these lines are almost equal to the compression index C_c. This fact satisfies the previous assumption (3) in section 6.2. Further, the points corresponding to OIC and OK_oC tests are closely adjacent to the w versus $\log p_f$ lines for NIC and NK_oC test, respectively. Therefore, the previous assumption of approximate equality of ξ and ρ will be permitted within the range of $n \leqq 10$.

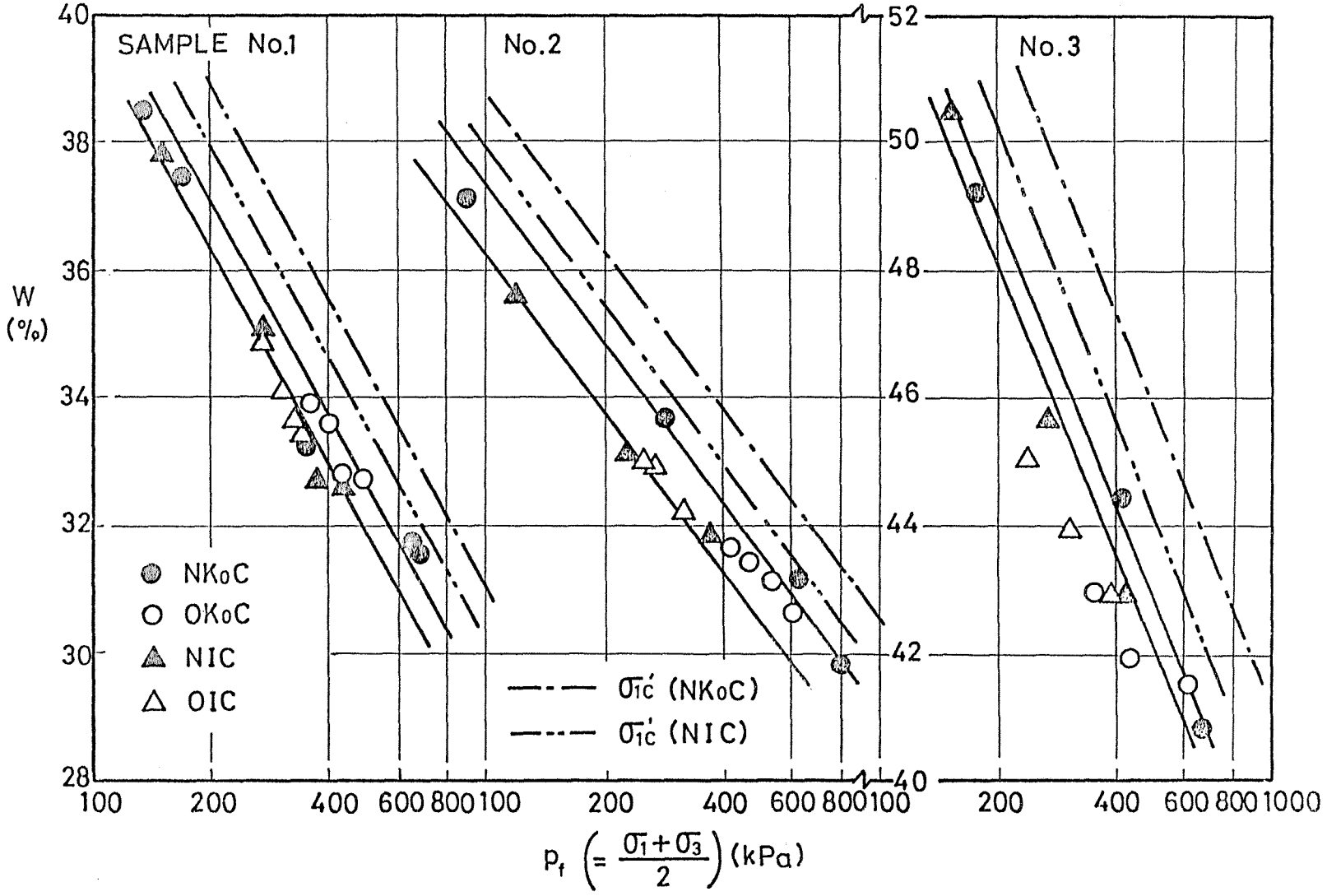

Fig.6-8 Relationship between water content and effective stress at failure

6.4 Change in Undrained Triaxial Compression Strength due to Consolidation and Swelling

The variation of the undrained strength S_u with the preshear effective stress p_v is shown in Fig. 6-9. The ratio S_u/p_v for normally consolidated clay in NIC tests are 5 to 12 per cent larger than those in NK_oC tests (see Table 6-2). These results coincide with that reported by others (e.g. Henkel and Sowa, 1963, Nakase et al. 1969).

Fig. 6-10 illustrates the relationships between the overconsolidation ratio n and the normalized ratio S_u/p_v in axi-symmetrical triaxial compression test, in which p_v is the preshear effective vertical stress. Broken lines are those replotted from the data given by Ladd and Foott (1974) in terms of S_u/p_v versus $\log n$. Their data were obtained by direct simple shear test, the test procedure of which corresponds to the OK_oC test by the present author.. As shown in Fig. 6-10, it is obvious that the relation between $\log S_u/p_v$ and $\log n$ is represented by a straight line (the data for Sample No.2 were not shown in this figure because they fall in the same range in Sample No.1), and the line for each OK_oC test is almost parallel to that for OIC test. Consequently, S_u/p_v versus n relationhip within the range of $n \geqq 10$ can be represented as follows.

$$\left(S_{un}/p_n\right)_{K_o} = \left(S_{u1}/p_1\right)_{K_o} n^{\beta} \qquad (6\text{-}24)$$

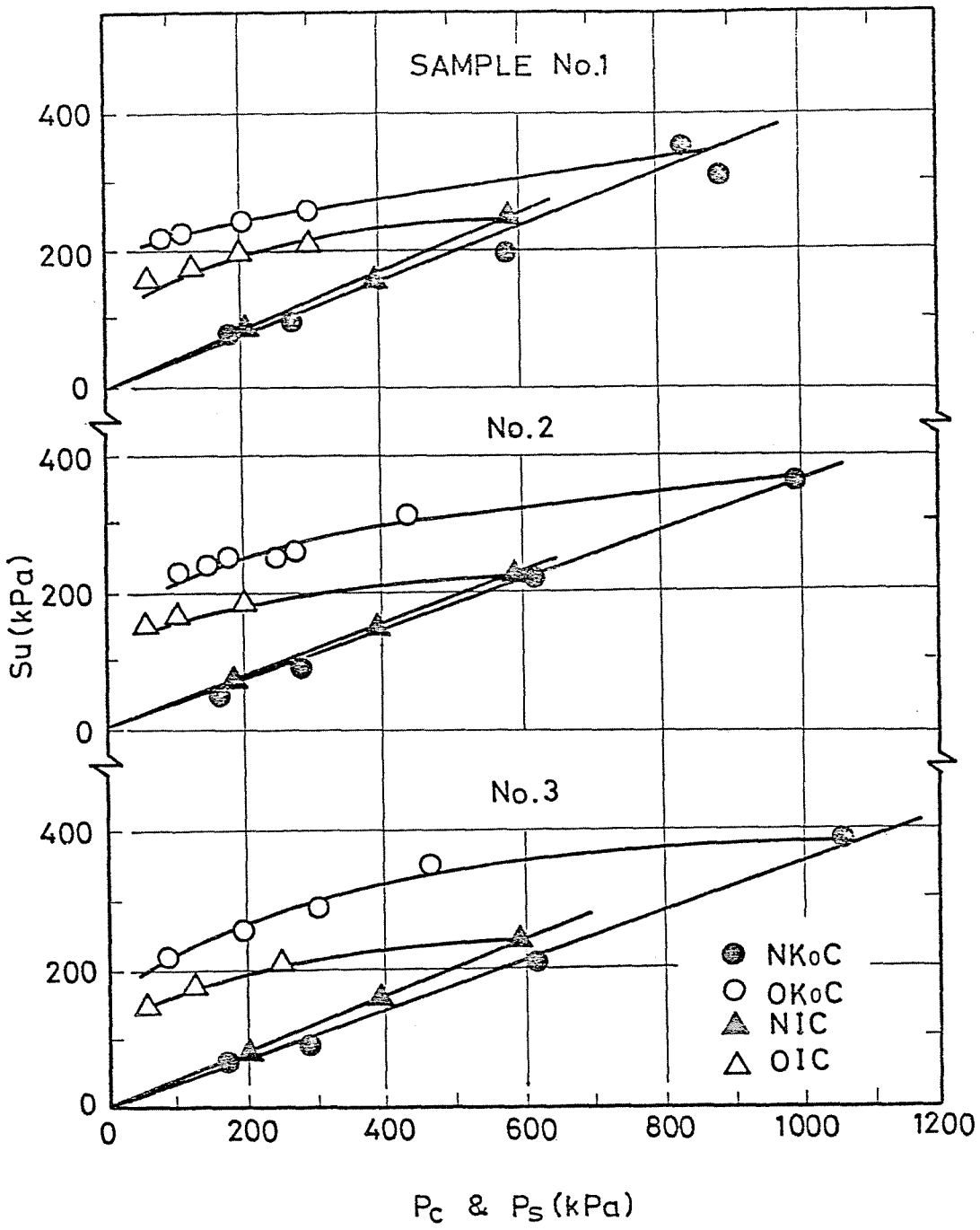

Fig.6-9 Undrained shear strength vs. preshear effective stress

Test	Sample number		
	1	2	3
NIC	0.42	0.36	0.41
NK_oC	0.40	0.34	0.36

Table 6-2 Comparison of the ratio S_u/p_v in NIC and NK_oC tests

Sample number	$1-\xi$	β
1	0.80	0.81
2	0.84	0.85
3	0.89	0.86

Table 6-3 Comparison of the value $(1-\xi)$ and β

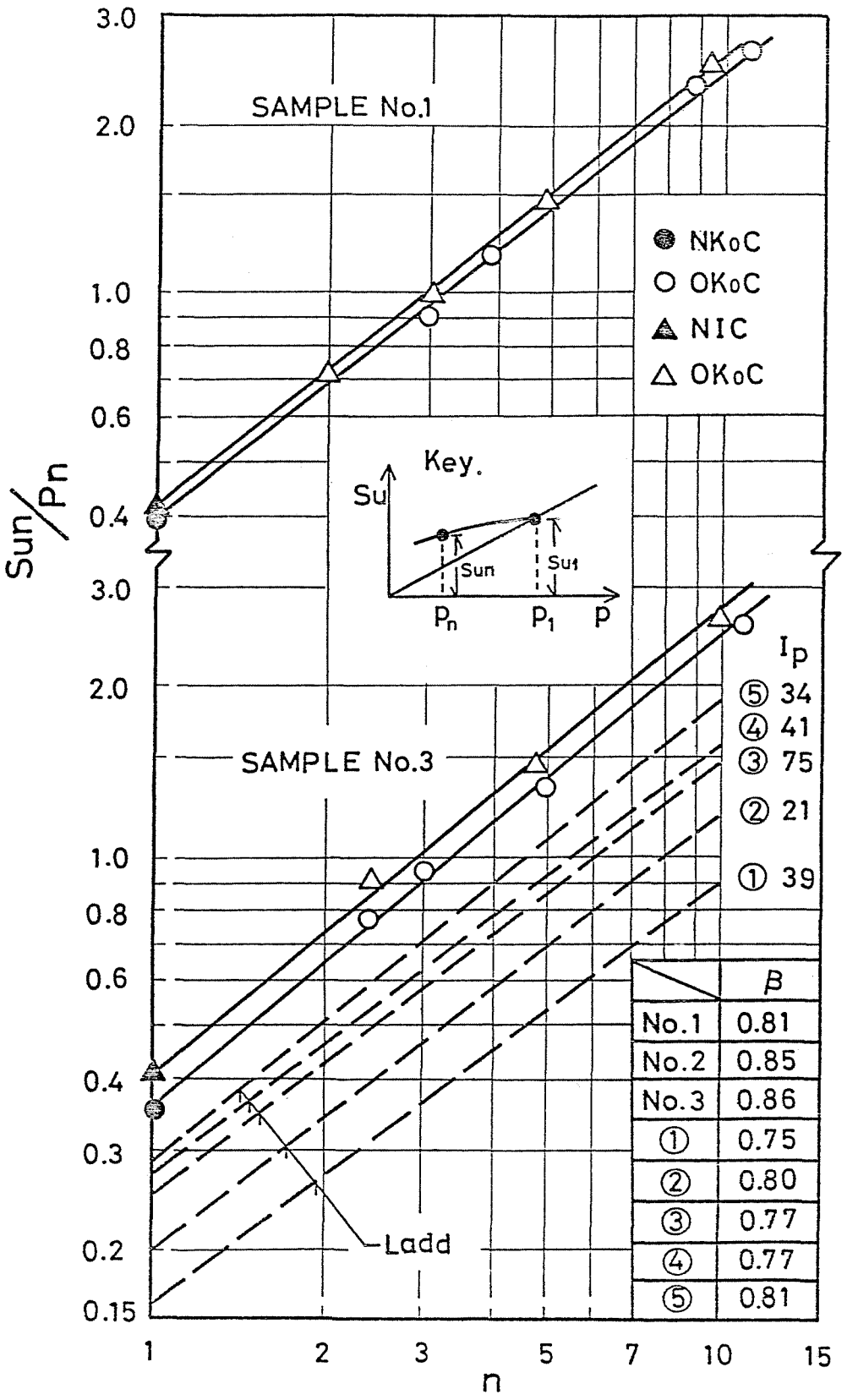

Fig.6-10 Rate of change in undrained shear strength vs. overconsolidation ratio (axi-symmetrical triaxial compression tests)

$$\left(Sun/p_n\right)_I = \left(Su1/p_1\right)_I n^{\beta} \qquad (6\text{-}25)$$

where, the subscripts K_0 and I represent the K_0 and isotropic stress condition, respectively, and the exponent β represents the slope of the $\log Su/p$ versus $\log n$ line.

The form of Eqs. (6-24) and (6-25) are quite the same as Eq. (6-10) and the exponent β in Eqs. (6-24) and (6-25) corresponds to $(1-\xi)$ in Eq. (6-10). By the way, the comparison of the values of $(1-\xi)$ with those of β indicates fairly good agreement as shown in Table 6-3.

In this study, the experimental data are limited within the range of $n \leqq 10$, whereas experiments in isotropic condition for wide range of n values up to 375 were carried out by Yudhbir and Varadarajan (1974). Their data indicate that $(Sun/p_n)_I$ values increase abruptly for n value greater than about 100. In any case, the in situ undrained shear strength of a clay soil with any value of n within the range of $n \leqq 10$ can be estimated by using the value $(Su1/p_1)_I$ obtained from the conventional CU triaxial compression test and ξ obtained from the oedometer test, provided that the relation between $(Su1/p_1)_I$ and $(Su1/p_1)_{K_0}$ is established.

Previously the present author (Mitachi and Kitago 1973) proposed a temporary method for estimating the $(Suy/p_1)_{K_0}$ from $(Suy/p_1)_I$.

This method was based on the experimental results of Henkel and Sowa (1963) and that of the present author (Mitachi and Ueda 1969, and Mitachi and Kitago 1973) that the water content in normal consolidation is uniquely defined by the average effective consolidation pressure irrespective of the stress systems during consolidation. The author's present test data indicate that the relationship mentioned above is not always be satisfied. Therefore, the previous method of estimation lost its basis.

Accordingly, let us now consider how to represent the relation between $(S_{ui}/p_i)_{K_o}$ and $(S_{ui}/p_i)_I$ in simple expression. From the experimental results in the past (e.g. Henkel and Sowa 1963, Ladd 1965, Nakase et al. 1969, Mitachi et al. 1970) the maximum difference between the values of $(S_{ui}/p_i)_I$ and $(S_{ui}/p_i)_{K_o}$ is about 20 %. Now, it should be noted that the undrained shear strengths S_u in S_u/p_v mentioned above are not the shear stresses acting upon the failure plane, but the ones exerted on the 45° plane. Mikasa (1969) proposed a convenient method to obtain the S_u on the failure plane from the conventional NIC test. His method is as follows (see Fig. 6-11). NIC test data are arranged as if they were conducted under the condition of constant average principal stress (in terms of total stress), and the plane on which this average principal stress acts is presumed to be the failure plane. The undrained shear strength obtained by this method is 6 % less than that obtained by assuming $\phi_u = 0$. Strictly speaking, the shear stress caluculated by this method is not always equal to that on the failure plane, but the difference between the shear stress on the 45° plane and that on the failure plane may be within this order.

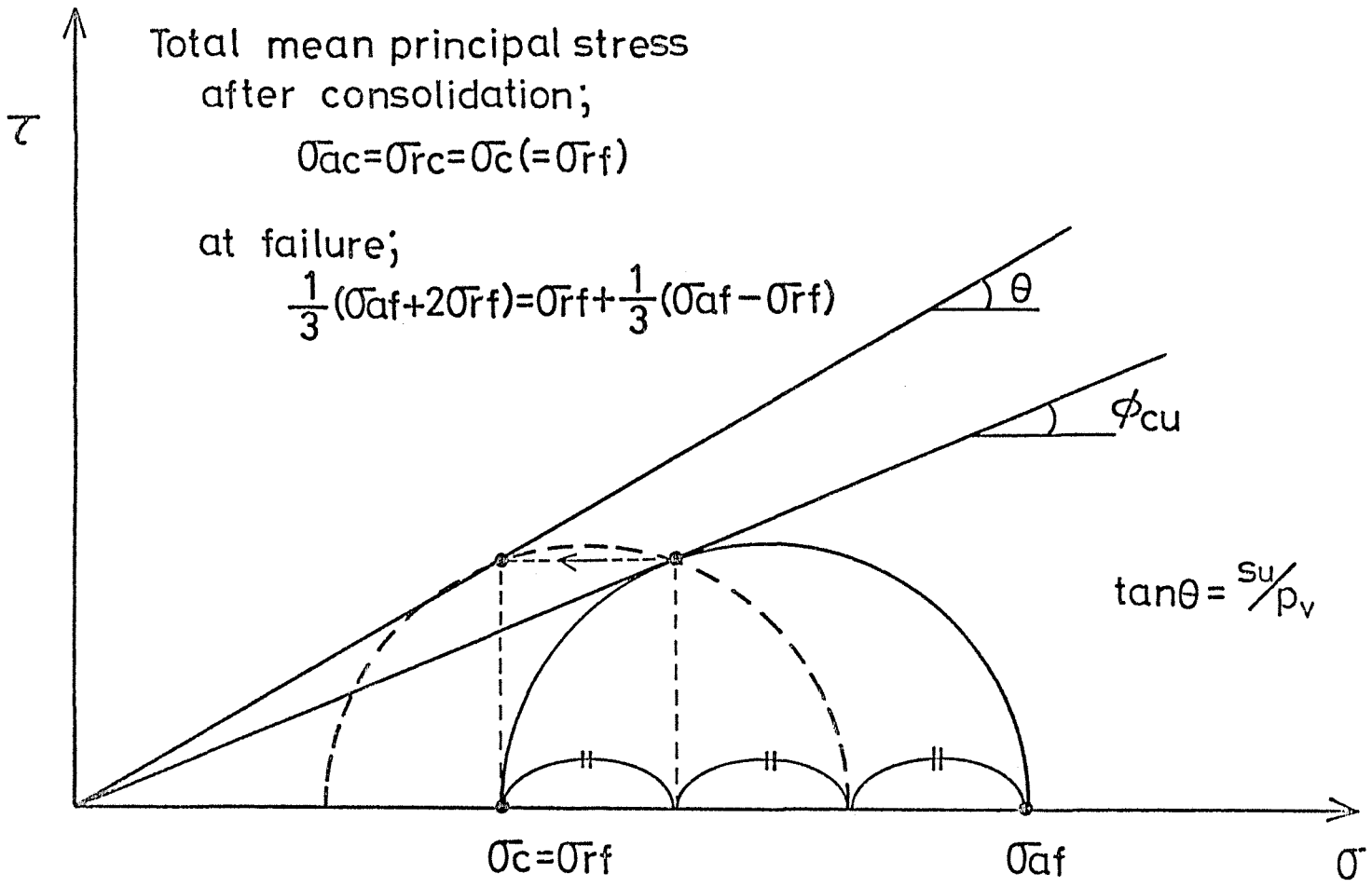

Fig.6-11 A method obtaining undrained shear strength by NIC test(Mikasa, 1969)

On the other hand, the undrained shear strengths for stability computation have to be obtained from the tests in plane strain condition, since the conditions of many field problems closely approximate to those of plane strain. As already mentioned in Chapter V, investigations hitherto (e.g. Henkel and Wade, 1966, Kitago et al. 1973 and Vaid and Companella, 1974) show that the S_u/p_v in plane strain condition is about 8 to 10% larger than that in axi-symmetrical stress condition. Therefore, it can roughly be assumed that both effects mentioned above cancel each other.

Consequently, for conservative estimate, let $(S_{u1}/p_1)_{K_0} \fallingdotseq 0.8\,(S_{u1}/p_1)_I$, and following equation is obtained

$$(S_{un}/p_n)_{K_0} \fallingdotseq 0.8\,(S_{u1}/p_1)_I\, n^{1-\xi} \qquad (6\text{-}26)$$

6.5 S_u/p_v versus n in Triaxial Extension and Plane Strain Tests

In this section, the effect of stress system during shear and, in addition, the effect of stress system during K_o consolidation on the S_u/p_v versus n relationship will be shown. To begin with, the relationship between consolidation pressure and undrained shear strength versus water content are examined.

There are a number of experimental evidence indicating that consolidation pressure versus water content relationship in normally consolidated clay is represented by straight lines in semi-logarithmic plot irrespective of stress system during consolidation, i.e. isotropic or anisotropic stress system. Fig.6-12 illustrates the preshear effective stress versus water content relationship before shear (end of consolidation and swelling). In this case, consolidation pressure for K_o consolidation(radial strain is kept to be zero) is effective axial stress and is effective radial stress for $\overline{K_o}$ consolidation (axial strain is kept to be zero), respectively. For isotropic and K_o consolidation in normally consolidated clay, the similar relationship as already mentioned in section 6.3.1 was obtained. In $\overline{K_o}$ consolidation the data points are plotted between the w versus $\log p_v$ curves for isotropic and K_o consolidation tests.

In overconsolidation state such a simple relationship as in normal consolidation does not appear. Even though it is assumed that w versus $\log p_v$ lines are straight, the slopes of these lines are different each other, depending on the way of defining

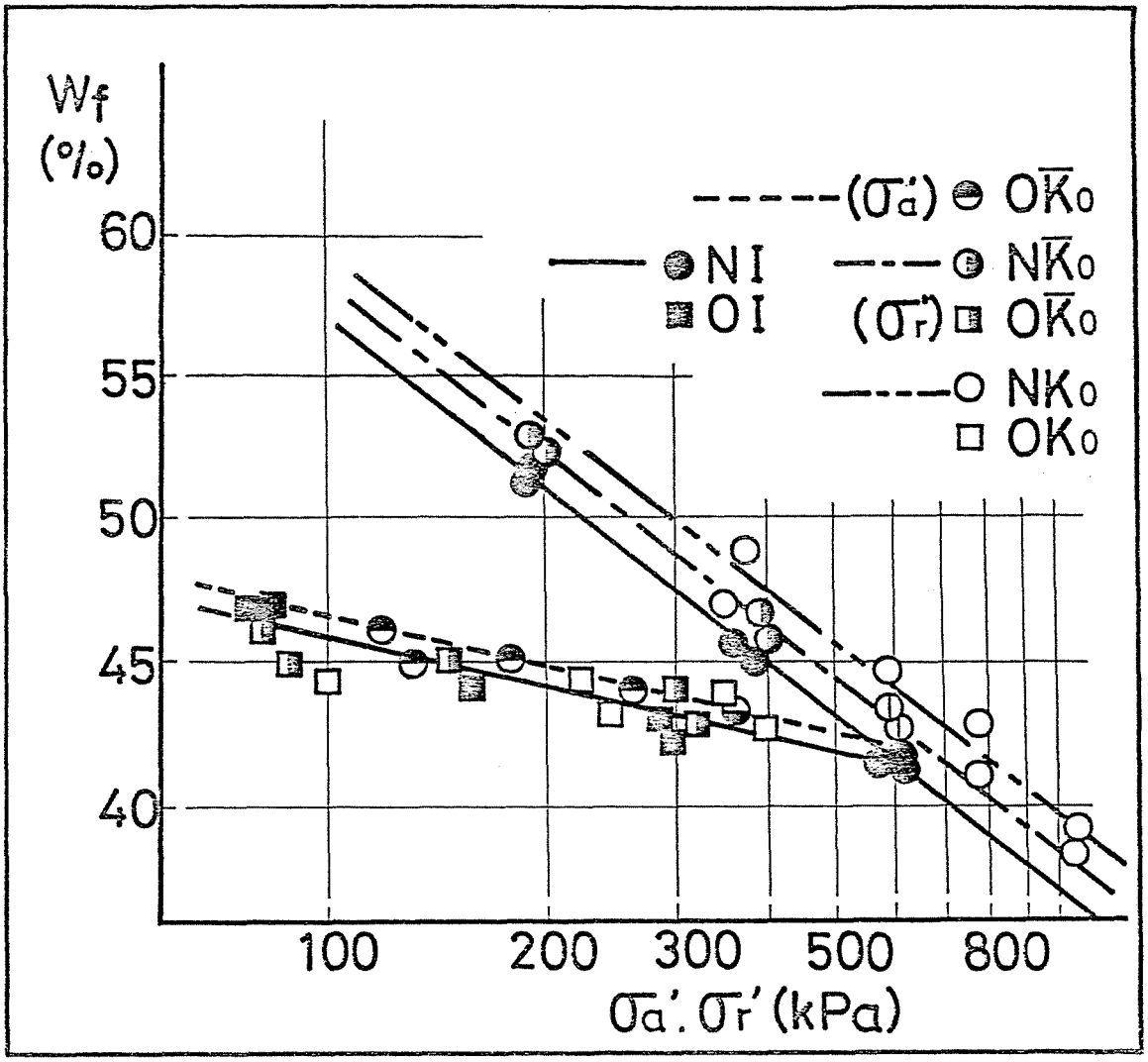

Fig.6-12 Preshear effective stress vs. water content relationship for 7 series of test on sample No.4

the consolidation (swelling) pressure, i.e. axial stress or radial stress.

Fig. 6-13 illustrates the relationship between water content versus deviatoric stress at failure. In extension test, the influence of stress system during consolidation on the undrained strength is striking, and the undrained strength in $N\overline{K_o}E$ test is about twice as large as that in NK_oE test. Considering the details of NK_oE and $N\overline{K_o}E$ tests, although the type of stress application is the same for two tests, there occurs an interchange of principal stress directions in NK_oE test while it doesn't occur in $N\overline{K_o}E$ test. On the other hand, the interchange of principal stress directions occurs in $N\overline{K_o}C$ while it doesn't occur in NK_oC test, although the type of stress application during shear is the same for the two compression tests. As stated above, although the point of difference between the two compression tests and that of two extension tests is the same, the strength difference between them is pronounced. One of the possible causes of this difference may be considered as follows. In compression tests, the intermediate principal stress is equal to minor one while it is equal to major one in extension tests.

In order to correlate the undrained shear strength S_u in normally consolidated clay to that in overconsolidated clay, assumptions (1), (2) and (3) are hold as mentioned previously in section 6.2. The experimental data in compression test indicating the validity of the assumption (3) has been shown previously. In extension test, Henkel et al. (1960) has already confirmed this fact in

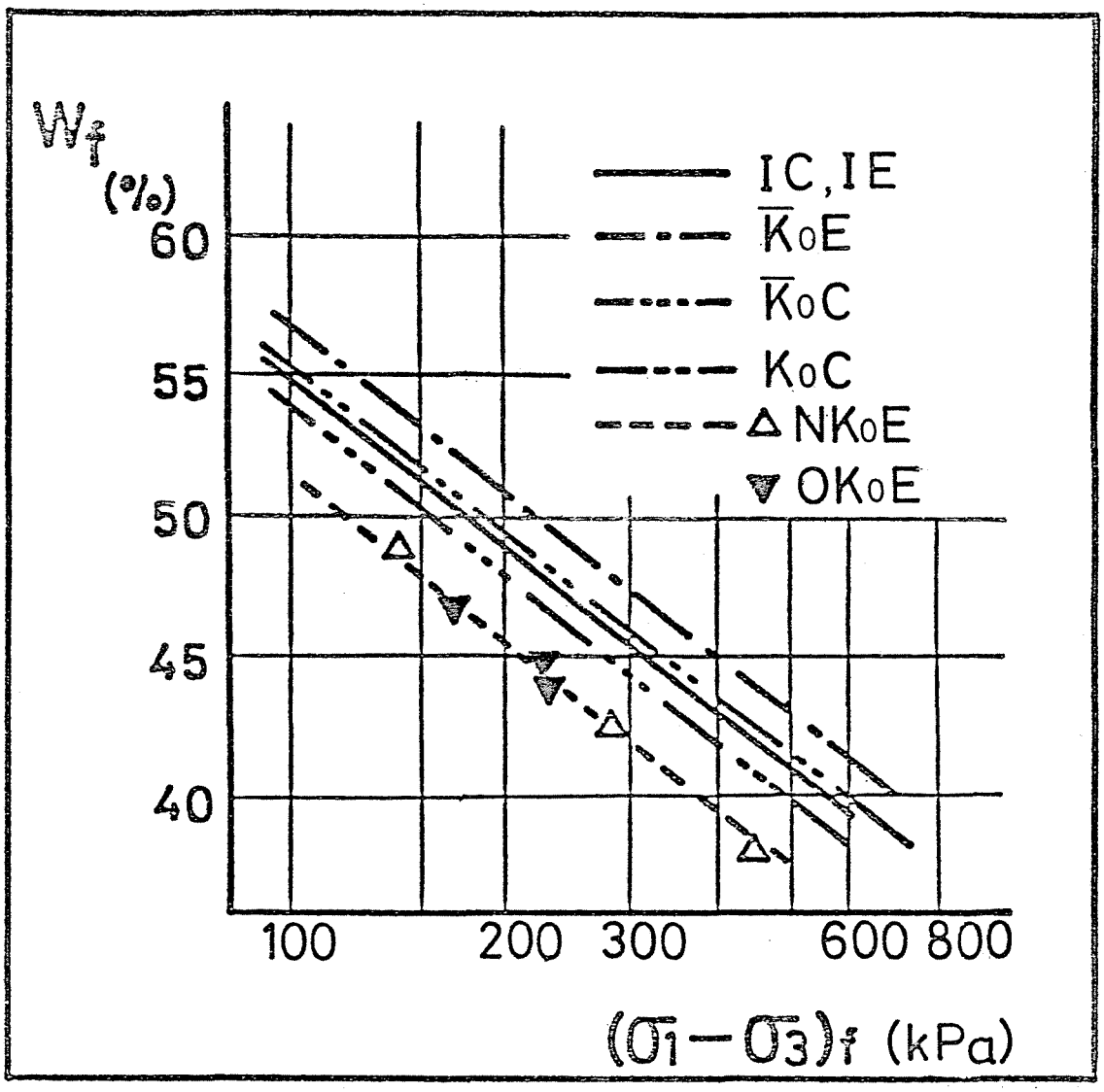

Fig.6-13 Water content vs. deviatoric stress at failure for 7 series of test on sample No.4

isotropically consolidated (and rebounded) undrained extension tests. From the experimental data by the present author, it can be extended to K_o consolidated (and rebounded) extension tests. Fig.6-14 illustrates the assumptions (1), (2) and (3) mentioned above. From this figure, following equation can be derived.

$$S_{un}/p_n = (S_{ui}/p_i)\, n^{(1-\rho)}$$

Fig.6-15 illustrates S_{un}/p_n versus n relationship for 12 types of test. Depending on the way of defining the consolidation presure p_n and overconsolidation ratio n, the slope and intercept of $\log S_{un}/p_n$ versus $\log n$ curves are different each other. One example for this is shown in the figure on the K_oE tests. The line denoted by $K_oE(\sigma_a')$ is based on the way of defining p_n and n by the axial stress, whereas the line denoted by $K_oE(\sigma_r')$ is based on the radial stress whose direction coincides with the major principal stress direction at failure. For the test data other than K_oE tests, consolidation pressure and overconsolidation ratio are all defined by the stress whose direction coincides with the major principal stress direction at failure. Thus, the slopes of each tests are almost identical, namely ρ is almost constant irrespective of the stress system during consolidation and swelling, provided that the consolidation pressure and overconsolidation ratio are defined as mentioned above. Accordingly, undrained shear strength of overconsolidated clay in axi-symmetrical extension condition can be estimated by the same method as in compression condition.

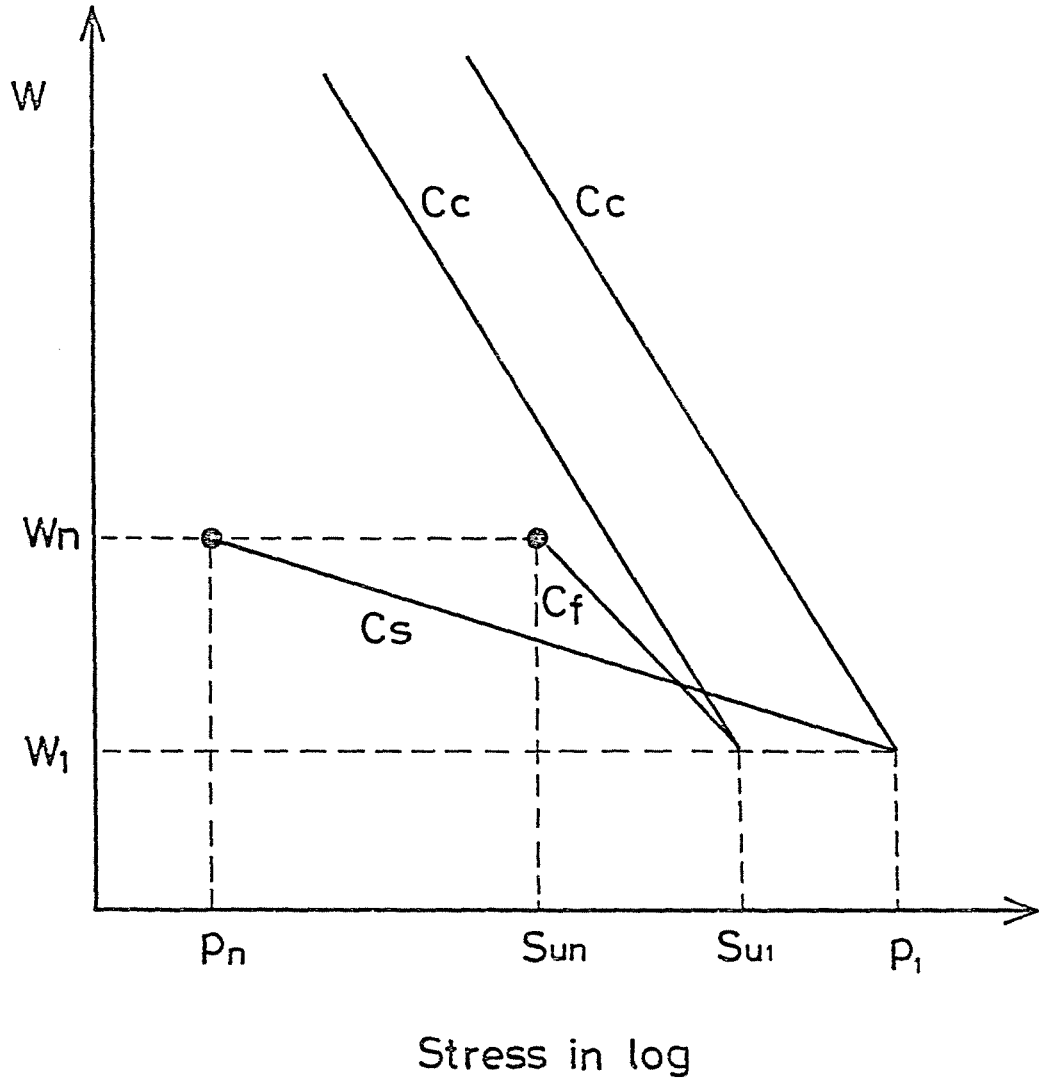

Fig.6-14 Idealized relationships between water content and stresses

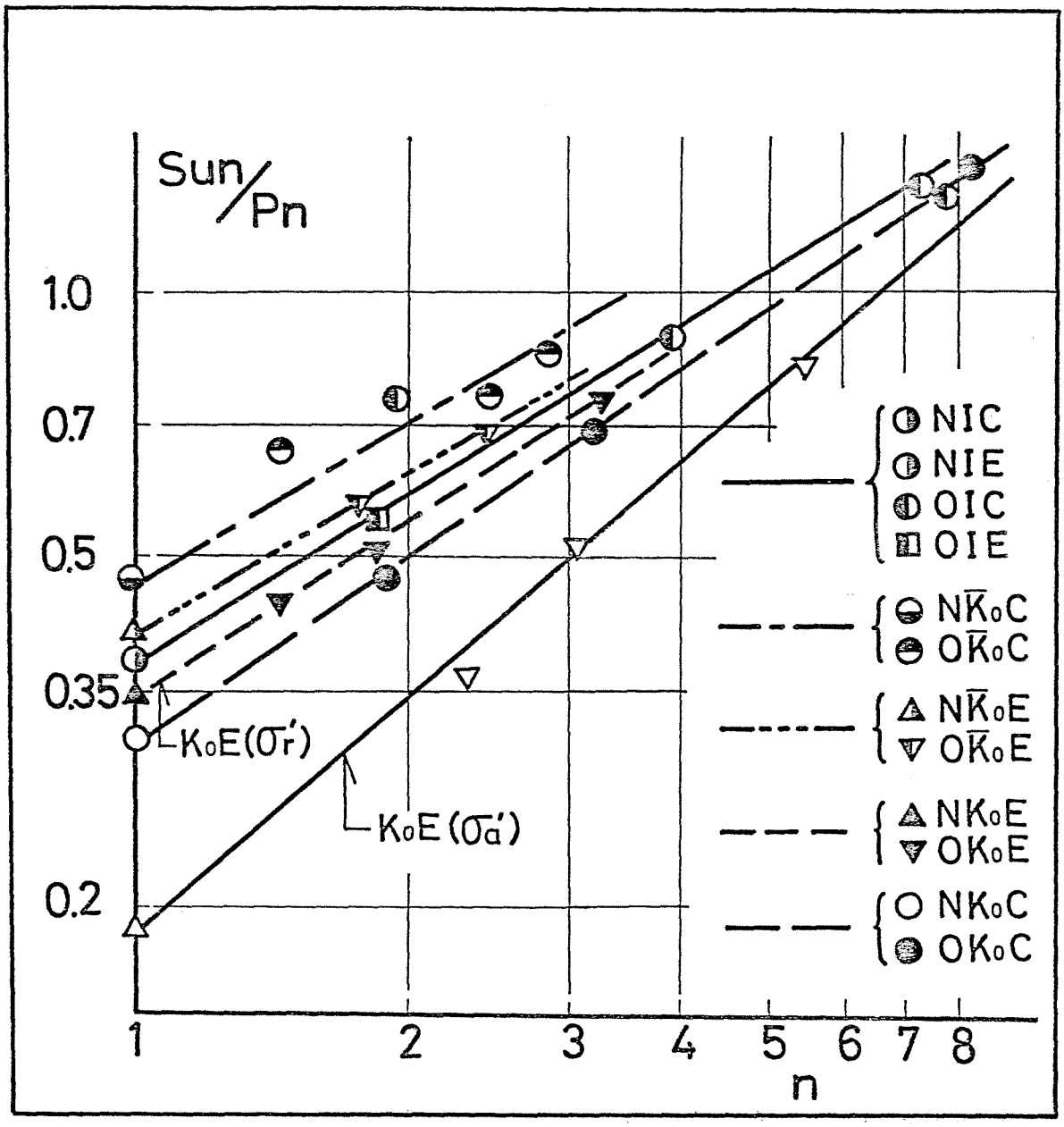

Fig.6-15 Rate of change in undrained shear strength versus overconsolidation ratio (axi-symmetrical triaxial compression and extension tests on sample No.4)

Fig. 6-16 illustrates the ratio Sun/p_n versus n relationship in plane strain and axi-symmetrical compression and extension tests. Although the scattering of the data is large at $n \fallingdotseq 10$ in compression tests, $\log Sun/p_n$ versus $\log n$ curve in plane strain condition is almost parallel to that in axi-symmetrical triaxial condition. In extension tests, the same conclusion as in compression tests can be drawn. Therefore, the convenient method for estimating the undrained shear strength of overconsolidated clay in axi-symmetrical triaxial condition mentioned previously can be extended for the conditions of plane strain compression and extension.

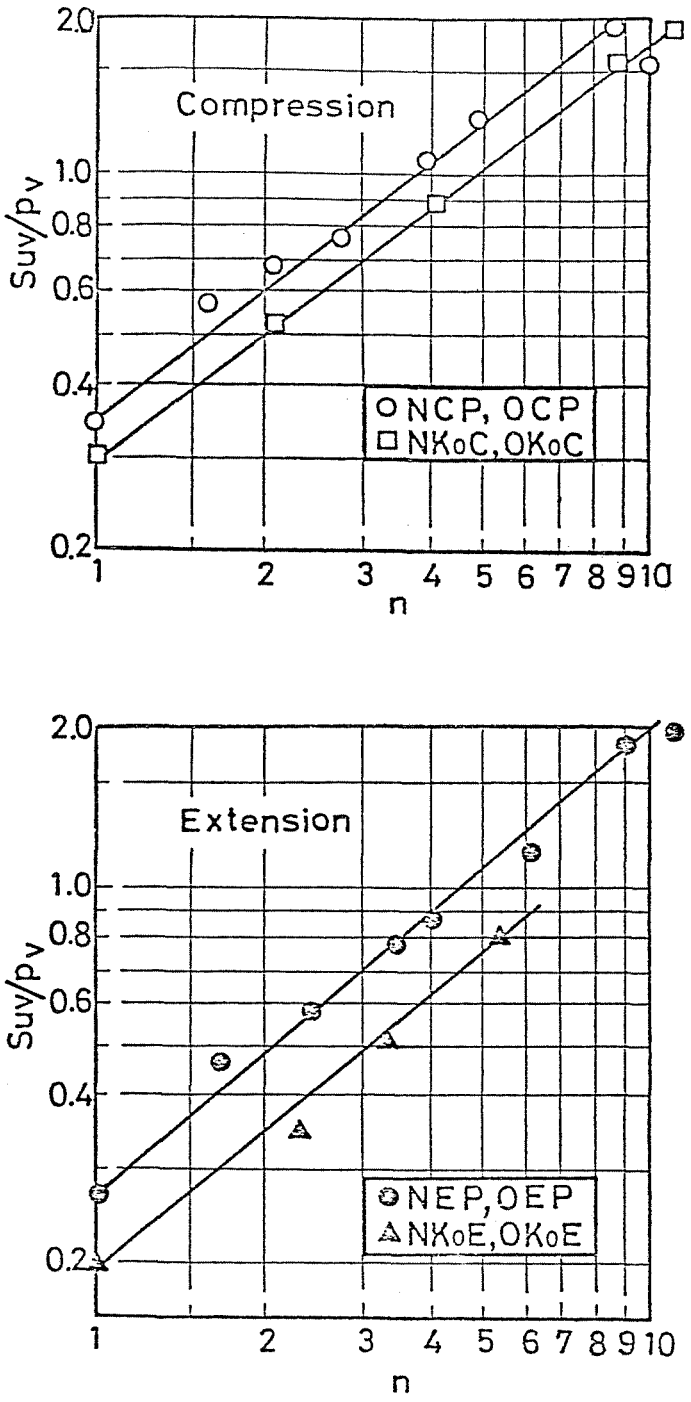

Fig.6-16 Rate of change in undrained shear strength vs. overconsolidation ratio (plane strain compression and extension tests on Sample No.4)

6.6 Prediction of in situ Undrained Strength of Overconsolidated Clay

As shown in previous sections, undrained strengths of overconsolidated clay under a variety of stress conditions can be estimated by using the data from convetional laboratory tests.

The procedure of estimation for the undrained compressive strength of overconsolidated clay is as follows.

1) Obtain the ratio $(Sui/p_i)_I$ by consolidating the undisturbed sample under the several steps of consolidation pressure which is greater than 1.5 to 2 times the in situ maximum past pressure (Ladd and Foott, 1974) and by shearing these specimen under undrained triaxial compression condition.

2) From a standard oedometer test, compression and swelling indices C_c and C_s are obtained.

3) Substituting the values of $(Sui/p_i)_I$, C_c and C_s into Eq. (6-26), $(Sun/p_n)_{K_o}$ can be obtained.

The method of prediction mentioned above is a procedure that may be used when the strengths have to be estimated with relatively high accuracy. However, triaxial and oedometer tests are not always be performed with ease. Accordingly a method of rough estimation of undrained strength by simpler test that can be performed within a short period will be considered as follows.

1) From the strength of unconfined compression test which is performed for normally consolidated clay and the corresponding value of overburden pressure, the value which corresponds to

0.8 $(S_{u1}/p_1)_I$ is obtained, namely $(\tau_u/2p_1)$ is regarded as equal to $(S_{u1}/p_1)_{K_0}$. The reason of this treatment is that the assumption $S_u = \tau_u/2$ gives satisfactory results in stability analysis (Nakase et al. 1969).

2) Let the value of $(1-\xi)$ be approximately equal to 0.8 irrespective of the value of PI, because the experimental data by Ladd and the present author show that the value of $(1-\xi)$ ranges from 0.75 to 0.86 and the difference between the values of true ξ and 0.8 does not yield so much error of strength estimation (for example, the difference of the value of S_{un}/p_n estimated by assuming $1-\xi = 0.8$ and the observed value at $n = 10$ is about ± 10 %).

3) Calculate the value of $(S_{un}/p_n)_{K_0}$ by setting

$$(S_{un}/p_n)_{K_0} \fallingdotseq (\tau_u/2p_1)\, n^{0.8}$$

Undrained strengths of overconsolidated clay in axi-symmetrical and plane strain extension conditions may be estimated by using the relationship between the strengths in undrained compression and extension conditions for normally consolidated clay, since the inclination of the $\log S_{un}/p_n$ versus $\log n$ curves are almost equal in compression and extension conditions.

CHAPTER VII CONCLUSIONS

From the experimental data and theoretical considerations described so far, the following conclusions are reached.

From the study for predicting stress-strain behaviour of isotropically normally consolidated clay in CHAPTER III, it may be concluded that;

(1) Cam-clay equations proposed by Roscoe et al. and subsequent equations proposed after them can not always give good prediction of stress-strain behaviour of isotropically consolidated clay because of the following fundamental defects.

a) Although the influence of the magnitude of K value on the prediction of the stress-strain relationships is dominant, the appropriate value of K is difficult to determine objectively.

b) As the Cam-clay equation is based on the energy concept, dilatancy characteristics of particular soil can not be introduced directly into the predicting equation.

(2) Isotropically consolidated undrained compression and extension stress-strain behaviour of clay can well be described by introducing dilatancy function $F(\eta)$ proposed by the present author into the predicting equation and overcoming the defects mentioned above.

From the study for stress-strain-strength behaviour of K_o normally consolidated clay in CHAPTER IV, it may be concluded that;

(1)The difference of stress system (compression or extension)

during shear affects the effective stress-strain behaviour of clay, but the type of stress application, i.e. increasing or decreasing stress, during shear does not make any influence upon the stress-strain properties of clay irrespective of the stress system during consolidation.

(2) Effective angles of shearing resistance ϕ' in extension tests are in general larger than those in compression tests, and the ϕ' values both in compression and extension are affected to a certain degree by the stress anisotropy during consolidation.

(3) Undrained shear strength S_u is greatly influenced by the difference of stress system during shear, especially in K_o consolidated clay, i.e. S_u in extension test is less than 70% of that in compression test.

(4) Stress-strain-strength behaviour of K_o consolidated clay during undrained compression and extension tests can be predicted by using the data obtainable from conventional isotropically consolidated undrained compression and extension tests on the same soil.

From the study for undrained plane strain stress-strain-strength behaviour of normally consolidated clay in CHAPTER V, it may be concluded that;

(1) Effective strength parameter $\tan\phi'$ and undrained shear strength S_u in plane strain test are greater than those in axi-symmetrical triaxial test in both compression and extension, and most markedly in extension.

(2) Interchange of principal stress directions in plane strain

extension test results in about 35% loss of undrained shear strength and more than 10 degrees increase of effective angle of shearing resistance in comparison with plane strain compression test.

(3) Octahedral stress ratio versus strain relationships and undrained stress paths in octahedral stress plane are almost identical for both triaxial and plane strain compression tests, but are appreciably different from each other in triaxial and plane strain extension tests.

(4) As dilatancy characteristics in extension appreciably differ from those in compression even in axi-symmetrical test as well as in plane strain test, it may be concluded that dilatancy characteristics of K_o consolidated clay is greatly influenced by the interchange of principal stress directions.

(5) Stress-strain behaviour of K_o consolidated clay during undrained plane strain compression and extension tests can be predicted by using the data obtainable from axi-symmetrical compression and extension tests, provided that appropriate information on the intermediate principal stress and correlation between effective stress path in plane strain and that in axi-symmetrical tests could be found.

From the study for undrained shear strength of overconsolidated clay in CHAPTER Ⅵ, it may be concluded that;

(1) The ratio of undrained shear strength under triaxial compression condition to effective vertical swelling pressure S_u/p_v for overconsolidated clay can be expressed by a simplified equation, irrespective of the stress systems during consolidation and swelling. By using this equation, in situ undrained shear strength of overcon-

solidated clay under the condition of axi-symmetrical compression condition can be estimated from the data obtained by conventional laboratory test.

(2) Coefficient of earth pressure at rest K_o and pore water pressure coefficient A at failure in overconsolidation state can both be expressed as a function of overconsolidation ratio.

(3) Undrained shear strengths of overconsolidated clay in axi-symmetrical and plane strain extension condition may be estimated by the same procedure as was done for overconsolidated clay in undrained triaxial compression condition.

ACKNOWLEDGEMENT

The author would like to express his appreciation to Prof. S. Kitago for the continuing guidance and encouragement and a critical reading of the manuscript.

He also wish to thank Prof. S. Toki and Mr. S. Miura for their many helpful suggestions during the course of this work.

The present study was supported by many colleagues in the Soil Mechanics and Foundation Engineering Laboratories of Hokkaido University. The author is indebted especially to Messrs. Y. Karoji, Y. Tanaka and S. Takeda who contributed to this study in developing automatic K_o control system, plane strain apparatus and loading extension apparatus. He is also indebted to Mr. Y. Kudo for his preparation of the figures.

REFERENCES

1) Adachi, T. and Tohgi, M.(1974): "Constitutive equations for normally and over consolidated clays," Proc., 9th Annual Meeting of JSSMFE, pp.251-254 (in Japanese).

2) Akai, K. and Adachi, T.(1965): "Study on the one-dimentional consolidation and the shear strength characteristics of fully-saturated clay, in terms of effective stress," Trans., JSCE, No. 113, pp.11-27 (in Japanese).

3) Bishop, A.W. and Bjerrum, L.(1960): "The relevance of the triaxial test to the solution of stability problems," Proc., ASCE Research Conf. on Shear Strength of Cohesive Soils, Boulder, Colorado, pp.437-501.

4) Bishop, A.W. and Henkel, D.J.(1957): "The measurement of soil properties in the triaxial test," Edward Arnold, London.

5) Bjerrum, L. and Lo, K.Y.(1963): "Effect of aging on the shear strength properties of a normally consolidated clay," Geotechnique, Vol. 13, No.2, pp.147-157.

6) Bjerrum, L. and Simons, N.E.(1960): "Comparison of shear strength characteristics of normally consolidated clays," Proc., ASCE Res. Conf. on Shear Strength of Cohesive Soils, Boulder, Colorado, pp.711-726.

7) Bjerrum, L., Simons, N.E. and Torblaa, I.(1958): "The effect of time on the shear strength of a soft marine clay," Proc., Brussels Conf. on Earth Pressure Problems, Vol.1, pp.148-158.

8) Boyce, J.R. and Brown, S.F.(1976): "Measurement of elastic strain in granular material," Geotechnique, Vol.26, No.4, pp.637-640.

9) Broms, B.B. and Casbarian, A.O. (1965): " Effects of rotation of principal stress axes and of the intermediate principal stress on the shear strength," Proc., 6th ICSMFE,Vol.1, pp.179-183.

10) Broms, B.B. and Ratnam,M.V.(1963): "Shear strength of an anisotropically consolidated clay," Proc., ASCE, Vol.89,No.SM6, pp.1-26.

11) Brooker, E.W. and Ireland, H.O.(1965): "Earth pressures at rest related to stress history," Canadian Geotechnical J., Vol.2, No.1, pp.1-15.

12) Brown, S.F. and Snaith, M.S.(1974): "The measurement of recoverable and irrecoverable deformations on the repeated load triaxial test," Geotechnique, Vol.24, No.2, pp.255-259.

13) Burland, J.B.(1965): "The yielding and dilation of clay," Correspondence, Geotechnique, Vol.15, No.2, pp.211-214.

14) Campanella, R.G. and Vaid,Y.P.(1972): "A simple K_o triaxial cell," Canadian Geotechnical J., Vol.9, No.3, pp.249-260.

15) Campanella, R.G. and Vaid, Y.P.(1973): "Influence of stress path on the plane strain behaviour of a sensitive clay," Proc., 8th ICSMFE,Vol.1, pp.85-92.

16) Casagrande, A. and Wilson, S.D.(1951): "Effect of rate of loading on the strength of clays and shales at constant water content," Geotechnique,Vol.2, No.4, pp.251-264.

17) Cheney,J.A.(1979): Discussion to "Deformation and strength characteristics of soft Bangkok Clay" Proc.,ASCE,Vol.105, No.GT9 pp.1129-1131.

18) Cornforth,D.H.(1964): "Some experiments on the influence of strain conditions on the strength of sand," Geotechnique, Vol.14, No.2, pp.143-167.

19) Drucker, D.C.(1959): "A definition of stable inelastic material" J. Appl. Mech., Trans. ASME,26, pp.101-106.

20) Dunkan, J.M. and Seed, H.B.(1966): "Anisotropy and stress reorientation in clay," Proc.,ASCE, Vol.92, No.SM5, pp.21-50.

21) Eekelen, H.A.M. van and Potts, D.M.(1978): "The behaviour of Drammen clay under cyclic loading," Geotechnique, Vol.28, No.2, pp.173-196.

22) El-Ruwayih, A.A.(1976): "Design manufacture and performance of a lateral strain device," Geotechnique, Vol.26, No.1, pp.215-216.

23) Hambly, E.C. and Roscoe, K.H.(1969): "Observations and predictions of stresses and strains during plane strain of 'wet' clays," Proc., 7th ICSMFE, Vol. 1, pp.173-181.

24) Hansen, J.B. and Gibson, R.E.(1949): "Undrained shear strength of anisotropically consolidated clays," Geotechnique, Vol.1, No.3, pp.189-204.

25) Hata, S., Ohta, H. and Yoshitani, S.(1969): "On the state surface of soils," Proc., JSCE, No.172, pp.71-92.

26) Henkel,D.J.(1960): "The shear strength of saturated remolded clays," Proc., ASCE Research Conf. on Shear Strength of Cohesive Soils, Boulder, Colorado, pp.533-554.

27) Henkel, D.J. and Sowa, V.A.(1963): "The influence of stress history on stress paths in undrained triaxial tests on clay," Laboratory Shear Testing of Soils, ASTM, STP, No.361, pp. 280-291.

28) Henkel, D.J. and Wade, N.H.(1966): "Plane strain tests on saturated remoulded clay," Proc., ASCE, Vol.92, No.SM6,pp. 67-80.

29) Hvorslev,M.J. (1936): " Conditions of failure for remolded cohesive soils," Proc., 1st ICSMFE, Vol.3, pp.51-53.

30) Hvorslev, M.J.(1960): "Physical components of the shear strength of saturated clays,"Proc., Res. Conf. on Shear Strength of Cohesive Soils, Boulder, Colorado, pp.169-273.

31) Jaky, J. (1948): " Pressure in silos" Proc.,2nd ICSMFE,Vol.1, pp.103-109.

32) Karube,D.(1975): "Special testing methods other than standardized triaxial test and their problems," Proc., 20th Symposium on Soil Mechanics, JSSMFE, pp.45-60 (in Japanese).

33) Karube, D. (1977): " A stress-strain-time equation of normally consolidated clay," Proc.,9th ICSMFE, Specialty Session No.9, pp.105-112.

34) Karube, D.(1978): "Strains in triaxial compression tests on normally consolidated clays," Proc., JSCE, No.273, pp.83- 97 (in Japanese).

35) Khera, R.P. and Krizek, R.J.(1967): "Strength behaviour of an anisotropically consolidated remolded clay," Highway Research Record, No.190,pp.8-18.

36) Kitago, S., Mitachi, T. and Kamiya, M. (1976): "Strength properties of saturated clay in undrained triaxial extension," Proc., 11th Annual meeting of JSSMFE, pp.239-242 (in Japanese).

37) Kitago, S., Mitachi, T. and Miura, S.(1973): "A plane strain apparatus and some test results for a saturated remolded clay," Proc., 28th Annual Meeting of JSCE, Vol.III, pp.25-26 (in Japanese).

38) Kitago, S., Mitachi, T. and Yamaguchi, H.(1979): "The influence of consolidation duration on the shearing behaviour of cohesive soils," Proc., 34th Annual Meeting of JSCE, Vol.III, pp.63-64 (in Japanese).

39) Kitago,S. et al.(1978): "Undrained shear strength characteristics of clay-glass beads mixtures," Technical Report, JSSMFE, Hokkaido Branch, No.18, pp.167-176 (in Japanese).

40) Kitago, S. et al.(1980): "The effect of time on the shearing behaviour of cohesive soil," Technical Report, JSSMFE, Hokkaido Branch, No.20, pp.89-98 (in Japanese).

41) Kjellman, W.(1936): "Report on a apparatus for consumate investigation of mechanical properties of soils," Proc., 1st ICSMFE, Vol.2, pp.16-20.

42) Ladd, C.C.(1965): "Stress-strain behaviour of anisotropically consolidated clays during undrained shear," Proc., 6th ICSMFE, Vol.1, pp.282-286.

43) Ladd, C.C.(1971): "Strength parameters and stress-strain behaviour of saturated clays," Text for MIT Special Summer Program 1.34S Soft Ground Construction.

44) Ladd, C.C.(1973): Discussion, Main Session IV , Proc., 8th ICSMFE, Vol.4-2, pp.108-115.

45) Ladd, C.C. and Foott, R.(1974): "New design procedure for stability of soft clays," Proc., ASCE, Vol.100, GT7, pp. 763-786.

46) Ladd, C.C. and Lambe, T.W.(1963): "The strength of 'undisturbed' clay determined from undrained tests," Laboratory Shear Testing of Soils, ASTM, STP, No.361, pp.342-371.

47) Lade, P.V.(1976): "Three-dimensional behaviour of normally consolidated cohesive soil," Report to the National Science Foundation.

48) Lade, P.V.(1978): "Cubical triaxial apparatus for soil testing," Geotechnical Testing J., Vol.1, No.2, pp.93-101.

49) Lade, P.V. and Musante, H.M. (1978):" Three-dimensional behavior of remolded clay," Proc., ASCE,Vol.104, No. GT2, pp.193-209.

50) Lambe, T.W. and Whitman, R.V.(1969): Soil Mechanics, John Wiley and Sons, Inc.

51) Leon, J.L. and Alberro, J.(1977): "Extension and compression tests on Mexico City clay," Proc., 9th ICSMFE, Vol.1, pp.193-196.

52) Lewin, P.I.(1971): "Use of servo mechanisms for volume change measurement and K_o consolidation," Geotechnique, Vol.21, No.3, pp.259-262.

53) Lewin, P.I.(1973): "The influence of stress history on the plastic potential," Proc., of the Symposium on the role of plasticity in soil mechanics, pp.96-106.

54) Lewin, P.I.(1975): "Plastic deformation of clay with induced anisotropy," Istanbul Conf. on SMFE, Vol.2, pp.137-148.

55) Lewin, P.I. and Burland, J.B.(1970): "Stress-probe experiments on saturated normally consolidated clay," Geotechnique, Vol.20, No.1, pp.38-56.

56) Lo, K.Y.(1969): "The pore pressure-strain relationships of normally consolidated undisturbed clays, Part I, Theoretical considerations," Canadian Geotechnical J., Vol.6, No.4, pp. 383-394.

57) Menzies, B.K., Sutton, H. and Davies, R.E.(1977): "A new system for automatically simulating K_o consolidation and K_o swelling in the conventional triaxial cell," Geotechnique, Vol. 27, No.4, pp.593-596.

58) Mikasa, M.(1962): "On the significance of the concept of 'structure' in soil mechanics," Proc., 17th Annual Meeting of JSCE, pp.35-38 (in Japanese).

59) Mikasa, M.(1964): "Classification table of the engineering property of soil and its significance," Tsuchi-to-Kiso, JSSMFE, Vol.12, No.4, pp.17-24 (in Japanese).

60) Mikasa, M.(1969): "Interpretation and utilization of testing results," Procedure for Testing Soils, Revised Edition, JSSMFE, Part 5, chapter 5, pp.429-450 (in Japanese).

61) Mikasa, M., Nishigaki, Y. and Okajima, Y.(1978): "Comparison of the ratio c_u/p obtained from different types of test," Proc., 13th Annual Meeting of JSSMFE, pp.325-328 (in Japanese).

62) Mitachi, T. and Ueda, K.(1969): "On the shear strength characteristics of anisotropically consolidated clays," Proc., 24th Annual Meeting of JSCE, Vol.III, pp.79-82 (in Japanese).

63) Mitachi, T. and Kitago, S. (1973): "The influence of stress history on the shear strength characteristics of cohesive soils," Bulletin of the Faculty of Engineering Hokkaido University, No.68,Part II , pp.253-268.

64) Mitachi , T. and Kitago, S. (1976): " Change in undrained shear strength characteristics of saturated remolded clay due to swelling," Soils and Foundations, Vol.16, No.1, pp.45-58.

65) Mitachi ,T., Kitago, S. and Karoji, Y. (1973):"The influence of consolidation duration on the shear strength characteristics of cohesive soils (3rd report), " Proc., 8 th Annual Meeting of JSSMFE, pp.299-302 (in Japanese).

66) Mitachi,T., Kitago, S. and Miura, S. (1976): "The influence of strain condition on the shear strength characteristics of cohesive soils," Proc., 31th Annual Meeting of JSCE, pp.147-148 (in Japanese).

67) Mitachi , T., Kitago, S. and Miyabe, K. (1979): " A consideration on the undrained stress-strain-time relationship of cohesive soil, " Proc., 34th Annual Meeting of JSCE, Vol.III, pp.61-62 (in Japanese).

68) Mitachi, T., Noto, S. and Ueda, K. (1970): "The effect of K_o consolidation on the shear strength of saturated clays," Technical Report, JSSMFE, Hokkaido Branch, No.10, pp.77-82 (in Japanese).

69) Mroz, Z., Norris, V.A. and Zienkiewicz, O.C. (1979): "Application of an anisotropic hardening model in the analysis of elasto-plastic deformation of soils," Geotechnique, Vol.29, No.1, pp.1-34.

70) Nakase, A., Kobayashi, M. and Katsuno, M. (1969): "Change in undrained shear strength of saturated clays through consolidation and rebound," Report of the Port and Harbour Research Institute, Vol.8, No.4, pp.103- 143 (in Japanese).

71) Noorany, I. and Seed, H.B.(1965): "In-situ strength characteristics of soft clays," Proc., ASCE, Vol.91, No.SM2, pp. 49- 80.

72) Ohta, H., Yoshitani, S. and Hata,S.(1975): "Anisotropic stress-strain relationship of clay and its application to finite element analysis," Soils and Foundations, Vol.15, No.4, pp.61-79.

73) Okumura, T.(1969): "Studies on the disturbance of clay samples (1st report)," Report of the Port and Harbour Research Institute, Vol.8, No.1, pp.59-84.

74) Parry, R.H.G.(1960): "Triaxial compression and extension tests on remoulded saturated clay," Geotechnique, Vol.5, pp.166-180.

75) Parry, R.H.G.(1971): "Undrained shear strengths in clays," Proc., 1st Australia-Newzealand Conf. on Geomechanics, pp.11-15.

76) Parry, R.H.G. and Nadarajah, V.(1973): "Observations on laboratory prepared, lightly overconsolidated specimens of kaolin," Geotechnique, Vol.24, No.3, pp.345-358.

77) Pender, M.J.(1978): "A model for the behaviour of overconsolidated soil," Geotechnique, Vol.28,No.1, pp.1-25.

78) Prevost, J.H.(1978): "Anisotropic undrained stress-strain behaviour of clays," Proc., ASCE, Vol.104,No.GT8, pp.1075-1090.

79) Prevost, J.H.(1979): "Undrained shear tests on clays," Proc., ASCE, Vol.105, No.GT1, pp.49-64.

80) Roscoe, K.H. and Burland, J.B.(1968): "On the generalized stress-strain behaviour of wet clay," Engineering Plasticity, Cambridge Univ. Press, pp.535-609.

81) Roscoe, K.H. and Poorooshasb, H.B.(1963): "A theoretical and experimental study of strains in triaxial compression tests on normally consolidated clays," Geotechnique Vol. 13, No.1, pp. 12-38.

82) Roscoe, K.H. and Thurairajah, A. (1964): " On the uniqueness of yield surfaces for wet clays," Proc., IUTAM Symposium pp. 364-384.

83) Roscoe, K.H., Schofield, A.N. and Thurairajah, A.(1963): "Yielding of clays in states wetter than critical," Geotechnique, Vol.13, No.3, pp.211-240.

84) Roscoe, K.H., Schofield, A.N. and Wroth, C.P.(1958): "On the yielding of soils," Geotechnique, Vol.8, No.1, pp.22-53.

85) Rowe, P.W. (1962): " The stress-dilatancy relation for static equilibrium of an assembly of particles in contact," Proc., Royal Society, London,Series A, Vol.269, pp.500-527.

86) Sawada, T., Hasegawa, T. and Shimada, K.(1977): "On the volume change characteristics of normally consolidated clays," Proc., 12 th Annual Meeting of JSSMFE, pp.315-318 (in Japanese).

87) Schofield, A.N. and Wroth, C.P. (1968) Critical State Soil Mechanics, McGraw-Hill, London.

88) Scott, R.F.(1963): Principles of Soil Mechanics, Addison-Wesley Publishing Co., Reading, Mass.

89) Sekiguchi, H. and Ohta, H.(1977): "Induced anisotropy and time dependancy in clays," Proc., ICSMFE, Specialty Session 9, pp. 229-238.

90) Shibata, T.(1963): "On the volume changes of normally consolidated clays," Disaster Prevention Research Institute, Kyoto Univ., Annuals No.6, pp.128-134 (in Japanese).

91) Shibata, T.(1975): "On the rate of increase in undrained shear strength c_u/p of saturated soils," Proc., 20th Symposium on Soil Mechanics, JSSMFE, pp.129-137 (in Japanese).

92) Shibata, T. and Karube, D.(1965): "Influence of the variation of the intermediate principal stress on the mechanical properties of normally consolidated clay," Proc., 6th ICSMFE, Vol.1, pp.359-363.

93) Shibata, T., Ohta, H. and Sekiguchi, H.(1976): "Stress-strain-strength characteritics of soil," Tsuchi-to-Kiso, JSSMFE, Vol. 24, No.8, pp.11-22 (in Japanese).

94) Skempton, A.W. and Sowa, V.A.(1963): "The behaviour of saturated clays during sampling and testing," Geotechnique, Vol.13, No.4, pp.269-290.

95) Sketchley, C.J. and Bransby, P.L.(1973): "The behaviour of overconsolidated clay in plane strain," Proc., 8th ICSMFE, Vol.1, pp.377-384.

96) Tsushima, M. and Miyakawa, I.(1977): "Experimental consideration on the strength properties of undisturbed organic soils," Proc., Symposium on the Engineering Properties of Organic Soils, JSSMFE, pp.53-56 (in Japanese).

97) Vaid, Y.P. and Campanella, R.G.(1974): "Triaxial and plane strain behaviour of natural clay," Proc., ASCE, Vol.100, No. GT3, pp.207-224.

98) Wong, P.K.K. and Mitchell, R.J.(1975): "Yielding and plastic flow of sensitive cemented clay," Geotechnique, Vol.25, No.4, pp.763-782.

99) Wroth, C.P.(1965): "The prediction of shear strains in triaxial tests on normally consolidated clays," Proc., 6th ICSMFE, Vol.1, pp.417-420.

100) Wroth, C.P.(1977): "The predicted performance of soft clay under a trial embankment loading based on the Cam-clay model," Chapter 6 of Finite Elements in Geomechanics,Wiley.

101) Wroth, C.P. and Bassett, R.H.(1965): "A stress-strain relationship for the shearing behaviour of a sand," Geotechnique, Vol.15, No.9, pp.32-56.

102) Wu, T.H., Loh, A.K. and Malvern, L.E.(1963): "Study of failure envelopes of soils," Proc., ASCE, Vol.89, No.SM1, pp.145-181.

103) Yamaguchi, H.(1972): "Some considerations on the earth pressure at rest," Proc., 27th Annual Meeting of JSCE, Vol.III, pp.109-110 (in Japanese).

104) Yamanouchi, T. and Yasuhara, K.(1974): "A consideration on the coefficient of earth pressure at rest in clayey soils," J. of JSSMFE, Vol.14, No.2, pp.113-118 (in Japanese).

105) Yudhbir and Varadarajan, A.(1974): "Undrained behaviour of overconsolidated saturated clays during shear," Soils and Foundations, Vol.14, No.4, pp.1-12.